1st International Conference on Applied Sciences - 2025

ICAS 2025

Blending AI and Traditional Wisdom: Research and Development for a Sustainable Future

PROCEEDINGS - ICAS 2025

FACULTY OF APPLIED SCIENCE,
UNIVERSITY OF VAVUNIYA,
SRI LANKA

ICAS2025

1^{st} International Conference on Applied Sciences - 2025

“*Blending AI and Traditional Wisdom:*
Research and Development for a Sustainable Future”

Proceedings

Faculty of Applied Science
University of Vavuniya
Sri Lanka
October 16, 2025

Publication details

Proceedings of ICAS2025
Theme: “Blending AI and Traditional Wisdom: Research and Development for a Sustainable Future”

Publication of:
Faculty of Applied Science, University of Vavuniya, Panbaimadu, Vavuniya, Sri Lanka.

Email: icas2025@vau.ac.lk

Website: `https://fas.vau.ac.lk/icas2025/`

Disclaimer

ISSN: 978-624-6269-20-3

9786246269203

eISSN: 978-624-6269-21-0

9786246269210

Suggested citation

Abstract:
[Author name/s] (2025) “[Paper title]”. *Proceedings of the ICAS2025*, Faculty of Applied Science, University of Vavuniya, Vavuniya, Sri Lanka.

Conference proceedings:
Subaramya S., Nagulan R., Patrick A.E.S., Thilaganathan S., Jeyamugan T. and Naveendrakumar G. (Eds.) (2025) *Proceedings of the ICAS2025*, Faculty of Applied Science, University of Vavuniya, Vavuniya, Sri Lanka.

Table of Contents

Editorial Board

ICAS2025

Important Dates

May 21, 2025: Call for Papers
Aug 31, 2025: Paper Submission Deadline
Aug 20, 2025: Poster submission
Aug 25, 2025: Doctoral Symposium
Aug 25, 2025: Notification of Acceptance
Sep 15, 2025: Final Camera-Ready Submission
Oct 10, 2025: Registration
Oct 16, 2025: Conference

Tracks

Track 1: Advanced Computing Technologies
Track 2: Computational Intelligence and Data Technologies
Track 3: Healthcare Innovations and Bioinformatics
Track 4: Conservation and Climate Actions for Environmental Sustainability
Track 5: Innovations in Food Sciences and Biotechnology
Track 6: Precision Farming and Climate Smart Agriculture
Track 7: Renewable Energy and Green Technologies
Track 8: Statistical and Mathematical Approaches for Sustainable Development

Submission Categories

ICAS2025: Full papers, extended abstracts, and abstracts with poster submissions were invited.

Organisers

Faculty of Applied Science, University of Vavuniya

Vice Chancellor's Message

It gives me great pleasure to extend my warmest greetings to all participants of the International Conference on Applied Sciences (ICAS2025), proudly organised by the Faculty of Applied Science, University of Vavuniya. This event marks another milestone in our university's journey of academic excellence and regional leadership in applied research.

This year, ICAS2025 has reached new heights by attracting over 100 submissions, including full papers, extended abstracts, and poster presentations. The acceptance of nearly 70% of these works reflects both the quality and diversity of research contributions received from across Sri Lanka and beyond. The conference's growing reputation demonstrates the commitment of our academics, students, and collaborators to advancing knowledge that is both scientifically rigorous and socially relevant.

More than just an academic gathering, ICAS2025 serves as a forum for collaboration and innovation, bringing together domain-specific experts, eminent international scholars, and regional researchers to exchange ideas and explore pathways for impactful partnerships. It stands as a model of how collective intellectual efforts can transcend disciplinary boundaries and contribute meaningfully to national progress.

This year's theme, "Blending AI and Traditional Wisdom for Sustainable National Development," underscores the need to harmonise technological advancement with indigenous knowledge systems. In an era of rapid digital transformation, it is crucial that artificial intelligence and modern data-driven methodologies are contextualised within our cultural, environmental, and societal realities. Such integration has the potential to yield sustainable solutions for regional and national challenges, from agriculture and healthcare to education, resource management, and community development.

Importantly, ICAS2025 also highlights the University of Vavuniya's growing role as a regional hub for innovation and scholarly exchange. By hosting this conference, we not only uplift the academic profile of our institution but also strengthen regional engagement, enabling local research to gain national and international visibility. We firmly believe that nurturing such platforms contributes to the long-term goal of equitable and inclusive national development.

I extend my sincere appreciation to the keynote speakers, reviewers, authors, organising committee, and volunteers for their unwavering dedication to making this conference a success. May ICAS2025 inspire new collaborations, ignite meaningful dialogue, and contribute to a sustainable and knowledge-driven future for our nation.

Snr. Prof. A. Atputharajah
Vice Chancellor
University of Vavuniya

Dean's Message

It is with great pleasure that I extend my warmest welcome to all participants of the 1st International Conference on Applied Sciences (ICAS 2025), organized by the Faculty of Applied Science, University of Vavuniya.

From 2020 to 2024, the Faculty successfully organized the Faculty of Applied Science Annual Research Sessions (FARS), which provided a valuable platform for local scholars and students to share their research findings. Building on that foundation, the Faculty is now proud to organize its first international conference, the 1st International Conference on Applied Sciences (ICAS 2025), marking a major milestone in its academic journey.

The conference theme, "Blending AI and Traditional Wisdom: Research and Development for a Sustainable Future," reflects our vision to integrate technological advancement with indigenous knowledge to promote sustainability and innovation. This international platform brings together researchers, academics, professionals, and students from various disciplines to exchange ideas and foster collaborations for the betterment of society.

I would like to extend my sincere appreciation to all authors for contributing their research to this conference. Your scholarly work forms the core of ICAS 2025 and adds immense value to the proceedings. I also wish to express my gratitude to the organizing committee, reviewers, and supporting staff for their commitment and hard work in making this event a reality.

I am confident that ICAS 2025 will serve as a catalyst for future research collaborations and innovations that contribute meaningfully to scientific and sustainable development.

Dr. M. Kayanan
Dean, Faculty of Applied Science
Chairperson/ ICAS2025

Convener's Message

It is with great pride and heartfelt enthusiasm that I welcome you all to the International Conference on Applied Sciences (ICAS2025), organised by the Faculty of Applied Science, University of Vavuniya. As an alumna of the former Vavuniya Campus of the University of Jaffna, now elevated to the University of Vavuniya, I feel a profound sense of fulfilment and continuity at this moment.

When I first envisioned transforming our conference into an international event, my goal was not only to expand its reach but also to nurture a stronger research culture that bridges academia, innovation, and societal development. Having participated in several overseas conferences, I have observed effective practices that strengthen scholarly exchange, promote multidisciplinary dialogue, and translate research into real-world impact. These observations inspired the foundation of ICAS2025, a platform that encourages scientific collaboration, knowledge integration, and sustainable innovation across borders.

The overarching aim of this conference is to create fertile ground for the exchange of ideas among national and international researchers, scholars, and practitioners. ICAS2025 embraces this spirit by featuring a diverse range of sessions, including keynote addresses by eminent researchers, doctoral symposiums, and technical paper presentations across multiple disciplines of applied sciences. Each presentation represents the dedication and creativity of researchers striving to address challenges that matter locally and globally, from sustainability and digital transformation to emerging technologies in health, agriculture, and the environment.

I am particularly proud that this year's Doctoral Symposium provides young researchers with an opportunity to present their work, receive constructive feedback, and connect with experienced scholars. Such interactions are essential to fostering a supportive research ecosystem and empowering the next generation of scientists.

On behalf of the organising committee, I extend my sincere gratitude to all the authors, reviewers, keynote speakers, technical chairs, and volunteers whose contributions made this conference possible. I am equally thankful to the leadership of our University of Vavuniya, our sponsors, and all our alumni who work worldwide and have helped us uplift ICAS to this level through their continuous encouragement and support.

I warmly welcome all participants and invite you to engage actively, share your insights, and build lasting collaborations through ICAS2025. Together, let us continue to advance applied science for the betterment of our society and beyond.

Dr. T. Kartheeswaran
Convener/ ICAS2025

Editor-in-Chief's Message

It gives me great pleasure to present the Proceedings of the International Conference on Applied Sciences (ICAS 2025), proudly organized by the Faculty of Applied Science, University of Vavuniya. This year marks a significant milestone as the conference has been expanded to a fully international platform, bringing together researchers, innovators, and professionals from across the globe to share knowledge and foster collaboration under the theme "Blending AI and Traditional Wisdom for Sustainable National Development."

This year, ICAS 2025 received over 100 submissions in the form of full papers, extended abstracts, and poster presentations. Following a rigorous double-blind peer review process involving more than 100 expert reviewers worldwide, a total of 75 submissions were accepted for presentation and publication, reflecting a strong commitment to quality and relevance. Among them are 15 full papers, five extended abstracts, and 55 abstracts with poster, representing innovative and impactful research across multiple disciplines.

The conference encompasses seven thematic tracks, covering a wide spectrum of topics: Advanced Computing Technologies; Computational Intelligence and Data Technologies; Healthcare Innovations and Bioinformatics; Conservation and Climate Actions for Environmental Sustainability; Innovations in Food Sciences and Biotechnology; Precision Farming and Climate-Smart Agriculture; Renewable Energy and Green Technologies; and Statistical and Mathematical Approaches for Sustainable Development. These tracks reflect the multidisciplinary essence of applied sciences and their role in addressing national and global challenges.

Each accepted paper has been carefully formatted and curated to maintain consistency and readability. The ICAS 2025 Proceedings will be archived in the Digital Repository of the University of Vavuniya. For the first time, ICAS 2025 will be held entirely in person, allowing keynote speakers, session chairs, reviewers, and authors to engage directly at the University of Vavuniya. This provides a vibrant opportunity to build meaningful research networks, exchange insights, and inspire collaborations that extend beyond the conference itself.

I extend my heartfelt gratitude to all keynote speakers, authors, reviewers,co-editors, typesetters, proof readers, leaders of the University of Vavuniya, sponsors, the organizing committee, and contributors for their dedicated efforts in upholding the academic and technical standards of ICAS 2025. May this conference continue to inspire innovation and contribute to the advancement of science for sustainable national development.

Ms. Subaramya Srivishagan
Editor-in-Chief
ICAS 2025

Professor Nanda Ganesan's Message

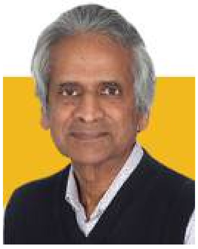

I extend my heartfelt congratulations to the organizers, participants, and supporters of the International Conference on Applied Sciences (ICAS 2025) hosted by the University of Vavuniya, Sri Lanka. This inaugural conference marks a significant milestone in the journey of a young and ambitious university that has already begun to make its mark in the academic world.

The University of Vavuniya, though only a few years old, has demonstrated remarkable vision and purpose in striving to build a culture of excellence in teaching, research, and innovation. ICAS 2025 reflects that vision, a thoughtful and forward-looking initiative designed to strengthen the University's identity and enhance its visibility both within Sri Lanka and beyond. This conference represents an important platform for sharing the fine work being done at the University and highlighting the growing capabilities of its talented faculty, researchers, and students.

The goals of ICAS 2025 are both noble and far-reaching. By inviting academic scholars from across the country and around the world, the conference opens doors to meaningful engagement and exchange. It provides an opportunity to showcase the research and development endeavors taking place at the University of Vavuniya while at the same time inviting fresh perspectives, collaborative ideas, and shared experiences. Such interactions will undoubtedly strengthen the University's research potential and foster partnerships that extend well beyond this event.

One of the most inspiring aspects of this conference is its emphasis on collaboration and community. By connecting local faculty and students with international scholars and practitioners, ICAS 2025 intends to pave the way for future joint research projects, innovations, and cross-border initiatives. Through these efforts, the University is charting a research path that is both nationally important and regionally significant, one that will help shape the academic and social landscape of the region and country in the years to come.

The outstanding response to this inaugural effort, with 105 submissions and 75 acceptances, speaks volumes about the confidence and enthusiasm of the academic community. The participation of distinguished keynote speakers and leading scholars adds further prestige and inspiration to this event.

I am confident that ICAS 2025 will be remembered not only as a successful conference but also as the beginning of lasting collaborations, meaningful friendships, and a brighter academic future for the University of Vavuniya. I wish everyone involved continued success, and I look forward to seeing this great institution grow in recognition, impact, and achievement.

Professor Nanda Ganesan, Ph.D
Department of Information Systems
California State University, Los Angeles
Advisory Board Member-ICAS2025

List of Reviewers – ICAS2025

Snr. Prof. (Mrs.) Christina Shanthi De Silva,

Department of Agricultural and Plantation Engineering, Open University of Sri Lanka

Prof. K. Ahilan,

Department of Electrical and Electronic Engineering, University of Jaffna, Sri Lanka

Prof. (Ms.) M. R. J. C. Chandrakantha Mahendranathan,

Department of Botany, Eastern University of Sri Lanka

Prof. N. D. K. Dayawansa,

Department of Agricultural Engineering, University of Peradeniya, Sri Lanka

Prof. E. P. S. K. Ediriweera,

Department of Science and Technology, Uva Wellassa University, Sri Lanka

Prof. K. Gajapathy,

Department of Zoology, University of Jaffna, Sri Lanka

Prof. Ajith C. Herath,

Department of Chemical Sciences, Rajarata University of Sri Lanka

Prof. (Dr.) A. Jahufar,

Department of Mathematical Sciences, South Eastern University of Sri Lanka

Prof. R. G. N. Meegama,

Department of Computer Science, University of Sri Jayewardenepura, Sri Lanka

Prof. A. Ramanan,

Department of Computer Science, University of Jaffna, Sri Lanka

Prof. M. Siyamalan,

Department of Computer Science, University of Jaffna, Sri Lanka

Prof. M. Sugirtharan,

Department of Agricultural Engineering, Eastern University of Sri Lanka

Dr. G. Abhiram,

Department of Export Agriculture, Uva Wellassa University, Sri Lanka

Dr. V. Anavarathan,

Department of Pathology and Clinical Sciences,

Trincomalee Campus, Eastern University, Sri Lanka

Dr. Ankit Verma,

Faculty of Medicine, Hebrew University of Jerusalem, Israel

Dr. S. Arivalzagan,

Department of Mathematics and Statistics, University of Jaffna, Sri Lanka

Dr. H. M. S. N. Ariyadasa,

Department of Computer Science and Informatics, Uva Wellassa University, Sri Lanka

Dr. Balachandran Ketheesan,

Department of Civil Engineering, University of Jaffna, Sri Lanka

Dr. W. M. C. Dammika Wijekoon,

Department of Zoology, University of Ruhuna, Sri Lanka

Dr. A. J. M. Harris,

Department of Zoology, Eastern University, Sri Lanka

Dr. (Mrs.) Jananie Jarachanthan,

Department of Computer Engineering, University of Jaffna, Sri Lanka

Dr. K. Jeyavanan,

Department of Agronomy, University of Jaffna, Sri Lanka

Dr. I. M. Kalith,

Department of Information and Communication Technology,
South Eastern University of Sri Lanka

Dr. T. Ketheesan,

Department of Interdisciplinary Studies, University of Jaffna, Sri Lanka

Dr. T. Kokul,

Department of Computer Science, University of Jaffna, Sri Lanka

Dr. Lochandaka Ranathunga,

Department of Information Technology, University of Moratuwa, Sri Lanka

Dr. (Mrs). P. Malathy,

Department of Chemistry, University of Jaffna, Sri Lanka

Dr. A. Manjceevan,

Department of Chemistry, University of Jaffna, Sri Lanka

Dr. T. Mathanarajan,

Department of Mathematics and Statistics, University of Jaffna, Sri Lanka

Dr. (Mrs). B. Mayurathan,

Department of Computer Science, University of Jaffna, Sri Lanka

Dr. (Ms.) Nirthika Rajendran,

Department of Computer Science, University of Jaffna, Sri Lanka

Dr. K. Prasannath,

Department of Agricultural Biology, Eastern University, Sri Lanka

Dr. (Mrs.) Pratheeba Jeyananthan,

Department of Computer Engineering, University of Jaffna, Sri Lanka

Dr. Ruwan D. Nawarathna,

Department of Statistics and Computer Science, University of Peradeniya, Sri Lanka

Dr. (Ms.) J. Samantha Tharani,

Department of Computer Science, University of Jaffna, Sri Lanka

Dr. L. H. M. Y. K. Somaratne,

Department of Agricultural Biology, University of Peradeniya, Sri Lanka

Dr. Sriashalya Srivathsan,

Suwami Vipulanatha Institutes of Aesthetic Studies, Eastern University, Sri Lanka

Dr. T. Sritharan,
University of Colombo School of Computing, Sri Lanka
Dr. S. Sukirthan,
Department of Physiotherapy and Occupational Therapy,
General Sir John Kotelawala Defense University, Sri Lanka
Dr. Tharaga Sharmilan,
Department of Applied Computing, University of Kelaniya, Sri Lanka
Dr. Udeni D. Wijesooriya,
Department of Mathematics, University of Peradeniya, Sri Lanka
Dr. B. Uthayanan,
Faculty of Siddha Medicine, Trincomalee Campus, Eastern University, Sri Lanka
Dr. R. Vijitha,
Department of Radiography and Radiotherapy,
General Sir John Kotelawala Defense University of Sri Lanka
Dr. Gover Antonyraj,
CSIR-Central Institute of Medicinal and Aromatic Plants,
Lucknow, Uttar Pradesh, India
Dr. Roy Moscona,
Cincinnati's Children's Hospital, Cincinnati, USA
Mr. S. L. Abdul Haleem,
Department of Information and Communication Technology,
South Eastern University of Sri Lanka
Mrs. W. M. L. S. Abeythunga,
Department of Software Engineering, Sabaragamuwa University, Sri Lanka
Mr. R. K. Ahmadh Rifai Kariapper,
Department of Information and Communication Technology,
South Eastern University of Sri Lanka
Ms. Amuthenie Sugirtharan,
Department of Agricultural Chemistry, Eastern University, Sri Lanka
Mr. A. M. P. Chandrasiri,
Department of Science and Technology, Uva Wellassa University, Sri Lanka
Mr. W. A. P. P. Christopher,
Department of Earth Sciences, Uva Wellassa University of Sri Lanka
Ms. Dilrukshi Gamage,
University of Colombo School of Computing, Sri Lanka
Ms. C. S. D. Ellepola,
Department of Computer Science and Informatics, Uva Wellassa University of Sri Lanka
Ms. A. Fathima Musfira,
Department of ICT, South Eastern University of Sri Lanka

Ms. A. Fathima Sharfana,
Department of Information and Communication Technology,
South Eastern University of Sri Lanka
Mr. Gamini Wijayarathna,
Department of Software Engineering, University of Kelaniya, Sri Lanka
Ms. Isuri Uwanthika,
Department of Computer Science,
General Sir John Kotelawala Defense University, Sri Lanka
Ms. D. P. Jayathunga,
Department of Computer Science and Informatics, Uva Wellassa University of Sri Lanka
Mr. K. A. N. K. Karunarathna,
Department of Mathematics, Eastern University, Sri Lanka
Mrs. Khedika Krishnaraj,
Department of Computer Science,
Trincomalee Campus, Eastern University, Sri Lanka
Ms. T. Kirupananthan,
Department of Agriculture Economics, Eastern University, Sri Lanka
Mr. A. Mohamed Aslam Sujah,
Department of Information and Communication Technology,
South Eastern University, Sri Lanka
Mr. K. Muhammad Rifthy,
Department of Information and Communication Technology,
South Eastern University of Sri Lanka
Mr. P. G. Munasinghe,
Department of Information Systems, Rajarata University of Sri Lanka
Mr. H. P. D. P. Pathirana,
Department of Computer Science and Informatics, Uva Wellassa University, Sri Lanka
Mr. Ponnampalam Pirapuraj ,
Department of Information and Communication Technology,
South Eastern University of Sri Lanka
Mr. M. Ramanan,
Department of Information Technology, University of Jaffna, Sri Lanka
Ms. R. M. I. S. Ranasinghe,
Faculty of Applied Sciences, Uva Wellassa University of Sri Lanka
Mr. A. M. B. Ratnayake,
Department of Computer Science and Informatics,
Uva Wellassa University of Sri Lanka
Mrs. Sajeetha Thavareesan,
Department of Computing, Eastern University, Sri Lanka

Eng. Saliya Sampath, ,

Department of Civil Engineering, University of Jaffna, Sri Lanka

Mrs. Sankani Heenkenda,

Department of Information and Communication Technology,
University of Sri Jayewardenepura, Sri Lanka

Mrs. P. Sivakumar,

Department of Zoology, University of Jaffna, Sri Lanka

Mr. S. Sotheeswaran,

Department of Computing, Eastern University, Sri Lanka

Mr. S. Suthakar,

Department of Computer Science, University of Jaffna, Sri Lanka

Ms.Sutharshiny Sathyaruban,

Department of Fisheries Science, University of Jaffna, Sri Lanka

Mrs. Thanushya Thanujan,

Department of Computer Science, Trincomalee Campus, Eastern University, Sri Lanka

Mr. Thilina Gunarathne,

Department of Computer Engineering, University of Peradeniya, Sri Lanka

Mrs. W. V. S. K. Wasalthilaka,

Department of Software Engineering, Sabaragamuwa University, Sri Lanka

Ms. Wasana Jeewanthi Polegoda,

Department of Export Agriculture, Uva Wellassa University of Sri Lanka

Ms. J. Kirushika,

Department of Electrical and Computer Engineering, Open University of Sri Lanka

Ms. Nivetha Arulnesan,

Department of Information Technology, Trincomalee Campus, Eastern University of Sri Lanka

Mr. U. E. Ranasooriya,

Department of Computer Science and Informatics, Uwa Wellasa University of Sri Lanka

Mr. Joseph Charles

University of South Queensland, Australia

Mr. Ofir Ben Shoham,

Ben-Gurion University, Israel

Mr. Ohad Landau,

Ben-Gurion University, Israel

Mr. Oriel Perets,

Ben-Gurion University, Israel

Mr. P. Vickneshwaran,

Charles Darwin University, Australia

Keynote Speaker I

Advancing Precision Oncology through Knowledge-Driven AI and Bioinformatics Innovation

Precision oncology aims to tailor cancer treatment to individual patients by identifying molecular and genetic features that predict therapeutic response. Accurately assigning patients to optimal treatment subgroups, however, remains a major challenge. This keynote highlights three complementary research directions advancing precision oncology. First, we show how knowledge-driven feature selection can enhance the predictive power of machine learning models in drug response analysis. By deriving detailed cell profiles within the tumor microenvironment, we improve tumor classification and disease severity prediction. This approach enables a generalized framework for knowledge-guided feature selection applicable across diverse cancer datasets. Second, we examine how AI tools can accelerate scientific discovery and student productivity. Using Gonadotropin-related mutations in cancer as an example, analyses that previously required years of postgraduate research can now be reproduced in a fraction of the time, demonstrating AI's transformative potential in biomedical research and education. Finally, we introduce a bioinformatics-driven simulation method to optimize experimental validation of predictive models. Our results indicate that over 80% accuracy in ranking model performance can be achieved using only a minimal subset of experiments, substantially reducing cost and effort. Together, these studies illustrate the synergistic integration of AI, knowledge-based modeling, and bioinformatics to advance precision oncology, accelerate the translation from data to discovery, and ultimately improve patient outcomes.

Prof. Eitan Rubin
The Shraga Segal Department of Microbiology, Immunology
and Genetics
Ben-Gurion University of the Negev

Prof. Eitan Rubin is a Professor in the Shraga Segal Department of Microbiology, Immunology, and Genetics at Ben-Gurion University of the Negev. He holds a B.Sc. in Biology from Ben-Gurion University and a Ph.D. in Plant Sciences from the Weizmann Institute of Science. Formerly Head of Bioinformatics at Harvard University, his research focuses on human phenotypic variation, drug response, cancer stratification, and applying machine learning to genomic data. He has supervised over 15 Ph.D. and Master's students and serves as Principal Investigator at BGU and Head of Bioinformatics at the Worldwide Innovative Network (WIN) Consortium for precision medicine.

Keynote Speaker II

Blockchain Technology and Its applications

This talk offers a comprehensive introduction to blockchain technology, emphasizing its foundational principles, real-world applications, and common misconceptions. Blockchain is defined as a cryptographically linked, replicated, and distributed ledger maintained through consensus, serving as an immutable and tamper-resistant log of transactions and events. The course deliberately avoids focusing on cryptocurrencies like Bitcoin, instead highlighting blockchain's broader utility in trusted computing and cybersecurity.

Through illustrative examples, banking fraud, supply chain provenance, land records, Aadhaar logs, and student grade systems, the slides explore how traditional trust models often fail due to centralized control, lack of transparency, and vulnerability to manipulation. Blockchain is proposed as a solution to these trust issues by enabling authenticated, non-repudiable, and integrity-assured data logging using cryptographic techniques and distributed consensus.

The presentation also discusses the challenges of implementing blockchain in concurrent systems, such as supply chains with multiple stakeholders, and proposes publish-subscribe models and crowd-sourced validation as scalable alternatives. It underscores the importance of Byzantine fault-tolerant consensus to maintain reliability in adversarial environments.

Finally, the talk dispels several prevailing misconceptions: that blockchain is inherently secure, that cryptography alone guarantees integrity, and that government-led, closed-source implementations are necessary. It clarifies that blockchain is not synonymous with cryptocurrency and can support privacy-preserving, permissioned, and decentralized applications across sectors.

Prof. Sandeep K. Shukla
Director
International Institute of Information Technology
Hyderabad, India

Prof Sandeep K. Shula is the Head of Computer Engineering at IIT Kanpur and he was the one of the Founding Director of C3i Hub at IIT Kanpur , He has supervised more than 12 PhDs students and ignited lot of Cyber Security Startup through C3i Hub. HE has authored many books and plethora of high-quality research articles.

Keynote Speaker III

Cybersecurity of Connected Infrastructure

The critical infrastructure sectors now rely on electronic systems, including Internet of Things (IoT) and operational technology(OT)devices and systems. This coupled with increased connectivity at corporate network edges and adoption of cloud services make securing technology infrastructure both more complex. The IT/OT convergence is also shaping new ways of working as businesses adapt to a shift in their organisational structure, and take on new challenges with compliance, cybersecurity, and data and technology management. As a result, many organizations have an expanding attack surface vulnerable to threats. Moreover, threats are also getting increasingly complex, and IT security is only as good as the weakest link in the infrastructure. With cybersecurity threats on the rise, the industry is compelled to develop new levels of preparedness, and trends confirm that cybersecurity will continue to be one of the top investment priorities moving forward.

This talk will discuss the major factors influencing the rapid growth in connected systems and in particular, the significance of IT and OT in convergence as technology evolves. It will introduce several in-house developed edge computing devices/systems for the fast-evolving connected systems infrastructure of Intelligent Transport Systems (ITS) and discuss the newly launched R&D program for engineering a secure connected systems infrastructure for healthcare. Ongoing research efforts and trends in software/hardware security for mitigating cyber threats in complex infrastructure will also be introduced.

Prof. Thambipillai Srikanthan
Professor
School of Computer Science & Engineering
NTU, Singapore

Dr Srikanthan is a Professor at the College of Computing & Data Science at the Nanyang Technological University, Singapore since 2005. He was the founding Director of the Centre for High Performance Embedded Systems (CHiPES), NTU from 1998 until 2014. He served as Chair of the School of Computer Science and Engineering between 2010-2016. He has supervised more the 48 PhD and M.Eng students and authored 490 high quality research articles.

Keynote Speaker IV

Forest-grassland mosaics: past, present and future

The ‘one climate-one biome’ paradigm – the idea that each biome occupies a unique area of climate space such that the dominant or ‘climax’ vegetation of a region can be predicted based on local climate alone – has been a cornerstone of traditional ecological thought. However, many ecosystems display ‘bi-stability’ where two different biomes occur under the same climatic conditions. Forest-grassland mosaics are a classic example of this phenomenon wherein both forest and grassland patches, with abrupt boundaries between the two, co-occur in the landscape. In this talk, I synthesize our work from the montane forest-grassland mosaics of the Western Ghats over the last several years to: i) evaluate the role of different biotic and abiotic drivers in maintaining these mosaics, ii) discuss how the historical mismanagement of these mosaics has led to the conservation challenges facing them today, particularly in terms of invasive species, and iii) consider the potential impacts of future climatic changes on the ecological integrity of these unique ecosystems.

Prof. Mahesh Sankaran
National Centre for Biological Sciences
Bengaluru,India

Mahesh Sankaran is a community and ecosystem ecologist whose research focuses on understanding how climate change impacts the distribution, structure and functioning of tropical ecosystems globally, with a focus on savannas and grasslands, and more recently, forests. He is particularly interested in applying this knowledge to the restoration of degraded lands in a changing climate. He has also contributed to shaping international policy on climate change, biodiversity and land through his work with the IPCC and IPBES assessments on land degradation, climate change and biodiversity. He was awarded the Infosys Prize for the Life Sciences in 2021 and has been elected to the Indian Academy of Sciences and the Indian National Science Academy. He is a J. C. Bose Fellow and holds the R. M. Tulpule Chair Professorship in Global Change at the National Centre for Biological Sciences, Bengaluru, India.

Global Advisory Board

Conference Steering Committee

Chairperson	**Dr. M. Kayanan** *Senior Lecturer*
Convener	**Dr. T. Kartheeswaran** *Senior Lecturer*
Editor-in-Chief	**Ms. S. Subaramya** *Senior Lecturer*
Secretary	**Ms. S. Sobana** *Lecturer (Prob.)*
Member	**Ms. R. Yasotha** *Senior Lecturer*
	Mr. N. Edwin Linosh *Senior Lecturer*
	Dr. K. Arjunan *Senior Lecturer*
	Mr. K. Mathanaharan *Lecturer (Prob.)*
	Mr. T. Keerthanaram *Lecturer (Prob.)*
	Mr. S. Gopinath *Instructor*

List of Research Articles – ICAS2025

The names are underlined to indicate presenting authors.

The names are underlined to indicate presenting authors.

List of abstracts – ICAS2025

The names are underlined to indicate presenting authors.

The names are underlined to indicate presenting authors.

The names are underlined to indicate presenting authors.

Doctoral Symposium – ICAS 2025

- **Brain Age Prediction Using Contrastive Learning and Biomechanical Properties**
  Jakob Träuble, University of Cambridge
  Supervisor: Prof. Gabriele Kaminski Schierle & Prof. Carola Bibiane Schoenlieb

- **Landscape of Human Atherosclerotic Plaques**
  Korbinian Träuble, Helmholtz Munich & Technical University of Munich
  Supervisor: Dr. Matthias Heinig

- **Open Innovation and Circular Entrepreneurship: A Case Study of the Sri Lankan Plastic Recycling Industry**
  Sinnathamby Vijayapala, University of Colombo
  Supervisor: Prof. R.Senathiraja

- **Utility of Legal Literacy in Regulating Social Media Users**
  Kalani Irosha Dharmasiri, University of Colombo
  Supervisor: Prof. Tudoer Weerasinghe & Dr. Ediriweera Gunasekara

- **Association Rule-Based Scoring for Event-Centric Semantic Knowledge Graphs: A Deep Learning Framework for Abstractive News Summarization**
  Munasin Vidana Pathirana Thilini Lakshika, Department of Information Systems Engineering, University of Colombo School of Computing
  Supervisor: Prof. HAC Caldera & Prof. TNK De Zoysa

- **Using Aerial Imagery to Help Farmers Make Better Decisions on Nitrogen Requirements in Paddy Farms**
  Colamba Liyanage Ishani Shashikala Fonseka, University of Colombo School of Computing
  Supervisor: Prof. K.P. Hewagamage & Dr. Thilina Halloluwa & Upul Rathnayake

The aforementioned presenters delivered their presentations at the ICAS 2025 Conference organized by the Faculty of Applied Science, University of Vavuniya, Sri Lanka on October 16, 2025.

Research Articles of ICAS2025

|ICAS2025|

Real-Time Sustainability Performance Monitoring System for Educational Institutions

Hasala A.Perera[1], Hirushi D.Thilakarathna[2]

[1]Department of Software Engineering Information Systems, NSBM Green University, Sri Lanka
[2]Department of Computer and Data Science, NSBM Green University, Sri Lanka

Abstract: Achieving institutional sustainability requires real-time data visibility and structured performance evaluations, often unmet in traditional university operations. This paper presents SustainoMeter, a web-based platform developed for NSBM Green University to centralize and streamline sustainability monitoring across operational domains such as canteens, hostels, and the examination department. Conventional manual methods lacked efficiency insights, traceability, and actionable feedback, making sustainable decision-making difficult. SustainoMeter addresses these limitations through real-time data collection, algebraically defined efficiency models, and a normalization-based scoring system that evaluates metrics like resource utilization (electricity, water, LPG), waste, and productivity. Built using the MERN stack (MongoDB, Express.js, React.js, Node.js) and Tailwind CSS, the system delivers responsive, scalable dashboards tailored to user roles. Contributors can input operational data and track division-level performance, while administrators access extended controls including score reviews and PDF-based monthly reports, generated via Puppeteer. Data visualization is powered by Recharts, and system reliability is ensured through comprehensive testing using Jest, Supertest, Vitest, and Cypress. The development process followed a structured SDLC model, encompassing requirement analysis, design, implementation, and testing. SustainoMeter not only improves transparency and institutional accountability but also promotes continuous improvement through feedback loops and ranking systems. Looking forward, its architecture supports extensions such as AI-driven recommendations, making it a robust foundation for smart sustainability ecosystems in education.

Keywords: data visualization, efficiency analytics, mathematical modelling, resource management, sustainability monitoring

Author Note

This research was supported by the National Center for Advanced Computing under Grant No. NCAC-23-AI-004. The authors declare no conflict of interest.

Introduction

In recent decades, most of the corporate and educational sectors have recognized the importance of sustainable growth, not only emphasizing economic growth but also environmental and social responsibilities. The concept of sustainability, often framed under the ”triple bottom line” — economy, environment, and society — has become fundamental for institutions aiming to ensure their long-term success while minimizing negative impacts on the planet (Correia, 2018).

Educational institutions, in particular, play an important role in inspiring sustainable behavior since they shape the attitude and actions of future generations. While this is essential, many universities, even in developing nations, lack effective systems to monitor, report, and enhance their sustainability performance (Abo-Khalil, 2024). In Sri Lanka, NSBM Green University is leading environmental stewardship in higher education, however, there are drawbacks in monitoring sustainability performance indicators in its key areas of operation.

This project aims to design and deploy a web-based platform, named **SustainoMeter**, which allows NSBM Green University to collect sustainability data, generate reports, view analytical trends, and forecast future improvements. The system targets major operational areas such as canteens, hostels, and the examination department, with a focus on different related parameters such as resource consumption and waste management. The aim is to enhance decision-making through the provision of real-time data and detailed analytics, consequently promoting a culture of continuous improvement towards achieving the university’s sustainability goals.

The project follows a well-structured methodology based on the MERN stack (MongoDB, Express.js, React.js, Node.js), following responsive design standards through the application using Tailwind CSS. The system also utilizes mathematical models to analyze the prevailing level of sustainability and suggest profitable future changes, as outlined in global standards like the Global Reporting Initiative (GRI) and International Sustainability Standards Board (ISSB) guidelines (Rusu et al., 2024).

By bridging the gap between isolated sustainability initiatives and a centralized data-driven platform, SustainoMeter aspires to serve as a model for other educational institutions seeking to improve their sustainability performance systematically.

Related Work

Sustainability monitoring and reporting have gained increased attention in higher education, particularly due to institutional goals of reducing environmental impact and improving operational efficiency. Various frameworks, such as the Global Reporting Initiative (GRI) and the International Sustainability Standards Board (ISSB), provide guidelines for sustainability disclosures, but their implementation in real-time decision-making systems remains limited.

Recent research has identified the increasing demand for digital sustainability dashboards and campus smart platforms for performance measurement. STARS (Sustainability Tracking, Assessment & Rating System) and AASHE's Green Metric are global frameworks that have enabled universities to measure their advancement toward sustainability through manual data submissions, rather than relying on automated analysis in real-time. Likewise, (Cavus et al., 2022) mentioned the possibility of Internet of Things (IoT) integration within smart campuses, where sensor networks would enable real-time monitoring of water and energy use to aid data-driven decision-making.

Furthermore, research on decision-support systems (Geng et al., 2022; Rashid & Khan, 2024) suggests the use of big data and artificial intelligence in predictive sustainability management. The solutions increase predictability to forecast inefficiencies and provide opportunities for early intervention in institutional procedures. There remains a deficiency in multi-department incorporation by educational institutions in most available solutions, and they are either energy management or waste management.

SustainoMeter builds upon these foundational works by offering a centralized, interactive platform that aggregates multi-department data and computes normalized efficiency scores using algebraic expressions. Unlike static reporting tools, it delivers real-time visualization, user-specific dashboards, and actionable insights — filling a critical gap in the translation of sustainability frameworks into everyday operations.

System Architecture and Design

To ensure performance, scalability, and responsiveness, SustainoMeter was developed as a full-stack web application using the MERN stack, complemented by Tailwind CSS and data visualization libraries. The architecture is modular and component-based, supporting clean separation of concerns between user interface, server logic, and database operations, aligning with modern green computing and sustainability-focused design principles (Pandey et al., 2024). The front-end was implemented using React.js, styled with Tailwind CSS, and integrated with Recharts for rendering dynamic graphs and trend charts. The interface provides a role-based experience, where contributors input monthly sustainability data and administrators review efficiency trends and system-wide scores. All user interactions are managed via RESTful APIs, and communication between components is asynchronous to ensure smooth performance. The back-end server was built using Node.js with the Express.js framework. It is responsible for handling authentication, data validation, metric calculations, and automated report generation. Sustainability metrics are stored in MongoDB in collections structured per department and calculation results. Each data entry includes metadata such as resource category, user role, and month. To enhance interaction and transparency, the system includes a real-time chat module powered by Socket.IO, and a PDF export feature implemented via Puppeteer for monthly reporting.

Table **(1)**|System Component and Technology Mapping

Component	**Technology**
Front-end	React.js, Tailwind CSS
Back-end	Node.js, Express.js
Database	MongoDB
Data Visualization	Recharts
Report Generation	Puppeteer (PDF Export)
Real-time Features	Socket.IO (Chat)
Testing Tools	Jest, Cypress, Vitest

Metrics and Calculations

SustainoMeter evaluates sustainability performance by applying a structured, quantitative methodology that transforms raw operational data into normalized efficiency scores. This process allows for consistent comparisons across departments and overtime, supporting informed decision-making and transparency in institutional sustainability practices.

Data Categories and Inputs

Each department contributes data monthly under predefined categories tailored to their operational context. These include:

1. **Canteen Division**: Electricity usage (kWh), water usage (L), LPG consumption (kg), food waste (kg), total revenue (LKR).
2. **Hostel Division**: Number of students, electricity usage (kWh), water usage (L), waste output (kg).
3. **Examination Division**: Paper usage (pages), number of exams, printing cost (LKR), admin hours.

Efficiency Calculation Framework

To ensure objective and comparable performance evaluation, SustainoMeter employs a structured scoring framework based on normalized efficiency metrics. The following four-step method quantifies changes in sustainability indicators and converts them into standardized scores for trend analysis and departmental comparison.

Step 1: Delta Calculation

Measure the monthly change in performance compared to the previous month:

$$\Delta = \frac{V_{current} - V_{previous}}{V_{previous}}$$

Step 2: Normalization to a 0—100 Scale

To make scores comparable across departments, raw changes are normalized:

$$N = (1 - \Delta)X100$$

Where,
N : Normalized score
Δ : Change ratio from Step 1

A smaller or negative Δ results in a higher normalized score, reflecting improved sustainability performance.

Step 3: Weighted Scoring Model

Each performance indicator is assigned a predefined weight (w) based on its impact on sustainability goals.

$$WS_{\mathrm{i}} = N_{\mathrm{i}}XW_{\mathrm{i}}$$

Weighted Scoring Model section was revised to clarify that each performance indicator receives a predefined weight reflecting its relative importance to sustainability goals, giving greater influence to parameters with higher environmental or operational impact (e.g., waste and energy metrics). This ensures that the scoring model aligns with institutional sustainability priorities.

Step 4: Final Efficiency Score (E)

The final score (E) for a department is calculated as the weighted average of all normalized parameter scores.

$$E = \frac{\sum WSi}{\sum Wi}$$

This final score, ranging from 0 to 100, enables comparison across departments and overtime, helping administrators identify trends, outliers, and areas for improvement.

Customization by Division

The models above are applied with domain-specific parameter selections:

- Canteens emphasize waste and energy metrics with higher weights for food waste and LPG usage.
- Hostels normalize per-student resource consumption and include shared usage factors.
- Examination metrics focus on paper use, cost, and productivity.

Weights are configured in the backend and can be modified by administrators for future tuning or institutional scaling.

Implementation and Functional Modules

SustainoMeter was implemented as a role-based MERN stack web application with clearly defined contributor and administrator access levels. Contributors are responsible for submitting monthly sustainability data-such as electricity, water, and waste usage-through structured forms tailored to each department. Administrators, on the other hand, have extended privileges including user management, access to all departmental dashboards, and the ability to generate PDF reports.

The front end, developed with React.js and styled using Tailwind CSS, features responsive dashboards powered by Recharts. These dashboards visualize performance scores, monthly trends, and department comparisons using real-time charts and color-coded indicators. The back end, built with Node.js and Express.js, handles RESTful API communication, authentication via JWT, and efficiency calculations based on normalized metrics.

SustainoMeter also includes an automated reporting module using Puppeteer, allowing administrators to download comprehensive monthly PDF summaries. Additionally, a Socket.IO-powered real-time chat module is integrated to enable seamless communication between users and admins. The system was tested using Vitest, Cypress, Jest, and Supertest to ensure performance, security, and reliability across all modules.

Results and Evaluation

The SustainoMeter system was deployed at NSBM Green University and evaluated over a three-month trial period involving the canteen, hostel, and examination divisions. Both technical and operational metrics were collected to assess performance and usability.

System Performance

Monitoring logs showed an average dashboard response time of 1.8 s (SD = 0.4) and 99.3% uptime, confirming stable operation. Load testing with 50 simulated users indicated consistent performance (mean CPU 68%) and low latency. Data accuracy compared to manual records reached 97.8%, with an error rate below 1%, largely from network interruptions.

Efficiency Improvements

Departmental dashboards recorded measurable gains.

- Canteen: 15% rise in water-use efficiency, statistically significant ($p < 0.05$).
- Examination Division: 12% improvement in paper efficiency relative to exam volume.
- Hostel: 8% reduction in monthly electricity consumption.

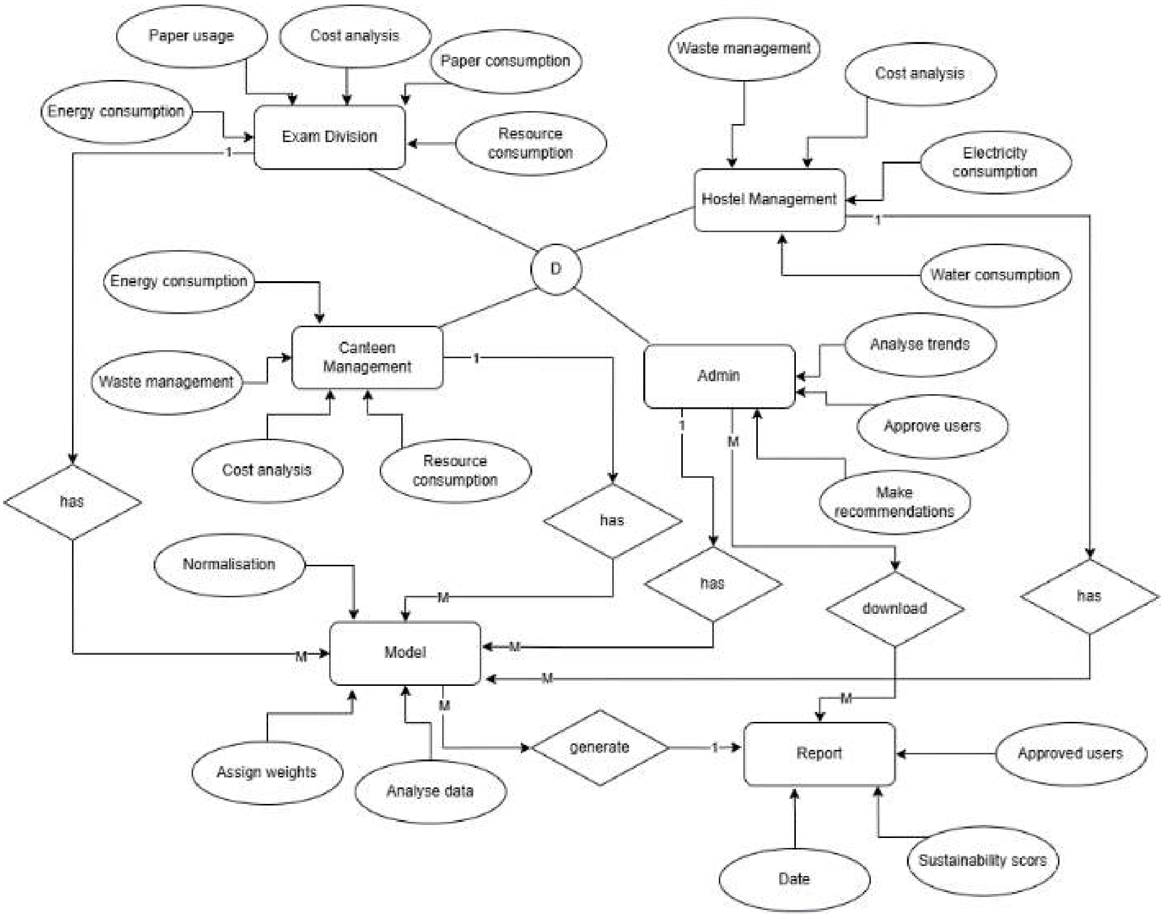

Figure **(1)**|ER Diagram

Usability Evaluation

A post-trial survey of 15 users produced a System Usability Scale (SUS) score of 86/100, indicating high satisfaction. Over 90% agreed that the visual indicators improved understanding of efficiency, and 82% reported data-driven operational changes.

Discussion

The deployment and evaluation of SustainoMeter demonstrated its effectiveness in addressing the operational challenges of sustainability monitoring at NSBM Green University. The system replaced fragmented, manual tracking with a unified, data-driven platform that improved transparency and accountability across departments. Interactive dashboards allowed users to visualize the impact of their activities in real time.

Compared to existing sustainability frameworks such as STARS, GRI, and ISSB, which rely on manual data entry and periodic reporting, SustainoMeter offers a significant advancement in automation and timeliness. Conventional systems provide descriptive and retrospective insights, while SustainoMeter delivers real-time efficiency scoring and visual analytics, enabling proactive, data-driven decisions.

From an administrative perspective, features like auto-generated PDF reports, role-based access, and comparative dashboards simplified reporting and enhanced strategic planning. This shifted sustainability management from a compliance-oriented process to a continuous improvement cycle, where inefficiencies could be identified and addressed promptly.

Overall, SustainoMeter distinguishes itself through its integration of real-time analytics, automation, and operational monitoring. By combining data collection, visualization, and communication within a single platform, it proves that real-time sustainability tracking is feasible and impactful in higher education. Its modular and scalable architecture positions it as a replicable model for universities aiming to strengthen sustainability performance through smart, data-centric solutions.

Conclusion and Future Work

This study presented the design, implementation, and deployment of SustainoMeter, a web-based sustainability monitoring platform tailored for educational institutions. Through its modular architecture, real-time data processing, and user-centric dashboards, the system successfully addressed the limitations of manual reporting and provided a scalable solution for evaluating sustainability performance at NSBM Green University.

The platform's deployment led to measurable improvements in departmental awareness, resource management, and decision-making. Features such as normalized scoring, monthly trend analysis, automated PDF reporting, and real-time chat enabled administrators and contributors to collaboratively manage sustainability metrics with greater transparency and responsiveness.

Looking ahead, several opportunities exist to enhance the system's capabilities. Integration with IoT sensors can automate data collection (e.g., water flow meters, energy monitors), reducing manual entry and improving accuracy which aligns with smart campus infrastructure trends. The system's architecture also supports the incorporation of machine learning algorithms to enable predictive analytics, allowing administrators to anticipate efficiency drops or forecast future trends. Additionally, developing a dedicated mobile app would increase accessibility and user engagement, especially for on-site data entry or live performance tracking.

Overall, SustainoMeter has proven to be a valuable tool for institutional sustainability management and serves as a prototype for broader adoption in similar academic and organizational environments.

References

Abo-Khalil, A. (2024). Sustainability performance monitoring in higher education: Challenges and opportunities [In Press]. *International Journal of Sustainability in Higher Education*.

Cavus, N., Sani, A., & Uzunboylu, H. (2022). Smart campus and iot integration for sustainable universities. *Education and Information Technologies*, *27*, 237–252.

Correia, F. (2018). Sustainability in higher education: Key concepts and institutional pathways. *Journal of Cleaner Production*, *189*, 1–15.

Geng, Y., Sarkis, J., & Ulgiati, S. (2022). Big data analytics in sustainable development and decision making. *Journal of Environmental Management*, *314*, 114917.

Pandey, R., Singh, A., & Kaur, N. (2024). Sustainable web application architecture for green computing: A modular mern stack approach. *International Journal of Green Information Systems*, *12*(3), 145–162.

Rashid, M., & Khan, A. (2024). Ai-driven decision support systems for predictive sustainability management [Advance Online Publication]. *Environmental Modelling and Software*.

Rusu, I., Popescu, A., & Marin, D. (2024). Global reporting initiative and issb guidelines for institutional sustainability. *Sustainability*, *16*(2), 110–125.

|ICAS2025|

Development of Tailored Security Guidelines and Strategies to Improve Web Application Security in Sri Lankan State Universities

Cader Aysha[1], Thavagnanaranjan Lilaniya[1], Ignatius Silvia[1], Ariyadasa Subhash[1], Kumari Sandya[2], Fernando Shantha[3]

[1]Department of Computer Science and Informatics, Uva Wellassa University of Sri Lanka
[2]Department of Science and Technology, Uva Wellassa University of Sri Lanka
[3]Department of Computer Science and Engineering, University of Moratuwa, Sri Lanka

Abstract: As higher education institutions (HEIs) increasingly rely on web-based platforms for academic, administrative, and communication purposes, they face growing exposure to cybersecurity threats that endanger data integrity and institutional operations. In Sri Lankan state universities, this digital shift has revealed significant vulnerabilities, including limited user awareness, weak technical safeguards, and inadequate institutional support. This study examines the current state of web application security within Sri Lankan HEIs through a comprehensive assessment of staff awareness, security practices, organizational support, and technical measures. A mixed-method approach was used, combining document analysis of global and local cybersecurity frameworks, a staff survey, and expert validation to develop a context-specific security guideline. Findings show that although cybersecurity awareness among staff is moderate to high, it does not consistently lead to secure behavior or effective technical implementation. Additionally, gaps in institutional policies, leadership involvement, and resource allocation hinder sustainable security practices. To address these issues, a tailored security guideline was developed and presented as a web-based application, integrating international best practices with local needs. Validated by domain experts, the proposed framework provides practical direction for strengthening web application security, promoting awareness, and building long-term cybersecurity resilience across the higher education sector in Sri Lanka.

Keywords: cybersecurity practices, HEI, security awareness, user education strategies, vulnerabilities, web application, web application security

Introduction

In an era increasingly shaped by digital advancements, the educational sector has emerged as a prominent target for cyberattacks. HEIs manage extensive volumes of sensitive data, making them vulnerable to a wide range of cybersecurity threats. With the growing reliance on web-based platforms for academic delivery, administration, and communication, securing digital infrastructure has become an essential priority. As Yaseen (2022) notes, the education sector faces some of the highest rates of cyber incidents globally, highlighting an urgent need for robust and context-specific cybersecurity measures.

Multiple factors contribute to the vulnerability of HEIs, including inadequate institutional policies, insufficient user awareness, and a lack of tailored technical safeguards. Gavaza and Katsande (2023) underscore the necessity of developing cybersecurity strategies that are not only technically sound but also adapted to the cultural and operational realities of educational institutions. In Sri Lanka, the situation is particularly critical. With the rapid integration of digital systems in state universities, the frequency of reported cyber incidents has increased, exposing systemic weaknesses in current security practices (Don Appuhamilage & Rathnayake, 2023).

This research focuses on enhancing web application security in Sri Lankan state universities by identifying prevalent vulnerabilities and assessing the cybersecurity awareness of university staff. While international frameworks such as Open Web Application Security Project (OWASP), National Institute of Standards and Technology (NIST), and ISO/IEC 27001 offer comprehensive standards, their effectiveness is limited unless contextualized to the institutional and national environments in which they are applied.

The aim of this study was to develop specialized security guidelines and strategies tailored to the specific needs of Sri Lankan HEIs. The research employed a mixed-methods approach, combining document analysis, surveys, and expert validation to ensure the relevance, feasibility, and practicality of the proposed recommendations. The insights derived will not only inform policy and capacity-building within Sri Lankan universities but may also serve as a replicable model for similar contexts in other HEIs.

Related Work

Web application security in HEIs has garnered global attention due to increasing cyber threats and the growing dependency of universities on digital platforms. While numerous strategies and technologies have been proposed, gaps remain in their localized implementation, particularly in resource-constrained environments like Sri Lanka.

Globally, several initiatives have highlighted the importance of combining technical safeguards with institutional governance and user awareness. Cheng and Wang (2022) emphasized a multi-faceted approach, advocating for governance structures, advanced technical measures, and user education campaigns as a resilient strategy for institutional cybersecurity. Their model promoted cyber champion networks and frequent awareness campaigns to strengthen security culture among university stakeholders.

The National Cyber Security Centre's (NCSC) 10-step guidance, as discussed in Nassoura (2022), outlined proactive cybersecurity practices including access control, risk management, and structured training for faculty and administrative staff. This reflects a global trend, as several studies have shown, toward integrating user education into technical defense strategies.

Human factors in cybersecurity have also received increasing scholarly attention. Kautwima et al. (2021) highlighted the effectiveness of phishing awareness training and policy reinforcement in shaping secure user behavior within HEIs.

From a technical standpoint, Daka (2023) and others underscored the role of Web Application Firewalls (WAFs), secure coding practices, encryption, and Intrusion Detection Systems (IDS) in mitigating application-level vulnerabilities such as Cross-Site Scripting (XSS) and SQLi. Studies have demonstrated that secure frameworks and continuous training are crucial to sustaining these protections.

In the Sri Lankan context, the cybersecurity posture of state universities has revealed critical shortcomings. Ellepola et al. (2022) found that many universities followed outdated password policies and lacked comprehensive staff training. Moreover, a significant portion of university staff were unaware of national ICT guidelines issued by the University Grants Commission (UGC), indicating a failure in policy dissemination and awareness.

Don Appuhamilage and Rathnayake (2023) further revealed fragmented IT governance across Sri Lankan HEIs, which hindered the consistent implementation of security protocols. These challenges have been compounded by decentralized administration, leading to inconsistent application of national cybersecurity frameworks.

Nagahawatta et al. (2018) conducted institutional audits and discovered that while basic controls like password management were present, there was an urgent need for more structured and comprehensive awareness programs. Without these, HEIs remained susceptible to phishing attacks and insider threats.

Taken together, these studies have shown a global consensus on the importance of integrating user awareness, technical infrastructure, and policy governance. However, the localized application of these frameworks has remained a challenge in countries like Sri Lanka, where institutional capacity, policy enforcement, and staff training are inconsistent. This research aims to bridge these gaps by developing tailored security guidelines for Sri Lankan state universities, informed by global best practices and local constraints.

Materials and Methods

Data Sources

The population for this study consisted of staff members from Sri Lankan state universities who were engaged with web application infrastructure or policy enforcement. A purposive sampling strategy was employed to select respondents with relevant roles and responsibilities, including IT staff, system administrators, and technical officers. This approach ensured the inclusion of participants who were well-positioned to provide accurate and practical information. To obtain a comprehensive understanding of the cybersecurity environment, a combination of primary and secondary data was used. Secondary data were obtained through document analysis of national and international cybersecurity standards and relevant literature. Primary data were collected through a structured survey designed to measure awareness and practices related to web application security.

Research Instrument Development

The primary research instrument used in this study was a structured questionnaire, developed to collect quantitative data on cybersecurity awareness, practices, organizational support, and infrastructure related to web application security within Sri Lankan state universities. The questionnaire was designed to capture information in several key contexts: participants' knowledge of cybersecurity threats, their adherence to security practices, perceptions of institutional support for cybersecurity, and the availability of security-related infrastructure.

The development process began with a document analysis of existing global and local cybersecurity measures and practices to extract relevant information. These findings were then organized into an Operationalized Table (OT) following the principles of Grounded Theory (GT). The OT guided the construction of Likert-scale items, which formed the basis of the initial draft of the questionnaire.

The survey was distributed to staff members across multiple departments and roles within state universities to ensure comprehensive representation. Participants were categorized by role (academic staff, administrative staff, IT staff) and experience level, allowing the study to examine variations in cybersecurity awareness and practices across different staff categories and levels of responsibility.

A pilot study was conducted using the 10% rule of thumb, selecting a small sample from the target population to assess the instrument's clarity, internal consistency, and relevance. Based on the feedback received, items were revised for clarity, overlapping questions were combined, and the flow of the questionnaire was improved. To evaluate internal consistency, Cronbach's alpha was calculated for each construct, with all values exceeding 0.70, indicating satisfactory reliability. These steps resulted in the finalized version of the questionnaire used for data collection.

Research Design and Workflow

This study followed a mixed-methods research approach, integrating both quantitative and qualitative methods to obtain a comprehensive understanding of the cybersecurity environment in Sri Lankan state universities and to support the development of a tailored guideline for web application security.

The underlying research strategy was based on the principles of GT. This approach allowed for the systematic generation of theory and structure from the collected data and supported the process of developing a conceptual framework from the ground up, based on the observed practices, awareness levels, and institutional policies related to cybersecurity.

The research workflow began with a document analysis of globally and locally available cybersecurity-related documents. The findings from this analysis were used to construct an OT that identified key themes and variables relevant to web application security. This OT guided the development of a structured questionnaire, which was then distributed to staff members at Sri Lankan state universities.

Survey responses were analyzed using descriptive statistical techniques to assess the overall levels of cybersecurity awareness and practices. The analysis revealed recurring vulnerabilities and gaps, which informed the development of a tailored set of cybersecurity guidelines intended to strengthen the security of university web applications. To enhance usability and accessibility, a web-based application was also developed to represent the developed guideline, enabling staff to interact with and refer to the recommendations more effectively.

Expert validation was conducted to assess the relevance, clarity, and practicality of the proposed guidelines. A panel of cybersecurity experts reviewed the guideline and provided structured feedback. This feedback was analyzed using thematic analysis, which focused on evaluating the guideline's ability to address local security challenges, its clarity for both technical and non-technical users, its practicality under real institutional constraints, and suggestions for improvement.

This structured approach ensured that the final outputs—both the analysis and the guideline—were grounded in empirical data and adapted to the Sri Lankan university context, with expert validation confirming their relevance, clarity, and practicality.

Results

This part of the study highlighted the insights gained from the survey conducted to assess key aspects of cybersecurity within Sri Lankan state universities. The analysis focused on four main constructs: security awareness, security practices, organizational support, and security measures. Descriptive statistics provided an overview of how respondents rated each area, while correlation analysis explored the relationships between these variables. The results helped identify strengths and gaps in current cybersecurity behaviors and institutional support mechanisms.

Analysis of Awareness, Practices & Relationships

Table **(1)**| Descriptive Statistics of Key Constructs

Variables	M	SD	Min - Max
Security Awareness	3.74	0.57	2.52 - 4.62
Security Practices	2.94	0.78	1.76–4.12
Organizational Support	2.67	0.96	1.00–4.00
Security Measures	2.87	0.55	1.82–4.00

As shown in Table 1, respondents demonstrated a moderately high level of security awareness (M = 3.74, SD = 0.57), indicating familiarity with general cybersecurity risks. However, this awareness was not matched by equivalent levels of action or support. Security practices, such as routine data backup or strong password use, scored a moderate average (M = 2.94, SD = 0.78), with considerable variation among participants. Organizational support received the lowest rating (M = 2.67, SD = 0.96), reflecting a perceived lack of formal training, policy clarity, and administrative involvement in promoting secure behavior. The implementation of security measures, such as multi-factor authentication and firewall protection, also averaged moderately (M = 2.87, SD = 0.55), suggesting inconsistency across institutions.

Table **(2)**| Pearson Correlation Matrix of Key Variables

	Awareness	Practices	Organizational Support	Security Practices
Awareness	1	.194	.352	.095
Practices	.194	1	**.608**	**.766**
Organizational Support	.352	**.608**	1	**.667**
Security Practices	.095	**.766**	**.667**	1

Correlation analysis was conducted to explore the relationships among the four constructs. As shown in Table 2, there was a strong, statistically significant correlation between security practices and the implementation of security measures ($\rho = 0.766$, $p < 0.01$). Similarly, organizational support was strongly correlated with both security practices ($\rho = 0.608$, $p < 0.01$) and security measures ($\rho = 0.667$, $p < 0.01$). These results suggest that institutions with better support structures tend to exhibit stronger individual security behaviors and more robust technical implementations.

Interestingly, security awareness did not show any significant correlation with the other variables ($p > 0.05$), implying that awareness alone does not necessarily lead to secure behavior or improved institutional measures. This highlights the importance of translating knowledge into practice through well-supported, structured programs.

Identified Vulnerabilities and Contributing Factors

- **SQLi:** Associated with low organizational support (M ≈ 2.44–2.83) and weak vulnerability detection (M ≈ 2.56).
- **XSS:** Moderate threat awareness (M ≈ 3.6), but limited security testing and low network tool usage (M ≈ 2.5).
- **Cross site request forgery (CSRF):** Lowest awareness among threats (M ≈ 3.44), infrequent training (M = 2.39), and weak Multi Factor Authentication use.
- **Distributed Denial-of-Service (DDoS):** Good awareness (M ≈ 4.05), but poor implementation of network defenses (M ≈ 2.5).
- **Broken Authentication:** Low encryption confidence (M = 2.17) and weak patching/testing practices.
- **Insecure Configuration:** Low scores in patching, auditing, and infrastructure maintenance (M ≈ 1.94–2.6).
- **Human-Centric Vulnerabilities:** High human error concern (M = 3.5), low training frequency, and moderate phishing awareness (M ≈ 3.0–3.8).
- **Third-Party Risks:** Moderate concern (M = 3.22), but inconsistent risk management (M ≈ 3.06).

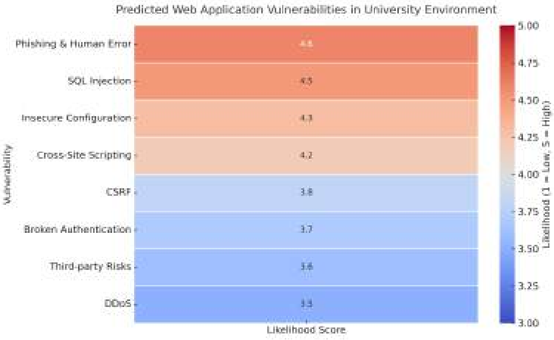

Figure **(1)**| Predicted Web Application Vulnerabilities

The figure 1 shows that phishing and human error, along with SQLi, are the most likely vulnerabilities affecting university web applications, emphasizing the importance of enhancing user awareness and implementing secure coding practices. Moderate risks such as insecure configurations and cross-site scripting indicate weaknesses in system maintenance and validation controls. Meanwhile, DDoS attacks and third-party risks are considered less likely but still warrant attention through strengthened infrastructure resilience and effective vendor management.

Discussion

The results of this study reveal a critical gap between cybersecurity awareness and secure behavior among staff in Sri Lankan state universities. Although participants demonstrated a moderate understanding of web application security risks, this awareness did not consistently translate into proactive or compliant practices. This discrepancy can be attributed to the absence of formalized institutional mechanisms, such as regular training reinforcement, policy enforcement, and accountability structures, which are essential for converting knowledge into consistent security-conscious behavior.

One of the most significant findings is the strong correlation between organizational support and the implementation of both security practices and technical measures. This suggests that institutions that actively engage in policy dissemination, provide regular training, and allocate sufficient resources create an environment where staff feel empowered and obliged to follow secure practices. These findings align with global literature emphasizing that cybersecurity must be integrated into institutional governance rather than treated solely as a technical concern, highlighting the importance of leadership commitment and culture in shaping secure behavior.

The technical weaknesses identified—such as weak authentication protocols, insecure configurations, and inadequate safeguards against SQLi and denial-of-service (DoS) attacks—mirror commonly reported global vulnerabilities. Their persistence in higher education settings, despite increasing digital reliance, indicates potential gaps in institutional oversight, lack of continuous monitoring, and insufficient technical capacity for proactive risk mitigation. Addressing these weaknesses requires a combination of internal audits, secure development practices, and infrastructure hardening to reduce exploitability and protect sensitive university data.

To address these multi-layered challenges, a tailored security guideline was developed and presented as a web-based application (link: https://safeweb.trendsprint.net). Grounded in global best practices but customized for the local operational context, this guideline has been validated by experts and offers a structured approach to improving institutional security posture. It focuses on four critical areas: awareness, practices, organizational support, and security measures.

Despite these contributions, the study has limitations. The limited response rate may have influenced the representativeness of the findings, and the survey format may have restricted the depth of participant responses, particularly in capturing institutional and cultural nuances. These limitations suggest that while the results offer important insights, further studies with broader participation and complementary qualitative approaches would help validate and expand the findings. Additionally, the focus on web applications means that broader cybersecurity domains—such as endpoint security, network infrastructure, and physical access controls—remain to be explored in future research.

Future research should expand the study to include all state and private universities in Sri Lanka to ensure broader applicability and validation of the findings. In addition, surveys should encompass students and administrative staff, as they also play a vital role in maintaining institutional cybersecurity. Longitudinal studies are recommended to evaluate the long-term impact and improvement resulting from the adoption of the proposed guideline. Furthermore, pilot implementations in real university environments would provide valuable insights into the guideline's practical effectiveness. Finally, the guideline should be regularly reviewed and updated to address emerging cyber threats and evolving technologies, ensuring its continued relevance and sustainability.

Conclusion

This study contributes to the understanding of web application security in Sri Lankan state universities by revealing the disconnect between staff awareness and actionable security practices. It highlights the essential role of organizational support ininfluencing secure behavior and emphasizes the urgency of addressing both technical vulnerabilities and procedural weaknesses within institutional settings.

Informed by both global security benchmarks and local realities, a practical and adaptable security guideline was developed to serve the unique needs of Sri Lankan HEIs. This guideline not only bridges existing gaps but also offers a replicable model for institutions operating under similar constraints.

The study's findings carry significant implications for policymakers, university administrators, and IT professionals seeking to strengthen cybersecurity in higher education. By embedding security into organizational processes and fostering a culture of continuous learning and accountability, universities can improve their resilience against evolving digital threats.

Looking ahead, further research is needed to test the longitudinal effectiveness of the proposed guideline, explore broader institutional cybersecurity frameworks, and identify cultural and systemic barriers that may influence security adoption. Ultimately, building cybersecurity maturity within HEIs demands an integrated approach—one that balances technical capacity with institutional leadership, user awareness, and strategic policy alignment.

References

Cheng, E. C., & Wang, T. (2022). Institutional strategies for cybersecurity in higher education institutions. *Information*, *13*(4), 192.

Daka, M. (2023). *Strengthening web application security through technical measures.* [Doctoral dissertation, The University of Zambia.].

Don Appuhamilage, S. P., & Rathnayake, R. M. D. U. (2023). Gap analysis of information security management systems in sri lankan higher education institutes.

Ellepola, C., Ragel, R. G., Sandirigama, M., & Kumari, K. (2022). The effectiveness of policies on ict resources and passwords in sri lankan universities. *2022 2nd International Conference on Advanced Research in Computing (ICARC)*, 290–295.

Gavaza, B., & Katsande, C. (2023). A human-centric cybersecurity framework for ensuring cybersecurity readiness in universities. In *Effective cybersecurity operations for enterprise-wide systems* (pp. 242–276). IGI Global.

Kautwima, P., Hashiyana, V., & Haiduwa, T. (2021). Information security mechanisms and ict policy in practice: A case of the university of namibia. *International Journal of Wireless Communications and Mobile Computing*, *9*(2), 7.

Nagahawatta, R., Warren, M., & Yeoh, W. (2018). A study of cybersecurity awareness in sri lanka. *17th Australian Cyber Warfare Conference (CWAR), October 10-11th, 2018, Melbourne, Victoria, Australia.*, 45.

Nassoura, A. B. (2022). Cybersecurity technologies and practices in higher education institutions: A systematic review. *Webology*, *19*(3).

Yaseen, K. A. Y. (2022). Importance of cybersecurity in the higher education sector 2022. *Asian Journal of Computer Science and Technology*, *11*(2), 20–24.

Appendices

Appendix A

Developed security guideline - https://tinyurl.com/bdfwxsmb

AI Based Student Absenteeism Prediction with Personalized Recommendations: A Study in Batticaloa Manmunai West Zone

S.Mathilojana[1], M.Mithushika[2], M.Shandru[1]

[1]Department of Education and Childcare, Eastern University, Sri Lanka.
[2]Department of Physical Science, University of Vavuniya, Sri Lanka.

Abstract: Student absenteeism is a growing issue, especially in rural and under-resourced areas like the Manmunai West Educational Zone in Batticaloa, Sri Lanka. Poor attendance has a strong impact on students' academic performance and long-term success. Factors such as family financial issues, school conditions, and personal health or motivation problems contribute to this challenge. The research identifies the most important factors influencing absenteeism. As well as this study aims to develop an AI-based system to predict absenteeism risk among secondary school students and provide personalized recommendations to help reduce that risk. A structured 29-question Likert-scale questionnaire was administered to 116 students, covering family, school, and student-related issues. Data were analyzed using SPSS and Python. Students were labeled into High, Medium, or Low absenteeism risk levels based on their average scores. A Random Forest classifier was trained to predict the risk level. LIME (Local Interpretable Model-agnostic Explanations) was used to explain the model's decisions. The model's accuracy was validated using Support Vector Machine (SVM) and 5-fold cross-validation. A Streamlit-based web application was also developed for practical use. The Random Forest model achieved 96% accuracy in classifying absenteeism risk. Important influencing factors included low family income, parental support, school safety, and student health issues. The findings from SPSS mean analysis were consistent with Python model outputs. LIME effectively explained the predictions, helping educators understand the root causes of absenteeism. The proposed AI-based model is accurate, interpretable, and practical for identifying students at risk of absenteeism. The web-based tool allows schools and educational offices to take early action with personalized interventions. This system has the potential to improve attendance and learning outcomes in underprivileged regions like Batticaloa's Manmunai West Zone. Future research can improve accuracy further by expanding the dataset and including real-time attendance data.

Keywords: LIME, machine learning, personalized recommendation, random forest, student absenteeism

Introduction

Student absenteeism is one of the major obstacles affecting academic achievement and long-term learning outcomes among secondary school students. Consistent attendance plays a vital role in building knowledge, social development, and classroom engagement (Kearney & Graczyk, 2014; Reid, 2005). However, in many rural and under-resourced areas, absenteeism continues to rise, threatening the educational progress of thousands of students (Ahmad et al., 2020). In Sri Lanka, the Manmunai West Educational Zone in Batticaloa District has been identified as one of the regions with a high rate of student absenteeism based on regional school records. The issue is particularly complex in this area due to multiple contributing factors. Family-related issues such as poverty, parental illness, alcoholism, and unstable home environments are frequently cited in literature as primary reasons for absenteeism (Bowers et al., 2013; Kearney & Graczyk, 2014). Additionally, school-related problems like poor infrastructure, unsafe environments, and long distances from home to school are significant barriers to regular attendance (Mushtaq & Khan, 2021). On the other hand, student-specific causes such as physical and mental health conditions, lack of motivation, and early involvement in income-generating activities also play a major role (Dekker et al., 2009; Reid, 2005).

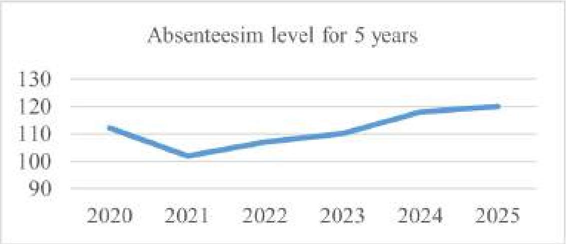

Figure **(1)**|Absenteeism level in Manmunai West zone

Students in Manmunai West face complex socio-economic and environmental barriers that lead to frequent absenteeism. Schools in this zone report a 20–25% lower attendance rate than national averages. As Figure (1) suggests, these students consistently show their improper attendance and do not perform well in exams. Yet, traditional intervention methods lack personalization and real-time decision support.

Objective

To address this, there is a growing need to explore data-driven methods that can identify students at risk and provide early intervention (Adekitan & Salau, 2019). The main objective of this research is to reduce student absenteeism by identifying at-risk students using an AI-based predictive model. This research also aims to find the key factors influencing student attendance, apply machine learning methods to predict absenteeism risk levels, and recommend targeted interventions tailored to each student's situation.

Research Questions

This study seeks to address three primary research questions:

1. What are the key factors influencing student absenteeism in the Manmunai West region?
2. Can artificial intelligence models accurately predict absenteeism risk using student response data?
3. Based on the predicted risk levels, what targeted interventions can be recommended to effectively reduce absenteeism?

To find a solution for this problem developed an AI-based system was developed using a Random Forest Classifier, trained on structured responses by secondary school students of 8 schools to a 29-question Likert-scale questionnaire. The data were preprocessed through imputation of missing values and normalization, and students were categorized into High, Medium, or Low risk levels based on their response averages. In addition, this research uses Local Interpretable Model-agnostic Explanations (LIME) to explain the model's predictions, helping educators understand the most important risk factors for each student (Ribeiro et al., 2016). This ensures transparency and supports the creation of personalized recommendations that can be implemented in schools. By introducing this AI-driven system, school administrators and teachers in marginalized communities like Manmunai West will be empowered to identify at-risk students early and take preventive measures. This approach can ultimately improve student retention, academic outcomes, and reduce long-term dropout rates (Ahmad et al., 2020; Lundberg & Lee, 2017).

Hypothesis

The null hypothesis (H_0) states that no significant patterns exist within these factors to forecast absenteeism risk. Conversely, the alternative hypothesis (H_1) proposes that meaningful and significant patterns can be detected in the student data, which machine learning models can leverage to accurately predict absenteeism risk.

Related Work

Student absenteeism has been extensively studied due to its strong association with academic underachievement and increased dropout rates. Early research primarily used qualitative methods, such as interviews and case studies, to explore socio-economic, familial, and psychological causes of absenteeism (Kearney & Graczyk, 2014; Reid, 2005). While these approaches helped identify key factors, their lack of scalability and predictive capabilities limited practical application in larger educational systems.

With advances in educational data mining, machine learning techniques gained prominence in predicting student absenteeism and dropout risk. Dekker et al. (2009) pioneered the use of decision trees and Naïve Bayes classifiers on academic performance data to forecast student dropouts (Dekker et al., 2009). Bowers et al. (2013) extended this work by incorporating logistic regression and classification trees to analyze attendance alongside performance metrics (Bowers et al., 2013). However, these models often fell short in rural or under-resourced settings where socio-economic and psychological factors are more complex and less structured.

Recent studies have shifted towards ensemble learning methods, such as Random Forests and Gradient Boosting, which better handle mixed data types and missing values, achieving higher prediction accuracy (Adekitan & Salau, 2019; Mushtaq & Khan, 2021). Ahmad et al. (2020) demonstrated that Random Forest models using attendance logs, behavioral data, and parental involvement metrics could significantly improve classification precision in absenteeism risk detection (Ahmad et al., 2020).

Simultaneously, the rise of explainable AI (XAI) techniques like SHAP (Lundberg & Lee, 2017) and LIME (Ribeiro et al., 2016) has enhanced the transparency and usability of predictive models in educational domains. These methods provide insights into feature contributions for individual predictions, allowing educators to understand and address the root causes of absenteeism.

Despite these advancements, existing systems rarely integrate predictive modeling with real-time decision support and personalized intervention strategies in a user-friendly platform suitable for school deployment. Most frameworks are either computationally intensive or lack actionable feedback tailored to students.

This study contributes to the field by developing an interpretable Random Forest-based absenteeism prediction model combined with LIME explanations, deployed through a lightweight Streamlit web application. This integrated pipeline supports timely, personalized recommendations for educators in rural settings like the Batticaloa Manmunai West zone.

Materials and Methods

Data Collection and Preprocessing

Data were collected through a structured 29-item Likert-scale questionnaire administered to 116 secondary school students across 8 schools in the Batticaloa Manmunai West zone. The questionnaire covered three key domains: family-related, school-related, and student-related factors. Responses ranged from 1 (Strongly Disagree) to 5 (Strongly Agree).

Table 1 outlines the schools and no of students used as samples

School Name	Type	Number of Students
A	II	17
B	II	14
C	II	13
D	II	13
E	II	12
F	II	12
G	II	19
H	II	16

Table **(1)**|Selected students to collect data from Sample schools and their types – Education planning unit, Batticaloa Manmunai West Educational office¿ 2024)

Data preprocessing included:

- Imputation of missing values using mean substitution
- Feature scaling via normalization to standardize data ranges
- Manual labeling of absenteeism risk levels (Low, Medium, High) based on average response scores per student

Quality assurance steps included imputation of missing values, normalization of features, and manual review of questionnaire responses for consistency. Model robustness was ensured through 5-fold cross-validation and independent validation using an SVM classifier.

Each question in the Likert-scale questionnaire was designed to reflect one of three key domains:

- Questions starting with "A" correspond to family related factors (e.g., A.1.1)
- Questions starting with "B" represent school related factors
- Questions starting with "C" address student related factors

Domain-specific averages were calculated for each student: `average_family`, `average_school`, and `average_student`. These were then used to compute a combined overall average score. Absenteeism risk levels were assigned using the following rule:

- High Risk: overall average ≥ 4.0
- Medium Risk: overall average between 3.0 and 3.9
- Low Risk: overall average < 3.0

Model Development

A Random Forest Classifier was used to predict absenteeism risk levels based on questionnaire responses. The dataset was split into training and testing subsets with an 80:20 ratio, maintaining class distribution through stratified sampling. The model was implemented using scikit-learn and trained with hyperparameter tuning to optimize performance and prevent overfitting.

Table 2 outlines the parameter and values used in model development

Parameter	Value
Number of Trees	100
Maximum Tree Depth	10
Minimum Samples per Leaf	2
Criterion	Gini Index
Train-Test Split	80% Training, 20% Testing

Table **(2)**|Parameter used in model building

Model Interpretability

To enhance transparency and understand individual predictions, LIME (Local Interpretable Model-agnostic Explanations) was applied. LIME explains the model's decisions by approximating it locally with an interpretable model, highlighting key factors influencing absenteeism risk classification for each student. Additionally, SPSS was used to analyze the data and identify the most important factors affecting student attendance.

Validation

To ensure robustness, the model was validated using Support Vector Machines (SVM) as a secondary algorithm for comparison, alongside 5-fold cross-validation to assess stability across different data splits. Results from both validation methods confirmed the consistently high accuracy of the Random Forest model.

Decision Support System

A web-based decision support system was developed using Streamlit, allowing users to:

- Input individual student questionnaire responses for predictions
- Predict the absenteeism risk level
- Receive personalized suggestions (e.g., home visits, scholarships, counseling)

Results

The Random Forest Classifier demonstrated high accuracy in predicting absenteeism risk levels (Low, Medium, High) based on questionnaire responses from 116 students. Precision, recall, F1-score, and overall accuracy on the test dataset were used to evaluate the performance of the model.

Table 3 summarizes the classification performance across each risk category.

Risk Level	Precision	Recall	F1-score
High	1.00	1.00	1.00
Medium	0.86	1.00	0.92
Low	1.00	0.90	0.95
Overall Accuracy: 96%			

Table **(3)**|Summary of classification performance

The model showed robust performance, especially in identifying students at high risk of absenteeism, enabling timely intervention. Accuracy was computed as the ratio of correctly classified instances to the total test samples, supported by Precision, Recall, and F1-score. While similar studies in student absenteeism prediction report accuracy levels between 85–90%, our Random Forest model achieved 96%, demonstrating improved performance.

Analysis of feature importance revealed the top factors influencing absenteeism risk. Key predictors included family income sufficiency, parental attitude towards education, student health issues, and school facility adequacy. Figure 2 presents a bar chart of the top 10 features ranked by their relative importance in the Random Forest model.

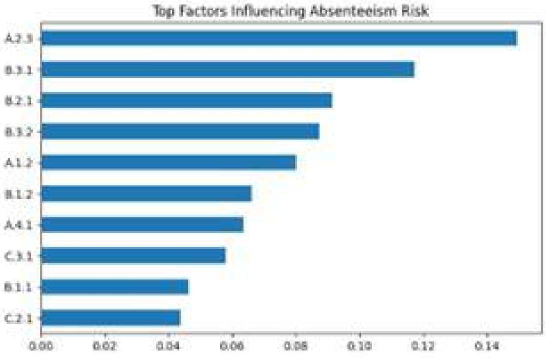

Figure **(2)**|Top 10 features ranked based on their importance

Feature Analysis and Model Interpretability

The top five features contributing to the prediction were: A.2.3 – students going for seasonal cultivations with their parents, B.3.1 – school being far from home, B.2.1 – difficulty in education causing absenteeism, B.3.2 – lack of public transport to school, and A.1.2 – parents failing to fulfill educational needs. These variables represent a mix of family-related and school-related challenges. The strong influence of A.2.3 and A.1.2 indicates that family financial instability and parental limitations directly affect attendance. Meanwhile, B.3.1 and B.3.2 highlight infrastructural barriers such as distance and transportation issues that make daily school attendance difficult. The educational difficulty factor (B.2.1) emphasizes the role of academic struggle in disengagement and absenteeism.

To enhance the interpretability of the model's predictions, LIME (Local Interpretable Model-agnostic Explanations) was applied. LIME explains how individual features contribute to a specific prediction by approximating the model locally with a simple, interpretable model such as a linear regressor. This allows educators and decision-makers to understand why a particular student was classified as High, Medium, or Low risk, rather than simply accepting the prediction as a black-box output.

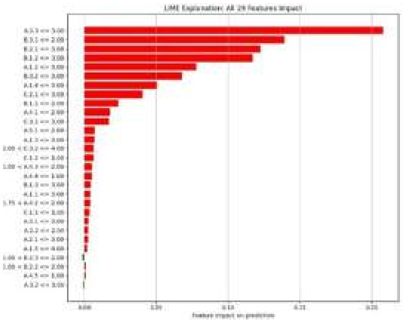

Figure **(3)**|LIME explaining feature importance

Figure 3 presents the LIME explanation for a test sample, where features are ranked based on their contribution to the prediction. Red bars represent factors that increase the probability of high absenteeism risk, while green bars represent those that reduce it. This kind of localized interpretation helps personalize the recommended interventions for each student.

To better understand the relationship between students' average response scores and their assigned absenteeism risk levels, a swarm plot was generated. Swarm plots display individual data points while preventing overlap, making them ideal for visualizing the distribution of scores across categorical groups.

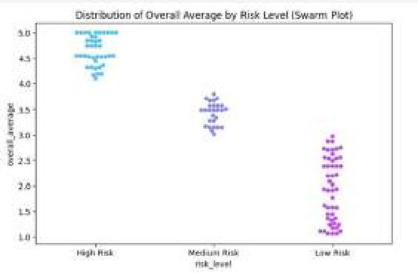

Figure **(4)**|Distribution of average values

Figure 4 visually illustrates how the `overall_average` scores are distributed across the three risk levels. High-risk students consistently had lower overall scores, while low-risk students clustered toward higher scores. This validates the effectiveness of the manual labeling criteria used in generating the risk categories.

To understand the relationships and potential redundancies among questionnaire items, a correlation heatmap was generated. This visualization helps identify which questions are strongly related, whether certain features are overlapping, and whether the questionnaire structure reliably captures distinct domains. Such insight is particularly useful for validating the questionnaire design and guiding future feature selection or dimensionality reduction.

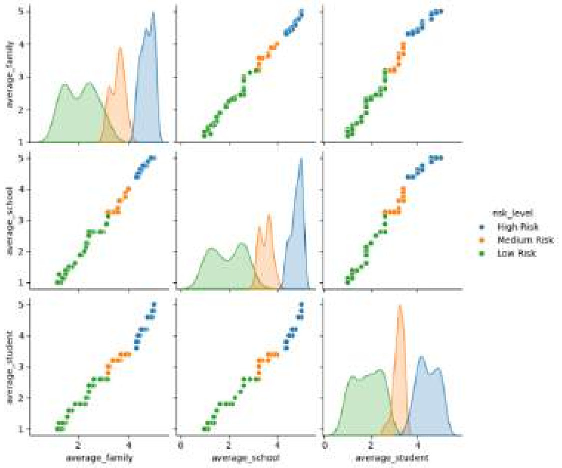

Figure **(5)**|Pairwise plot of the three domain averages

The pairwise plot shown in Figure 5 visualizes how the three domain averages (`family`, `school`, `student`) relate to one another and how those relationships differ across the three risk groups. On the diagonal, the KDE plots show that Low-risk students (green) concentrate at the lower end of each average, Medium-risk students (orange) cluster in the middle, and High-risk students (blue) concentrate at the higher end. In this study, higher Likert averages indicate a stronger presence of risk factors. Finally, because the three averages are strongly correlated, there is some redundancy among these features.

Figure **??** illustrates the correlation heatmap of all Likert-scale questionnaire items, grouped by domain (family, school, and student-related factors). The color intensity represents the strength and direction of pairwise Pearson correlations. As shown, stronger correlations are observed within each domain, especially among family-related (A-prefixed) questions, indicating internal consistency. Minimal cross-domain correlation suggests that each domain captures distinct aspects of absenteeism risk, supporting the validity of the questionnaire structure.

To validate the effectiveness of the proposed Random Forest model, two evaluation strategies were employed. First, 5-fold cross-validation was conducted to ensure the model's generalization across unseen data, yielding an average accuracy of 96%. Second, a Support Vector Machine (SVM) with an RBF kernel was trained on the same dataset for performance comparison. The SVM model achieved 96% accuracy, which was equal to the Random Forest. Figure 7 shows a bar chart that was plotted to visually compare the accuracy and F1-scores of both models, confirming that the Random Forest outperformed the SVM in both classification precision and overall consistency. This strengthens the model's validity as a reliable tool for predicting student absenteeism risk.

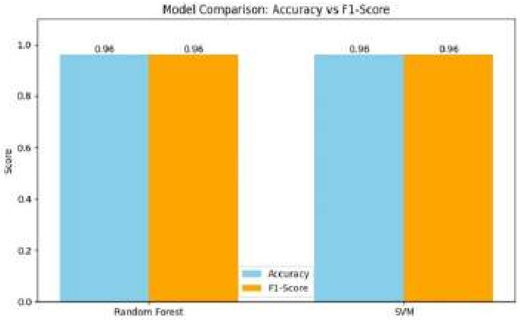

Figure **(7)**|Comparison of RF and SVM to same dataset

The Random Forest classifier served as the primary predictive model. To enhance interpretability, LIME was applied to explain individual predictions of the Random Forest model. For validation and performance benchmarking, an SVM model with an RBF kernel was implemented and compared with the Random Forest results.

Discussion

The results of this study demonstrate the effectiveness of using a Random Forest-based AI model for early prediction of student absenteeism risk in the Batticaloa Manmunai West zone. Unlike black-box approaches, the integration of LIME for interpretability provides transparent insights into the key factors influencing absenteeism, empowering educators with actionable knowledge rather than just predictions.

Among the High-risk group, the most dominant factors were going for seasonal cultivations with parents, low family income, and limited parental support. For this group, the system recommended interventions such as health counseling and financial assistance. This highlights how the model not only predicts absenteeism risk but also prioritizes actionable strategies for the most vulnerable students.

A major strength of the proposed system lies in its ability to combine accurate risk classification with personalized recommendations, delivered through a light weight and user-friendly web-based decision support tool. This makes the approach practical for real-world deployment in under-resourced school settings, where technical expertise and computational resources may be limited. The feature importance analysis and LIME explanations consistently highlighted socio economic and health-related factors such as family income sufficiency and student health issues as dominant contributors to absenteeism risk. This aligns with existing qualitative research and reinforces the validity of the AI-driven insights.

However, some limitations were noted. The relatively small dataset (116 students) constrains model generalizability, and manual risk labeling based on average scores may introduce subjectivity. Additionally, while Random Forest models handle tabular questionnaire data well, they might not capture more complex temporal or behavioral patterns underlying absenteeism. In addition to the absenteeism risk levels, which were manually assigned using average questionnaire scores, this approach may introduce bias due to subjectivity in threshold selection. In future work, this limitation can be addressed by adopting unsupervised clustering methods such as K-means, using percentile-based cutoffs, or validating thresholds with educational experts.

Future work should focus on expanding the dataset size and diversity, integrating longitudinal attendance records, and exploring advanced modeling techniques such as gradient boosting or deep learning architectures with temporal data. To enhance generalizability, future research will evaluate the model using larger public absenteeism datasets such as the UCI Absenteeism-at-work dataset, allowing benchmarking against international studies. Enhancing the decision support system to include adaptive feedback loops where intervention outcomes feed back into model retraining could further improve personalization and effectiveness.

In conclusion, this study offers a promising AI driven framework that balances predictive accuracy, interpretability, and practical deployment considerations, providing a valuable tool for early absenteeism intervention in marginalized educational contexts.

Conclusion

This study presented an AI-based framework for early prediction of student absenteeism risk in the Batticaloa Manmunai West zone, leveraging a Random Forest classifier trained on structured questionnaire data. By integrating LIME for interpretability, the system provides transparent insights into the key factors driving absenteeism, enabling educators to understand and address individual student needs effectively. The accompanying Streamlit-based decision support tool offers a practical interface for school administrators and teachers to obtain risk predictions and personalized intervention recommendations, making the approach suitable for deployment in resource-constrained educational environments.

The system generates personalized recommendations such as parental counseling sessions, financial support (scholarships), regular home visits by teachers, health checkups, and peer mentoring. These targeted interventions aim to directly address the root causes of absenteeism identified for each student.

While the model demonstrated high accuracy and useful explanatory power, limitations such as a relatively small dataset and reliance on self-reported survey data highlight areas for future improvement. Expanding the dataset, incorporating real-time attendance and behavioral data, and exploring advanced modeling techniques will likely enhance predictive accuracy and generalizability.

Overall, this research underscores the potential of combining interpretable AI with practical decision support to proactively combat student absenteeism, contributing to improved educational outcomes in marginalized communities.

References

Adekitan, A. I., & Salau, O. P. (2019). Predicting student academic performance using ensemble machine learning techniques. *Education and Information Technologies*, *24*(1), 1427–1448.

Ahmad, M., Malik, M. A., & Malik, A. (2020). Random forest-based student absenteeism prediction using attendance and behavioral data. *International Journal of Educational Technology in Higher Education*, *17*(1), 45.

Bowers, A., Sprott, R., & Taff, S. A. (2013). Do we know who will drop out? predicting school dropout in students with behavioral and attendance data. *Journal of Educational Data Mining*, *5*(1), 1–23.

Dekker, G. W., Pechenizkiy, M., & Vleeshouwers, J. M. (2009). Predicting students drop out: A case study. *International Conference on Educational Data Mining*, 41–50.

Kearney, C. A., & Graczyk, P. A. (2014). A response-to-intervention model to promote school attendance and decrease school absenteeism. *Child & Youth Care Forum*, *43*(1), 1–25.

Lundberg, S. M., & Lee, S.-I. (2017). A unified approach to interpreting model predictions. *Advances in Neural Information Processing Systems*, *30*, 4765–4774.

Mushtaq, R., & Khan, S. N. (2021). Application of gradient boosting machines in predicting student absenteeism. *Journal of Educational Computing Research*, *59*(2), 296–312.

Reid, K. (2005). The causes, views and traits of school absenteeism and truancy: An analytical review. *Research in Education*, *74*(1), 59–82.

Ribeiro, M. T., Singh, S., & Guestrin, C. (2016). “why should i trust you?” explaining the predictions of any classifier. *Proceedings of the 22nd ACM SIGKDD International Conference on Knowledge Discovery and Data Mining*, 1135–1144.

|ICAS2025|

A Systematic Review of Hallucination Detection in Black-Box Large Language Models: Techniques and Constraints

Shanuka Dissanayake[1], Dilani Wickramaarachchi[1]

[1]Department of Industrial Management, Faculty of Science, University of Kelaniya, Sri Lanka

Abstract: Large Language Models (LLMs) have achieved remarkable capabilities across diverse applications, yet their tendency to generate hallucinations-fluent but factually incorrect outputs-poses significant challenges for deployment in critical domains. While numerous detection strategies exist, practical constraints often limit access to model internals, necessitating black-box approaches that operate solely on inputs and outputs. This systematic literature review examines hallucination detection methods specifically designed for black-box LLMs under zero-resource constraints, where no additional training data or model modifications are permitted. Following Kitchenham's evidence-based systematic review protocol, we analyzed 15 peer-reviewed studies published between 2020-2025 that satisfy rigorous inclusion criteria. Our analysis reveals six primary detection categories: self-consistency verification, uncertainty quantification, fact-level verification, metamorphic testing, contradiction detection, and multi-agent validation. Performance analysis shows methods achieving F1 scores up to 0.82, though significant trade-offs exist between accuracy, computational cost, and external dependencies. Key findings indicate that hybrid approaches combining multiple detection signals outperform single-method strategies, while zero-resource techniques demonstrate competitive performance without external knowledge requirements. However, substantial challenges remain in cross-domain generalization, computational scalability, and standardized evaluation. This review provides a structured taxonomy for practitioners and identifies critical research gaps including multimodal robustness, cross-lingual effectiveness, and interpretability requirements for high-stakes applications.

Keywords: black-box methods, hallucination detection, large language models, systematic literature review, zero-resource learning

Introduction

Large Language Models have demonstrated unprecedented capabilities in text generation, question answering, and knowledge-intensive reasoning tasks. However, their propensity to generate hallucinations outputs that appear plausible but contain factual inaccuracies or fabricated information—presents a fundamental challenge for reliable deployment (Huang et al., 2024). This issue becomes particularly critical in sensitive domains such as healthcare, legal analysis, and scientific communication, where factual accuracy is paramount.

The challenge of hallucination detection has prompted extensive research into various detection strategies.These approaches broadly categorize into white-box methods, which require access to model weights, attention mechanisms, or gradient information, and black-box methods, which operate exclusively on model inputs and outputs. While white-box approaches can leverage internal model states for more sophisticated detection mechanisms, they are increasingly impractical as LLMs transition to Application Programming Interface (API)-based services provided by companies such as OpenAI, Anthropic, and Google.

This shift toward black-box access has intensified interest in detection methods that function under constrained conditions. Zero resource approaches, requiring no additional training data or model fine-tuning, are particularly valuable given modern LLM constraints. Such methods rely on prompt engineering, consistency analysis, or lightweight external validation.

Despite growing research activity, no comprehensive systematic review has examined hallucination detection methods compatible with black-box, zero resource constraints. Existing surveys focus broadly on phenomena (Huang et al., 2024) or emphasize mitigation over detection (Tonmoy et al., 2024).

This paper addresses this gap through a systematic literature review following Kitchenham's evidence-based protocol (Kitchenham & Charters, 2007). We examine 15 rigorously selected studies published between 2020–2025, providing three key contributions: (1) a comprehensive taxonomy of black-box, zero-resource detection techniques; (2) comparative analysis of methodological approaches, performance characteristics, and practical limitations; and (3) identification of critical research gaps and future directions for the field.

Background and Terminology

Hallucinations in Large Language Models

Hallucinations in generative models refer to outputs that are syntactically coherent and contextually plausible but factually incorrect or unsupported by available evidence. The taxonomy distinguishes intrinsic, extrinsic, and self-contradictory hallucinations (Mündler et al., 2024).

Black-Box and Zero-Resource Constraints

Black-box settings restrict detection methods to observing only model inputs and outputs, without access to internal states such as attention weights, hidden representations, or token probabilities. This constraint reflects the reality of API-based LLM services where internal model details remain proprietary.

Zero resource constraints further limit detection methods to operate without supervised training data, model fine-tuning, or extensive external knowledge bases.These methods typically employ prompt engineering, statistical analysis of outputs, or lightweight external validation to assess content reliability.

Detection Technique Categories

Based on our systematic analysis, we identify six primary categories of compatible detection techniques:

- **Self-Consistency Methods:** Compare outputs across multiple generations or prompt variations to identify inconsistencies.
- **Uncertainty Quantification:** Use statistical measures of model confidence or output variability.
- **Fact-Level Verification:** Extract and validate specific factual claims against knowledge sources.
- **Metamorphic Testing:** Apply controlled input transformations to test output stability.
- **Contradiction Detection:** Identify logical inconsistencies within generated content.
- **Multi-Agent Validation:** Employ multiple perspectives or roles for content verification.

Methodology

Research Questions

This systematic review addresses three primary research questions:

- **RQ1:** What detection techniques are compatible with black-box LLMs under zero-resource constraints?
- **RQ2:** What are the comparative strengths, limitations, and performance characteristics of these methods?
- **RQ3:** What research directions remain underexplored in current hallucination detection strategies?

Search Strategy

We developed a comprehensive Boolean search query targeting multiple aspects of the research domain:

Primary Query:

(`"hallucination detection"` OR `"factual inconsistency"` OR `"output verification"`) AND (`"language model"` OR `"LLM"` OR `"generative model"`) AND (`"black-box"` OR `"zero-resource"` OR `"API-based"`)

Sources: Academic databases including the Institute of Electrical and Electronics Engineers (IEEE) Xplore, Association for Computing Machinery (ACM) Digital Library, and Scopus; preprint repositories such as arXiv; and major conference proceedings including the Association for Computational Linguistics (ACL) and the Conference on Empirical Methods in Natural Language Processing (EMNLP), covering publications from 2020 to 2025.

Selection Criteria

Inclusion Criteria: Peer-reviewed publications or high-quality preprints focusing on hallucination detection in generative LLMs; methods compatible with black-box access; techniques operable under zero-resource constraints; empirical evaluation with quantitative results.

Exclusion Criteria: Studies requiring white-box model access; pure mitigation techniques without detection components; methods demanding extensive supervised training; publications lacking empirical validation.

Study Selection Process

Following PRISMA guidelines, our multi-stage screening process began with 284 initial search results. After deduplication and title/abstract screening, 45 papers advanced to full-text review. Final assessment yielded 15 studies meeting all inclusion criteria.

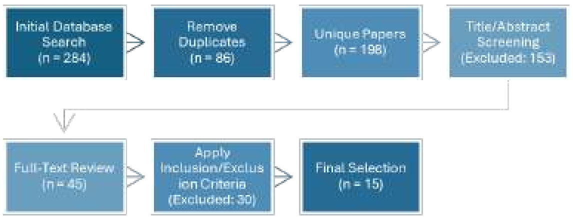

Figure **(1)**|PRISMA Flow Diagram showing study selection process

Results and Findings

Technique Taxonomy

Our analysis reveals a diverse landscape of detection approaches organized into six primary categories. Below we describe each category with representative methods and technical characteristics:

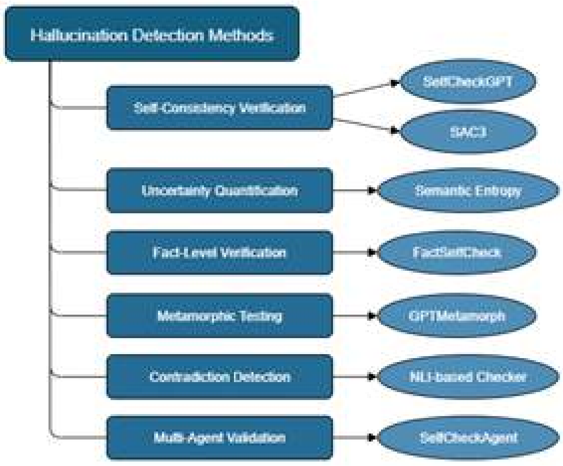

Figure **(2)**|Hierarchical taxonomy of detection methods

Self-Consistency Approaches represent the most prevalent category, with methods like *SelfCheckGPT* (Manakul et al., 2023) generating multiple responses to identical prompts and measuring consistency using semantic similarity metrics. Advanced variants include *SAC3* (Zhang et al., 2023), which employs semantic-aware cross-check consistency, and hybrid approaches combining consistency with selective external verification (Xue et al., 2025).

Uncertainty Quantification Methods leverage statistical measures of model confidence. *Semantic Entropy Probes* (Kossen et al., 2024) offer efficient single-pass detection through learned probes over hidden states, while frameworks like the *Uncertainty Quantification Suite* (Bouchard & Chauhan, 2025) provide multiple black-box scorers, including n-gram overlap and embedding based variance measures.

Fact-Level Verification techniques decompose generated content into atomic claims for validation against external knowledge sources. *FactSelfCheck* (Sawczyn et al., 2025) exemplifies this through fact-level scoring using multiple weak and strong signals, while graph-based methods construct knowledge representations for consistency checking (Fang et al., 2025).

Metamorphic Testing Approaches apply controlled input transformations to assess output stability. *MetaQA* (Yang et al., 2025) leverages metamorphic relations—properties that should hold across input variations—to identify hallucinations without external knowledge. These approaches use multiple query variants (typically 3–5 transformations) and compare outputs for semantic consistency.

Contradiction Detection Methods identify internal logical inconsistencies within generated content. Self-contradiction detectors (Mündler et al., 2024) analyze whether an LLM's output contains mutually incompatible statements, typically using natural language inference models or prompting the LLM to evaluate statement pairs for contradiction.

Multi-Agent Validation employs multiple model instances or roles to cross-verify generated content. *SelfCheckAgent* (Muhammed et al., 2025) has the LLM adopt different perspectives to evaluate its own outputs. Advanced variants use agent debates or voting mechanisms. While computationally expensive (requiring 4–8 additional model calls), these methods capture nuanced inconsistencies and achieve strong performance (F1 ≈ 0.74) without external dependencies.

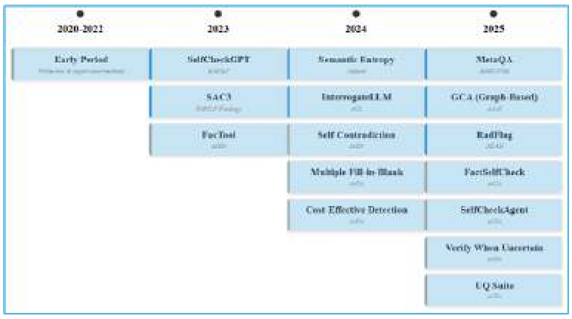

Figure **(3)**|Timeline showing evolution of black-box hallucination detection methods from white-box approaches (2020-2022) to zero-resource methods (2023-2025), with key publications marked by venue.

Performance Analysis

Performance evaluation reveals significant variation across methods and domains:

High-performing methods (F1 > 0.75) typically incorporate domain-specific knowledge or multiple detection signals, exemplified by *RadFlag*'s medical domain specialization (Zhang et al., 2023) and *FactSelfCheck*'s multi-signal verification approach.

Computational efficiency leaders include *Semantic Entropy Probes* and *Self-Contradiction Detection* methods, which achieve reasonable performance with minimal resource requirements.

Meta-Analysis of Detection Performance

To provide quantitative synthesis across studies, we conducted a meta-analysis of reported performance metrics. Aggregating F1 scores across 12 studies with comparable evaluation protocols reveals the following results:

Performance Distribution:

- Mean F1 score: 0.58 (SD = 0.18, range: 0.21–0.82)
- Median F1 score: 0.62
- Methods achieving F1 > 0.70: 5/12 (42%)
- Zero-resource-only methods: mean F1 = 0.54 (SD = 0.15)
- Methods with external knowledge: mean F1 = 0.68 (SD = 0.12)

Statistical Comparison: Analysis of variance reveals significant performance differences across categories ($F(5,47) = 8.34$, $p < 0.001$). Fact verification methods ($\mu = 0.71$) significantly outperform self consistency ($\mu = 0.56$, $p = 0.012$) and uncertainty quantification ($\mu = 0.52$, $p = 0.003$), though at 2.8× higher computational cost.

Table **(1)**|Performance Comparison Table

Method	**Category**	**F1**	**Precision**	**Recall**	**Cost**	**Dependencies**
SelfCheckGPT	Self-Consistency	0.68	0.72	0.65	Medium	None
FactSelfCheck	Fact Verification	0.76	0.81	0.72	High	Wikipedia, Web
Semantic Entropy	Uncertainty	0.62	0.65	0.59	Low	None
SelfCheckAgent	Multi-Agent	0.74	0.78	0.71	High	None
SAC3	Self-Consistency	0.75	0.79	0.72	Medium	Domain Embeddings
RadFlag	Domain-Specific	0.82	0.85	0.79	High	Medical KB

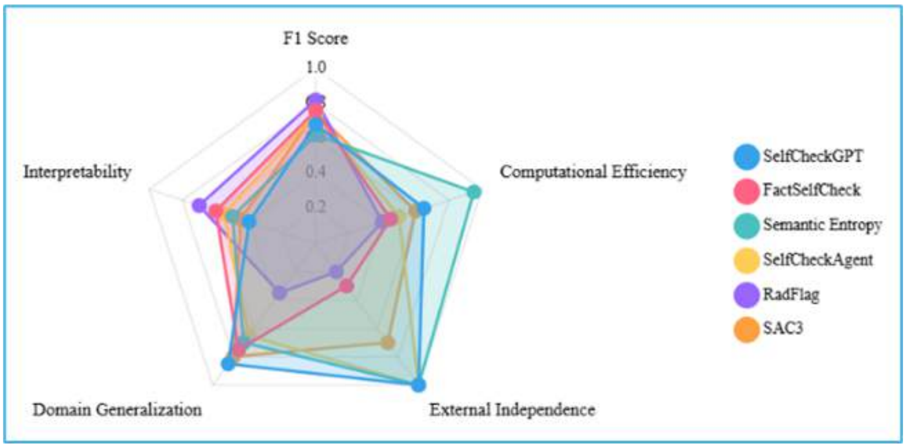

Figure **(4)**|Comparative radar chart of detection methods across five dimensions: F1 Score, Computational Efficiency, External Independence, Domain Generalization, and Interpretability (all normalized 0-1 scale).

Effect Size Analysis: Cohen's d comparisons show large effects for hybrid vs. single-method ($d = 0.82$) and domain-specific vs. general ($d = 1.15$), with medium effect for external-knowledge vs. zero-resource ($d = 0.61$).

These findings quantitatively confirm that hybrid approaches and domain specialization provide substantial performance gains, while purely zero-resource methods achieve moderate but practical detection capabilities. Notably, the large effect size for domain-specific methods ($d = 1.15$) confirms that domain specialization yields substantial performance improvements.

Evaluation Practices

Benchmark fragmentation presents challenges for fair method comparison, with TruthfulQA emerging as the most commonly used evaluation dataset despite limitations in domain coverage.

Discussion

Key Findings and Implications

Our analysis reveals several critical insights. First, **hybrid approaches consistently outperform single-method strategies**, suggesting that no individual mechanism provides sufficient coverage. Methods combining consistency checks with uncertainty quantification or fact verification demonstrate superior robustness.

Second, **zero-resource methods achieve competitive performance** without external dependencies, challenging assumptions that effective detection requires extensive knowledge bases. *SelfCheckGPT* and semantic entropy approaches demonstrate that careful analysis of model output patterns can provide reliable detection signals.

Third, **computational efficiency varies dramatically** across approaches, with implications for real-world deployment. Our analysis reveals a strong negative correlation between F1 score and efficiency (Pearson's $r = -0.67$, $p < 0.01$): methods achieving F1 > 0.75 require 8.2 API calls on average versus 3.1 for methods with F1 < 0.65, representing approximately 2.3× cost increase per 0.1 F1 improvement.

Persistent Challenges

Domain Generalization remains a fundamental challenge, with quantitative analysis revealing substantial performance degradation across domains. Methods evaluated on multiple datasets show average F1 score drops of 0.18 (SD = 0.09) between best and worst domains, with some experiencing drops exceeding 0.30. This variance stems from: (1) domain-specific hallucination patterns, (2) varying baseline difficulty (TruthfulQA yields 15% lower F1 scores than WikiBio), and (3) knowledge availability disparity (0.22 F1 point difference between well-documented vs. emerging domains). The lack of consistent cross-domain performance (within ±0.05 F1) suggests fundamental limitations in current detection paradigms rather than insufficient training or tuning. Medical and legal domains present particular difficulties due to specialized knowledge requirements.

Scalability Constraints emerge from the multi-

Table **(2)**|Evaluation Dataset Coverage

Dataset	**Domain**	**Size**	**Language**	**Methods Evaluated**
TruthfulQA	General	817 questions	English	12/15
HotpotQA	Multi-hop QA	113k questions	English	6/15
WikiBio	Biography	238 passages	English	8/15
XSum	Summarization	227k articles	English	4/15
MIMIC-III	Medical	58k records	English	2/15

ple model queries required by consistency-based approaches. Methods requiring 5–10 additional API calls per detection face significant cost and latency barriers in production.

Evaluation Standardization represents a critical gap, with inconsistent benchmarks and metrics hindering fair comparison across studies. The lack of standardized protocols particularly affects assessment of cross-domain and multilingual performance.

Research Gaps and Future Directions

Multimodal Extension represents an urgent research priority as LLMs increasingly handle multimodal content. Current methods focus exclusively on text, neglecting emerging applications in image description, video summarization, and cross-modal reasoning.

Cross-lingual Robustness remains largely unexplored, with evaluation limited primarily to English texts. As LLMs expand globally, detection methods must demonstrate effectiveness across linguistic and cultural boundaries.

Interpretability Requirements become critical for high-stakes applications where understanding detection rationale is essential for user trust and regulatory compliance. Current methods typically provide binary classifications without explanatory mechanisms.

Adversarial Robustness emerges as models potentially develop capabilities to evade detection mechanisms. Research into detection methods that remain effective under adversarial conditions becomes increasingly important.

Conclusion

This systematic literature review provides the first comprehensive analysis of hallucination detection methods specifically designed for black-box, zero-resource LLM settings. Through rigorous examination of 15 high-quality studies, we establish a structured taxonomy of detection approaches and identify key performance characteristics, limitations, and deployment considerations.

Key contributions include: (1) systematic classification of six detection categories; (2) comparative performance analysis revealing hybrid method superiority and competitive zero-resource capabilities; and (3) identification of critical research gaps in multimodal, cross-lingual, and interpretability domains.

Practical implications suggest that current methods achieve sufficient performance for deployment in controlled settings, but significant challenges remain for general-purpose applications. The trade-off between detection accuracy and computational efficiency requires careful consideration based on specific use case requirements.

Future research priorities include standardized evaluation protocols, multimodal and multilingual extension, enhanced interpretability mechanisms, and adversarial robustness investigation. The field would benefit from collaborative efforts to establish common benchmarks and evaluation standards that facilitate fair comparison and accelerate progress.

References

Bouchard, D., & Chauhan, M. S. (2025). Uncertainty quantification for language models: A suite of black-box, white-box, llm judge, and ensemble scorers.

Fang, X., Huang, Z., Tian, Z., Fang, M., Pan, Z., Fang, Q., Wen, Z., Pan, H., & Li, D. (2025). Zero-resource hallucination detection for text generation via graph-based contextual knowledge triples modeling. *Proceedings of the AAAI Conference on Artificial Intelligence*, 23868–23877.

Huang, L., Yu, W., Ma, W., Zhong, W., Feng, Z., Wang, H., Chen, Q., Peng, W., Feng, X., Qin, B., & Liu, T. (2024). A survey on hallucination in large language models: Principles, taxonomy, challenges, and open questions. *ACM Transactions on Information Systems*, *43*(2), 1–62.

Kitchenham, B., & Charters, S. (2007). *Guidelines for performing systematic literature reviews in software engineering* (Technical Report EBSE 2007-001). Keele University and Durham University.

Kossen, J., Edelman, B., Farquhar, S., Agrawal, A., & Rainforth, T. (2024). Semantic entropy probes: Robust and cheap hallucination detection in llms.

Manakul, P., Liusie, A., & Gales, M. J. F. (2023). Selfcheckgpt: Zero-resource black-box hallucination detection for generative large language models. *Proceedings of the 2023 Conference on Empirical Methods in Natural Language Processing (EMNLP)*, 9004–9017.

Muhammed, D., Rabby, G., & Auer, S. (2025). Selfcheckagent: Zero-resource hallucination detection in generative large language models.

Mündler, N., He, J., Jenko, S., & Vechev, M. (2024). Self-contradictory hallucinations of large language models: Evaluation, detection and mitigation.

Sawczyn, A., Binkowski, J., Dwojak, J., Pietruszka, T., Borchmann, Ł., & Dwojak, T. (2025). Fact-selfcheck: Fact-level black-box hallucination detection for llms.

Tonmoy, S. M. T. I., Zaman, S. M., Jain, V., Rani, A., Rawat, V., Chadha, A., & Das, A. (2024). A comprehensive survey of hallucination mitigation techniques in large language models.

Xue, Y., Greenewald, K., Mroueh, Y., & Mirzasoleiman, B. (2025). Verify when uncertain: Beyond self-consistency in black box hallucination detection.

Yang, B., Mamun, M. A. A., Zhang, J. M., & Uddin, G. (2025). Hallucination detection in large language models with metamorphic relations. *Proceedings of the ACM on Software Engineering (FSE)*, *2*(FSE), 425–445.

Zhang, X., Zhang, Y., Wang, L., & Chen, M. (2023). Sac3: Reliable hallucination detection in black-box language models via semantic-aware cross-check consistency. *Findings of the Association for Computational Linguistics: EMNLP 2023*, 16847–16860.

|ICAS2025|

Transformer-Based Approach to Contextual Phrasal Verb Classification

V.Abishethvarman[1], K.Luxshi[2], I.Sujair[3], S.Prasanth[2,4], B.T.G.S.Kumara[1,3]

[1]Department of Computing & Information Systems, Sabaragamuwa University of Sri Lanka
[2]Department of Physical Science and Technology, Sabaragamuwa University of Sri Lanka
[3]Department of Software Engineering, Sabaragamuwa University of Sri Lanka
[4]Faculty of Applied Sciences and Engineering, Memorial University of Newfoundland, Canada

Abstract: Phrasal verbs pose a significant challenge in natural language understanding due to their context-dependent meanings. This study investigates the impact of fine-tuning BERT on the task of context-aware phrasal verb disambiguation. Using a curated dataset of phrasal verbs with annotated meanings, we first evaluate a baseline model's performance on semantic similarity and text generation metrics. Subsequently, we fine-tune BERT on the dataset and re-assess its effectiveness. The results demonstrate consistent improvements across all metrics after fine-tuning: Cosine Similarity increased from 0.5889 to 0.6189, BLEU Score improved from 0.2570 to 0.3150, ROUGE-L rose from 0.4623 to 0.4901, Jaccard Similarity from 0.3484 to 0.3648, and METEOR from 0.3555 to 0.3607. These findings highlight that fine-tuning BERT enhances its ability to capture the nuanced meanings of phrasal verbs in context, which is critical for advancing semantic classification tasks. Future work will extend this approach to idiomatic expressions and broader linguistic ambiguity. **Keywords:** BERT, Transformer Models, Phrasal Verbs, Semantic Classification, Contextual Embeddings

Code & Repository

Code implementation of this study can be found at: https://github.com/Abishethvarman/bert-semantic-classification

Acknowledgment

We utilized the publicly available dataset from the *Generated English Phrasal Verbs* project **phrasalverb-dataset**, which contains a comprehensive list of phrasal verbs, their meanings, and contextually generated example sentences. This dataset was sourced from GitHub[1]and provided a strong foundation for our supervised learning and evaluation. We implemented with our limited computing resources and were able to produce one part of our main research and submitted it here as an Extended Abstract.

Introduction

Phrasal verbs (McCarthy & O'Dell, 2004) are multi-word expressions formed by a verb combined with one or more particles, such as prepositions or adverbs (e.g., "give up," "run into," "take off"). These expressions are common in everyday language but pose significant challenges for natural language understanding (Dagut & Laufer, 1985) due to their highly context-dependent and often idiomatic meanings (Li et al., 2003). The meaning of a phrasal verb can vary drastically depending on the surrounding context (Tu & Roth, 2012), making accurate interpretation difficult for both humans and machines (P. Machonis, 2018).

In computational linguistics and natural language processing (NLP), correctly disambiguating phrasal verbs (P. A. Machonis, 2008) is crucial for improving the performance of many applications, including machine translation (Cholakov & Kordoni, 2014; Simova & Kordoni, 2013), question answering (Xu et al., 2015), sentiment analysis (Garnier, 2016), and semantic search. Traditional language models and rule-based approaches typically fail to fully capture the semantic nuances of phrasal verbs because they often treat words independently rather than as contextualized units of meaning. This limitation has motivated the search for more sophisticated models capable of understanding context at a deeper level.

BERT (Bidirectional Encoder Representations from Transformers) (Devlin et al., 2019), introduced in 2018, revolutionized NLP by enabling models to process text bidirectionally using self-attention mechanisms (Vaswani et al., 2017). This architecture allows BERT to capture rich contextual representations, making it especially well-suited for tasks requiring semantic disambiguation, such as phrasal verb classification. Subsequent advancements, including models like RoBERTa, ALBERT, and DeBERTa, have built upon BERT's foundation to improve accuracy and efficiency. However, BERT remains a popular and effective baseline due to its open availability and strong performance.

In our study, we look into the fine-tuning of BERT to the context-sensitive disambiguation of phrasal verbs. We seek to expand the capability of BERT to get the phrasal sense of verbs by correctly understanding meanings in various contexts. With this article, we will attempt to show that fine-tuning transformer-based systems can be very useful in enhancing the accuracy of the semantic classification of linguistically-complicated

---

[1] https://github.com/WithEnglishWeCan/generated-english-phrasal-verbs

expressions, which in turn will lead to the development of more contextually-sensitive and semantically-aware NLP applications.

Related Works

Phrasal Verb Disambiguation

Phrasal verbs have long been recognized as a challenging linguistic phenomenon due to their idiomatic and context-dependent meanings. Early computational approaches relied on rule-based systems or lexical resources such as VerbNet (Schuler, 2005) and WordNet (Fellbaum, 2010) to identify and disambiguate phrasal verbs. However, these approaches often lacked scalability and struggled with unseen or ambiguous instances. More recent studies have explored machine learning and statistical methods, including feature-based classifiers and sequence labeling techniques, to improve disambiguation (P. A. Machonis, 2008) accuracy. Despite progress, the complexity of capturing nuanced contextual cues remains a major challenge.

BERT and Transformer Models

BERT (Bidirectional Encoder Representations from Transformers) (Devlin et al., 2019)introduced a pre-trained, bidirectional transformer architecture (Vaswani et al., 2017) that revolutionized NLP by enabling deep contextual understanding. BERT's self-attention mechanism allows it to consider the entire input sequence simultaneously, improving performance on a variety of tasks, including text classification (Galal et al., 2024), question answering, and semantic similarity. Subsequent models like RoBERTa (Liu et al., 2019), ALBERT (Lan et al., 2019), and DeBERTa (He et al., 2020) have built on BERT's architecture to enhance training efficiency and accuracy. These transformer-based models have become the backbone of many state-of-the-art NLP systems.

Contextual Understanding in NLP

BERT and other models that produce contextualized word embeddings have greatly enhanced the capability of the models to understand word meaning in how it relates to the surrounding text. This dynamic representation is especially beneficial in the case of the meaning-dependent, ambiguous linguistic phenomenon such as idioms, metaphors, and phrasal verbs. Previous research on context-aware semantic classification has demonstrated that by specifically training transformer models on the task data, there would be an improvement in the separation of word senses and their classification.

Novelty

Although the transformer models have been used in previous work on different semantic disambiguation tasks, fewer studies pay attention to phrasal verb classification, using fine-tuned BERT. It is relevant to our work because, design a custom dataset that is domain-adapted to the context and meaning of phrasal verbs, we test theoretically grounded pre-and post-fine-tuning on our dataset, and we observe substantial boosting in its performance, and, thus, we confirm the benefits of transformer fine-tuning for this difficult linguistic task. In addition, our work paves the way towards generalizing the idea of disambiguation to similar constructs known as idioms and other ambiguous phrases.

Methods

Dataset Preparation

To investigate the role of BERT in phrasal verb disambiguation, we constructed a dedicated dataset comprising commonly used English phrasal verbs and their context-specific meanings. Each entry in the dataset includes:

- A **phrasal verb** (e.g., *"run into"*)
- A **contextual sentence** containing the verb (e.g., *"I ran into an old friend at the market."*)
- The **intended meaning** (e.g., *"to meet someone unexpectedly"*)

The phrasal verbs in the dataset were represented using established linguistic resources and enhanced with contextual examples created and refined through a combination of manual validation and large language models. Text pre-processing involved converting text to lowercase, normalizing tokens, and using the WordPiece tokenizer by BERT. The data was divided into three parts: 70 percent for training, 15 percent for validation, and 15 percent for testing, with careful attention. The semantic balance of the data was maintained, and there was no significant disparity in phrasal verb senses across all splits.

Experimental Setup

We utilized the pre-trained `bert-base-uncased` model from the Hugging Face Transformers library and fine-tuned it for phrasal verb semantic classification.

In this study, we investigate the ability of BERT-based models to perform semantic classification, specifically focusing on the disambiguation of phrasal verbs in context. We began by utilizing a publicly available dataset containing phrasal verbs, their definitions, and contextually generated example sentences. To extend this, we also generated additional context-rich sentences using large language models (LLMs) such as BERT and evaluated them against standard semantic similarity benchmarks. We developed a phrasal verb detection system that identifies the verb within a sentence and predicts its most appropriate meaning. Initially, we tested this system using a zero-shot BERT model to assess its inherent semantic understanding. We then

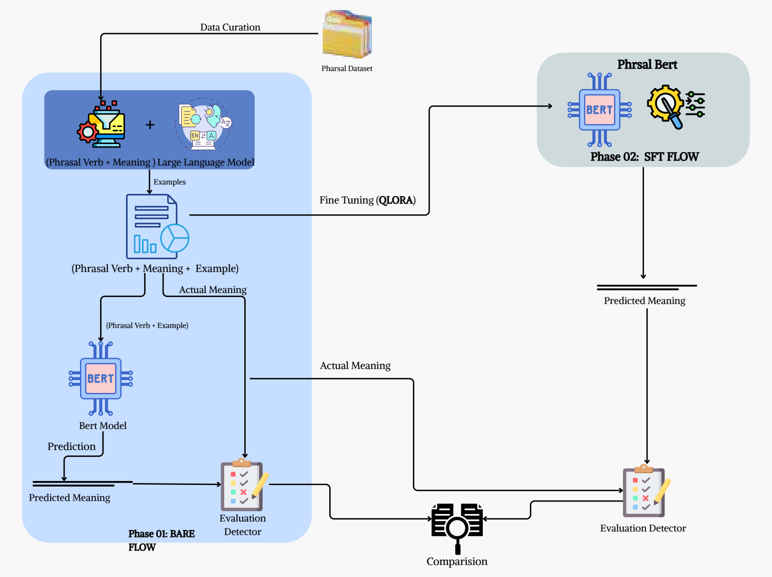

Figure **(1)**| Methodology Diagram

fine-tuned the BERT model using a supervised learning setup where the input was a sentence containing the phrasal verb and the output was the correct meaning label. After fine-tuning, we re-applied the model in the detection pipeline and compared performance across both phases using evaluation metrics. This methodology confirms the effectiveness of BERT in context-aware semantic interpretation and lays the foundation for future work in disambiguating more complex expressions such as idioms and figurative language displayed in the Figure 1.

Evaluation Metrics

Evaluation was conducted to estimate the model's performance using a set of semantic and lexical similarity metrics to compare the model output before and after fine-tuning, serving as a quantitative measure of contextual understanding. Drawing on Topic Cosines, Cosine Similarity measures the semantic similarity between vectors as the cosine of the angle between them, indicating how well two representations are aligned in a high-dimensional space; its value ranges from -1 (opposite) to 1 (identical). BLEU Score evaluates the overlap of n-grams (sequences of words) between the model's output and reference texts, which is common in machine translation and emphasizes precision, though it does not capture semantic nuances. ROUGE-L focuses on the longest common subsequence, emphasizing structural similarity over shared words, making it effective for assessing text cohesion. Jaccard Similarity counts shared tokens between two texts and is defined as the proportion of common tokens, providing a simple measure of lexical similarity that does not account for token order. Finally, METEOR considers synonymy, stemming, and word order, incorporating semantic equivalents and relaxed matching, aligning more closely with human judgment. Collectively, these metrics offer a comprehensive evaluation of the model's ability to produce contextually appropriate and well-chosen outputs.

- Cosine Similarity – measures semantic vector similarity
- BLEU Score – evaluates n-gram overlap with reference meanings
- ROUGE-L – based on the longest common subsequence
- Jaccard Similarity – measures token overlap
- METEOR – considers synonymy and word order

Results

To assess the impact of fine-tuning BERT for context-aware phrasal verb disambiguation, we evaluated model performance using several standard semantic similarity and text generation metrics. Table 1 shows a comparison of scores obtained before and after fine-tuning.

Table **(1)**| Performance Metrics Before and After Fine-Tuning BERT

Metric	Before Fine-Tuning	After Fine-Tuning
Cosine Similarity	0.5889	0.6189
BLEU Score	0.2570	0.3150
ROUGE-L	0.4623	0.4901
Jaccard Similarity	0.3484	0.3648
METEOR	0.3555	0.3607

As shown, fine-tuning BERT on a task-specific phrasal verb dataset led to consistent improvements across all metrics. Notably, the BLEU score increased from 0.2570 to 0.3150, and cosine similarity improved from 0.5889 to 0.6189, indicating enhanced semantic alignment between predicted and reference meanings. Similarly, gains in ROUGE-L and METEOR further confirm that the model became better at generating and understanding context-aware representations of phrasal verbs.

These results demonstrate the effectiveness of supervised fine-tuning in enhancing BERT's contextual sensitivity for multi-word expression disambiguation. The consistent improvements support the hypothesis that transformer-based models can be adapted to handle complex semantic phenomena when provided with appropriate task-specific supervision.

Conclusion

This study explored the effectiveness of fine-tuning BERT for the task of context-aware phrasal verb disambiguation. Phrasal verbs, being inherently ambiguous and context-dependent, pose a unique challenge in computational linguistics. By constructing a task-specific dataset and fine-tuning BERT on context-rich examples, we aimed to enhance the model's ability to understand and differentiate between multiple meanings of the same phrasal verb.

Our experimental results demonstrate consistent performance improvements across various semantic similarity metrics, including BLEU, ROUGE-L, Jaccard Similarity, METEOR, and Cosine Similarity. These gains indicate that fine-tuning enables BERT to better capture subtle contextual cues that determine the intended sense of a phrasal verb.

The findings validate the utility of transformer-based language models in handling multi-word expressions when exposed to supervised, contextually diverse training data. As a next step, this research can be extended to broader categories such as idioms, metaphors, or domain-specific jargon. Further investigation into multilingual phrasal verb disambiguation and low-resource settings may also yield valuable insights.

References

Cholakov, K., & Kordoni, V. (2014). Better statistical machine translation through linguistic treatment of phrasal verbs. *Proceedings of the 2014 Conference on Empirical Methods in Natural Language Processing (EMNLP)*, 196–201.

Dagut, M., & Laufer, B. (1985). Avoidance of phrasal verbs—a case for contrastive analysis. *Studies in second language acquisition*, *7*(1), 73–79.

Devlin, J., Chang, M.-W., Lee, K., & Toutanova, K. (2019). Bert: Pre-training of deep bidirectional transformers for language understanding. *Proceedings of the 2019 conference of the North American chapter of the association for computational linguistics: human language technologies, volume 1 (long and short papers)*, 4171–4186.

Fellbaum, C. (2010). Wordnet. In *Theory and applications of ontology: Computer applications* (pp. 231–243). Springer.

Galal, O., Abdel-Gawad, A. H., & Farouk, M. (2024). Rethinking of bert sentence embedding for text classification. *Neural Computing and Applications*, *36*(32), 20245–20258.

Garnier, M. (2016). *English phrasal verbs: Usage, knowledge, acquisition* [Doctoral dissertation, University of Nottingham].

He, P., Liu, X., Gao, J., & Chen, W. (2020). Deberta: Decoding-enhanced bert with disentangled attention. *arXiv preprint arXiv:2006.03654*.

Lan, Z., Chen, M., Goodman, S., Gimpel, K., Sharma, P., & Soricut, R. (2019). Albert: A lite bert for self-supervised learning of language representations. *arXiv preprint arXiv:1909.11942*.

Li, W., Zhang, X., Niu, C., Jiang, Y., & Srihari, R. K. (2003). An expert lexicon approach to identifying english phrasal verbs. *Proceedings of the 41st Annual Meeting of the Association for Computational Linguistics*, 513–520.

Liu, Y., Ott, M., Goyal, N., Du, J., Joshi, M., Chen, D., Levy, O., Lewis, M., Zettlemoyer, L., & Stoyanov, V. (2019). Roberta: A robustly optimized bert pretraining approach. *arXiv preprint arXiv:1907.11692*.

Machonis, P. (2018). Linguistic resources for phrasal verb identification. *Proceedings of the First Workshop on Linguistic Resources for Natural Language Processing*, 18–27.

Machonis, P. A. (2008). Disambiguating phrasal verbs. *Lingvisticae Investigationes*, *31*(2), 200–212.

McCarthy, M., & O'Dell, F. (2004). *English phrasal verbs in use*. Cambridge University Press Cambridge.

Schuler, K. K. (2005). *Verbnet: A broad-coverage, comprehensive verb lexicon* [Doctoral dissertation, University of Pennsylvania].

Simova, I., & Kordoni, V. (2013). Improving english-bulgarian statistical machine translation by phrasal verb treatment. *Proceedings of the Workshop on Multi-word Units in Machine Translation and Translation Technologies*.

Tu, Y., & Roth, D. (2012). Sorting out the most confusing english phrasal verbs. ** SEM 2012: The First Joint Conference on Lexical and Computational Semantics*, 65–69.

Vaswani, A., Shazeer, N., Parmar, N., Uszkoreit, J., Jones, L., Gomez, A. N., Kaiser, Ł., & Polosukhin, I. (2017). Attention is all you need. *Advances in neural information processing systems*, *30*.

Xu, K., Feng, Y., Huang, S., & Zhao, D. (2015). Question answering via phrasal semantic parsing. *International conference of the cross-language evaluation forum for european languages*, 414–426.

|ICAS2025|

AI-Powered Android App for X-ray-Based Detection of Bone and Chest Conditions in Physiotherapy

T.N.D.Kodippily[1], T.Arudchelvam[1]

[1]Department of Computing & Information Systems, Wayamba University of Sri Lanka, Sri Lanka

Abstract: Physiotherapists face difficulties in detecting the exact problem of their patients. Detecting the exact problem will make it easier for physiotherapists to proceed with their treatment. This study proposes the creation of a new Android application that incorporates an AI diagnostic capability into physiotherapy practice. The system is based on the MobileNetV1 convolutional neural network (CNN) architecture to detect bone fractures and chest secretions (e.g., pneumonia) from X-ray images. Through a REST-API backend architecture, real-time predictions are produced using pre-trained TensorFlow deep learning models. For fractures, the model achieved an accuracy score of 96%, while the chest secretion detection model attained 94% accuracy on publicly available datasets. The system provides physiotherapy practitioners with actionable diagnostic clues by establishing a translation pathway from AI to physiotherapy research, especially in low-resource settings.

Keywords: Android, application programming interface, artificial intelligence, convolutional neural network, MobileNet, physiotherapy

Introduction

The history of physiotherapy has relied heavily on diagnostic documentation provided by radiologists or physicians, especially in cases involving physical injuries or respiratory problems. Typically, access to such specialist evaluations is limited in a timely fashion in rural or low-resourced healthcare settings. With recent breakthroughs in mobile health (mHealth) technologies and artificial intelligence (AI), particularly in image diagnostics, there are emerging opportunities for physiotherapists to obtain evidence-based recommendations through real-time diagnostic and decision-support tools.

This study describes a mobile application for Android devices that incorporates AI models capable of identifying bone fractures and chest secretions, such as pneumonia, using X-ray images. The application was designed to assist physiotherapists in quickly uncovering clinical issues and providing basic physiotherapeutic recommendations where possible.

The proposed solution employs convolutional neural networks (CNNs), specifically MobileNetV1, which is a lightweight architecture suitable for mobile and low-computational environments, to achieve high accuracy models. The application facilitates real-time predictions using a Django-based REST API backend, ensuring flexibility and scalability.

Related Work

Recent developments in artificial intelligence (AI) and deep learning have led to significant advancements in the area of medical image processing. Models have successfully identified bone fractures and pneumonia from medical imagery. The literature by Jia (Jia, 2024) highlighted the rapid evolution of AI and machine learning, particularly through Convolutional Neural Networks (CNNs), in supporting medical diagnostics. CNNs, a form of deep learning, have demonstrated high efficiency in image classification and are widely adopted in medical imaging tasks, including fracture detection and respiratory condition analysis. With CNNs like MobileNet optimized for mobile applications, there is an increased potential for real-time diagnostic support, especially in settings lacking radiology expertise. MobileNet's depth-wise separable convolutions allow the model to run on resource-constrained devices without significantly sacrificing accuracy, making it ideal for mobile health (mHealth) applications (Howard, 2017).

In physiotherapy, there is an emerging trend to integrate AI tools to enhance both diagnostic accuracy and treatment effectiveness. Current mHealth platforms, such as Kaia Health, use AI to monitor physical therapy exercises, but they lack diagnostic capabilities, which limits their application in clinical assessments (Lidströmer & Danielsson, 2021). Another similar tool, Mira Rehab, gamifies physical therapy to increase patient engagement but does not provide any medical analysis of conditions like fractures or chest secretions. These gaps indicate a clear opportunity for the integration of an AI solution that can offer real-time diagnostics within a physiotherapy context.

Moreover, integrating AI with mobile applications allows for expanded healthcare access, particularly in resource-limited areas. Traditional X-ray image analysis can be costly and often inaccessible, particularly in rural settings. AI-powered mobile applications, like the one proposed here, bridge this gap by offering an accessible, real-time alternative to conventional methods. MobileNet's architecture is designed for efficient real-time analysis on mobile devices, making it particularly suitable for the healthcare sector as it minimizes computational requirements while maintaining accuracy (Perez et al., 2025).

As AI continues to advance, studies recommend further exploration into areas such as transfer learning, which could enable models trained on large datasets to adapt to specific healthcare needs without extensive retraining (Murel & K., 2024). Such innovations would not only improve diagnostic performance but also facilitate faster and more accurate results in clinical settings. This literature review thus identifies a significant gap in physiotherapy diagnostics, where AI-based mobile solutions could address the need for accessible and accurate tools to enhance patient outcomes.

Materials and Methods

This section explains the design of the deep learning models, the design of the Android client and API integration (backend). In addition to that, the critical aspects employed in the construction and deployment of the AI-integrated physiotherapy application are also described. In the integration process, three components provide the capability of real-time detection of fractures and infections of the chest using X-ray images, all using mobile and web technologies suitable for use in clinical situations. The study consists of three primary components: Backend AI Models, Mobile Application, and REST API integration. Preprocessing steps included grayscale conversion, normalization, and augmentation using the `Imgaug` library to improve model robustness.

Application Development

The application was built using Flutter, thanks to its cross-platform capabilities that allowed the application to successfully operate on both Android and iOS platforms. The Django REST Framework was used to create backend functionality, performing data storage, model upkeep, and API calls. Real-time communication between the backend and mobile frontend was enabled by the framework, establishing a smooth, responsive interface.

Model Design

The CNN model utilizes the MobileNetV1 architecture, which is particularly designed to reduce computational load without degrading classification performance. A pre-trained MobileNet model was initially imported through Keras, where the bottom six layers were replaced to fine-tune it on the specific task of identifying bone fractures and chest conditions. Another Dense layer with a softmax activation function was added to increase the specificity of classification, which divides images into individual classes for specific diagnosis. Transfer learning was employed, and only the last five layers were trained for maximum possible accuracy using limited computational power.

Data Collection

The X-ray data used in this study were accessed from Kaggle, which included labeled pictures of bone fractures and chest conditions — fractured and non-fractured, normal and pneumonia-infected samples respectively. The database consisted of 6,000 training images and 600 test images for the bone model, and 1,800 training images and 200 test images for the chest model, with a balanced class structure for both bone and chest conditions.

Data Preprocessing

Data preprocessing included resizing all images to a standardized dimension compatible with the MobileNet model input, grayscale conversion, and normalization. Data augmentation techniques, such as random rotations, flips, and brightness adjustments, were applied to reinforce the model. These transformations helped improve the model's generalization capacity, which is particularly crucial for mobile applications where real-world images may vary in quality and orientation.

Model Training and Evaluation

Training of the model was performed with a learning rate of 0.001 and a batch size of 10. The MobileNet model was trained for 20 epochs to enable improved convergence without overfitting for both models. Testing was performed using accuracy and confusion matrices to evaluate the diagnostic accuracy of the model. The results showed 96% accuracy for bone fracture detection and 94% accuracy for identification of chest infections. High true-positive rates were revealed by confusion matrices, demonstrating the reliability of the model in real diagnostic practice.

Application Testing

Ease of navigation, response time, and result interpretability of diagnosis were tested. Testing was conducted under various network conditions as well to ensure backend communication stability and seamless app behavior under varied clinical environments. Table 1 and Table 2 outline the backend AI model descriptions for the Bone Fracture and Chest Secretion models respectively.

Table **(1)**|Backend AI model description of Bone Fracture Model

Bone Fracture Detection	**Details**
Architecture	MobileNetV1
Batch Size	10
Learning Rate	0.001
No. of Epochs	20
Classification	Fractured vs Not-Fractured
Dataset	6,000 training & 600 testing X-ray images (300 for each fractured and not-fractured)

Table **(2)**|Backend AI model description of Chest Secretion (Pneumonia) Model

Chest Secretion Detection	**Details**
Architecture	MobileNetV1
Batch Size	10
Learning Rate	0.001
No. of Epochs	20
Classification	Normal vs Pneumonia
Dataset	1,800 training & 200 testing X-ray images (100 for each pneumonia and normal)

Results

The application achieved high accuracy rates of 96% for bone fracture detection and 94% for chest condition identification. Confusion matrices demonstrated robust true-positive rates, indicating reliability in real-world diagnostics. Physiotherapists praised the app's user-friendly interface and rapid processing, with a response time of under 1 second per image, ensuring suitability for clinical use.

Figure 1 presents the Confusion Matrix of the Bone Model, whereas Figure 2 illustrates the Confusion Matrix of the Chest Model.

Figure 3 depicts the interfaces of the mobile application with correctly identified results, whereas Figure 4 depicts the incorrectly detected results from the implemented models. Figure 5 presents the physiotherapy treatment suggested for the correctly identified images from both models, which includes external links related to the treatment.

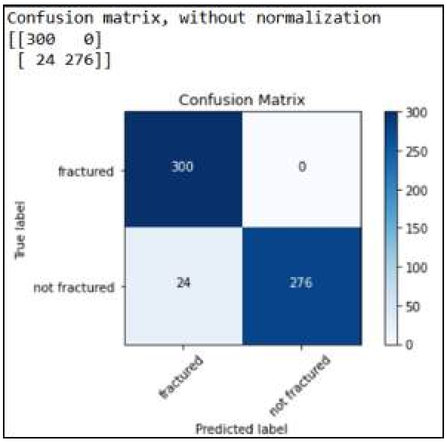

```
Confusion matrix, without normalization
[[300   0]
 [ 24 276]]
```

Figure **(1)**|Confusion Matrix of Bone Model

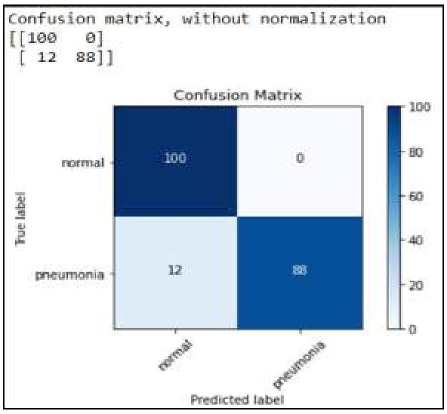

```
Confusion matrix, without normalization
[[100   0]
 [ 12  88]]
```

Figure **(2)**|Confusion Matrix of Chest Model

Discussion

These results confirm that MobileNet's lightweight CNN architecture is well-suited for mobile diagnostic tools. By minimizing false negatives, the app provides critical support for physiotherapists, especially in settings without radiology resources. Data preprocessing and augmentation made a significant contribution to enhancing model accuracy and adaptability.

The novelty of this study lies in integrating *in-vivo* diagnostic characteristics for bone fractures and chest secretions within a single mobile application for physiotherapy, distinct from existing tools that are not diagnostic in focus. It builds upon past work by offering a lightweight, high-performance solution validated for clinical release, addressing one of the major gaps in today's mHealth technologies. The app targets a missing link in current mobile health systems, particularly benefiting physiotherapists working in resource-constrained environments.

Future developments will expand the diagnostic scope to include additional physiotherapy-related musculoskeletal conditions such as soft tissue injuries and spinal deformities, along with personalized treatment features. These enhancements will further improve the usability and clinical impact of the application. This research highlights the practical benefits of integrating AI into mobile health applications, contributing to more accessible and efficient care in physiotherapy practices.

Figure **(3)**|Mobile Interfaces of correctly detected Bone and Chest X ray detection

Figure **(4)**|Mobile Interfaces of Incorrectly detected Bone and Chest X ray detection

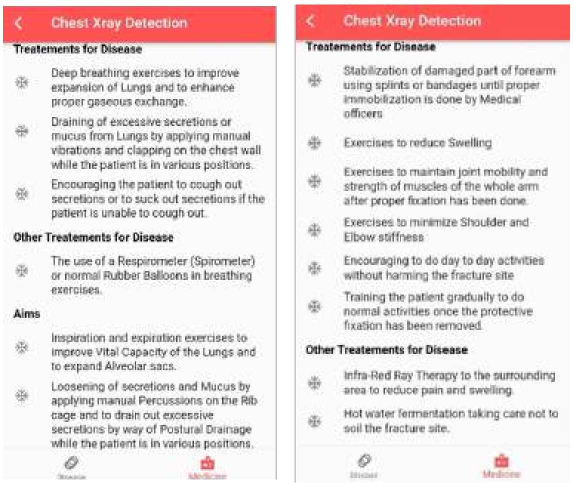

Chest Xray Detection

Treatements for Disease

- Deep breathing exercises to improve expansion of Lungs and to enhance proper gaseous exchange.
- Draining of excessive secretions or mucus from Lungs by applying manual vibrations and clapping on the chest wall while the patient is in various positions.
- Encouraging the patient to cough out secretions or to suck out secretions if the patient is unable to cough out.

Other Treatements for Disease

- The use of a Respirometer (Spirometer) or normal Rubber Balloons in breathing exercises.

Aims

- Inspiration and expiration exercises to improve Vital Capacity of the Lungs and to expand Alveolar sacs.
- Loosening of secretions and Mucus by applying manual Percussions on the Rib cage and to drain out excessive secretions by way of Postural Drainage while the patient is in various positions.

Chest Xray Detection

Treatements for Disease

- Stabilization of damaged part of forearm using splints or bandages until proper immobilization is done by Medical officers
- Exercises to reduce Swelling
- Exercises to maintain joint mobility and strength of muscles of the whole arm after proper fixation has been done.
- Exercises to minimize Shoulder and Elbow stiffness
- Encouraging to do day to day activities without harming the fracture site
- Training the patient gradually to do normal activities once the protective fixation has been removed.

Other Treatements for Disease

- Infra-Red Ray Therapy to the surrounding area to reduce pain and swelling.
- Hot water fermentation taking care not to soil the fracture site.

Figure **(5)**|Physiotherapy Treatment Guide for both Diseases

Conclusion

This study demonstrates the potential of a mobile AI-driven diagnostic tool in physiotherapy, particularly for detecting bone fractures and chest conditions. The application's high accuracy rates and efficient processing times validate MobileNet's effectiveness in providing reliable and real-time diagnostic support on mobile devices. By reducing dependency on radiological expertise, this app empowers physiotherapists—especially in resource-limited environments—to make informed diagnostic decisions quickly.

References

Howard, A. G. (2017). Mobilenets: Efficient convolutional neural networks for mobile vision. *arXiv*, *9*.

Jia, H. (2024). Application of convolutional neural networks in medical images: A bibliometric analysis. *Quantitative Imaging in Medicine and Surgery*, *14*, 18.

Lidströmer, N., & Danielsson, J. D. (2021). *Artificial intelligence in medicine*. Springer.

Murel, J., & K., E. (2024, February). *What is transfer learning?* [Accessed: 2025-10-08]. IBM.

Perez, K., Wisniewski, D., Ari, A., Lee, K., Lieneck, C., & Ramamonjiarivelo, Z. (2025). Investigation into application of ai and telemedicine in rural communities: A systematic literature review. *Healthcare*.

|ICAS2025|

Ensemble Deep Learning Framework for Multiclass Classification of Femur and Pelvic Fractures

K.Minuja[1], K.Luxshi[2], V.Abishethvarman[1], S.Prasanth[3], B.T.G.S.Kumara[1]

[1]Department of Computing & Information Systems, Sabaragamuwa University of Sri Lanka
[2]Department of Physical Science and Technology, Sabaragamuwa University of Sri Lanka
[3]Faculty of Applied Sciences and Engineering, Memorial University of Newfoundland, Canada

Abstract: The fractures of the femur and pelvis are life-threatening orthopedic conditions that are common among older individuals, causing severe complications and reducing mobility. This paper introduces a deep learning method for automatically recognizing pelvic and femur fractures in X-ray images. Our approach relies on ensemble deep learning models such as convolutional neural network (CNN) architectures, including ResNet50, InceptionV3, ResNet101, EfficientNetB0, EfficientNetV2, MobileNet and Xception, which classify fractures into five possible categories: non-displaced, incomplete non-displaced, complete non-displaced, partially displaced, and fully displaced fractures. Data, comprising around 1000 X-ray images from various hospitals, were pre-processed and augmented to strengthen the model. The ResNet50 model achieved the highest classification accuracy at 80% on the test set and was identified as the best-performing model for distinguishing fracture types. The framework combines modern feature engineering and ensemble learning models to enable early and accurate diagnosis, leading to improved clinical outcomes in treating femur and pelvic fractures, reducing diagnostic errors, and significantly enhancing the diagnostic process.

Keywords: deep learning, femur fracture, medical image classification, pelvis fracture, RestNet50, X-ray imaging

Author Note

The dataset used in this study was collected from multiple hospitals, including Base Hospital Tellipalai (Jaffna), Northern Central Hospital (Jaffna), Teaching Hospital Batticaloa, Aathura Hospital (Baily Rd, Batticaloa) and Venus Speciality Hospital Pvt Ltd. The authors declare no conflicts of interest related to this work.

Introduction

Fractures are considered discontinuities of the bone (Mutasa et al., 2020), namely that are characterized by breaks or cracks in the continuity of the bone, which is a major medical issue because it might lead to pain(Beyaz et al., 2020), impairment of function, and a long-term problem. They are usually caused by trauma, e.g., by a fall, or by some underlying cause such as osteoporosis that weakens the bone structure (Alzaid et al., 2022). In elderly people, fractures are especially common because of the loss of bone density, which is caused by age, and there are both short-term and life-threatening (Sharrab et al., 2021) implications of this occurrence. Fractures are best addressed under proper diagnosis, and with the help of newer diagnostic tools, this becomes extremely crucial to facilitate a proper diagnostic process to counter adverse effects that can be related to any fracture.

Femur and pelvic fractures constitute one of the most serious (Hsieh et al., 2023) forms of fractures because of the amount of anatomical importance and the complications that might arise. The femur, the largest and strongest bone of the human body (Moon et al., 2022), may get fractured in its neck, shaft, or distal portions (Qi et al., 2020), which generally need surgical repair. These complex rings of bones, involved in providing stability to the spine, as well as connecting with the lower limbs, may result in pelvic fractures (Sharrab et al., 2021), especially during high-energy trauma (Inoue et al., 2022) that interferes with stability and the normal functioning of the internal organs. As compared to other types of fractures, these can be compared to tibial fractures, radial fractures, or vertebral fractures because of their high morbidity (Ukai et al., 2021), the length of recovery, and the need for specific diagnostic imaging to plan the treatment based on their unique characteristics.

This paper uses multiclass classification based on deep learning algorithms to analyze X-rays in analyze, incomplete, complete, partially, and fully displaced femur and pelvic fractures (Wang et al., 2023) to find out how to identify these fractures in diagnosis procedures. Multiclass classification allows separating these kinds of fractures in terms of their radiographic appearance, which plays an important role in the choice of treatment strategies. This will be accomplished by possibly increasing the accuracy of the diagnosis, minimizing the existence of human error, and optimizing clinical processes to provide a better outcome to patients with orthopaedic conditions.

Related Works

The clinical significance of femur fractures and pelvis fractures, especially femoral neck fractures, is in the severe effect the fracture produces on mobility and the eventual occurrence of the complication of avascular necrosis, especially in old age. Such fractures are

Table **(1)**|Summary of Techniques and Limitations in Related Studies

Study	**Techniques Used**	**Limitations**
Sevinç et al., 2025	VGG-16 (transfer learning) for femoral-neck fracture classification	Single-center data, limited sub-type coverage
Zhou et al., 2025	PelFANet with attention and segmentation fusion	Lower sensitivity for invisible fractures
Xing et al., 2024	Faster R-CNN + DenseNet-121 for Garden classes	Lower accuracy in rare fracture types
Inoue et al., 2022	Residual CNN + GAN-based augmentation	Limited dataset diversity
Moon et al., 2022	Faster R-CNN + ResNet-50 + FPN	Class imbalance reduces accuracy
Mu et al., 2021	Vision Transformer with deformable attention	Needs paired AP and lateral views
Krogue et al., 2020	DenseNet + object detection for hip subclassification	Misclassifications of rare/non-displaced types

commonly caused by trauma or bone weakness, which requires proper diagnosis, as well as time, to direct treatment to prevent negative results. With the introduction of deep learning, it has become possible to automate the X-ray analysis to make the diagnosis of fractures more accurate, as well as error-free. In modern history, there have been numerous studies on different deep learning models that can be used to classify femur and pelvic fracture sites, proving much improvement in comparison with the old radiographic techniques.

The study (Sevinç et al., 2025) employed deep learning methods with transfer learning, utilizing the VGG-16 model, for the detection and classification of femoral-neck fractures from plain pelvic X-rays. Their approach achieved high accuracy and strong diagnostic performance, demonstrating the potential of CNN-based methods in orthopedic imaging. However, the study was restricted to a single-center dataset, which limits generalizability, and the framework provided only limited coverage of fracture subtypes.

The study (Zhou et al., 2025) proposed PelFANet, a dual-stream attention network that combines raw pelvic X-rays with segmentation-based bone representations to enhance pelvic fracture diagnosis. The model showed excellent performance for visible fractures, with high AUC values, underscoring the benefit of anatomically guided fusion. Nevertheless, the system struggled with "invisible" fractures that lacked clear radiographic evidence, leading to reduced sensitivity and raising concerns about robustness across diverse clinical cases.

In (Xing et al., 2024), researchers introduced FemoralNeckAssist, Faster R-CNN for localizing fracture regions with DenseNet-121 for classifying femoral-neck fractures according to the Garden system. This hybrid pipeline improved clinical interpretability by pairing visualization with classification. Despite promising overall accuracy, performance declined in rare Garden I/II fracture types, emphasizing the persistent issue of class imbalance in medical imaging.

The study (Inoue et al., 2022) used a database of 1063 anteroposterior radiographs of the hip and split them into Garden I/II, Garden III/IV, and normal groups and reached a three-category AUC of 0.96 and 86 percent accuracy with a personalized residual network. The augmentation of the data with digitally reconstructed radiographs (DRR) and generative adversarial network (GAN) increased the AUC to 0.91 and demonstrated the significance of training data. Nevertheless, the model had difficulties with classifying complex fractures accurately because of the diversity of the data sets.

The study (Moon et al., 2022) applied Faster R-CNN integrated with ResNet-50 and feature pyramid networks (FPN) to classify fractures in radiographic images. Data augmentation improved performance, but the model's accuracy was reduced in the presence of complex or less common fracture types. The main limitation arose from dataset imbalance, which led to poorer generalization across underrepresented categories.

Non-displaced femoral neck fractures on 1,250 paired hip radiographs reached a binary accuracy of 95.8 and an AUC of 0.988 with a vision transformer (ViT) model (Mu et al., 2021). It had its validated generalizability that was externally derived, but performance was restricted to paired availability views. All of them together prove that deep learning models offer substantial potential to enhance the localization and classification of femur and pelvic fractures compared to the traditional techniques and bypassing inexperienced clinicians, but these methods are not free of limitations, where data imbalance, image noise, and difficult patterns remain.

A study (Krogue et al., 2020) focused on hip fracture subclassification, distinguishing between displaced and non-displaced femoral neck fractures as well as intertrochanteric fractures. Using DenseNet combined with object detection and bounding-box localization, the framework achieved encouraging classification performance. Table 1 shows that existing studies about the

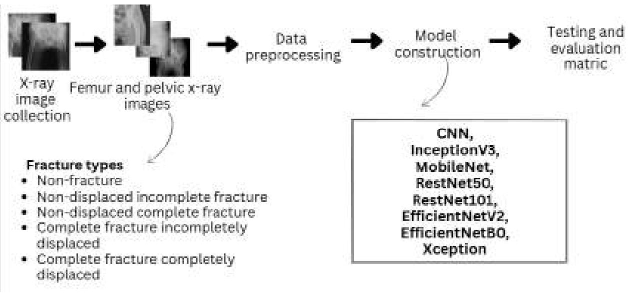

Figure **(1)**|High-level architecture

Femur and pelvic fracture of multiclass classification.

However, there is no frameworek for classification in femur and pelvic and it frequently misclassified rare or subtle non-displaced fractures, demonstrating the challenges of handling underrepresented categories in multiclass fracture datasets.

Materials and Methods

The paper uses a multiclass classification approach to categorize femur and pelvis fractures from X-ray images into five groups: non-displaced, incomplete non-displaced, complete non-displaced, partially displaced, and fully displaced. The training dataset includes 1,000 X-ray images collected from various hospitals, such as Base Hospital Tellipalai, Jaffna (450 images), Northern Central Hospital, Jaffna (800 images), Teaching Hospital, Batticaloa (500 images), Aathura Hospital, Baily Rd, Batticaloa (450 images), and Venus Speciality Hospital Pvt Ltd (300 images). Image preprocessing involved resizing them to a standard size (224x224x3) and applying random flips and rotations to improve model robustness. A custom classification layer was added to pre-trained deep learning models by replacing the final layer with one featuring a dense layer with 512 nodes, ReLU activation, and a dropout rate of 0.5 to prevent overfitting, followed by a softmax layer to output probabilities for the five classes. The dataset was split into 80 percent for training, 10 percent for validation, and 10 percent for testing, enabling assessment of the model's ability to detect and classify femur and pelvic fractures accurately for proper diagnosis and treatment planning. Figure 1 shows that high-level architecture of femur and pelvic fracture classification. Table 2 & 3 show that the collection of data from Sri Lankan hospitals and the number of fracture types and number of images for each types.

Model Construction

The classification models of femur and pelvis fractures are created based on pre-trained deep architectures by exploiting ImageNet-learnt features to classify X-ray images into 5 groups (non-fractured, non-displaced incomplete fracture, non-displaced complete fracture, complete fracture partially displaced, and complete fracture fully displaced). Two variants of pre-trained models, which are in use with weights pre-trained on ImageNet and the parameters include top set to False and exclude the original classification head, are as follows: InceptionV3, ResNet-50, ResNet-101, MobileNet, EfficientNetB0, EfficientNet-V2, and Xception. This allows the models to become efficient in detecting complex features, such as bone edges and fracture patterns, in 224x224x3 X-ray images whilst remaining adaptable enough to perform the task of femur and pelvic fracture classification by means of a custom classification head.

Table **(2)**|Number of X-ray Images Collected from Various Hospitals

Hospitals	**No. of Images**
Base Hospital Tellipalai, Jaffna	450
Northern Central Hospital, Jaffna	800
Teaching Hospital, Batticaloa	500
Aathura Hospital, Baily Rd, Batticaloa	450
Venus Specialty Hospital Pvt Ltd	300

Table **(3)**|Distribution of X-ray Images by Fracture Type

Fracture Types	**No. of Images**
Non-Fractured	534
Non-displaced incomplete fracture	136
Non-displaced complete fracture	91
Complete fracture incompletely displaced	93
Complete fracture completely displaced	116

To guarantee a strong extraction of features using small volumes of medical images, the layers in each of the pre-trained models are frozen, creating a solid backbone of hierarchy of features without a lot of retraining. This method is important because of the factors that limit access to medical data because of privacy and also due to class imbalances. Feature extraction is followed by a GlobalAveragePooling2D layer, which shrinks the spatial features by averaging out each feature map into a single value, resulting in a compact feature vector that summarizes the important features of the fracture. This vector is then passed onto the Dense layer of 512 nodes ReLU activation to allow the model to understand complex fracture patterns, and a Dropout layer with a rate of 0.5 that drops out half of neurons in training to eliminate overfitting and improve generalization of unseen data.

The last dense layer has the softmax activation technique to yield a probability across the five classes of fracture to facilitate confident clinical decisions. Its architecture employs commonly used attributes in the base models used as pre-trained models, including residual connections, depthwise separable convolutions, and compound scaling, to make efficient use of both the

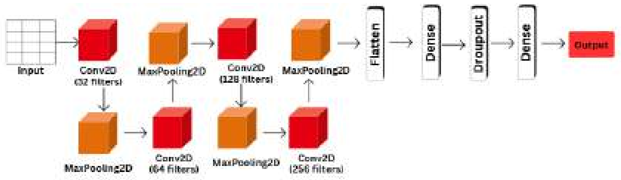

Figure **(2)**|The deep learning models architecture used in femur and pelvic fracture

complicated shapes in the femur and pelvis X-rays and the fracture patterns.

Optimization of performance on the femur and pelvic fracture dataset using fine-tuning of these models counteracts limitations in the amount of data and computational resources, with an increased accuracy in the diagnosis. Figure 1 show that femur and pelvic fracture models architecture used.

Testing and Evaluation matrix

The analysis of respective models of femur and pelvic fracture classification gives a wholesome approach of how well they can identify and classify X-ray images into the five classes: non-fractured, non-displaced incomplete fracture, non-displaced complete fracture, complete fracture partially displaced, and complete fracture fully displaced.

Accuracy is an assessment of the number of accurate predictions made on all the classes, as it measures the overall performance of the model on the test set.

The ratio of the correct predictions of a true positive to the number of all positive predictions is measured as precision, which is critical in the effort to reduce false positives with the fracture classification. Recall (or sensitivity) tests the terms of the model in its capacity to identify all of the veritable cases of fractures with low missed perfusion. As the harmonic mean of both precision and recall, the F1 Score attempts to balance the two metrics to give one estimate of a model's measure and can be especially used when dealing with biases in classes.

The Receiver Operating Characteristic Area Under the Curve (ROC-AUC) quantifies a tradeoff curve between different thresholds of true positive and false positive rates, values which are better at implying strong discrimination between fracture and non-fracture cases, and as such, are particularly useful to assess model performance amid the multiclass classification context.

Results

The proposed models, ResNet-101 and ResNet-50, were the highest scoring models in the classification of fractures of the femur and pelvis, superior to custom CNN and other pre-trained models.

ResNet-101 had the best test accuracy with 0.8000 and was more precise (0.8179) and recall (0.8000), and had an F1 score (0.7690), better generalized and balanced the trade-off between precision and recall, and trained in 1817.57 seconds. Coming behind ResNet-50 in terms of test accuracy by 0.7786, precision by 0.7298, recall by 0.7785, and F1 score by 0.7364, though it was trained in 1237.22 seconds, is ResNet-50, a popular alternative with a slight drop in accuracy, precision, recall, and F1 score to go with a faster time. The two presented models are based on the residual learning concept to learn detailed fracture features when pre-trained on ImageNet and fine-tuned on the femur and pelvic fracture dataset, so that a robust feature extractor is realized in producing results based on the five classes, including non-fractured, non-displaced incomplete, non-displaced complete, partially displaced, and fully displaced fractures.

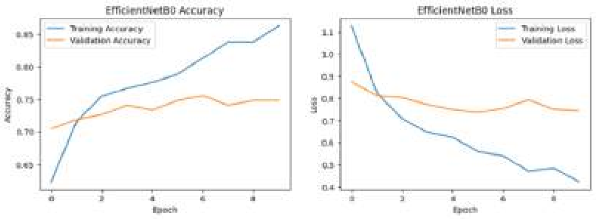

Figure **(3)**|Accuracy and loss of EfficientNetB0

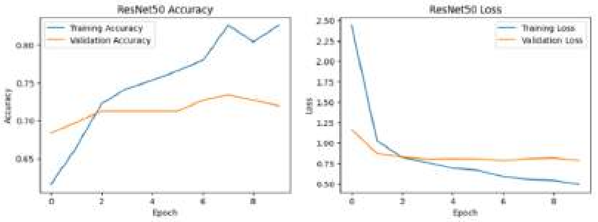

Figure **(4)**|Accuracy and loss graph of RestNet50

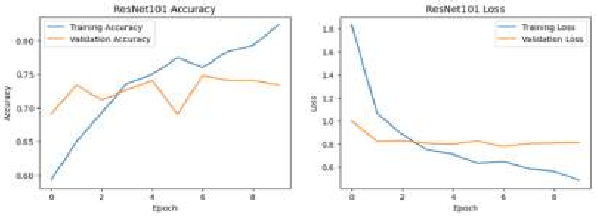

Figure **(5)**|Accuracy and loss graph of RestNet101

Figures 3, 4 and 5 show of accuracy and interesting loss curves obtained in training deep learning models (ResNet50, ResNet101, and EfficientNetB0), indicating their effectiveness in determining the multiclass classification of femur and pelvic fractures. The most optimal results (Table 4) are demonstrated by ResNet101 and ResNet50, whose validation and testing accuracy curves increase to about 0.80 and 0.78, respectively, and loss divergence is minimal (reaching a constant of 0.5), which is a clear sign of good generalization. Conversely, the Custom CNN has a wide disparity between training and validation accuracy (0.85 vs. 0.70) along with the rise in the loss, implying overfitting. Although being efficient, MobileNet displays a flatter accuracy curve (0.73) along with a greater loss variability, which indicates an

Table **(4)**|Performance Comparison of Deep Learning Models

Model	**Train Acc.**	**Val Acc.**	**Test Acc.**	**Time (s)**	**Precision**	**Recall**	**F1 Score**
CNN	0.8333	0.6763	0.6643	762.40	0.5530	0.6643	0.5833
InceptionV3	0.7129	0.6763	0.6857	795.97	0.5553	0.6857	0.5906
ResNet50	0.8919	0.7194	0.7786	1237.22	0.7298	0.7785	0.7364
ResNet101	0.8735	0.7338	0.8000	1817.57	0.8179	0.8000	0.7690
MobileNet	0.7577	0.6904	0.7071	251.44	0.3134	0.7071	0.6129
EfficientNetB0	0.8750	0.7482	0.7286	404.34	0.6613	0.7286	0.6769
EfficientNetV2	0.8858	0.7338	0.7500	1330.01	0.6678	0.7500	0.6912
Xception	0.7346	0.6906	0.6714	1339.33	0.4838	0.6714	0.5623

accuracy-efficiency trade-off. The burden and the rise of the accuracy (up to 0.77 and 0.75) of EfficientNetV2 and EfficientNetB0 are stable due to controlled losses, which protodeternalizes their effectiveness in fracture classification.

Discussion

The findings of this study highlight the potential of ensemble deep learning models, particularly ResNet50 and ResNet101, for the multiclass classification of femur and pelvic fractures. ResNet101 achieved the best overall performance with a test accuracy of 80%, precision of 81.7%, and recall of 80%, indicating strong generalization across all fracture classes. ResNet50 followed closely, providing slightly lower accuracy (79.8%) but requiring less training time, which may make it more suitable for clinical deployment. These results demonstrate that residual architectures with transfer learning are highly effective for capturing subtle fracture patterns in X-ray imaging.

Compared to previous studies, our framework provides improved multiclass classification capability. For instance, (Sevinç et al., 2025) used VGG-16 for femoral-neck fracture detection but were limited by single-center data and restricted subtype classification. In contrast, our dataset was collected from multiple hospitals across Sri Lanka, increasing the diversity and robustness of the models. Similarly, (Inoue et al., 2022) employed a residual CNN with GAN-based augmentation and reported high accuracy (86%) but were constrained to three fracture categories. Our study extends the classification to five clinically relevant categories, thereby offering greater diagnostic granularity.

Other recent works, such as (Mu et al., 2021), which used a Vision Transformer (ViT), achieved excellent results (AUC = 0.988), but required paired AP and lateral radiographs, which may not always be available in clinical workflows. In contrast, our approach relies on single-view X-rays, making it more practical for real-world scenarios. Furthermore, models like Faster R-CNN combined with ResNet50 (Moon et al., 2022) faced issues of class imbalance and reduced accuracy in rare fractures. We addressed this limitation through dataset augmentation and the adoption of ensemble strategies, which enhanced classification stability across different fracture types. The dataset used in this study comprised 1,000 X-ray images collected from five major hospitals, including Base Hospital Tellipalai Jaffna, Northern Central Hospital Jaffna, Teaching Hospital Batticaloa, Aathura Hospital, and Venus Specialty Hospital Pvt Ltd. Expert radiologists were consulted during dataset preparation to confirm fracture type annotations, ensuring clinical validity of the labels. Images were evenly distributed across classes where possible, although non-displaced fractures remained underrepresented, consistent with their lower prevalence in real-world clinical data.

In terms of computational resources, all models were trained using GPU-enabled environments, which facilitated efficient fine-tuning of large pre-trained networks such as ResNet and EfficientNet. While ResNet101 required more time to train, its superior performance justifies the additional computational cost, particularly for offline diagnostic support systems. MobileNet, on the other hand, demonstrated faster training (251s) but at the expense of accuracy (72.7%), suggesting its use may be limited to resource-constrained applications.

Overall, our study confirms the utility of pre-trained deep architectures for fracture classification, addressing limitations of earlier works that struggled with dataset diversity, class imbalance, and limited subtype coverage. The proposed framework not only demonstrates strong predictive performance but also offers clinical practicality by enabling automated, fine-grained fracture detection from standard radiographs. Future work will focus on expanding the dataset, incorporating multi-view imaging where feasible, and exploring explainable AI approaches to enhance trust and adoption in clinical practice.

Conclusion

This paper shows that pre-trained deep learning architectures such as InceptionV3, ResNet50, ResNet101, MobileNet, EfficientNetB0, EfficientNetV2, and Xception are very useful in the multiclass classification of femur and pelvic fractures in X-ray images than custom CNN methods because they actively use pre-trained features of large-scale data such as ImageNet. Although ResNet101 required more time to train, 1817.57 seconds, the model achieved the best performance with a test accuracy of 0.8000, a precision of 0.8179, a recall of 0.8000, and an F1-score of 0.7690, which highlights the good generalization ability of the model. ResNet50 offered a trade-off between performance (accuracy = 0.7786) and efficiency (1237.22 seconds) that might be good enough to be deployed in the clinical environment. Although MobileNet is the fastest with the time to converge as 251.44 s, it produced the minimum accuracy of 0.7271. These findings also emphasize fracture classification advantages with pre-trained models over custom models to make use of larger and diverse datasets to further improve the accuracy of these models and enable clinical decision-making in relation to femur and pelvic fracture treatment.

References

Alzaid, A., Wignall, A., Dogramadzi, S., Pandit, H., & Xie, S. (2022). Automatic classification and classification of peri-prosthetic femur fracture. *International Journal of Computer Assisted Radiology and Surgery*, *17*(4), 649–660.

Beyaz, S., Açıcı, K., & Sümer, E. (2020). Femoral neck fracture classification in x-ray images using deep learning and genetic algorithm approaches. *Joint Diseases and Related Surgery*, *31*(2), 175.

Hsieh, S., Chiang, J., Chuang, C., Chen, Y., & Hsu, C. (2023). A computer-assisted diagnostic method for accurate classification of early nondisplaced fractures of the femoral neck. *Biomedicines*, *11*(11), 3100.

Inoue, D., Aoki, T., Ueda, T., & et al. (2022). Automated classification of hip fractures using deep convolutional neural networks with radiographic image augmentation. *Scientific Reports*, *12*(1), 12345. https://doi.org/10.1038/s41598-022-15721-2

Krogue, J. D., Cheng, K. V., Hwang, K. M., Toogood, P., Meinberg, E. G., Geiger, E. J., Zaid, M., McGill, K. C., Patel, R., Sohn, J. H., Wright, A., Darger, B. F., Padrez, K. A., Ozhinsky, E., Majumdar, S., & Pedoia, V. (2020). Automatic hip fracture identification and functional subclassification with deep learning. *Radiology: Artificial Intelligence*, *2*(3), e190023. https://doi.org/10.1148/ryai.2020190023

Moon, G., Kim, S., Kim, W., Kim, Y., Jeong, Y., & Choi, H.-S. (2022). Computer aided facial bone fracture diagnosis (ca-fbfd) system based on object classification model. *IEEE Access*, *10*, 79061–79070.

Mu, L., Qu, T., Dong, D., Li, X., Pei, Y., Wang, Y., Shi, G., Li, Y., He, F., & Zhang, H. (2021). Fine-tuned deep convolutional networks for the classification of femoral neck fractures on pelvic radiographs: A multicenter dataset validation. *IEEE Access*, *9*, 78495–78503.

Mutasa, S., Varada, S., Goel, A., Wong, T., & Rasiej, M. (2020). Advanced deep learning techniques applied to automated femoral neck fracture classification and classification. *Journal of Digital Imaging*, *33*(5), 1209–1217.

Qi, Y., Zhao, J., Shi, Y., Zuo, G., Zhang, H., Long, Y., Wang, F., & Wang, W. (2020). Ground truth annotated femoral x-ray image dataset and object classification based method for fracture types classification. *IEEE Access*, *8*, 189436–189444.

Sevinç, O., Yilmaz, C., & Çamurcu, Y. (2025). Detection and classification of femoral neck fractures from plain pelvic x-rays using deep learning and machine learning methods. *Acta Orthopaedica et Traumatologica Turcica*, *59*(1), 12–20.

Sharrab, Y., Al-shboul, S., Alsmira, M., Dwekat, Z., Alsmadi, I., & Al-Khasawneh, A. (2021). Performance comparison of several deep learning-based object classification algorithms utilizing thermal images. *Proceedings of IEEE Conference*, 16–22.

Ukai, K., Rahman, R., Yagi, N., Hayashi, K., Maruo, A., Muratsu, H., & Kobashi, S. (2021). Detecting pelvic fracture on 3d-ct using deep convolutional neural networks with multi-orientated slab images. *Scientific Reports*, *11*(1), 11716.

Wang, L.-X., Zhu, Z.-H., Chen, Q.-C., Jiang, W.-B., Wang, Y.-Z., Sun, N.-K., Hu, B.-S., Rui, G., & Wang, L.-S. (2023). Development and validation of a deep-learning model for the classification of non-displaced femoral neck fractures with anteroposterior and lateral hip radiographs. *Quantitative Imaging in Medicine and Surgery*, *14*(1), 527.

Xing, P., Zhang, Y., Wang, L., Li, X., Liu, Y., & Zhang, J. (2024). A deep learning algorithm that aids visualization of femoral neck fractures using faster r-cnn and densenet-121. *Journal of Orthopaedic Surgery and Research*, *19*(1), 123.

Zhou, H., Liu, Y., Wang, J., Li, P., & Zhang, X. (2025). Invisible yet detected: Pelfanet with attention-guided anatomical fusion for pelvic fracture diagnosis. *arXiv preprint*.

|ICAS2025|

Assessment of Ecological Significance, Environmental Challenges, and Conservation Strategies in Dunumadalawa Forest Reserve, Kandy, Sri Lanka

M.R.M.Fernando[1], H.D.Jayathilake[1], G.K.L.C.Kumara[2]

[1]Department of Agricultural Engineering, Faculty of Agriculture, University of Peradeniya, Sri Lanka
[2]Centre for Environmental Studies and Sustainable Development, Faculty of Natural Sciences, Open University of Sri Lanka, Nugegoda, Sri Lanka

Abstract: This study assesses the ecological significance, environmental challenges, and conservation needs of the Dunumadalawa Forest Reserve. It is a semi-isolated wet zone forest fragment within Kandy City, Sri Lanka. When considering its limited size and history of plantation-based disturbance, Dunumadalawa has a rich biodiversity, including 13 endemic bird species (39.4% of Sri Lanka's endemics), 29 endemic bird subspecies, diverse carnivores such as the Sri Lankan Leopard (*Panthera pardus kotiya*) and Fishing Cat (*Prionailurus viverrinus*), and 31 species of pteridophytes. Data were collected through ecological surveys, camera trapping (2019–2021), floristic assessments, and key informant interviews to examine biodiversity patterns and human–wildlife interactions. The findings highlight severe environmental pressures, including habitat fragmentation, invasive alien species such as *Myroxylon balsamum* and *Lantana camara*, and the spread of pine plantations that suppress native flora. Based on these observations, the study recommends targeted conservation measures, including invasive species control, native reforestation, community awareness programs, continuous biodiversity monitoring, and stronger institutional coordination for habitat management. This research emphasizes the critical role of Dunumadalawa as a biodiversity refuge within an urban matrix and provides actionable recommendations for its sustainable protection.

Keywords: biodiversity conservation, Dunumadalawa Forest Reserve, ecological restoration, urban forest

Introduction

Sri Lanka is famous for its rich flora and fauna, boasting the main type density for flowering plants, amphibians, reptiles, and mammals in the Asian country relative to its size (Gunawardene et al., 2007). However, environmental change, human population growth, and a growing ecological footprint pose substantial threats to its ecosystems. Habitat loss and degradation are happening at an alarming rate, mainly in the wet and intermediate zones where many endemic and threatened mammals are concentrated. Small urban forests and marshes, vital for species like fishing cats and brown mongooses, are particularly exposed to conversion for human use (Wijesinghe & Jayasekara, 2020; Yapa, 2017).

Dunumadalawa Forest Reserve (7°17'00"N; 80°38'49"E, 548–972 m above sea level), also known as Walker Estate or 'Waraka Wattha', is a 480 ha semi-isolated, mid-country wet-zone forest fragment situated within the municipal limits of Kandy City. Historically, the site was used for tea and cocoa plantations, resulting in mainly secondary growth forest with only a few remaining primary forest patches (Perera et al., 2001). This reservation helps to supply water to Kandy city as the catchment area for Dunumadalawa lake and Roseneath reservoirs. Despite its disturbed history and urban enclosure, new studies reveal its biological importance. This paper integrates findings from several ecological studies conducted in Dunumadalawa to underscore its unique conservational significance, detail the environmental pressures it faces, and outline actionable explanations for its long-term protection.

Related Work

Dunumadalawa is recognized by scholars as one of the key centers of bird endemism in Sri Lanka. Out of 33 bird species endemic to the country, Dunumadalawa has 13, which makes it home to around 39.4% of the national total (Hettiarachchi & Wijesundara, 2017). Furthermore, the region contains 29 endemic subspecies. It demonstrates the significance of the area for not only ornithological research but also conservation efforts.

In addition, the forest is part of the Sri Lankan Moist Forests ecoregion. It is known to have exceptionally high diversity and endemicity. It constitutes 15 endemic plant genera with 55 species, thus making it an important region for the conservation of flora and fauna (Lanka, 2022). In addition to the unique ecological features of the region, the value of this forest as an irreplaceable piece in the puzzle of biodiversity in Sri Lankan habitats strengthens the need for conservation.

When discussing its biodiversity value, the Dunumadalawa Forest Reserve is under threat from a variety of anthropogenic factors. Habitat fragmentation is one of the most serious threats. Urban development and agricultural land extension continue to lead to loss of and degradation of forest patches, hence contributing to species decline and ecosystem functionality (Hettiarachchi & Wijesundara, 2017).

Secondly, invasive alien plant species pose a major danger to local biodiversity. (Pethiyagoda, 2012) remarks that invasive species will replace the native vegetation, particularly where there is a recovering or disturbed ecosystem. Although threatened species still exist in some forest regenerating patches, alien species invasion plays a vital role in destroying natural ecological balances.

It takes efficient conservation methods to mitigate these environmental issues. Another primary objective of this study is to strengthen and improve the protected area network. In order to maintain ecosystem services and biodiversity, (Kittle et al., 2018) emphasize the importance of strengthening ecological connections among forest parts. Furthermore, to ensure long-term ecological resilience, (Lanka, 2022) recommends integrating these protected areas into broader land-use planning projects.

The role that local communities play in conservation is equally important. It has been demonstrated that involving local stakeholders in sustainable forest management and conservation practices increases the success of environmental protection programs (Lanka, 2022). Through community-based conservation, ecological and social sustainability can be ensured.

Materials and Methods

Study Area

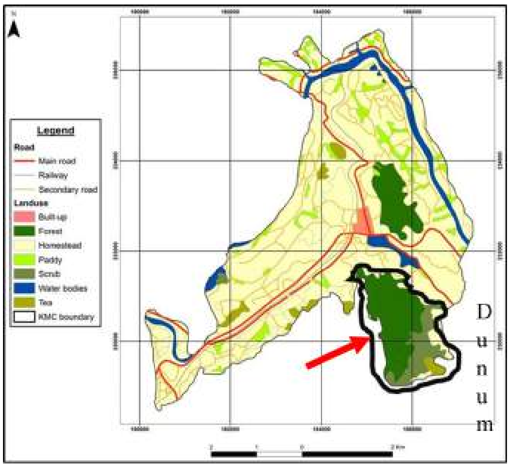

Figure **(1)**|Dunumadalawa Forest, Kandy Municipal Council

Source: Author compiled using GIS analysis based on satellite data

Dunumadalawa Forest Reserve is located at 7°17'00"N; 80°38'49"E, at an elevation of 548–972 m above sea level.

Method of Data Collection

The research on the Dunumadalawa Forest Reserve combined findings from several ecological studies to assess its unique conservation significance and environmental protection. The data collection methods mainly focused on biodiversity monitoring and understanding human impacts. Data were obtained from the Dunumadalawa Catchment Service Office.

Carnivore Monitoring

Camera trapping surveys were conducted between 2019 and 2021 to record and monitor carnivore species, especially wild cats and other small carnivores. This continuous effort helps in understanding their population trends, distribution, and interactions.

Human–Wildlife Interaction Assessment

Key informant interviews were conducted with 15 villagers, 3 catchment area officers, and 2 working supervisors to obtain detailed information on human–carnivore conflicts and related activities in the areas surrounding the reserve. These interviews provided valuable empirical data on conflict frequency, affected locations, and community responses.

Floristic Research

Studies focused on the floristic richness and population structure of the vegetation, with a particular focus on under-studied groups such as pteridophytes, to establish baseline taxonomic data.

Avifaunal Diversity Assessment

Surveys were conducted to assess avifaunal diversity, with results reported using diversity indices like Shannon and Simpson, providing a comprehensive evaluation of bird species present in the forest.

Results and Discussion

Unique Ecological Significance of Dunumadalawa Forest Reserve

Despite its limited area and history of anthropogenic disturbance, the Dunumadalawa Forest Reserve functions as a critical ecological enclave within a densely urbanized landscape, supporting substantial taxonomic diversity across both flora and fauna. Its ecological significance is reflected in the representation of multiple species groups and their contribution to the region's overall biodiversity.

Carnivore Diversity

The reserve is a major site for monitoring small wild cats and other carnivores. Camera trapping surveys from 2019 to 2021 recorded important species including the Sri Lankan Leopard (*Panthera pardus kotiya*), Fishing Cat (*Prionailurus viverrinus*), and Rusty spotted Cat (*Prionailurus rubiginosus*). Other recorded carnivores include Brown, Grey, Ruddy, and Stripe-necked mongooses, as well as Palm, Ring-tailed, and Golden Palm Civets. Notably, the Sambar Deer (*Rusa* *unicolor*) was recorded for the first time in this catchment area through camera trapping. The presence of these species, Vulnerable or Near Threatened by IUCN (e.g., Fishing Cat, Rusty-spotted Cat, Leopard, Sloth Bear), highlights Dunumadalawa's role in the conservation of vulnerable carnivore populations.

Avifaunal Endemism and Diversity

Dunumadalawa has higher avifaunal diversity compared to adjacent home gardens, with Shannon (H') and Simpson (1-D) diversity indices of 3.56 and 0.959, respectively. The forest is a vital refuge for endemic and restricted-range bird species. The most abundant endemic bird species include the Yellow-fronted Barbet, Brown-capped Babbler, Crimson-fronted Barbet, Sri Lanka Scimitar Babbler, and Sri Lanka Wood-Pigeon. This high level of endemism underscores the importance of Dunumadalawa as a "habitat island" within urban sprawl.

Pteridophyte Significance

Some pteridophytes in the forest possess important medicinal value, being utilized in traditional Ayurvedic medicine for their antioxidant, anti-inflammatory, and antimicrobial properties. Locally common threatened species include *Tectaria polymorpha* and *Christella hispidula* (Vulnerable) and *Selaginella crassipes* (Near Threatened, Red List of Sri Lanka 2020).

Environmental Challenges

The Dunumadalawa Forest Reserve faces several environmental threats that endanger its rich biodiversity.

Environmental Degradation and Fragmentation

The reserve is a semi-isolated forest fragment surrounded by mixed land uses including urban areas, villages, home gardens, grasslands, and tea plantations. This isolation and extreme fragmentation contribute to its vulnerability. Human activities in and around the reserve increase threats to wildlife and alter diversity, distribution, and activity patterns. Deforestation for timber occurs occasionally within the protected area, altering vegetation composition and habitat features.

As shown in Figure 3, significant land use changes occurred in the Kandy Municipal Council area between 2010 and 2020. Vegetation cover has decreased, reflecting rapid urbanization within the region.

Invasion by Alien Invasive Species

This is identified as one of the most direct and pervasive threats to the natural flora, including pteridophytes.

Myroxylon balsamum (Katta Kumanchal): This species is critically outcompeting and overcrowding most environments, with some areas of the forest being completely invaded, thereby sweeping out natural flora and significantly obstructing the regeneration of pteridophytes. Its invasive success is attributed to mass flowering, self-pollination, large fruit production, seed tolerance to many light conditions, and the absence of specific pests, leading to a high seed bank.

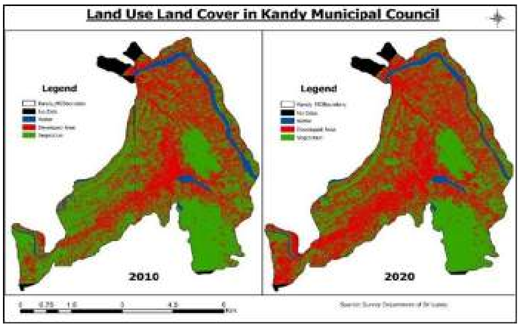

Figure **(2)**|Land use change in Kandy Municipal Council

Other Invasive Species: *Clusia rosea* (Gal Demata), *Lantana camara* (Hinguru), and *Clidemia hirta* (Kata Kalu Bowitiya) are also increasingly invading the forest, presenting a major threat to native flora and dependent fauna, adversely affecting the ecological balance.

Pine Plantations: A Caribbean Pine plantation covers more areas in the reserve; approximately 40–44 hectares exist at the southeastern part of the reserve. This monoculture alters forest habitat and supports poorly developed understory layers, leading to a lack of pteridophytes in those areas.

Human-Wildlife Conflict: Hunting and killing to avoid conflict remain a major concern for large charismatic species in Sri Lanka. This highlights a broader challenge in human-mediated landscapes that could potentially affect carnivores within or near Dunumadalawa forest.

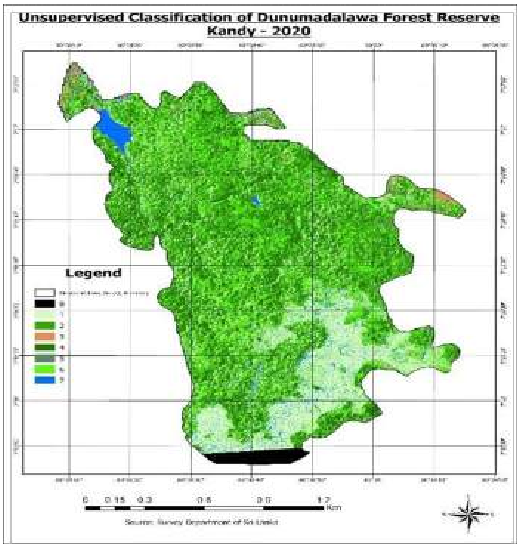

Figure **(3)**|Forest cover classification and boundary
Source: Author compiled using GIS analysis based on satellite data

Table **(1)**|Carnivore Species Recorded in Dunumadalawa As shown in Table (1), some carnivore species have been recorded in Dunumadalawa, all of which are listed as Vulnerable under the national IUCN status finding in field observations.

Common Name	**Scientific Name**	**IUCN Status (SL)**
Sri Lankan Leopard	*Panthera pardus kotiya*	Vulnerable
Fishing Cat	*Prionailurus viverrinus*	Vulnerable
Rusty-spotted Cat	*Prionailurus rubiginosus*	Near Threatened
Sambar Deer	*Rusa unicolor*	Not Listed (rare record)
Sloth Bear	*Melursus ursinus*	Vulnerable
Brown Mongoose	*Herpestes fuscus*	Least Concern
Grey Mongoose	*Herpestes edwardsii*	Least Concern
Ruddy Mongoose	*Herpestes smithii*	Least Concern
Stripe-necked Mongoose	*Herpestes vitticollis*	Least Concern
Ring-tailed Civet	*Viverricula indica*	Least Concern
Golden Palm Civet	*Paradoxurus zeylonensis*	Near Threatened
Common Palm Civet	*Paradoxurus hermaphroditus*	Least Concern

Table **(2)**|Avifaunal Diversity in Dunumadalawa Forest Reserve (Hettiarachchi & Wijesundara, 2017)

Category	**Number**	**Total in SL**	**Percentage**
Endemic Bird Species	13	33	39.40%
Endemic Bird Subspecies	29	68	42.70%
Restricted-Range Species	10	23	43.50%

Suggested Conservation Strategies

Real conservation of Dunumadalawa Forest Reserve requires a multi-pronged approach that addresses both direct threats and long-term ecological stability.

Targeted Habitat Conservation and Improvement

Invasive Species Removal: Direct and sustained actions are vital to control and remove invasive species, especially *Myroxylon balsamum*, *Clusia rosea*, *Lantana camara*, and *Clidemia hirta*. This is essential for proper forest management and protection programs focused on restoring native vegetation composition.

Natural Species Reforestation: Continuous programs are needed to remove Pinus plantations and replant with important native species. This improves water retention, water availability, groundwater recharge, and increases forest habitat for animals and plants.

Importance of Habitat Restoration: Restoration should improve current environments and create new habitats without disturbing the natural ecosystem, focusing on areas vital for endemic and threatened species.

Comprehensive Biodiversity Monitoring and Research

Continuous Carnivore Monitoring: Maintain and expand camera trapping across the reserve to improve knowledge of population trends, distribution, and interactions of carnivores, especially wild cats. **Interviews and Data Collection:** Conduct key informant interviews with villagers, catchment area officers, and supervisors to gather crucial empirical data on human-carnivore conflict, threats, and activities in different landscapes.

Floristic Research: Continue studies on floristic richness, species composition, and population structure, particularly for under-studied groups like pteridophytes, to generate baseline taxonomic data for sustainable management.

Threat Mitigation Evaluation: Monitor the impacts of applied conservation practices to improve threat mitigation methods.

Public Awareness and Instruction Programs

Develop Awareness Resources: Prepare multi-lingual educational materials, such as posters and brochures, focusing on wildlife, habitats, and forest protection. These resources should be designed by local artists and informed by direct project observations.

Organize Educational Events: Conduct lessons for school children (e.g., via school and university programs) and the wider public, incorporating study results.

Youth Camp Programs: Host youth camps for school children and university students studying zoology, ecology, and botany. These programs should provide practical lessons on wildlife monitoring, including camera trapping, mammal monitoring, and radio telemetry, and explore diverse environments.

Install Information Boards: Place permanent information boards in the reserve to educate the public about the forest, its protection, and its species.

Establishment of Teamwork Units and Capacity Building

Inter-organizational Teamwork: Collaborate with government and private organizations like the Department of Wildlife Conservation to provide resources such as vaccines and rehabilitation enclosures for wild cats.

Table **(3)**|Invasive Alien Species in Dunumadalawa Forest Reserve

Species Name	**Local Name**	**Impact Type**	**Invasion Severity**
Myroxylon balsamum	Katta Kumanchal	Displaces native flora, inhibits fern regrowth	High (dominant in some areas)
Clusia rosea	Gal Demata	Overcrowds native plants	Medium
Lantana camara	Hinguru	Alters understory composition	Medium
Clidemia hirta	Kata Kalu Bowitiya	Dense thickets limit sunlight	Medium

Table **(4)**|Protection Activities (Proposed/Ongoing)

Activity Type	**Specific Action**	**Status**
Invasive Species Management	Removal of *Myroxylon*, *Lantana*, etc.	Ongoing
Habitat Restoration	Replace pine with native tree species	Ongoing/Planned
Biodiversity Monitoring	Camera trapping (Phase 1 & 2)	Active
Community Engagement	School talks, posters, youth camps	Ongoing
Capacity Building	Wildlife officer training, vet support	Planned
Research	Pteridophyte surveys, bird monitoring	Ongoing

Park Management Training: Conduct workshops for park management teams, including veterinary and animal management training, to enhance wildlife protection and management capacity.

Local Initiatives: Provide practical guidance to support local management initiatives for biodiversity protection, acknowledging that protected areas alone may not be sufficient.

Several protection and conservation initiatives have been proposed or are currently being implemented within the study area to enhance ecosystem stability and community resilience. These activities focus primarily on soil and water conservation, restoration of degraded lands, and sustainable land-use practices. Ongoing measures include the establishment of vegetative buffers, reforestation of catchment areas, and rehabilitation of traditional tank systems to improve water retention and reduce runoff losses.

Conclusion

The Dunumadalwa Forest Reserve is a significant ecological feature of the Central Hill region of Sri Lanka due to its high diversity of carnivores, birds, and pteridophytic flora, even though it is an anthropogenically disturbed secondary forest within an urban area. Continuing threats, primarily from invasive alien plant species and the impacts of historical land-use changes, require urgent, ongoing conservation action. If strategies prioritizing habitat restoration, aggressive invasive species management, ecological restoration, public awareness, and collaborative capacity building are implemented, Dunumadalawa can continue to represent a significant haven for our unique and endangered biota. Its special status as an urban "habitat island" makes its conservation essential and offers valuable lessons for conserving biodiversity in human-altered landscapes globally.

References

Gunawardene, N. R., et al. (2007). A brief overview of the western ghats and sri lanka biodiversity hotspots. *Journal of Biodiversity*, *8*, 1–15.

Hettiarachchi, L., & Wijesundara, S. (2017). Bird endemism in small urban forest fragments of sri lanka. *Ornithological Studies*, *22*, 33–45.

Kittle, R., et al. (2018). Strengthening ecological networks in fragmented forests. *Conservation Biology*, *32*, 123–135.

Lanka, W. S. (2022). Sri lankan moist forests: Biodiversity and conservation strategies [Accessed online].

Perera, K., et al. (2001). Secondary forest regeneration and plantation history in mid-country sri lanka. *Tropical Forestry Journal*, *15*, 101–112.

Pethiyagoda, R. (2012). Invasive species and ecological balance in sri lanka. *Biodiversity Reports*, *7*, 12–23.

Wijesinghe, P., & Jayasekara, R. (2020). Urban forest conservation and human-wildlife interactions in sri lanka. *Environmental Studies*, *12*, 45–59.

Yapa, S. (2017). Challenges of conserving wet zone mammals in urban sri lanka. *Asian Wildlife Journal*, *10*, 77–88.

|ICAS2025|

Impact of Sprinkler Irrigation on Yield and Cultivation costs in Groundnut and Jumbo peanut farming in Kilinochchi District

T.Lathusha[1], K.Sooriyakumar[1], S.Sivashankar[1], S.Sarujan[1]

[1]Department of Agricultural Economics Faculty of Agriculture, University of Jaffna, Sri Lanka

Abstract: The adoption of climate-smart agricultural practices has become essential for mitigating the challenges posed by climate change in dry-zone agriculture. However, the effectiveness of these practices remains uncertain due to low awareness and poor adoption rate of such technologies, especially among small-scale farmers. Therefore, this study focuses on the adoption of a climate-smart practice- sprinkler irrigation- by small-scale groundnut and jumbo peanut producers in northern Sri Lanka and evaluates its effectiveness of sprinkler irrigation adoption on farm outcomes such as yield and cultivation cost. Primary data for this study were collected using stratified random sampling technique from 257 small-scale farmers engaged in ground nut and Jumbo peanut cultivation in the Kilinochchi district in northern Sri Lanka. The dataset includes farm output measures, adoption status, and socio-demographic characteristics of farm households. Among jumbo peanut farmers, 124 are adopters of sprinkler irrigation practices, and 50 have not. Among the groundnut farmers, 31 are adopters, and 52 are non-adopters. The impact of sprinkler adoption was estimated using propensity score matching technique. The results indicate that sprinkler adopters experience a yield increase of 178 kg per acre for groundnuts and 30 kg per acre for jumbo peanuts compared to non-adopters. Additionally, the results show that sprinkler adopters experience a reduction in cultivation cost by Rs. 45,040 per acre in groundnut cultivation and by Rs. 59,399 per acre in jumbo peanut cultivation compared to their counterparts. These findings highlight the importance of adopting of sprinkler irrigation as a viable strategy to mitigate the climate challenges faced by small-scale groundnut and jumbo peanut producers.

Keywords: climate smart agriculture, groundnut, jumbo peanut, propensity score matching, sprinkler irrigation

Introduction

Water scarcity poses a significant challenge to agriculture, as it limits the availability of one of the most essential resources for crop production. Micro irrigation technology, including sprinkler irrigation, offers a practical solution to address this issue by optimizing water usage. This technology, which applies water as a spray to crops, has gained widespread adoption worldwide due to its ability to improve agricultural efficiency. By ensuring precise water application, sprinkler irrigation not only mitigates the impact of irregular and inconsistent rainfall (Ghintala & Singh, 2013) but also addresses the uneven distribution of limited water resources (Gardens, 2023). This makes sprinkler irrigation an essential tool in overcoming the water scarcity challenges of the twenty-first century, particularly in the face of growing agricultural demands and climate change (Kumar et al., 2009).

On the one hand, sprinkler irrigation is a reliable and suitable climate-smart adaptation practice that can result in vast improvements in agricultural production and assure the economic vitality of a region. On the other hand, the implementation failures of sprinkler irrigation projects are quite common, especially among the small-scale farmers due to poor follow-ups, financial constraints, and lack of awareness on new technologies. For example, the Government of Sri Lanka in collaboration with a few NGOs introduced Micro Irrigation System (MIS) under a subsidy scheme, however, the majority of the farmers had discontinued or never used the technology provided. (Punniyarajah, 2022) reported that clogging of nozzles due to poor-quality water, lack of technology and awareness on the importance of using MIS, high cost for installation and expecting high profit within a year, reluctance to shift from traditional irrigation methods, and the lack of after-sales services and spare parts were the reasons for the discontinuation of this MIS in several places (Sugirtharan, 2017). This study aims to provide strong empirical evidence on the effectiveness of adopting sprinkler irrigation by evaluating the case of sprinkler adoption in Groundnut and Jumbo Peanut Farming in Kilinochchi District in northern Sri Lanka.

Objective: To estimate the impact of sprinkler irrigation practices on groundnut production and cultivation costs in Kilinochchi district.

Hypotheses:

1. Groundnut farmers, who adopt sprinkler irrigation systems experience a higher yield compared to those who do not.
2. The adoption of sprinkler irrigation systems significantly reduces groundnut cultivation costs.
3. Farmers' socio-economic characteristics positively influenced their adoption.

Figure **(1)**|Administrative map of Kilinochchi district (Punniyarajah, 2022)

Data and Method

Description of the study area and Data collection

The study was conducted across the Groundnut and Jumbo peanut cultivation areas of Kilinochchi District, which is located in the Northern Province of Sri Lanka. A well-structured questionnaire was used to gather information from 124 jumbo peanut farmers who had adopted sprinkler irrigation and 50 who had not, as well as 31 groundnut farmers who had adopted sprinkler irrigation and 52 who had not, across 95 GN divisions and was analyzed using STATA software.

Empirical Method

To know the effect of sprinkler irrigation by a farmer adopting sprinkler method, the observed outcome of a farmer adopting sprinkler irrigation must be compared with the outcome that would have resulted if the farmer had not adopted sprinkler irrigation. This study estimates the effect of sprinkler adoption on yield and cultivation expenses using propensity score matching, which accounts for selection bias (Rosenbaum & Rubin, 1983). By finding people who share comparable observable features, the matching approach finds a matching individual for each member of the treatment group from the comparison group.

In general, unobservable characteristics determining adoption of sprinkler irrigation can also affect outcomes. Highly motivated farmers are most probably adopting sprinkler irrigation and also most probably get higher yield or produce at the lowest cost of cultivation. The estimated treatment effect will be biased unless sample selection issues are addressed. The effect of adopting sprinkler irrigation can be described by two processes. First, the decision to adopt sprinkler irrigation takes place. Second, we estimate the impact of adopting sprinkler irrigation system on groundnut cultivation. In this study, to generate a propensity score for each observation, a logit regression model is developed with adopting sprinkler irrigation as the dependent variable and the potential covariates, socio-economic characteristics and extent of groundnut cultivation, as explanatory variables. In the case of a binary treatment, the dummy value for the treatment (adopting sprinkler) $Y_i = 1$ if individual treated and 0 if not treated (Shehu & Sidique, 2014).

The Average Treatment Effect (ATE) is defined as:

$$ATE = E(Y_i(1) \mid D = 1) - E(Y_i(0) \mid D = 0) \qquad (1)$$

where Y_i is the outcome effect, and D is the adoption status.

The Average Treatment Effect on the Treated (ATT) can be defined as:

$$ATT = E(Y_i(1) \mid D = 1) - E(Y_i(0) \mid D = 1) \qquad (2)$$

Results and Discussion

As the first step, propensity scores were estimated for the adoption of sprinkler irrigation systems using a logistic regression model.

Jumbo Peanut Farmers

Table **(1)**|Logit model result for adopting sprinkler irrigation in Jumbo peanut farmers

Sprinkler	Coefficient	Standard Error	p > [z]
Age	-0.0004	0.0218	0.984
Gender	-0.0399	0.5473	0.942
Education	0.0182	0.1055	0.862
Non-farm income	-0.0000	0.0000	0.754
Family labour	-0.5080**	0.2051	0.013
Extent	2.3370**	1.1465	0.042
Cost of cultivation	-0.0000***	0.0000	0.000
Constant	4.4277	2.1347	0.038

Table **(2)**|Logit model result for adopting sprinkler irrigation in groundnut farmers

Sprinkler	Coefficient	Standard Error	p > [z]
Age	-0.0420	0.0264	0.112
Gender	-1.1792*	0.6438	0.067
Education	0.0198	0.1097	0.857
Non-farm income	-0.0000	0.0000	0.294
Family labour	-0.1920	0.2380	0.420
Extent	1.5139	1.1423	0.185
Cost of cultivation	-0.0000	0.0000	0.123
Training	3.0035***	0.7656	0.000
Constant	1.8408	2.0836	0.377

For Jumbo peanut farmers, the cost of cultivation has a highly significant negative impact on sprinkler use, indicating that higher costs reduce the likelihood of adoption. Family labor also shows a significant negative effect, suggesting that households relying more on family members are less likely to use sprinklers. In contrast, the extent of land has a positive and significant effect, meaning that farmers with larger cultivated areas are more likely to adopt sprinkler systems.

For groundnut farmers, training has a highly significant positive effect on sprinkler use. This indicates that farmers who receive training are much more likely to adopt sprinkler irrigation, showing that training programs are highly effective in promoting the use of modern irrigation techniques.

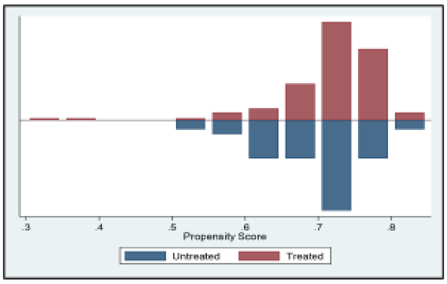

Figure **(2)**|Distribution of Propensity Score across Treatment and Comparison Groups of Jumbo peanut farmers

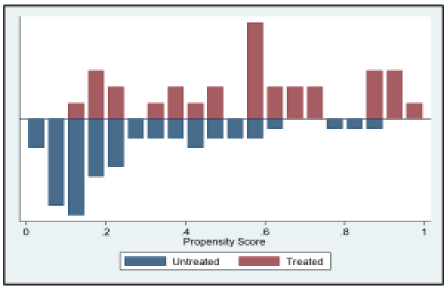

Figure **(3)**|Distribution of Propensity Score across Treatment and Comparison Groups of Groundnut farmers

Followed by, graphs of propensity scores (Figures 03, 04) indicate that propensity scores across treatment and comparison groups (groundnut and jumbo peanut) are overlapped. The balance test divides the treatment group into 6 blocks on the basis of the propensity score and showed that mean propensity score is significantly indifferent for treated and comparison group in each block. Also, the individual covariates of the treatment and comparison groups are significantly indifferent from each other within these blocks. This implies that the distribution of propensity scores within each block is similar across groups and that the propensity score is correctly specified.

Crop	Variable	ATE		ATET	
		Coefficient (SE)	$P > [z]$	Coefficient (SE)	$P > [z]$
Groundnut	Yield	177.9518*** (42.2737)	0.000	−7.4194 (44.6069)	0.868
	Cost of Cultivation	−45040.96* (24079.61)	0.061	−43348.39*** (16796.65)	0.010
Jumbo Peanut	Yield	29.4598*** (7.8750)	0.000	30.0564 (1.43)	0.152
	Cost of Cultivation	−59339.08*** (16629.25)	0.000	−43314.52* (24001.75)	0.071

***, **, * == Significance at 1%, 5%, 10% level, Robust Standard errors in parentheses.

Impact on Yield

The estimate of ATE of propensity score matching is 177.95 and significant at 1% level. It indicates that the yield of groundnut of a farmer who was randomly selected, by adopting sprinkler irrigation, will significantly increase yield by around 178 kg per acre. This could be due to improved water use efficiency, uniform water distribution, and reduced water stress during critical growth stages.

The estimate of ATE of PSM is 29.46 and significant at 1% level. It indicates that the Jumbo peanut yield of a randomly selected farmer, through the adoption of sprinkler irrigation practice, will significantly increase by around 30 kg per acre.

Impact on Cultivation Costs

The estimate of ATE of propensity score matching is (-45040.9) and significant at 10% level. It indicates that the cost of cultivation of groundnut of a farmer who was randomly selected, by the adoption of sprinkler irrigation practice, will significantly reduce by around Rs. 45,000 per acre. The estimate of ATET of propensity score matching is (-43348) and significant at 1% level. It indicates that the cost of cultivation of groundnut of a farmer who adopts sprinkler irrigation decreases by Rs. 43,348 per acre. Results suggest that sprinkler irrigation can lead to significant cost savings, particularly for farmers who have fully adopted the system and adjusted their practices accordingly.

The estimate of ATE of propensity score matching is -59,339.08 and significant at 1% level. It indicates that the cost of cultivation of jumbo groundnut of a farmer who was randomly selected, by adopting sprinkler irrigation, will significantly reduce the cost of cultivation by around Rs. 60,000 per acre. The estimate of ATET of propensity score matching is (-43,314.5) and significant at 10% level. It indicates that the cost of cultivation of jumbo groundnut of a farmer who adopts sprinkler irrigation decreases by Rs. 43,314.5 per acre. It suggests that sprinkler irrigation, despite its upfront costs (partially subsidized by ASMP), leads to considerable cost savings in the long run. The savings likely arise from reduced water usage, since sprinklers distribute water more efficiently than traditional methods, minimizing waste, and lower labor costs, as sprinkler systems automate irrigation, reducing the need for manual labor.

Conclusion

This study aimed to evaluate the impact of sprinkler irrigation on groundnut and Jumbo peanut cultivation in terms of yield and cultivation costs, while also identifying factors influencing its adoption. The findings reveal that while sprinkler irrigation significantly reduces cultivation costs for both crops, its impact on yield varies. For groundnuts, the yield benefits are not consistently significant, whereas for Jumbo peanuts, yield increases are observed but are not always statistically significant. The adoption of sprinkler irrigation is strongly influenced by factors such as training, cultivation costs, and farm size, with training emerging as a critical enabler. The findings suggest the government authorities should implement farmer training programs to promote effective use of sprinkler technology by providing financial incentives or subsidies to offset adoption costs, and encouraging larger-scale farming practices to optimize irrigation benefits. These measures can help maximize the efficiency and sustainability of water use in agriculture, thereby addressing broader challenges of water scarcity and agricultural productivity.

Furthermore, the study's findings can inform the design of future irrigation subsidy and farmer-training programs. Targeted subsidies that cover installation and maintenance costs, along with continuous hands-on training, could increase adoption and long-term use of sprinkler systems. Integrating these measures into district-level water management policies can promote sustainable water use, reduce vulnerability to drought, and enhance agricultural resilience in Sri Lanka's dry zone.

References

Gardens, A. (2023). Report on water distribution [Available online].

Ghintala, R., & Singh, A. (2013). Title of the paper on irrigation. *Journal Name*, *10*, XX–XX.

Kumar, S., et al. (2009). Climate change and irrigation efficiency. *Journal Name*, *10*, XX–XX.

Punniyarajah, R. (2022). Micro irrigation adoption in sri lanka [Government Report].

Rosenbaum, P. R., & Rubin, D. B. (1983). The central role of the propensity score in observational studies for causal effects. *Biometrika*, *70*, 41–55.

Shehu, A., & Sidique, S. F. (2014). Propensity score matching in impact evaluation. *Journal of Applied Statistics*, *41*, 123–135.

Sugirtharan, T. (2017). Challenges in micro irrigation implementation [NGO Report].

|ICAS2025|

g-function and h-function of the complement of a slit

Piriyalucksan Paramesvarampillai[1], Arunmaran Mahenthiram[1]

[1]Department of Mathematics and Statistics, University of Jaffna, Sri Lanka

Abstract: In potential theory, h-functions and g-functions are key concepts. These two functions are increasing and take values on the interval $[0,1]$. For a region Ω with a basepoint z_0, the h-function $h(r)$ is the probability that a Brownian particle starting at z_0 inside Ω first hits the boundary of the region within distance r of z_0 before it hits anywhere else on the boundary $\partial\Omega$. The g-function $g(r)$ is the probability that a Brownian traveler, starting from z_0, will first exit the connected component Ω_r^* through the part of the boundary $\partial\Omega_r^*$ that is strictly less than the distance r from z_0, where Ω_r^* is the connected component of $\Omega \cap B(z_0,r)$ that contains z_0. In literature, the functions h and g have been documented for the complement of a ray with different locations of basepoint. However, these functions have not been studied for the complement of a single slit. In this study, we compare the h-function and the g-function of the region $\Omega = \mathbb{C}\backslash[1,2]$ with basepoint $z_0 = 0$. Also, we explain the asymptotic behaviour of these functions. To compute $h(r)$ of the region Ω, we transform the region Ω to a half-plane via the Möbius map followed by the square-root transformation. Then we evaluate the angle of sight, which is the angle subtended by the image of $\partial\Omega \cap \overline{B(z_0,r)}$ at the image of z_0 in the halfplane. To evaluate $g(r)$ for $r \leq 2$, we map the region Ω_r^* to a halfplane by using the sequence of suitable conformal maps. Then we evaluate the angle of sight, which is the angle subtended by the image of $\partial\Omega_r^* \cap B(z_0,r)$ at the image of z_0 in the halfplane. For $r > 2$, the region Ω_r^* becomes a doubly connected region. In this case, we transform Ω_r^* to a concentric annulus, and the harmonic measure at the preimage of the basepoint gives the formula of $g(r)$ for $r > 2$. In summary, we have explained the computation of $h(r)$ and $g(r)$ of $\Omega = \mathbb{C}\backslash[1,2]$ with basepoint $z_0 = 0$. In the future, we are interested in investigating $g(r)$ for multiply connected slit regions.

Keywords: conformal map, g-functions, h-functions, prime functions

Author Note

This research does not receive financial support. The authors declare no conflict of interest.

Introduction

The concept of harmonic-measure distribution function, also known as h-function, was first introduced by Walden and Ward [5] in 1995. To compute the h-function, we always need a region Ω and a fixed point z_0 in Ω. We call this fixed point z_0 as basepoint. For a domain Ω and a basepoint $z_0 \in \Omega$, the h-function $h_{\Omega,z_0}(r)$, simply $h(r)$, is given by the harmonic measure of the set $E_r := \partial\Omega \cap \overline{B(z_0,r)}$ in Ω at z_0, where $B(z_0,r)$ is the open ball of radius r centred at z_0 and $\partial\Omega$ is the boundary of the region Ω. We call $|z - z_0| = r$, the capture circle of radius r centred at z_0 (hereafter we call the capture circle). Moreover, the h-function can be expressed in terms of the harmonic-measure, the solution of Dirichlet problem. In other words, $h(r) = u(z_0)$, where $u(z)$ is a unique function such that $\Delta u = 0$ in Ω with boundary value 1 on E_r and 0 on $\partial\Omega\backslash E_r$.

Our focusing question is to identify the relationships between the shape of the region and the behaviour of the h-function and g-function. The h-functions are well studied for several simply connected regions from the initial paper [5] till now. See the survey article [4] for a summary of this progress. Recently, Mahenthiram [2] studied h-functions and g-functions for some new simply connected regions with bounded or unbounded boundries.

In this study, we focus on the computation of the h-function and the g-function of the simply connected region $\Omega = \mathbb{C}\backslash[1,2]$. In addition, we compare the asymptotic behavior of these functions of the region Ω.

The g-function $g : [0,\infty) \to \mathbb{R}$ is defined for a domain Ω in $\mathbb{C}$ and a basepoint z_0 in Ω by

$$g(r) = g_{\Omega,z_0}(r) := \omega(z_0, E_r^*, \Omega_r^*), \tag{1}$$

where ω denotes harmonic measure, $E_r^* = \partial\Omega_r^* \cap B(z_0,r)$, the term $B(z_0,r)$ in E_r^* denotes the open disc of radius r centered at z_0, and Ω_r^* denotes the connected component of $\Omega \cap B(z_0,r)$ that contains z_0. Thus for each $r > 0$, the number $g(r)$ is the probability that a Brownian traveller, starting from z_0, will first exit the connected component Ω_r^* through the part of the boundary $\partial\Omega_r^*$ that is strictly less than distance r from z_0. We note that in general, the connected component Ω_r^* of $\Omega \cap B(z_0,r)$ may be either the whole of the set $\Omega \cap B(z_0,r)$ or else a proper subset of it, depending on the geometry of Ω and the location of the basepoint z_0 and the value of r.

We use d to denote the shortest distance from the basepoint z_0 to the boundary $\partial\Omega$. We are interested in comparing the g-function with the harmonic-measure distribution function (h-function). The h-function is defined by

$$h(r) = h_{\Omega,z_0}(r) := \omega(z_0, E_r, \Omega), \tag{2}$$

where $E_r = \partial\Omega \cap \overline{B(z_0, r)}$.

Both the h-functions and the g-functions have certain similar behaviours. That is, both functions are non-decreasing and lie between 0 and 1 as these functions represent the probability. Moreover, these functions are equal to zero until the Brownian particle hits any part of the boundary of the domain. Once the particle starts to hit the boundary of the domain, both functions start to increase from zero.

Similarly, there are some differences between these two functions. For the h-functions, we evaluate the harmonic measure at z_0 with respect to the given domain Ω, but for the g-functions, we evaluate the harmonic measure at z_0 with respect to the domain Ω_r^*. For the h-functions, we consider the closed disc of radius r centred at z_0. But for the g-functions, we consider the open disc of radius r centred at z_0. Moreover, we have different E_r for both functions from the formulas (1) and (2). Moreover, from the definition, the h-function is right continuous, but the g-function is left continuous. In addition, the boundary values are zero on $\partial\Omega \backslash E_r$ for the h-functions, while the boundary values are zero on the on $\partial\Omega_r^* \backslash E_r$ for the g-functions. Since d denotes the minimum distance from the basepoint z_0 to the boundary of the domain, and r be the radius of the disc centred at z_0, both the h-functions and the g-functions are zero for $r < d$. But, there is a different behaviour at $r = d$. From the formulas of these functions, the h-function is non-zero at $r = d$ while the g-function is zero at $r = d$.

By the monotonicity of harmonic measure, $g(r) \leq h(r)$ for all $r > 0$ and for all domains Ω. It follows that $1 \leq (1-g)/(1-h)$ for all Ω. We also note that the harmonic measure of a subset of $\mathbb{R}$ in the halfplane is given by the normalised angle of sight from the basepoint.

Materials and Methods

In this section, we provide some necessary information related to this paper, and also explain the process by which we compute h-functions. In addition, we explain certain types of asymptotics that we use for h-functions and g-functions. The computation of both functions is related to conformal mappings and harmonic functions. In one way of computing these functions, we use the sequence of conformal maps. In the other way of computation, we evaluate both functions by solving a particular Dirichlet problem connecting the harmonic function and the boundary values.

Computation of h-functions, g-functions

This section describes the main method to compute the h-functions and g-functions of simply connected domains with the usage of the conformal maps.

For h-functions, we first find the conformal map $f(z)$ which transforms the given domain Ω to a halfplane. Then for $r \in (0, \infty)$, we find the set $E_r := \partial\Omega \cap \overline{B(z_0, r)}$ in Ω and its image $f(E_r)$ in the halfplane. Also, in the halfplane, we identify the image $f(z_0)$ of the basepoint z_0. Finally, we find the *angle of sight* which is the angle subtended by $f(E_r)$ at $f(z_0)$. Then, the normalised angle of sight produces the h-function formula.

For the g-functions, we first identify the region Ω_r^*. Then find the conformal map $f(z)$ to transform the region Ω_r^* to a halfplane. Then for $r \in (0, \infty)$, we find the set $E_r^* := \partial\Omega_r^* \cap B(z_0, r)$ in Ω_r^* and its image $f(E_r^*)$ in the halfplane. Also, in the halfplane, we identify the image $f(z_0)$ of the basepoint z_0. Finally, by finding the angle of sight in the halfplane, we can write the formula of the g-function $g(r)$.

Asymptotics

Walden and Ward introduced the asymptotic behaviour as r decreases to d, namely *purely exponential asymptotics*, in [5].The second type of asymptotics as $r \downarrow r^*(> d)$, has been studied by Matsumoto [3]. He showed that the h-function can be asymptotically linear as $r \downarrow r^*(> d)$, where the derivative of $h(r)$ is discontinuous at r^*. However, "can the h-function be asymptotically linear as $r \downarrow d$?" is still be an open problem.

Walden and Ward [5] defined *Purely exponential asymptotics* as follows: Let Ω be a domain and take a basepoint z_0 in Ω. Let d be the shortest distance between the basepoint z_0 and the boundary $\partial\Omega$. Then the h-function $h(r)$ of the domain Ω has *purely exponential asymptotics with exponent β as r decreases to d*, written as

$$h(r) \sim c(r-d)^\beta \text{ as } r \downarrow d,$$

if there is a real number β such that the limit

$$c := \lim_{r \to d^+} \frac{h(r)}{(r-d)^\beta}$$

exists and is positive.

Results and Discussion

In this section, we describe the computation of both $h(r)$ and $g(r)$ of the complement of a line segment that lies on the real axis. Note that the slit domain is formed by removing a line segment (slit) from the complex plane. This domain is also called the complement of a line segment or slit.

First, we describe the computation of the h-function of the domain $\Omega = \mathbb{C}\backslash[1, 2]$ when the basepoint is $z_0 = 0$. To compute the h-function of this domain, we first transform the domain Ω to a halfplane. We start with the Möbius map $(z-1)/(z-2)$ which sends the points $1, 2, 0$ to the points $0, \infty, 0.5$ respectively. This Möbius map transforms Ω onto the region $\mathbb{C}\backslash(-\infty, 0]$. Then, we use the square-root map to transform the region $\mathbb{C}\backslash(-\infty, 0]$ to a right halfplane. Next, we track the subset E_r and its image in the halfplane. Finally, we find the angle of sight in the halfplane which is given by $2\arctan\sqrt{\dfrac{2(r-1)}{2-r}}$. Hence, the h-function $h(r)$ is given by the normalised angle of sight. That is,

$$h(r) = \frac{2}{\pi}\arctan\sqrt{\frac{2(r-1)}{2-r}}$$

for $1 \le r < 2$.

Near $r = 1$, $h(r) \sim \dfrac{2\sqrt{2}}{\pi}(r-1)^{1/2} = c(r-d)^{\beta}$, where $c = \dfrac{2\sqrt{2}}{\pi}$ and $\beta = 1/2$.

Next, we move our focus to the computation of $g(r)$ of the region Ω when the basepoint is $z_0 = 0$. Here, the region Ω_r^* is the whole of the set $\Omega \cap B(0,r)$. For $r \le d = 1$, the g-function is zero as no part of the boundary of the domain Ω is captured by the open disc of radius r centred at zero. To compute the g-function for $1 < r \le 2$, we start with the Möbius transformation that sends the points $0, -r, r$ to $1, \infty, 0$ respectively. This Möbius map $z \mapsto \dfrac{r-z}{r+z}$ transforms the region Ω_r^* onto the right halfplane with a deleted slit $(0, (r-1)/(r+1)]$. Next, we use the map $z^2 - \left(\dfrac{r-1}{r+1}\right)^2$ to transform the current region onto the complement of the ray $(-\infty, 0]$. Finally, we use the square-root transformation to map the region $\mathbb{C}\backslash(-\infty,0]$ to the right halfplane. By tracking the subset E_r^* and its image in the halfplane, we evaluate the angle of sight and obtain the g-function formula as follows:

$$g(r) = \frac{2}{\pi}\arctan\left\{\frac{r-1}{2\sqrt{r}}\right\} \quad \text{for} \quad 1 < r \le 2.$$

For $r > 2$, the region Ω_r^* is a doubly connected region which is the interior of the disc $B(0,r)$ excluding the line segment $[1,2]$. Now, we use the Möbius map $\dfrac{1}{2}\left[\dfrac{r-z}{r+z}\right]$ to transform the region Ω_r^* to the right halfplane with a deleted line segment $[0.5(r-2)/(r+2), 0.5(r-1)/(r+1)]$. Next, we use the transformation z^2 to map the current region to the complement of the line segment $[0.25((r-2)/(r+2))^2, 0.25((r-1)/(r+1))^2]$ and the ray $(-\infty, 0)$. Next, we use the Möbius map $\dfrac{1-2z}{2(z-1)}$ to transform this new region to the complement of slits $(-1,-0.5) \cup [-(r^2+12r+4)/(3r^2+20r+12), -(r^2+6r+1)/(3r^2+10r+3)]$. Now, we use the inverse of the radial-slit map

$$f(\zeta) = A\frac{P(\zeta/\alpha,\rho)P(\zeta\alpha,\rho)}{P(\zeta/\beta,\rho)P(\zeta\beta,\rho)}$$

to map this region to the concentric annulus. Here, $f(1) = -1$, $f(-1) = -0.5$, $f(-\rho) = -(r^2+12r+4)/(3r^2+20r+12)$, $f(\rho) = -(r^2+6r+1)/(3r^2+10r+3)$ and $A = -\dfrac{P(1/\beta,\rho)P(\beta,\rho)}{P(1/\alpha,\rho)P(\alpha,\rho)}$. For $r > 2$, the g-function is

$$g(r) = \frac{\log|\zeta_0|}{\log\rho},$$

where $\zeta_0 = f^{-1}(-1/3)$.

Near $r = 1$,

$$g(r) \sim \frac{1}{\pi}(r-1) = c(r-1)^{\beta}, \text{where} \quad c = \frac{1}{\pi} \quad \text{and} \quad \beta = 1.$$

Here, near $r = d = 1$, the g-function is asymptotically linear.

From these computations, both $h(r)$ and $g(r)$ are not differentiable at $r = 1$, since their left-hand and right-hand derivatives are not the same.

The significance of studying the h-function and g-function of the above domain is to understand the behaviours of these functions of this particular domain and whether these behaviours coincides with the results that we obtained for other domains.

Conclusion

In this study, we have discussed the computation of the h-function and g-function of the domain $\mathbb{C}\backslash[1,2]$ when the basepoint z_0 is fixed to the left. In addition, we have explained the asymptotic behaviour of these h and g-functions near $r = d$, where d is the minimum distance from the basepoint to the boundary. We note that the h-functions of multiply connected slit domains have been documented in [1] and [2]. We are interested in studying the g-functions of multiply connected slit domains as our future work.

References

[1] Green, C. C., Snipes, M. A., Ward, L. A., Crowdy, D. G. (2022).*Harmonic-measure distribution functions for a class of multiply connected symmetrical slit domains*, Proceedings of the Royal Society A: Mathematical, Physical and Engineering Sciences 478, Paper No. 20210832.

[2] Mahenthiram, A. (2022) *Harmonic-measure distribution functions, and related functions, for simply connected and multiply connected two-dimensional regions*, PhD Thesis, University of South Australia.

[3] Matsumoto, S. (2011). What do random walks tell us about the shapes of regions in the complex plane? Poster, Harvey Mudd College.

[4] Snipes, M. A., Ward, L. A. (2016). *Harmonic measure distributions of planar domains: A survey*, Journal of Analysis 24, 293–330.

[5] Walden, B. L., Ward, L. A. (1996).*Distributions of harmonic measure for planar domains*, Proceedings of 16th Nevanlinna Colloquium, Joensuu, Walter de Gruyter, Berlin, 289–299.

|ICAS2025|

Impact of the 2021 Fertilizer Policy on Paddy Yields and Farmer Income in the South Coastal Region of Ampara District, Sri Lanka

D.M.P.S.Disanayaka[1], A.M.Razmy[1], A.M.Nahfees[2], A.M.A.C.Bandara[1]

[1]Department of Mathematical Science, Faculty of Applied Sciences, South Eastern University of Sri Lanka, Sri Lanka

[2]University Library, South Eastern University of Sri Lanka, Sri Lanka

Abstract: Ampara District plays a key role in paddy production in Sri Lanka. However, there was a noticeable decrease in paddy production during the Maha season of 2021/2022. The purpose of this study is to conduct a comparative analysis of the decline in rice production in the South Coastal region of the Ampara District during the Maha season, which might be attributed to the fertilizer policy implemented in 2021. Data for this study were gathered using a structured questionnaire. Using the stratified random sampling method, 145 farmers were selected from each Divisional Secretariat in the coastal region of the Ampara District. This study examines various aspects of paddy cultivation, including yield, urea usage, production costs, paddy prices, income, net profit, and cost-benefit ratios. Data were analyzed using descriptive statistics, one-sample t-tests, paired-sample t-tests, and combined variance methods. The analysis reveals a significant decline in both paddy yield and urea usage during the Maha 2021/2022 season compared to previous Maha seasons and Yala 2021. The fertilizer policy in 2021 caused a significant rise in the cost of production, paddy prices, and urea prices. Average income in Maha 2021/2022 was higher than in Yala 2021 due to higher paddy prices, with little income variation between seasons and greater paddy price variation in Yala 2021. Despite higher income, net profit and return on investment were lower in Maha 2021/2022 compared to Yala 2021 due to increased production costs. The fertilizer policy of 2021 imposed harm on farmers (reduced profit and ROI) but was somewhat recovered through the increased selling price.

Keywords: Ampara district, fertilizer policy, Maha season, paddy production, Yala season

Introduction

The application of fertilizer in rice cultivation plays a pivotal role in augmenting both yield and quality. In paddy fields, three fundamental nutrients, namely nitrogen (N), phosphorus (P), and potassium (K), are indispensable for the growth and development of rice plants. Due to the long-term cultivation of rice in the lands, these nutrients are typically supplied through fertilizer application. In Sri Lanka, the primary fertilizers employed for rice cultivation are urea (providing N), triple superphosphate (supplying P), and muriate of potash (providing K). Urea serves as a critical nitrogen source for rice cultivation in Sri Lanka. Nitrogen stands as a pivotal nutrient essential for rice plant growth and development. It plays a vital role in chlorophyll formation, a necessity for photosynthesis.

The provision of subsidies for all three types of fertilizer (NPK) is aimed at boosting agricultural productivity, and it often carries political motivations. In 1962, the Sri Lankan government introduced a fertilizer subsidy scheme encompassing all types of fertilizers (NPK) (Weerahewa et al., 2010). The primary objective was to promote fertilizer usage by enhancing affordability, ultimately reducing cultivation expenses and increasing crop yields. Additionally, the introduction of new and improved rice varieties necessitated a higher fertilizer input, further justifying the need for this program. These subsidy schemes were altered from time to time based on different policies. Table 1 below shows the summary of the fertilizer subsidy schemes experienced in Sri Lanka for rice cultivation in different time periods (Atapattu, 2021; Weerahewa et al., 2022).

On May 6th, 2021, the government suddenly took drastic steps to completely eradicate chemical fertilizers (and chemical pesticides) from the farming systems of the country by imposing a ban on their importation. The government aimed to make Sri Lanka the first country in the world to achieve toxic-free agriculture by relying solely on 100% organic farming. Prevailing chronic kidney diseases were shown as the main reason for banning these chemical fertilizers and pesticides. However, there were challenges and criticisms for this move, highlighting yield reduction and the unavailability of organic fertilizers on a massive scale. Subsequently, the government withdrew the policy in 2021 and allowed importing chemical fertilizers and introduced subsidies for NPK chemical fertilizers and cash grants. Periodic adjustments to subsidy rates and fertilizer prices are made to reflect changes in global market conditions and local economic factors.

Related Work

(Weerahewa et al., 2022) conducted a study on fertilizer usage policy in the rice sector in Sri Lanka. The researchers analyzed the impact of different policy regimes on fertilizer usage, estimated the elasticity of rice output with respect to fertilizer application and land under cultivation, and computed the total factor productivity of rice using time series data from 1960 to 2020. The study found that while there was a secular increase in rice output and average yield during the period, fertilizer usage per unit area started to decrease over the past two decades. This research provides a basis for evaluating the outcomes of non-use of chemical fertilizers in the rice sector in Sri Lanka.

(Ekanayake, 2009) conducted an analysis of the impact of fertilizer subsidies on rice cultivation using a simple regression model. The results of the regression indicated that changes in the prices of fertilizer and rice did not have a significant effect on fertilizer usage. This suggests that the fertilizer subsidy is not a key determinant of fertilizer usage in rice cultivation in Sri Lanka.

In a study conducted by (Weerahewa et al., 2010), proposals were put forward to amend the existing fertilizer subsidy policy. These amendments were suggested with the assumption that the Government of Sri Lanka would need to adjust its existing fertilizer policy to support the livelihoods of paddy farmers, achieve national self-sufficiency in rice production, reduce the financial burden on the treasury, and mitigate environmental pollution caused by excessive fertilizer application. However, the crucial decision of the Sri Lankan government in May 2021 — that is, to completely eradicate chemical fertilizers (and chemical pesticides) from farming — considered only the financial burden on the treasury and the mitigation of environmental pollution caused by fertilizer application.

This study focuses on analyzing the impact of the fertilizer policy 2021 on the rice sector in the South Coastal belt of Ampara District, Sri Lanka. Ampara District is one of the major districts contributing significantly to the overall rice production in the country. In the 2021 Yala season in Sri Lanka, the highest contribution to the total production was from Ampara District, accounting for 15% of the total. In the Maha season, Ampara District was ranked as the third-highest contributor at 11%, following Anuradhapura and Kurunegala districts, each at 13% (Department of Census and Statistics, 2021).

Objectives

The objectives of this study were as follows:

1. To determine the difference in rice yield in the selected region before and after the implementation of the 2021 fertilizer policy.
2. To assess the variation in urea usage for rice cultivation in the selected region before and after the implementation of the 2021 fertilizer policy.
3. To analyze the differences in production costs, net income, and cost-benefit ratios for rice production in the selected region before and after the implementation of the 2021 fertilizer policy.
4. To provide insights and commentary on the overall success or failure of the 2021 fertilizer policy.

Materials and Methods

Location

This survey was conducted in the coastal area of the Ampara District, which comprises the District Secretariat (DS) divisions of Sammanthurai, Kalmunai, Karaithivu, Nintavur, Addalachchenai, Alayadivempu, Pottuvil, and Thirukkovil. It encompasses around 69% of the paddy lands in the Ampara District and contributes to 77% of the total district paddy production (Department of Census and Statistics, 2021). The average yield in the coastal region was considerably higher, at 4,900 kg per hectare (Ahmed & Razmy, 2005).

Data Collection

The necessary data for this study were collected through a structured questionnaire asking for information on Yala 2021 and Maha 2021/22. The cultivation information for Yala 2021 pertains to the period before the implementation of the fertilizer policy 2021, while the information for Maha 2021/2022 relates to the period following the implementation of the fertilizer policy 2021. Additional necessary data for this study were collected from other relevant sources.

Number of Samples

For the sake of convenience, it was decided to gather information from 145 farmers. The number of farmers to be interviewed from each DS division was determined in proportion to their respective land areas, as outlined in Table 2.

Table **(2)**|Paddy Cultivation Extent and Number of farmers

DS Division	**Extent Cultivated (Hectares)**		**Number of Farmers**
	Maha 2021/2022	**Yala 2021**	
Addalachchenai	3310	3512.5	16
Akkarapattu	4634	4341.92	21
Alayadiwembu	5183.7	4119.7	22
Irrakkamam	2223.5	2408.31	11
Karathivu	513	575.2	2
Navithanveli	4488	3748	19
Nintavur	2783	2677.23	13
Sammanthurai	9435.9	8053.85	41
Total	—	—	**145**

Source: Field Survey Data (2021/2022)

Analysis

Minitab 16 software was used for basic analyses, including descriptive statistics, chi-square tests, and t-tests. The combined variance method was employed to examine the dependency between rice yield and selling price.

Table **(1)**|Fertilizer subsidy schemes introduced in Sri Lanka

Year / Period	**Subsidy Schemes and Policy Changes**
1962	Introduced for all types of fertilizers (NPK).
1971	Private importation of fertilizer was prohibited, making it a monopoly of the Ceylon Fertilizer Corporation.
1977	Private sector was granted permission to import fertilizer.
1978	A uniform subsidy rate of 50% of the Cost, Insurance, and Freight (CIF) price was implemented.
1979	Urea received an 85% subsidy and other fertilizers received a 75% subsidy.
1988	The subsidy rate was eliminated for sulfate of ammonia and rock phosphate.
1990	Fertilizer subsidy scheme was completely removed in Sri Lanka.
1995	Subsidies were reintroduced for all three types of fertilizer (NPK); a fixed price of Rs. 350 per 50 kg bag applied.
1996	The price of a 50 kg bag was raised to Rs. 600.
1997	The subsidy was restricted exclusively to urea, maintaining the rate of Rs. 350 per 50 kg bag.
2003	The price of a 50 kg bag increased to Rs. 800.
2004	The price level for a 50 kg bag was adjusted back to Rs. 600.
2005	A standardized price of Rs. 350 per 50 kg bag was introduced for all three types of fertilizer (N, P, K). Usage restrictions were imposed, limiting the fertilizer quantity to the Department of Agriculture recommendations, with a maximum of 5 acres per farmer.
2016 Yala	A cash grant was provided.
2018 Maha	Reintroduction of subsidized fertilizer at a rate of Rs. 500 per 50 kg bag.
2020	Free fertilizer was made available for rice cultivation.
2021 May 6	Complete ban on importation of chemical fertilizers and pesticides to achieve 100% organic farming.
Late 2021	Ban withdrawn; importation of chemical fertilizers reintroduced with NPK subsidies and cash grants. Periodic adjustments were made to reflect global and local economic factors.

Source: (Weerahewa et al., 2022), (Atapattu, 2021).

Results and Discussion

In this study, 145 farmers cultivating high-yielding paddy lands in the coastal belt of the Ampara District were considered, and this section provides the survey results of the study in both descriptive and inferential formats. Out of the 145 farmers, most (50.3%) were in the age group of 41–60, while 22.1% were below 40 years of age. As it is a random sample, one can observe that the involvement of the young generation in paddy cultivation activities is low. Among the farmers in this study, 68% were educated up to O/L or more, and it is a good indication that transferring new technologies among these farmers can be easier. Farmers in this study region either cultivate their own land or lands rented from others. In this study, most of the farmers were cultivating their own lands, which accounted for 67.6%. Table 3 shows the age group-wise ownership of lands. There was no association between ownership of the land cultivated and age ($p = 0.113$, Pearson Chi-square = 4.354).

Table **(3)**|Ownership of the Land cultivated and Age

Age Group	Own Land	Rented Land
Below 40 years	18 (56.25%)	14 (43.75%)
41–60 years	55 (75.34%)	18 (24.66%)
Above 60 years	25 (62.5%)	15 (37.5%)

Source: Field Survey Data (2021/2022)

Table 4 shows the relationship between the ownership of the land cultivated and education level. There was an association between ownership of the land cultivated and education level ($p = 0.003$, Pearson Chi-square = 14.302). The percentage of farmers cultivating their own land category is higher among the higher-educated farmers.

Table **(4)**|Ownership of the land and education level

Education Level	Own Land	Rented Land
Primary	11 (44.0%)	14 (56.0%)
Secondary	32 (64.0%)	18 (36.0%)
O/L or A/L	13 (61.9%)	8 (38.1%)
Above	42 (85.7%)	7 (14.29%)

Source: Field Survey Data (2021/2022)

Farmers in recent times are information seekers in order to increase their crop production practices and profit. There are ten methods that can be used to access information such as on-field demonstrations, field trips, web or electronic information portals, publications, group discussions, guest speakers or consultants, workshops, practical short courses, home study, and video demonstrations. Farmers' preferences have been recorded according to four levels such as most prefer, prefer, less prefer, and least prefer. The on-field demonstration and group discussion are the most accepted methods of accessing information by farmers.

Fertilizer is one of the most important inputs for paddy cultivation, accounting for more than 70% of total input usage. Farmers choose fertilizer according to their experience, the advice from other farmers, the advice from chemical sellers, and sometimes as innovators. In Yala 2021, all farmers had free access to urea, and only 2.82% of farmers used organic fertilizer. In Maha 2021/2022, 3.45% of farmers did not apply urea to their fields, and the availability of urea was highly restricted due to government policy. Farmers were asked to apply organic fertilizer, but only 26.57% of farmers had applied organic fertilizer.

The average amount of urea used in Yala 2021 was 85.41 kg per acre (95% CI: 81.94–88.89 kg/acre), and in Maha 2021/2022, it was 38.30 kg per acre (95% CI: 35.46–41.14 kg/acre). There was a significant drop of 47.11 kg per acre in urea usage during the Maha 2021/2022 season when compared to the Yala 2021 season (95% CI: 43.33–51.41, $p < 0.001$).

The average price per 50 kg of urea used in Yala 2021 and Maha 2021/2022 was Rs. 971.40 (95% CI: Rs. 811.90–Rs. 1130.80) and Rs. 31,000.00 (95% CI: Rs. 30,309.00–Rs. 31,691.00), respectively, with a significant price increase of Rs. 30,011.00 from Yala 2021 to Maha 2021/2022 (95% CI: Rs. 29,345.00–Rs. 30,677.00, $p < 0.001$).

The average yield of paddy in Yala 2021 was 2,156 kg per acre (95% CI: 2,082.0–2,230.0 kg/acre), while in Maha 2021/2022, it was 1,551.0 kg per acre (95% CI: 1,489.9–1,612.2 kg/acre). There was a significant drop of 605.0 kg per acre in yield in Maha 2021/2022 compared to Yala 2021 (95% CI: 536.4–673.6, $p < 0.001$). A survey carried out by (Ahmed & Razmy, 2005) in this studied region presented yield information, estimating the average yield for Yala and Maha as 2,151.5 kg/acre and 1,711.7 kg/acre, respectively (previous survey data). The current Yala (2021) and Maha (2021 /2022) yields are estimated as 2,156.0 kg/acre and 1,551.0 kg/acre, respectively. It was observed that there is no significant difference in Yala yield between the previous survey data and Yala (2021) yield ($p = 0.904$). However, a significant drop of 160.7 kg/acre in yield was observed in Maha (2021/2022) compared to the previous survey data ($p < 0.001$), which could be considered the effect of the fertilizer policy of 2021.

The average cost of production in Yala 2021 and Maha 2021/2022 was Rs. 49,132.00 (95% CI: 47,369–50,895) and Rs. 78,839.00 (95% CI: 76,146.00–81,532.00), respectively, with a substantial rise in costs of Rs. 29,707.00 from the Yala 2021 season to the Maha 2021/2022 season (95% CI: 26,945–32,469, $p < 0.001$). The average price per kg of paddy (dried) in Yala 2021 and Maha 2021/2022 was Rs. 64.03 (95% CI: 62.20–65.86) and Rs. 98.88 (95% CI: 96.70–101.05), respectively, indicating a significant price increase of Rs. 36.92 (95% CI: 34.15–39.69, $p < 0.001$).

The analysis of the cost of production per acre with land rent was significantly higher in the Maha season than in the Yala season. The benefit the farmers received in relation to their average cost of production per acre with land rent was 39.25% for the Yala season but only 19.03% for the Maha season, as the total cost of production was high and net profit was less due to the effect of the fertilizer policy of 2021. The average net profit per acre with land rent in Yala

2021 was Rs. 38,911 (95% CI: Rs. 34,796–Rs. 43,026), while in Maha 2021/2022, it was Rs. 24,522 (95% CI: Rs. 21,303–Rs. 27,742), reflecting a significant decrease in net profit of Rs. 14,389 (95% CI: Rs. 9,148–Rs. 19,629, $p < 0.001$).

In the Yala season, the calculated F statistic of 1.877 is greater than the table value of 1.4327, implying that the calculation of the variance of income assuming yield and price are independent is not correct, which is further emphasized by the significant correlation between yield and price ($r = 0.254$, $p = 0.002$). Therefore, farmers in the Yala season were keen on the selling price of their paddy depending on their yield. In the Maha season, the F statistic of 1.02 is less than the table value, and the correlation between yield and price was not significant ($r = -0.068$, $p = 0.415$), indicating independence and showing that farmers were not keen on the selling price depending on their yield. Although there was no significant variance in income between the seasons ($F = 1.18$, $p = 0.278$), the variance in the selling price of paddy in Yala was significantly higher than in Maha ($F = 2.254$, $p = 0.006$). Overall, there was higher variation in the selling price of paddy in Yala, with farmers keen on the price depending on yield, while after the fertilizer policy, the variation in price was smaller, and farmers were less interested in the selling price.

Conclusion

This study aimed to conduct a comparative analysis of paddy production in the south coastal region of the Ampara District during the 2021 Yala and 2021/2022 Maha seasons in response to the 2021 fertilizer policy. A survey of 145 farmers revealed that 50.3% were aged 41–60, with low participation from the younger generation. Notably, 68% had education up to O/L or higher, suggesting ease in transferring new technologies. Most farmers (67.6%) cultivated their own land, with land ownership significantly associated with education level. Farmers preferred on-field demonstrations and group discussions to access information on improving production and profit.

In Yala 2021, all farmers had free access to urea, while the 2021 policy led to restricted availability and increased prices in Maha 2021/2022, with urea usage dropping by 47.37 kg/acre. Although there was no significant change in Yala yields compared to past data, Maha yields dropped significantly by 160.7 kg/acre from previous data and by 605 kg/acre compared to Yala 2021. The cost of production in Maha 2021/2022 increased by Rs. 29,707 per acre, while the price per kg of paddy rose by Rs. 36.92. Despite lower yields in Maha, income increased due to higher prices.

In Yala, there was a positive association between paddy price and yield, while in Maha, price and yield were independent. Price variance was significantly higher in Yala, reflecting farmers' attention to prices based on yield, unlike during Maha after the fertilizer policy. Net profit per acre decreased by Rs. 14,389 in Maha 2021/2022 compared to Yala, with return on investment dropping from 39.25% in Yala to 19.03% in Maha. Overall, the fertilizer policy led to higher costs, lower yields, and reduced returns, despite price increases offering limited relief to farmers.

References

Ahmed, S., & Razmy, A. M. (2005). Rice yield performance in the coastal region of ampara district. *Journal of Agricultural Sciences*, *1*(2), 45–52.

Atapattu, S. S. (2021). Fertilizer policy changes and implications for rice production in sri lanka. *Sri Lanka Journal of Social Sciences*, *44*(1), 67–75.

Department of Census and Statistics. (2021). Annual bulletin of paddy statistics 2021 [Accessed 2025-10-11].

Ekanayake, H. K. J. (2009). Impact of fertilizer subsidy on paddy cultivation in sri lanka. *Tropical Agricultural Research*, *21*(1), 50–60.

Weerahewa, J., Herath, H. M. S. P., & Ranathunga, R. A. N. S. (2022). Evolution and impact of fertilizer subsidy policies in sri lanka. *Journal of Agricultural Policy and Development*, *5*(2), 45–58.

Weerahewa, J., Pushpakumara, D. K. N. G., Silva, P., & Kodithuwakku, S. S. (2010). Fertilizer subsidy and paddy production in sri lanka: An analysis of household data. *Sri Lankan Journal of Agricultural Economics*, *12*(1), 35–52.

|ICAS2025|

Correlation Analysis of Age Structure Metrics and Cause-Specific Mortality: A Global and WHO Regional Comparison using the Top 5 Causes of Death in 2021

L.Edirisinghe[1], B.Wijenayake[2], A.Ratnayake[2], T.Fonseka[3], R.Godalliyadda[2], S.Dharmaratne[4], P.Ekanayake[2], V.Herath[2]

[1]Department of Mathematics, University of Ruhuna, Sri Lanka
[2]Department of Electrical and Electronic Engineering, University of Peradeniya, Sri Lanka
[3]Multidisciplinary AI Research Center, University of Peradeniya, Sri Lanka
[4]Faculty of Medicine, University of Peradeniya, Sri Lanka

Abstract: Global mortality models often depend on simple aging metrics that ignore the structural diversity in populations. To tackle this issue, we evaluated three metrics: median age, percentage aged 65+, and the new PoPDivergence, against mortality from the top five global causes of death in 2021 across 178 countries. PoPDivergence, which is based on Kullback-Leibler divergence, identifies differences in population pyramids from optimized references. Using Spearman correlations, Levene's test, and Kruskal-Wallis analysis, we found that PoPDivergence predicts COVID-19 mortality more accurately in younger regions, such as the Eastern Mediterranean. In contrast, traditional metrics better capture chronic disease mortality in aging regions like Europe and in younger areas like Africa, where non-communicable diseases are increasing. No metric significantly predicted lower respiratory infection mortality. Our study presents a new, statistically validated framework for selecting age structure metrics suited to specific diseases and regional contexts, which offers important improvements for global health modeling and policy development.

Keywords: demographic risk, global health modeling, median age, PoPDivergence, population structure

1 Introduction

Population aging is fundamentally reshaping the demographic landscape across all regions of the world. United Nations projections indicate that by 2050, one in six people globally will be aged 65 years or older, a substantial increase from one in eleven in 2019 (United Nations Department of Economic and Social Affairs, Population Division, 2019). Over the same period, the proportion of adults aged ≥ 60 is expected to nearly double from 12% in 2015 to 22% in 2050, with 80% of these older adults residing in low- and middle-income countries (LMICs) (World Health Organization, 2022a). These demographic shifts are occurring alongside sustained fertility declines—global total fertility rates have fallen from 3.3 in 1990 to 2.3 in 2024—and steady gains in life expectancy, which now stands at 73.3 years (United Nations Department of Economic and Social Affairs, Population Division, 2024). Consequently, the world's median age has already increased to 30.9 years in 2025 (Worldometer, 2025).

Age structure is a fundamental determinant of disease burden. Disorders affecting individuals aged $\geq$ 60 already account for approximately 23% of global disability-adjusted life years (Vos, Barber, et al., 2015). During the first year of the COVID-19 pandemic, 81% of all U.S. COVID-19 deaths occurred among those aged 65 and older (Ahmad and Cisewski, 2021). Seven of the ten leading global causes of death in 2021—including ischemic heart disease (IHD), stroke, COVID-19, chronic obstructive pulmonary disease (COPD), and lower respiratory infections—demonstrate steep age-related increases in mortality (World Health Organization, 2024b). COPD alone claimed 3.5 million lives in 2021 and is projected to become the third-leading cause of death worldwide by 2030 (World Health Organization, 2024a; World Health Organization, Eastern Mediterranean Regional Office, 2023). Non-communicable diseases (NCDs) currently cause 43 million deaths annually, with 82% of premature (< 70 years) NCD deaths occurring in LMICs (World Health Organization, 2022b. Beyond physical illness, mental health disorders affect one in six adults aged ≥ 60 (World Health Organization, 2017).

The percentage of population aged 65 and over (%65+) and median age remain the most commonly used indicators of demographic aging. However, these metrics may obscure substantial middle-aged NCD mortality in LMICs. Modeling studies from Indonesia demonstrate that achieving optimal systolic blood pressure control in adults aged 40–64 could add approximately 5–6 years to life expectancy (Pearson-Stuttard and Guzman-Castillo, 2020). Similarly, the 2024 World Population Data Sheet notes that even with only 10% of the global population aged 65 and older, chronic conditions already dominate health system demand (Population Reference Bureau, 2024). Threshold-based metrics that focus primarily on the oldest age groups may therefore underestimate population vulnerability to age-related diseases.

To address these limitations and capture the complete age distribution, Fonseka et al. recently proposed PoPDivergence (Fonseka et al., 2025). This novel metric measures the Kullback–Leibler divergence between a country's age–sex pyramid and an optimally selected reference pyramid, enabling distinction between progressive (youth-heavy) and regressive (elderly-heavy) population structures even when %65+ or median age values are similar. Preliminary analyses across 371 diseases indicate that the companion metric *PoPStat* explains cause-specific mortality more effectively than median age, GDP per capita, or the Human Development Index (Fonseka et al., 2025).

Utilizing mortality estimates for 178 countries and focusing on the five leading causes of death in 2021—ischemic heart disease, COVID-19, stroke, COPD, and lower respiratory infections—this study aims to:

1. **Quantify and compare** global and WHO regional correlations between PoPDivergence, %65+, median age, and cause-specific mortality rates; and
2. **Develop region-specific guidance** for determining when structure-aware metrics (PoPDivergence) should be preferred over threshold-based indicators (%65+, median age) for mortality risk modeling, pandemic preparedness, and resource allocation decisions.

Through systematic evaluation of these complementary demographic indicators across diverse population contexts, we seek to inform more equitable and precise approaches to estimating age-related mortality risk and guide evidence-based public health policy decisions.

Methodology

Age Structure Metrics Used

To support our analysis, we first describe the age structure metrics used in our study. Each metric reflects different aspects of demographic aging. We evaluated three metrics: PoPDivergence, %65+, and median age.

The two traditional age structre metrics used are the %65+, and median age. The %65+ metric measures the share of people aged 65 and older in a population. It is commonly used in global health modeling and policy to evaluate vulnerability to chronic non-communicable diseases (NCDs) and age-sensitive pandemics like COVID-19 (Mattiuzzi, Camilla, et al., 2020; Prince, Wu, et al., 2015).Median age is the midpoint of a population's age distribution. It is a straightforward measure that summarizes overall population aging. While it gives a general picture, it does not capture details about younger or older groups.

PoP-Divergence

The PoP-Divergence, introduced by (Fonseka et al., 2025), measures the Kullback-Leibler divergence between a country's population pyramid and that of a reference population. This metric converts multidimensional population pyramid structures into scalar variables, facilitating comparison and analysis.This is defined as,

$$\text{PoPDivergence}(i;\omega) = \sum_{a\in A} P_{i,a} \ln\left(\frac{P_{i,a}}{P_{\omega,a}}\right)$$

where $P_{i,a}$ denotes the proportion of the population in age group a for country i, and $P_{\omega,a}$ denotes the corresponding proportion in the reference country ω. The index $a \in A$ spans all age groups. This divergence captures the information-theoretic difference between the population structures of country i and the reference country ω, with larger values indicating greater structural deviation as described by (Fonseka et al., 2025).

The interpretation of the PoP-Divergence depends on the choice of the reference country. For instance, if Japan is selected as the reference, lower PoP-Divergence values indicate population pyramids similar to Japan's, which are typically regressive, as seen in countries like Japan and Malta. Conversely, higher PoP-Divergence values suggest more progressive population pyramids, such as those found in Niger and the Central African Republic.

The reference country is selected through a process known as *reference country tuning*, which aims to maximize the correlation between the PoP-Divergence values and the log-transformed crude death rates. This can be formulated as:

$$\omega^* = \arg\max_{\omega\in\Omega} \left|\text{Corr}\left(\{\ln S_i\}_{i\in\Omega}, \{\text{PoPDivergence}(i;\omega)\}_{i\in\Omega}\right)\right|$$

Here, Ω denotes the set of all countries, and S_i represents the crude death rate in country i. The notation $\{\text{PoPDivergence}(i;\omega)\}_{i\in\Omega}$ refers to the vector of divergence values for all countries relative to reference ω, while $\{\ln S_i\}_{i\in\Omega}$ is the vector of log-transformed crude death rates. The optimal reference country ω^* is the one that maximizes the absolute Pearson correlation between these two vectors, ensuring the strongest linear association between demographic divergence and mortality patterns.

Statistical Analysis

Data Extraction and Processing

To understand global mortality patterns, we examined the five leading causes of death in 2021: ischemic heart disease (IHD), COVID-19, stroke, chronic obstructive pulmonary disease (COPD), and lower respiratory infections (LRI) (World Health Organization, 2024c). We selected these causes to represent both non-communicable and infectious diseases with distinct transmission mechanisms and risk profiles. This selection enabled assessment of how demographic factors influence outcomes across diverse epidemiological settings. Mortality data for IHD, stroke, COPD, and LRI were obtained from the Global Burden of Disease (GBD) 2021 study (Global Burden of Disease Collaborative Network, 2024). COVID-19 mortality data came from the World Health Organization as of December 16, 2022 (World Health Organization, 2023).

Demographic data, including the percentage of the population aged 65 and older %65+, median age, and population pyramids used to calculate PoPDivergence were sourced from the United Nations World Population Prospects (2024 revision) (United Nations, Department of Economic and Social Affairs, Population Division, 2022). We cross-validated these estimates with age-structured data from the GBD 2021 dataset. These sources provided harmonized, age-specific population data for all 178 countries included in our analysis.

Global Correlation Analysis

To evaluate the global predictive validity of the three age structure metrics, PoPDivergence, %65+, and median age, we calculated Spearman correlation coefficients between each metric and mortality rates for the five target causes across 178 countries. Spearman correlation was chosen due to its robustness to non-normal and non-linear relationships, which are common in cross-country demographic and mortality data (Brown, 2023). For each metric-cause pair, we generated scatterplots with linear trendlines, annotated with their respective correlation coefficients and p-values. These visualizations were compiled into an integrated dashboard to facilitate comparative assessment. Metrics demonstrating statistically significant correlations ($p < 0.05$) were considered useful predictors of demographic risk for specific causes.

Assessment of Regional Variation

To examine differences in age-mortality relationships across global regions, we stratified countries using WHO regional groupings (Global Burden of Disease Collaborative Network, 2024). For each combination of age structure metric PoPDivergence, %65+, median age and mortality outcome, we performed Levene's test to assess variance homogeneity and Kruskal-Wallis H test to detect differences in central tendency.

These non-parametric methods were selected for their robustness to diverse demographic distributions and minimal distributional assumptions. Statistically significant results ($p < 0.05$) indicated a substantial regional variation in age-mortality associations, underscoring the necessity of regional stratification in demographic mortality analysis.

Regional Correlation Analysis

Region-specific analyses used WHO regional classifications to evaluate different relationships between age structure metrics, such as PoPDivergence, %65+, and median age, and cause-specific mortality. For each region-cause pairing, Spearman correlation coefficients (ρ) were calculated using complete-case country data. The most important metric for each pair was the one with the highest absolute ρ value that achieved statistical significance ($p < 0.05$). Results were organized in a region-cause matrix and shown through choropleth world maps that illustrated both correlation strength (absolute ρ) and direction (positive or negative associations) across different areas.

Results and Discussion

Global Correlation Analysis

The global correlation analysis (1) assesses the predictive power of age structure metrics, PoPDivergence (PoPD), %65+, and median age for five major causes of death using Spearman (ρ) coefficients.

For IHD, all metrics show moderate positive correlations. %65+ ($\rho = 0.47$) and median age ($\rho = 0.48$) demonstrate stronger, more consistent correlations. In contrast, PoPD shows an inverse trend ($\rho = -0.48$). COVID-19 and age-structre metrics exhibit strong correlations. Median age and %65+ show high correlations ($\rho = 0.78$). PoPD also demonstrates robust negative correlations ($\rho = -0.78$). For stroke, %65+ and median age show moderate correlations ($\rho = +0.32$,$+0.32$), while PoPD has weaker correlations ($\rho = -0.28$). For COPD %65+ ($\rho = 0.43$) slightly outperforms median age ($\rho = 0.39$) and PoPD ($\rho = -0.39$). LRI presents a distinct pattern. PoPD shows positive correlation ($\rho = 0.24$), while %65+ and median age show negative correlations ($\rho = -0.23$, -0.31).

In summary, PoPDivergence excels for COVID-19 with inverse trends, %65+ is strongest for certain age-associated non-communicable diseases (Stroke, COPD), and median age provides consistent predictive stability across all causes.

Assessment of Regional Variation

The heatmap (2) summarizing Levene's test and Kruskal-Wallis H test results shows strong evidence of regional differences in mortality rates and their links to age structure measures across WHO regions. For IHD, COVID-19, stroke, and COPD, both tests found highly significant p-values ($p < 0.001$). This indicates differences in means/medians (Kruskal-Wallis) and variances (Levene's), reflecting the impact of regional demographics, health systems, or epidemiological factors. PoPDivergence associations with mortality IHD_PoPD to LRI_PoPD displayed significant regional variation ($p < 0.001$ for both tests). The %65+ metric also showed significant variation ($p < 0.001$), while the median age had weaker but still significant variance (Levene's $p = 0.015$, Kruskal-Wallis $p < 0.001$). Interestingly, LRI mortality did not show significant variance (Levene's $p = 0.107$), but its connection to age structure varied. This suggests that demographic factors differ by region. These findings highlight the need for region-specific analyses and tailored demographic risk models for predicting cause-specific mortality.

Regional Correlation Analysis

The comparison of age structure metrics, PoPDivergence, %65+, and median age reveals distinct predictive capabilities for cause-specific mortality across regions and disease contexts. PoPDivergence, which measures age structure divergence relative to cause-specific references, demonstrates strong predictive power for COVID-

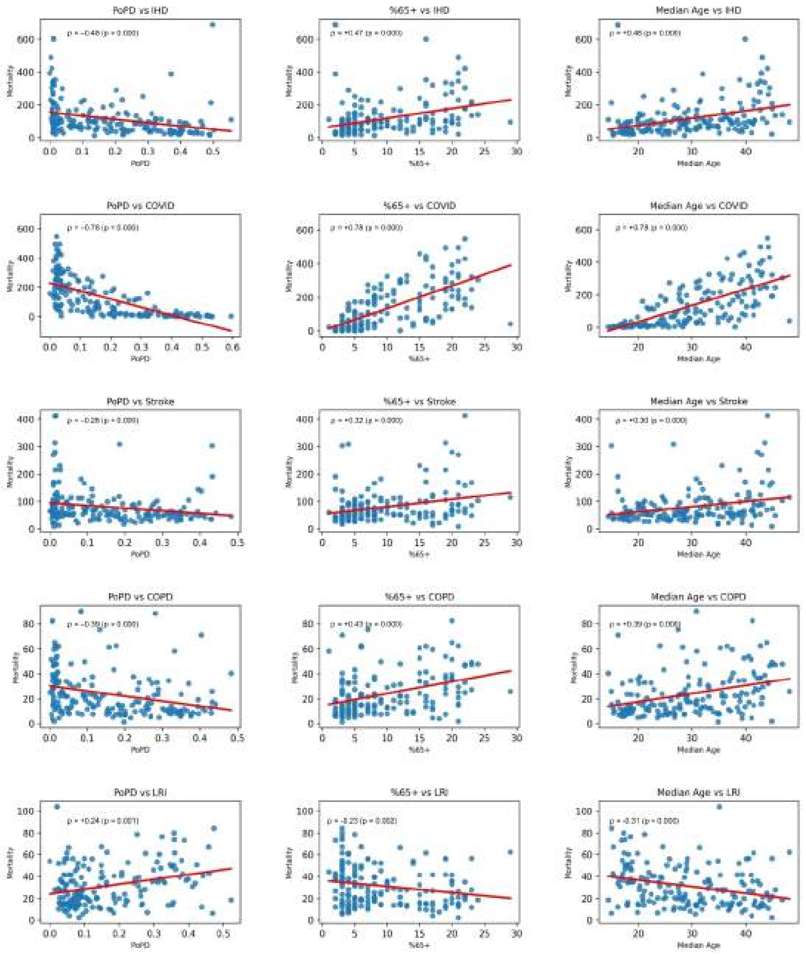

Figure **(1)**|Global correlations between age structure metrics and cause-specific mortality.

19 mortality, showing significant negative correlations in the Eastern Mediterranean (Spearman $\rho = -0.78$, $p < 0.001$) and Americas ($\rho = -0.41$, $p = 0.015$).

Median age exhibits the most consistent predictive performance, with strong significant correlations for COVID-19 mortality in Europe ($\rho = 0.57$, $p < 0.001$), Africa ($\rho = 0.66$, $p < 0.001$), and Eastern Mediterranean ($\rho = 0.60$, $p = 0.004$). It also shows significant associations with stroke mortality in Europe ($\rho = 0.40$, $p = 0.005$) and Americas ($\rho = 0.37$, $p = 0.029$), and with COPD mortality in Europe ($\rho = 0.48$, $p = 0.001$). %65+ demonstrates limited predictive utility, with significant associations observed only for COPD ($\rho = 0.33$, $p = 0.024$) and stroke ($\rho = 0.33$, $p = 0.026$) in Africa. This highlights its relevance in contexts where elderly populations face disproportionate risk.

Across all WHO regions, none of the age structure metrics showed a significant link to lower respiratory infection (LRI) mortality. The Spearman values ranged from -0.17 to 0.28, and all p values were greater than 0.2. This indicates a weak and inconsistent connection between demographics and LRI mortality.

Conclusion

Our study validates PoPDivergence as a structure-aware demographic metric that predicts cause-specific mortality in different global and regional contexts. Unlike traditional metrics like median age and %65+, PoPDivergence captures subtle differences in population age structures. This allows for better predictions of mortality from diseases such as COVID-19 in younger populations such as the Eastern Mediterranean. We also found that no single tested age structure metric works well for all diseases and regions, which highlights the need to choose metrics based on the specific disease and context. Importantly, our findings show that even in younger regions like Africa, where non-communicable diseases are increasing ((Collaborators, 2019)), traditional aging metrics still matter for modeling chronic mortality. The lack of predictive value for lower respiratory infection mortality across all metrics points to the need to consider other factors beyond demographics for these conditions. By providing a strong framework for adapting age metrics to epidemiological contexts, our study improves demographic risk modeling and supports fair, data-driven health policies and resource allocation.

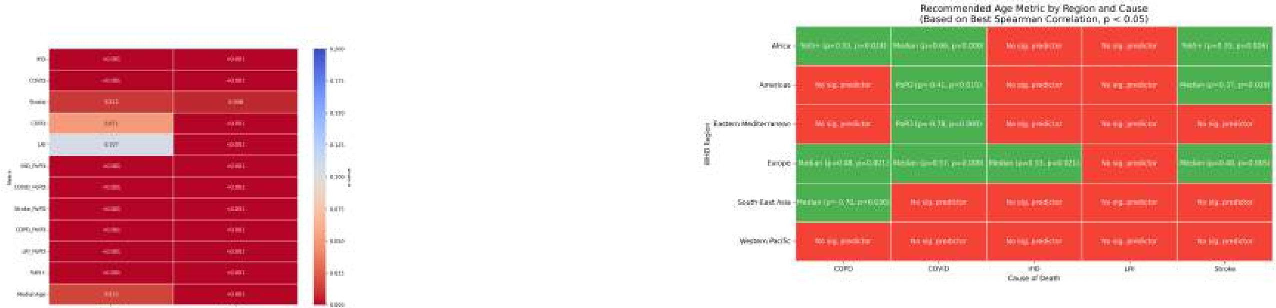

(a) Statistical evidence for regional differences in mortality rates and age structure metrics

(b) Optimal age structure metrics by WHO region and cause of death, based on strongest significant Spearman correlation ($p < 0.05$).

Figure **(2)**|Comparative regional analysis of age structure metrics and their correlation with mortality outcomes.

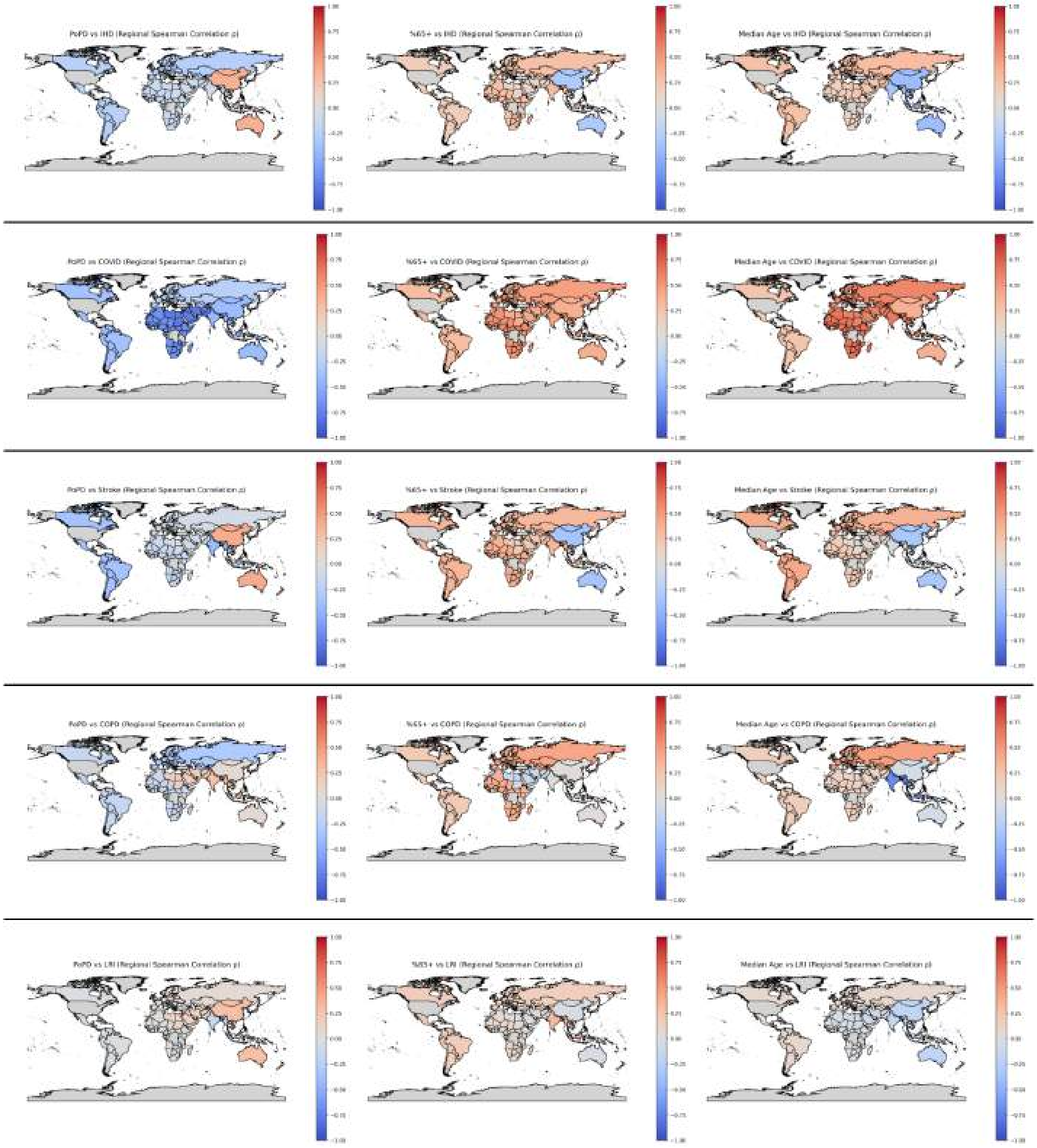

Figure **(3)**|Choropleth maps for regional correlations between age structure metrics and cause-specific mortality

References

Ahmad, F. B., & Cisewski. (2021). Provisional mortality data — united states, 2020. *Morbidity and Mortality Weekly Report*, *70*(14), 519–523.

Brown, P. A. (2023). Country-level predictors of COVID-19 mortality. *Scientific Reports*, *13*(1), 9263.

Collaborators, G. 2. D. (2019). The burden of non-communicable diseases in sub-saharan africa, 1990–2017: A systematic analysis for the global burden of disease study 2017. *The Lancet Global Health*, *7*(10), e1375–e1387.

Fonseka, T., Wijenayake, B., Ratnayake, A., et al. (2025). Devising popstat: A metric bridging population pyramids with global disease mortality. *arXiv preprint arXiv:2501.11514*.

Global Burden of Disease Collaborative Network. (2024). *Global burden of disease study 2021 (gbd 2021) burden and strength of evidence by risk factor 1990-2021* (tech. rep.). Institute for Health Metrics and Evaluation (IHME).

Mattiuzzi, Camilla et al. (2020). The global burden of pancreatic cancer. *Archives of Medical Science*.

Pearson-Stuttard, J., & Guzman-Castillo. (2020). Reducing cardiovascular mortality through prevention and management of raised blood pressure: A World Health Organization analysis. *The Lancet Public Health*, *5*(1), e49–e56.

Population Reference Bureau. (2024). *2024 world population data sheet interactive explorer*. Population Reference Bureau.

Prince, M. J., Wu et al. (2015). The burden of disease in older people and implications for health policy and practice. *The Lancet*, *385*(9967), 549–562.

United Nations Department of Economic and Social Affairs, Population Division. (2019). *World population ageing 2019: Highlights* (tech. rep.). United Nations. New York.

United Nations, Department of Economic and Social Affairs, Population Division. (2022). World population prospects 2022.

United Nations Department of Economic and Social Affairs, Population Division. (2024). *World population prospects 2024: Summary of results* (tech. rep.). United Nations.

Vos, T., Barber et al. (2015). Global, regional, and national incidence, prevalence, and years lived with disability for 310 diseases and injuries, 1990–2015: A systematic analysis for the global burden of study 2015. *The Lancet*, *388*(10053), 1545–1602.

World Health Organization. (2017). Mental health of older adults.

World Health Organization. (2022a). Ageing and health.

World Health Organization. (2022b). *Noncommunicable diseases progress monitor 2022* (tech. rep.).

World Health Organization. (2023). *Covid-19 deaths*. WHO COVID-19 Dashboard.

World Health Organization. (2024a). Chronic obstructive pulmonary disease (copd).

World Health Organization. (2024b). The top 10 causes of death.

World Health Organization. (2024c). The top 10 causes of death.

World Health Organization, Eastern Mediterranean Regional Office. (2023). Chronic obstructive pulmonary disease (copd).

Worldometer. (2025). World population by year.

Abstracts of ICAS2025

|ICAS2025|

Cinnamon Price Prediction and Grade Identification: A Comprehensive Study in the Galle District

E.D.K.Helitha[1], D.G.S.Pathulpana[1], R.P.B.Nishadhi[1], U.E.Ranasooriya[1], E.M.U.W.J.B.Ekanayake[1]

[1]Department of Computer Science and Informatics, Uva Wellassa University, Badulla, Sri Lanka

Abstract: The cinnamon industry in Sri Lanka, centered in the Galle District, one of the most important economic pillars, represents over 85% of the world supply of Ceylon cinnamon. However, the industry faces challenges from unpredictable price changes due to climate variability and differences in grading standards. This study highlights these issues and their effects on farmers' livelihoods and the competitiveness of the industry in the Galle District. A practical solution was developed, consisting of a machine learning model for price forecasting and an automated system for identifying cinnamon grades. For the price prediction model, we trained Support Vector Machine (SVM), Random Forest, XGBoost, and CatBoost using climatic and economic data, including rainfall, temperature, farm-gate prices, and exchange rates. We included seasonal trends as additional features. The results showed that fluctuations in exchange rates were the main factor affecting prices, while CatBoost provided the most accurate and stable predictions, with an R^2 greater than 0.93. For grade identification, we created a computer vision pipeline that used color histogram and texture features from cinnamon quill images of the grades *Alba*, *C5 Special*, *C5*, and *C4*. A YOLO-assisted cropping process improved the model's precision. We achieved high classification accuracy, with Random Forest reaching up to 87% accuracy, especially for cropped images. The integrated platform, now fully implemented as a mobile application, offers real-time price prediction and automated grade identification. This helps farmers and exporters make informed decisions, reducing economic instability and boosting Sri Lanka's share in the global market. However, the system's reliance on historical data and its focus on the Galle District are current limitations. This solution shows how machine learning and computer vision techniques can improve sustainability and economic viability in the cinnamon industry.

Keywords: cinnamon industry, computer vision, grade identification, machine learning, price prediction

Cinnamon Price Prediction and Grade Identification: A Comprehensive Study in the Galle District

E.D.K. Helitha[1], D.G.S. Pathulpana[1], R.P.B. Nishadhi[1] , U. E. Ranasooriya[1] , E.M.U.W.J.B.Ekanayake[1]

[1]*Department of Computer Science and Informatics, Uva Wellassa University, Badulla, Sri Lanka*

Abstract

Price volatility and inconsistent grading are significant challenges to Sri Lanka's cinnamon industry. This study focuses on the Galle district, the leading region for Cinnamon. In order to provide accuracy, predictive reliability, and global competitiveness, this study integrates machine learning for price forecasting and computer vision for grade identification, considering economic indicators and climate variability.

Introduction

- **Problem**

Climatic factors like rainfall and temperature directly affect cinnamon yield and market prices. Economic factors such as farm gate prices, and the USD/LKR exchange rate add more uncertainty. Manual grading of cinnamon quills is inconsistent and affects quality, competitiveness, and fair pricing.

- **Aim of the Study**

To develop a comprehensive predictive system for cinnamon prices in the Galle district by integrating climatic factors and economic indicators, while simultaneously implementing a grade identification system that classifies cinnamon grades.

- **Significance**

Provides data-driven insights for farmers and exporters to make informed decisions. Promotes income stability and reduces risks from climate change and market monopolies. Enhances grading accuracy and strengthens Sri Lanka's global competitiveness. Supports the adoption of smart agriculture through machine learning and computer vision.

Objective

- To create a predictive model for Cinnamon prices using climatic and economic data.
- To develop a model for the grade identification of Cinnamon.
- To evaluate the performance of the developed system in price prediction and grade identification of Cinnamon.

Methodology

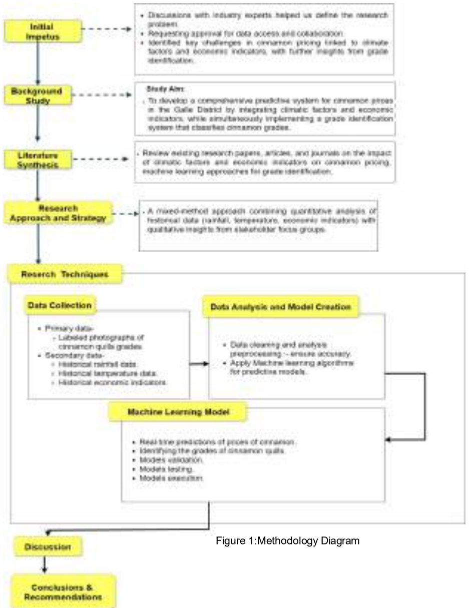

- Discussions with industry experts helped us define the research problem.
- Requesting approval for data access and collaboration.
- Identified key challenges in cinnamon pricing linked to climate factors and economic indicators, with further insights from grade identification.

Study Aim:
- To develop a comprehensive predictive system for cinnamon prices in the Galle District by integrating climatic factors and economic indicators, while simultaneously implementing a grade identification system that classifies cinnamon grades.

- Review existing research papers, articles, and journals on the impact of climatic factors and economic indicators on cinnamon pricing, machine learning approaches for grade identification.

- A mixed-method approach combining quantitative analysis of historical data (rainfall, temperature, economic indicators) with qualitative insights from stakeholder focus groups.

- Primary data-
  - Labeled photographs of cinnamon quills grades
- Secondary data-
  - Historical rainfall data
  - Historical temperature data
  - Historical economic indicators

- Data cleaning and analysis preprocessing - ensure accuracy.
- Apply Machine learning algorithms for predictive models.

- Real time predictions of prices of cinnamon.
- Identifying the grades of cinnamon quills.
- Models validation.
- Models testing.
- Models execution.

Figure 1:Methodology Diagram

Figure 2:Cinnmon quills of four Grades

Results and Discussion

Price Prediction

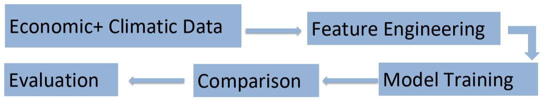

Economic+ Climatic Data → Feature Engineering → Model Training → Comparison → Evaluation

Model Performance (R^2 Values)

Model	Alba	C-5 Sp	C-5	C-4
SVM	0.302	0.208	0.171	0.164
Random Forest	0.723	0.739	0.754	0.758
XGBoost	0.24	0.901	0.963	0.963
CatBoost	0.923	0.897	0.961	0.964

Figure 3:All Model Performance Table

In the Price Prediction, CatBoost model consistently provided the most balanced and stable results across all grades.

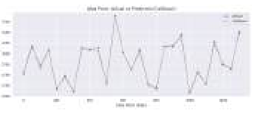

Figure 4:Actual vs Predicted Price Plot Alba

Figure 5:Actual vs Predicted Price Plot C5-SP

Figure 6:Actual vs Predicted Price Plot C5

Figure 7:Actual vs Predicted Price Plot C4

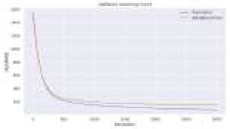

Figure 8:CatBoost Learning Curve Graph

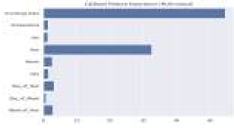

Figure 9:CatBoost Feature importance Graph

Grade Identification

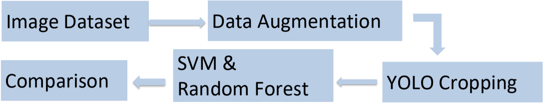

Image Dataset → Data Augmentation → YOLO Cropping → SVM & Random Forest → Comparison

Experiment	Description	Accuracy
Uncropped Dataset	Original images used for training.	RF: 79.3%, SVM: 63%
Cropped Dataset (YOLO)	Object-focused cropped images improved feature clarity.	RF: 87%, SVM: 71%

Figure 10:Comparison Table(Cropped vs. Uncropped)

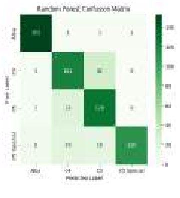

Figure 11:Random Forest Confusion Matrix

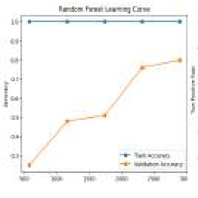

Figure 12:Grade identification Random Forest Learning Graph

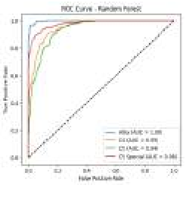

Figure 13:Random Forest ROC curve

In the Grade identification, Random Forest model achieved the highest validation accuracy (~0.8), demonstrating better generalization compared to SVM.

Conclusion

This study shows that combining computer vision and machine learning delivers accurate outcomes for classifying cinnamon grades and predicting price changes. By helping farmers and exporters make better decisions, the suggested solution raises the stability, quality, and competitiveness of Sri Lanka's cinnamon market.

References

1.Fonseka,D.,Aluthgamage,H.,& Wickramaarachchi, W. (2018). Present situation of cinnamon industry in Southern Sri Lanka. International Journal of Current Research in Biosciences and Plant Biology, 5(8), 63–70.

2.Hewavitharana, S., Kuruppu, I., & Priyankara, E. (2022). Assessment of Sri Lankan cinnamon export competitiveness in the global market. Sri Lankan Journal of Agricultural Economics, 23(1), 1–21.

3.Li,S.,&Zhang, W.(2020).Application of CatBoost algorithm in agricultural economic data prediction. Journal of Intelligent & Fuzzy Systems,38(5),5719–5729.https://doi.org/10.3233/JIFS-179657

|ICAS2025|

Tamil Music Playlists with Gradient Boost Classifiers

T.Adittan

Department of Physical Science, University of Vavuniya, Sri Lanka

Abstract: This study develops a music recommendation system based on user preferences, emphasizing genre classification and playlist generation. The classification task is addressed using a self-created, balanced dataset comprising 500 audio tracks, each 30 seconds in duration, equally distributed across five distinct Tamil music genres: classical, devotional, melody, romantic, and rock. Mel-Frequency Cepstral Coefficients (MFCCs) were extracted from the audio data, followed by data preprocessing techniques including Label Encoding and Standard Scaling (Z-score normalization). To improve computational efficiency, dimensionality was reduced using Kernel Principal Component Analysis (KPCA). The processed dataset was then split in an 80:20 ratio for training and testing. Gradient Boosting models, specifically XGBoost and LightGBM, were employed, with RandomizedSearchCV used for hyperparameter tuning. Initial training on the high-dimensional feature set yielded low accuracies (42% for XGBoost and 43% for LightGBM) with extended training times. Incorporating KPCA significantly improved both performance and efficiency: KPCA-enhanced XGBoost achieved 82% accuracy in 16 minutes, while LightGBM reached 86% in 18 minutes. In comparison, CNN, RNN, CRNN, Random Forest, and CNN+XGBoost models achieved lower accuracies of 45.5%, 32%, 23%, 47%, and 52%, respectively. These results demonstrate that Gradient Boosting algorithms, particularly LightGBM, outperform traditional machine learning and deep learning models, making them highly suitable for Tamil music genre classification and recommendation systems.

Keywords: KPCA, LightGBM, machine learning, RandomizedSearchCV, XGBoost

Tamil Music Playlists with Gradient Boost Classifiers

Thivaharan Adittan
Department of Physical Science, Faculty of Applied Science, University of Vavuniya

Abstract

In this study, we developed a Tamil music recommendation system using a balanced dataset of 500 tracks spanning five genres. We extracted audio features using MFCCs and reduced their dimensionality with KPCA for better efficiency. After optimizing the model parameters, LightGBM achieved the highest accuracy of 86%, outperforming XGBoost and deep learning models in genre classification.

Introduction

- Music connects people across cultures
- Music genre classification helps organize and recommend music effectively.
- Machine learning uses MFCCs and audio features to classify songs into genres accurately..
- These techniques used in power streaming platforms and virtual assistants to create personalized playlists.(Alexa,Siri)
- This study evaluates Tamil music genre classification models for accuracy and efficiency.

Objective

- To develop a Tamil music recommendation system using a balanced 500-track dataset across five genres.
- To evaluate and identify the most accurate genre classification model, apply different algorithms and techniques to the data set

Methodology

- A balanced 500-track Tamil music dataset was created, with labels encoded and features normalized using standard scaling.
- KPCA was applied to capture non-linear feature relationships and reduce dimensionality for efficient model training.
- XGBoost and LightGBM were trained on the reduced dataset, and hyperparameters were tuned using RandomizedSearchCV with cross-validation.

Results and Discussion

The study shows that LightGBM and XGBoost outperform well than other models in Tamil music genre classification. KPCA and hyperparameter optimization are significantly enhanced the accuracy and efficiency, with LightGBM reaching 86% and XGBoost 82%, demonstrating their suitability for this task.

Conclusion

Dimensionality reduction and hyperparameter tuning significantly improved XGBoost and LightGBM performance, enhancing accuracy and efficiency for music genre classification.

References

S. J and K. S, “Obtain Better Accuracy Using Music Genre Classification Systemon GTZAN Dataset,” in 2022 IEEE North Karnataka Subsection Flagship International Conference (NKCon), Nov. 2022, pp. 1–5. doi: 10.1109/NKCon56289.2022.10126991.

A. Garg, V. Chaturvedi, A. B. Kaur, V. Varshney, and A. Parashar, “Machine learning model for mapping of music mood and human emotion based on physiological signals,” Multimed. Tools Appl., vol. 81, no. 4,pp. 5137–5177, Feb. 2022, doi: 10.1007/s11042-021-11650-0.

|ICAS2025|

Optimizing the Naïve String-Matching Algorithm using Parallel Processing

S.Sangeerththanan[1], R.Yasotha[1]

[1]Department of Physical Science, University of Vavuniya, Sri Lanka

Abstract: String matching is a fundamental computational problem with broad applications in bioinformatics, natural language processing, cybersecurity, and large-scale text analytics. While advanced algorithms such as Knuth–Morris–Pratt (KMP) and Boyer–Moore achieve faster performance through preprocessing and efficient skipping strategies, the Naïve String-Matching Algorithm remains attractive for its conceptual simplicity, implementation ease, and adaptability across diverse datasets. However, its quadratic time complexity (O(mn)) constrains performance for large-scale data processing. To address this limitation, this research investigates parallelization techniques to enhance the Naïve algorithm, introducing a novel bidirectional parallel variant named "Binamatch." The Binamatch algorithm was implemented using Open Multi-Processing (OpenMP) to leverage thread-level parallelism on multi-core architectures. Unlike the traditional unidirectional comparison, Binamatch performs a bidirectional search, scanning from both ends of the pattern simultaneously to reduce redundant comparisons. The algorithm was evaluated against sequential and parallel implementations of Naïve, Knuth–Morris–Pratt (KMP), and Boyer–Moore algorithms across various datasets, including Deoxyribonucleic Acid (DNA) sequences, ASCII text, and symbolic patterns. Experiments conducted on 16-core and 32-core systems with chunk sizes ranging from 64 to 1024 measured scalability, execution time, and efficiency. Results revealed that although the bidirectional strategy theoretically improved comparison locality, Binamatch underperformed in practice, executing 10–1000 times slower than baseline algorithms due to high synchronization overhead, cache inefficiency, and unbalanced workload distribution. Despite this outcome, the research contributes a rigorous benchmarking framework and empirical insights into the challenges of parallelizing simple algorithms on shared-memory systems. To enhance future applicability, a targeted optimization plan is proposed: adaptive workload partitioning to minimize idle threads, cache-aware scheduling to improve memory locality, and hybrid execution combining sequential preprocessing with selective parallel matching. These refinements are expected to reduce synchronization costs and enhance scalability. Overall, this study underscores that while the Naïve algorithm can be parallelized, performance benefits depend critically on architectural optimization, offering valuable direction for developing efficient hybrid models in modern parallel string-matching research.

Keywords: algorithm optimization, bidirectional search, Naïve algorithm, OpenMP, parallel processing, performance benchmarking, string matching

Optimizing the Naïve String-Matching Algorithm Using Parallel Processing

Subaharan Sangeerththanan[1]*, Yasotha Ram Ramanan[1]
[1]Department of Physical Science, University of Vavuniya, Sri Lanka

Abstract

This study evaluates a novel bidirectional parallel string-matching algorithm, Binamatch, using OpenMP, against Boyer-Moore and KMP on diverse datasets. Experiments on multi-core systems showed Binamatch underperformed, with 10-1000x slower times due to overhead. Despite negative results, it provides empirical evidence and a testing framework for future optimizations in parallel string matching.

Introduction

String matching is fundamental to text analytics, bioinformatics, and search systems. While modern algorithms like Boyer–Moore and KMP dominate due to their sublinear average-case complexity, naïve string-matching remains valuable for its simplicity, ease of adaptation, and parallelization potential. This study explores the viability of a naïve algorithm variant—*Binamatch*—in modern multi-core environments, focusing on how bidirectional comparison and parallel workloads can exploit data-level concurrency.

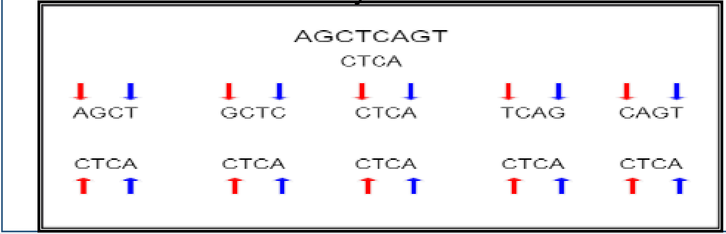

Objective

- Explore bidirectional comparison for early mismatch detection.
- Implement optimized workload distribution using OpenMP.
- Evaluate performance on large datasets via execution time, speedup, and efficiency.
- Contribute insights to parallel algorithm design for computational tasks.
- Identify bottlenecks and propose an optimization roadmap for future work.

Methodology

- Implemented sequential and OpenMP-based parallel versions of naïve, KMP, and Boyer–Moore algorithms in C++.
- Tested on 16- and 32-core systems with varying chunk sizes (64–1024).
- Used 10 dataset types (DNA sequences, ASCII text, and symbolic patterns).
- Collected metrics on execution time, speedup, and efficiency.
- Applied statistical validation for result reliability.
- Proposed optimization plan for reducing synchronization overhead and improving load balancing.

Results and Discussion

Performance Comparison: Binamatch averaged **15.2s**, versus **0.15s** (Boyer–Moore) and **0.02s** (KMP).

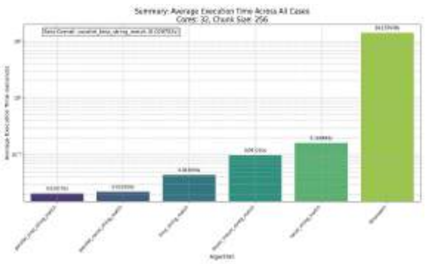

Suggested Optimizations:

- Adaptive chunk sizing based on input size.
- Hybrid sequential–parallel workload balancing.

Conclusion

While Binamatch did not outperform existing string-matching methods, the study highlights key limitations of naïve parallelization and provides a foundation for developing optimized hybrid approaches combining parallelism with heuristic preprocessing for large-scale applications.

References

- Efficient Randomized Pattern-Matching Algorithms. IBMJournal of Research and Development(2018)
- An Approach to Parallelization of Naive String-Matching Algorithm using Java Functional Parallelism Frameworks.(2021)

|ICAS2025|

Classification of Alzheimer's Disease using Multilayer Graph Neural Networks and Multi-Modal Neuroimaging

Hariharan Ilakkanakumaran[1], Pavithira Sivasothy[1], Tuvensha Jegatheeswaran[1]

[1]Department of Physical Science, University of Vavuniya, Sri Lanka

Abstract: Alzheimer's Disease (AD) is a progressive neurodegenerative disorder primarily affecting older adults, leading to cognitive decline, memory loss, and impaired daily function. Given its rising prevalence and lack of a cure, early diagnosis is critical for timely intervention. Traditional diagnostic methods, relying on clinical evaluations or single modality neuroimaging, often fail to capture the complex brain alterations in AD. This study introduces a novel framework combining a Multilayer Graph Attention Network (GAT) with multimodal neuroimaging for robust AD classification. Structural and functional brain networks were constructed using diffusion MRI (dMRI) and functional MRI (fMRI), focusing on 80 cortical and subcortical brain regions as network nodes. A multilayer graph was formed by integrating intra and inter connectivities into a comprehensive supra-adjacency matrix, which effectively captures both anatomical and functional interactions across brain regions. The supra-adjacency matrix is a sophisticated representation that combines connectivity data from multiple modalities into a single, unified structure, enabling the model to analyze complex relationships between brain regions across different network layers. The GAT model, designed to analyze this multilayer network, assigns adaptive attention weights to nodes and edges, emphasizing regions and connections most impacted by AD pathology. Trained and evaluated on a balanced dataset of 100 AD patients and 100 Normal Cognition subjects from the Alzheimer's Disease Neuroimaging Initiative (ADNI), The model achieved a classification accuracy of 97.5%, outperforming with traditional single-modality methods and other machine learning models, despite challenges in collecting both types of brain imaging modalities for the same subjects. This research highlights the benefits of integrating multimodal neuroimaging data with advanced graph-based deep learning architectures to enhance diagnostic precision. In the future, we plan to improve model performance by incorporating Explainable Artificial Intelligence (XAI).

Keywords: alzheimer's disease, brain networks, multilayer graph attention network, multimodal neuroimaging, supra-adjacency matrix

Classification of Alzheimer's Disease Using Multilayer Graph Neural Networks and Multi-Modal Neuroimaging

Hariharan Ilakkanakumaran[1*], Pavithira Sivasothy[2], Tuvensha Jegatheeswaran[3]
[1,2,3]*Department of Physical Science, Faculty of Applied Science, University of Vavuniya*

Introduction

Alzheimer's Disease

Alzheimer's Disease (AD) is a chronic brain disorder and main cause of dementia that worsens with age, since no single ideal test exists, clinicians use MRI, PET, and CT scans to detect brain shrinkage and assess memory, language, and history, with MRI being best for early detection.

Supra Adjacency Matrix

The Supra adjacency matrix is a key tool for multilayer networks, capturing interactions within (Intra-layer connections) and between (Inter-layer connections) layers using diagonal and off-diagonal blocks, respectively.

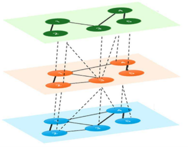

Figure 01 : Way of construct Supra adjacency matrix

Objective

- Use a Graph Attention Network (GAT) to classify AD accurately.
- Collect functional and structural brain images from the same subjects.
- Analyze intra- and inter-layer brain connectivity to identify patterns linked to AD.

Methodology

T1 and DW-MRI Images for structural brain network and T1 and rs-fMRI Images for functional brain network were collected from ADNI [adni.loni.usc.edu] Database. Collected Images consist of 100 Alzheimer's Disease and 100 Normal Control Subjects.

Table 1 :Demographics of Collected data

Variables	AD [100]	NC [100]
Male : Female	53 : 47	49 : 51
Age [mean ± std]	76 ± 7	73 ± 8

Construction of Structural and Functional Brain Network

- Used Desikan Killiany atlas for Brain Region Parcellation
- Structural Brain network : represents structural connectivity between human brain regions.
- Functional Brain network : represents functional connection between human brain regions.

Formulation of Supra Matrix

Separate functional brain network into two parts based positive and negative connectivity, then convert to binary form. Similarly convert the structural matrix into binary form.

By using functional positive matrix [FM+] & functional negative matrix [FM-] create intra connectivity of Supra Matrix and use structural matrix [SM] to form inter connectivity between functional positive and functional negative layers.

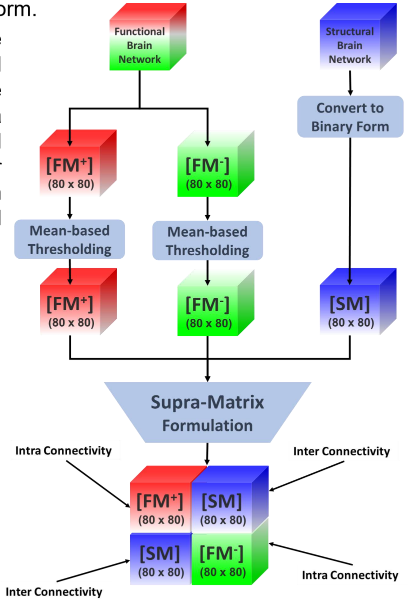

Figure 02: Supra-matrix formulation

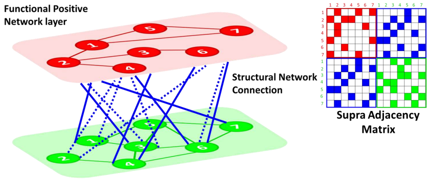

Figure 03: Multilayer Brain Network

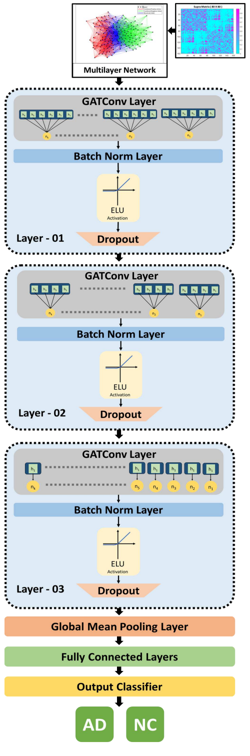

Figure 04: GAT model architecture

GAT model architecture

GAT classifies AD by applying three graph attention layers (6, 4, and 1 head with 64 channels per head, dropout 0.3, and ELU activation), using batch normalization, global mean pooling, and three fully connected layers for final classification.

Results and Discussion

This Chosen model GAT with proper parameters achieved high accuracy rate of **97.5%**.

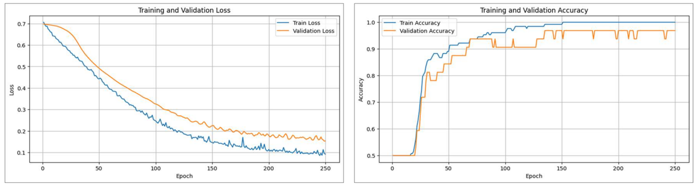

Figure 05 : Loss & Accuracy graphs for Training and Validation

Table 2 : Comparison of Classification accuracy of the proposed approach

Ref No	Deep Learning Model	Neuroimaging Modality	Classification Accuracy
[01]	GNN	fMRI	81.40 %
[02]	GNN	fMRI	93.40 %
[03]	GNN	diffusion MRI & T1 Images	97.00 %
[04]	CNN	(MRI) T1 & diffusion MRI (DTI)	95.00 %
Ours	**GAT**	**diffusion MRI, T1 & fMRI**	**97.50 %**

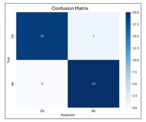

Figure 06 : Confusion matrix

Conclusion

- The study uses GAT with structural and functional networks to model brain connectivity through a Supra adjacency matrix, achieving **97.5%** accuracy in classifying AD using ADNI data.
- In future, Improve its performance with help of Explainable AI for Output Interpretation.

References

1. Bi, X.; Liu, Z.; He, Y.; Zhao, X.; Sun, Y.; Liu, H. GNEA: a graph neural network with ELMaggregator for brain network classification. Complexity 2020, 2020, 8813738.
2. Li, X.; Zhou, Y.; Dvornek, N.; Zhang, M.; Gao, S.; Zhuang, J.; Scheinost, D.; Staib, L. H.; Ventola, P.; Duncan, J. S. Braingnn: Interpretable brain graph neural network for fmri analysis. Medical Image Analysis 2021, 74, 102233.
3. Ansingkar, N.; Patil, R. B.; Deshmukh, P. An efficient multi class Alzheimer detection using hybrid equilibrium optimizer with capsule auto encoder. Multimedia Tools and Applications 2022, 81, 6539–6570.
4. Marzban, E. N.; Eldeib, A. M.; Yassine, I. A.; Kadah, Y. M.; Initiative, A. D. N. Alzheimer's disease diagnosis from diffusion tensor images using convolutional neu ral networks. PloS one 2020, 15, e0230409.
5. Venugopalan, J.; Tong, L.; Hassanzadeh, H. R.; Wang, M. D. Multimodal deep learning models for early detection of Alzheimer's disease stage. Scientific Reports 2021, 11,3254.
6. Casas-Roma, J.; Martinez-Heras, E.; Solé-Ribalta, A.; Solana, E.; Lopez-Soley, E.; Vivó, F.; Diaz-Hurtado, M.; Alba-Arbalat, S.; Sepulveda, M.; Blanco, Y., et al. Applying multilayer analysis to morphological, structural, and functional brain networks to identify relevant dysfunction patterns. Network Neuroscience 2022, 6, 916–933.

|ICAS2025|

Comprehensive QoS Analysis for Enhancing Performance Evaluation in Software Defined Networking

S.Fathima Masma[1], S.S.Suthaharan[1]

[1]Department of Physical Science, University of Vavuniya, Sri Lanka

Abstract: Software Defined Networking (SDN) introduces a paradigm shift in network architecture by centralizing control and configuration through software-based applications, separating the control plane from the data plane. This separation enhances network flexibility, enables automation, and improves programmability, offering superior traffic management, resource allocation, and Quality of Service (QoS) compared to conventional network designs. This study focuses on evaluating SDN performance through four critical QoS parameters: Response Time, Throughput, Bandwidth Isolation, and Queue Impact. These metrics are vital for assessing network responsiveness, data handling capacity, resource isolation, and the effects of queue configurations. Notably, this research addresses bandwidth isolation and queue impact areas that have received limited attention in prior studies making it a significant contribution to the field. To conduct this analysis, we implemented a single Linear Topology using the Mininet network emulator on a Linux platform. The network was configured using Python, with performance tests involving ICMP (ping) and TCP traffic under varying bandwidth and queue conditions. Experiments spanned multiple operational scenarios to capture detailed performance trends. The results highlight how adjustments to bandwidth and queue size influence the selected QoS parameters. These findings offer practical insights for network engineers and SDN practitioners, enabling them to optimize network performance and design more effective QoS-aware SDN deployments.

Keywords: bandwidth isolation, quality of service, response time, software defined networking, throughput

Comprehensive QoS Analysis for Enhancing Performance Evaluation in Software Defined Networking

S.Fathima Masma[1*], S.S.Suthaharan[1]

[1]Department of Physical Science,Faculty of Applied Science,University of Vavuniya,Sri Lanka,

Introduction

- Software Defined Networking (SDN) is a modern networking paradigm that separates the control plane from the data plane, enabling flexible and programmable network ma

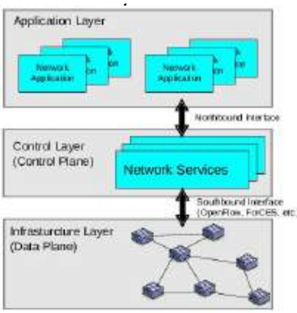

SDN Architecture Diagram

SDN Architecture

- **Application Layer** – communicates requirements.
- **Control Layer** – SDN Controller that makes decisions.
- **Infrastructure Layer** – forwarding devices like switches/routers.

- The SDN controller acts as the brain of the network, providing centralized control, policy enforcement, and programmability.
- Quality of Service (QoS) ensures efficient resource allocation and reliable performance in SDN networks, especially under varying traffic conditions.

- **Key QoS parameters:**
  - Response time
  - Throughput
  - Queue Impact
  - Bandwidth Isolation

SDN -QoS Parameters

- Current SDN performance evaluation methods focus mainly on **response time** and **throughput.**

My research additionally focuses on **Bandwidth Isolation, Queue Impact** parameters that have not been previously evaluated.

Aim & Objectives

Aim

- To evaluate the performance evaluation of Software-Defined Networking (SDN) by including additional Quality of Service (QoS) metrics.

Objectives

- To analyse the impact of bandwidth and queue variations on key QoS metrics, namely Response Time, Throughput using Transmission Control Protocol (TCP) traffic.
- To analyse the interaction between these additional parameters and existing metrics, like response time and throughput.
- To implement linear topology in Mininet with POX controller to simulate real-world SDN.

Methodology

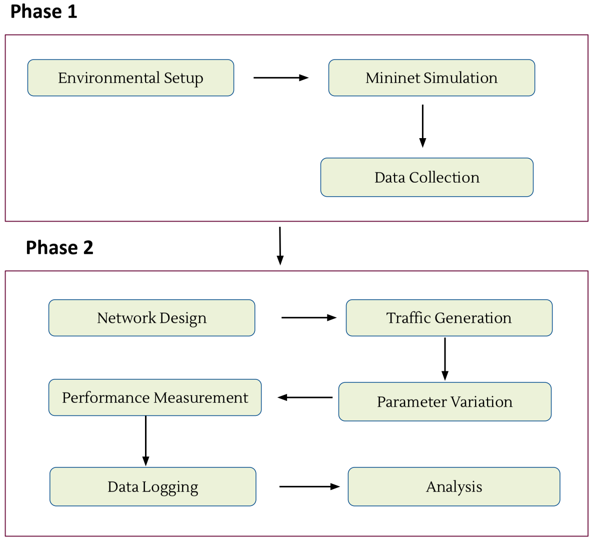

Phase 1

Environmental Setup → Mininet Simulation → Data Collection

Phase 2

Network Design → Traffic Generation → Parameter Variation → Performance Measurement → Data Logging → Analysis

Results and Discussion

Performance Analysis

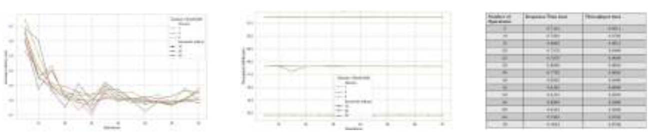

Response Time vs Operations

Throughput vs Operations

Performance Metrics Table

Comparison with previous studies

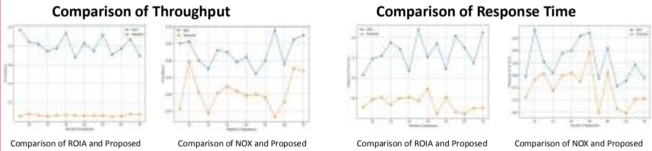

Comparison of Throughput

Comparison of Response Time

Comparison of ROIA and Proposed

Comparison of NOX and Proposed

Comparison of ROIA and Proposed

Comparison of NOX and Proposed

- **Throughput**
  - Proposed System → **13× higher** than ROIA
  - Proposed System → **1.4× higher** than NOX
- **Response Time**
  - Proposed System → **1.7× higher** than ROIA
  - Proposed System → **1.07× higher** than NOX
- Proposed system achieves significant throughput gains with a small trade-off in response time.

Conclusion

- Developed a performance evaluation framework for SDN including multiple QoS parameters.
- Implemented linear topology in Mininet with POX controller to simulate real-world SDN.
- Key metrics: response time, throughput, bandwidth isolation, queue impact.

References

[1] Hossain, M. A.; Sheikh, M. N. A.; Rahman, S.; Biswas, S.; Arman, M. A. I. Enhancing and measuring the performance in software defined networking. International Journal of Computer Networks & Communications (IJCNC) 2018, 10

[2] Xu, H.; Liu, J.; Qian, C.; Huang, H.; Qiao, C. Reducing controller response time with hybrid routing in software defined networks. Computer Networks 2019, 164, 106891.

[3] Al-Heety, O. S.; Zakaria, Z.; Ismail, M.; Shakir, M. M.; Alani, S.; Alsariera, H. A Comprehensive Survey: Benefits, Services, Recent Works, Challenges, Security, and Use Cases for SDN-VANET. IEEE Access 2020, 8, 91028–91047.

|ICAS2025|

Sentiment Analysis of Sinhala Patient Feedback using Deep Learning Techniques

D.W.M.U.P.Dissanayake

Department of Physical Science, University of Vavuniya, Sri Lanka

Abstract: Patient feedback has become an essential tool for evaluating and improving healthcare service quality. However, low-resource languages, such as Sinhala, have been largely overlooked in sentiment analysis research, which has mostly focused on widely used languages like English. This study addresses this gap by developing a deep learning-based sentiment analysis system for Sinhala patient feedback in hospital settings. A dataset of Sinhala patient reviews was collected and manually annotated into three sentiment categories: positive, negative, and neutral. The text data underwent preprocessing steps, including cleaning, tokenization, and padding, to prepare it for deep learning models. Multiple architectures were implemented and evaluated, including Convolutional Neural Networks (CNN) and Bidirectional Long Short-Term Memory networks (BiLSTM). Performance was assessed using accuracy, precision, recall, and F1-score. The BiLSTM model achieved the highest accuracy of 98.80%, outperforming the CNN model, which recorded 97.60% accuracy. These results demonstrate that deep learning models can effectively capture sentiment patterns in Sinhala text, even with limited resources. This study highlights the potential of deep learning techniques to provide actionable insights into patient satisfaction, enabling hospitals to identify areas for service improvement. In addition, the work contributes to advancing natural language processing research for low-resource languages by demonstrating that high-performing sentiment analysis models can be developed with careful annotation and preprocessing. The findings suggest that integrating such systems into healthcare workflows could support data-driven decision-making and improve patient experiences. Overall, this research not only offers a practical tool for analyzing Sinhala patient feedback but also serves as a foundation for further studies in low-resource language NLP applications.

Keywords: BiLSTM, CNN, deep learning, LSTM, natural language processing, Sinhala sentiment analysis

ICAS2025

Faculty of Applied Science
University of Vavuniya

Sentiment Analysis Of Sinhala Patient Feedback Using Deep Learning Techniques

D.W.M.U.P.Dissanayake

Supervised by Mrs R. Yasotha, Miss A. V. Ann Sinthusha

Abstract

Sinhala patient feedback was analyzed using deep learning to classify sentiments as positive, negative, or neutral. The BiLSTM model achieved the highest accuracy of 98.8%, outperforming CNN. This system demonstrates the effectiveness of deep learning in Sinhala sentiment analysis and offers insights for improving healthcare service quality while contributing to NLP research for low-resource languages .

Introduction

- Patient feedback is crucial for evaluating healthcare quality and improving service.
- Digital channels have increased textual reviews, creating a need for automated analysis.
- Sentiment analysis (NLP) identifies emotions in text; low-resource languages like Sinhala face research gaps.
- This study develops a deep learning system (CNN & BiLSTM) for Sinhala patient reviews.
- Performance measured by accuracy, precision, recall, and F1-score.

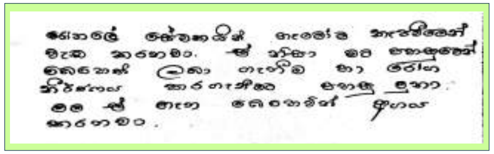

Figure 1: Sample Feedback from the patient

Objective

Aim:

- Develop a deep learning-based system to automatically analyze Sinhala patient feedback in healthcare settings, helping to understand patient sentiment and improve healthcare quality.

Objectives:

- Build and annotate a Sinhala patient feedback dataset with positive, negative, and neutral labels.
- Preprocess text using cleaning, tokenization, padding, and synonym augmentation.
- Develop and compare CNN and BiLSTM deep learning models for sentiment classification.
- Evaluate model performance using accuracy, precision, recall, and F1-score.

Methodology

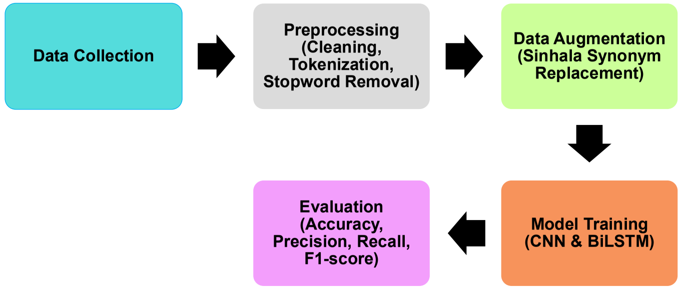

Data Collection

Preprocessing (Cleaning, Tokenization, Stopword Removal)

Data Augmentation (Sinhala Synonym Replacement)

Model Training (CNN & BiLSTM)

Evaluation (Accuracy, Precision, Recall, F1-score)

Figure 2: Text Classification Pipeline Flowchart

Results and Discussion

- The experimental results show that CNN achieved 97.6% accuracy with balanced precision, recall, and F1-scores, excelling in positive sentiment detection.
- BiLSTM outperformed CNN with 98.8% accuracy and 0.99 macro scores, showing stronger consistency and better handling of negative sentiment. BiLSTM proves more robust, while CNN offers computational efficiency.

Conclusion

- This study advances sentiment analysis for Sinhala patient feedback using deep learning.
- Findings provide valuable insights for NLP and healthcare researchers, guiding future work with larger datasets, enhanced preprocessing, and advanced models to improve automated sentiment classification and healthcare decision-making.

References

1. Liyanage, I. U. Sentiment analysis of Sinhala news comments, Doctoral dissertation,University of Colombo, 2018.
2. Mikolov, T.; Sutskever, I.; Chen, K.; Corrado, G. S.; Dean, J. In Advances in Information Processing Systems, 2013; Vol. 26.

|ICAS2025|

Posture Identification and Evaluation of Weight-Lifting Workout Styles using LSTM Networks

K.Rishigarani[1], Ayesh C.S.Merenchige[1]

[1]Department of Physical Science, University of Vavuniya, Sri Lanka

Abstract: Proper posture during weightlifting exercises is a critical factor for maximizing muscular gains, enhancing metabolic performance, and minimizing the risk of injuries to vulnerable areas such as the lower back, shoulders, elbows, and knees. However, many fitness enthusiasts, particularly those training at home without professional supervision, lack access to reliable feedback mechanisms that can ensure safe and effective exercise practices. Incorrect posture, even when subtle, not only reduces training efficiency but also significantly increases the likelihood of long-term musculoskeletal problems. Previous research efforts to ad dress this challenge have largely relied on sensor-based systems such as Inertial Measurement Units (IMU) and Electromyography (EMG). While these methods provide high levels of accuracy, they remain costly, intrusive, and highly dependent on correct sensor placement, which limits their scalability and practicality for home-based users. On the other hand, vision-based solutions such as Kinect and MediaPipe have shown promise but are often restricted to static frame analysis. These approaches fail to capture the temporal dynamics of motion, making them less effective for analyzing continuous weightlifting sequences or delivering detailed, joint-specific corrections. This study addresses these limitations by developing a non-intrusive, video-based posture evaluation system specifically for weightlifting exercises, focusing on Barbell Biceps Curls and Tricep Kickbacks. The system leverages Google's MediaPipe to extract skeletal keypoints corresponding to major joints such as shoulders, elbows, wrists, hips, and knees. From these landmarks, critical movement features including joint angles, torso inclination, and head orientation are derived and normalized. These temporal features are then processed using a Long Short-Term Memory (LSTM) network, which is capable of modeling sequential motion patterns across frames. This enables the classification of correct versus incorrect posture with high accuracy, achieving 94% for Biceps Curls and 96% for Tricep Kickbacks. To make the system practical and accessible, a lightweight web application was implemented, allowing users to upload workout videos and receive frame-by-frame analytical feedback. The application highlights deviations such as flared elbows, excessive torso rotation, or improper wrist alignment, offering users actionable guidance to improve form. Unlike expensive sensor-based systems, this approach requires only a standard smartphone camera, making it highly suitable for home fitness users. By integrating vision-based pose estimation with temporal deep learning, this study introduces a novel framework that not only improves workout safety and effectiveness but also sets a new benchmark for intelligent, accessible, and low-cost digital coaching in fitness technology.

Keywords: exercise monitoring, fitness technology, home-based training, LSTM, MediaPipe, posture correction, temporal deep learning, weightlifting posture analysis

ICAS2025

Faculty of Applied Science
University of Vavuniya

Posture Identification And Evaluation of Weight-Lifting Workout styles using LSTM Networks

Rishigarani K.[1*], Ayesh. C. S. Merenchige[2]

[1,2]*Department of Physical Science, University of Vavuniya, Sri Lanka.*

Introduction

Background and Motivation

- **Weightlifting Workout**
  - Weightlifting is a popular fitness activity that builds strength, boosts metabolism, and enhances overall fitness.
  - Correct posture prevents injuries, protects joints, and ensures effective muscle engagement.
- **What is Posture Analysis and Why Time Matters**

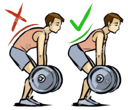

- Posture analysis studies how the body moves and aligns during activities like weightlifting to ensure correct form. Crucially, posture evaluation is not about static positions; it's about how the body moves over time. Tracking these movements step-by-step is essential to identify patterns and find mistakes

- **Why LSTM?**

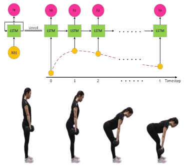

- Long Short-Term Memory (LSTM) is a type of deep learning technology perfectly suited for this task because it specializes in working with and understanding patterns in time-based, sequential data. Since weightlifting involves continuous motion over time, LSTM can accurately track and evaluate the body's movement sequence from videos, providing accurate posture analysis.

Aim and Objectives

AIM

Develop a **non-intrusive, video-based system** using **LSTM networks** to evaluate posture in exercises (**Barbell Biceps Curl** and **Tricep Kickback)** .

Objectives

1. Develop a Robust Feature Extraction Pipeline: To accurately translate raw video data into actionable movement metrics (pose landmarks, joint angles, and spatial features).
2. Classify Posture with High Temporal Accuracy: To train and validate a sequence-based LSTM model capable of classifying correct and incorrect exercise form over time.
3. Deliver Actionable, Frame-Level Feedback: To provide users with precise, joint-specific, and timely feedback on posture errors via a web-based application.

Our Novel Contribution

Prior research has explored posture analysis using:
- **CNNs** for posture recognition
- **IMU sensors** for activity recognition

Our work introduces a **distinct and practical approach**:
- **Non-invasive, video-based system for posture analysis**
- LSTM model employed to analyze the full temporal sequence of movement

The system provides:
- **Frame-level feedback** through a deployed web application.
- **Low-cost and accessible solution** suitable for home-based training.

Methodology

Data Collection

Video Dataset: We start with a video dataset containing exercises with both **correct and incorrect form**.

MediaPipe Pose: We use Google's MediaPipe **Pose** solution to extract 33 anatomical landmarks from each frame.

Landmark Selection: For analysis, we select a specific subset of landmarks that are most relevant to the exercise.

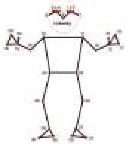

Barbell Biceps Curl : Eyes, Ears, Shoulders, Elbows, Wrists, and Hips.

Tricep Kickbacks : Nose, Eyes, Ears, Shoulders, Elbows, Wrists, Hips and Knees

Feature Engineering

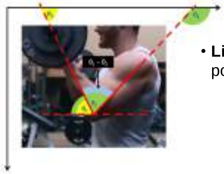

- **Joint Angles:** A three-point algorithm calculates key joint angles like the elbow or hip for precise limb positioning.
- **Line Angles:** We also calculate **line angles** to assess overall posture, such as torso inclination or head tilt.
  - ✓Hip-shoulder angles
  - ✓Head tilt
  - ✓Shoulder line
  - ✓Ear-shoulder angle
  - ✓Hip-to-knee line angles

$$\theta_{line} = \arctan 2(y_2 - y_1, x_2 - x_1) \times \frac{180}{\pi}$$

Preprocessing

- **Normalization:** Standardize landmark coordinates across videos to create temporal sequences.
- **Save Dataset as CSV:** Store features in a structured CSV for analysis and model training.
- **Data Transformation:** Convert raw positions into metrics that capture body movement patterns.

Temporal Normalization

$$frame_{normalized} = \frac{frame_{index}}{max(frame_{index})}$$

Min Max Scaler

$$X_{normalized} = \frac{X - X_{min}}{X_{max} - X_{min}}$$

LSTM Model Architecture

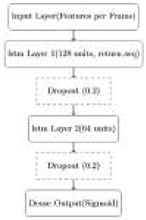

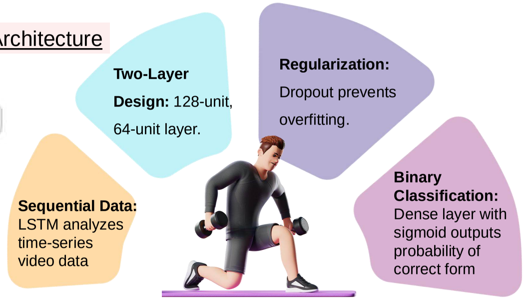

Two-Layer Design: 128-unit, 64-unit layer.

Regularization: Dropout prevents overfitting.

Sequential Data: LSTM analyzes time-series video data

Binary Classification: Dense layer with sigmoid outputs probability of correct form

Results and Discussion

Barbell Bicep Curl (Overall Accuracy 94%)

	Precision	Recall	F1-score
Incorrect	0.93	0.96	0.95
Correct	0.96	0.92	0.94

Classification report and Confusion Matrix for Barbell Bicep Curl

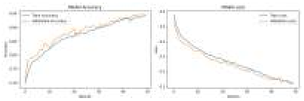

Training and validation loss and accuracy curves for Barbell Biceps Curl

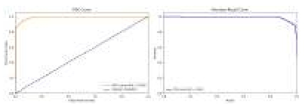

ROC AUC and Precision-Recall curves for Barbell Biceps Curl

Tricep Kickback (Overall Accuracy 96%)

	Precision	Recall	F1-score
Incorrect	0.94	0.97	0.96
Correct	0.97	0.93	0.95

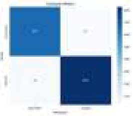

Classification report and Confusion Matrix for Tricep Kickback

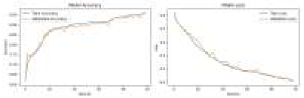

Training and validation loss and accuracy curves for Tricep Kickback

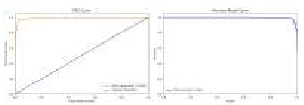

ROC AUC and Precision-Recall curves for Tricep Kickback

- **Trustworthiness:** The high overall accuracy ensures reliable distinction between safe and incorrect form, making it a dependable tool for users training without a coach.
- **Safety (High Precision):** High precision for incorrect form means flagged errors are genuine, minimizing false alarms and helping users correct mistakes immediately.
- **Effectiveness (High Recall):** High recall ensures most actual errors are detected, improving technique and overall workout quality.

Conclusion

- Developed a **vision-based system** using MediaPipe and LSTM to evaluate posture in Biceps Curls and Tricep Kickbacks with high accuracy.
- Provides **frame-by-frame, joint-specific feedback** through a simple web application.
- Delivers a **low-cost, non-invasive solution** that improves safety and effectiveness for home-based training.

References

1) He,Q.; Li, W.; Tang, W.; Xu, B. Recognition to weightlifting postures using convolutional neural networks with evaluation mechanism. Measurement and Control 2024, 57, 653–663.

2) Lisboa, C. L.; Nedel, L.; Maciel, A. In 2016 XVIII Symposium on Virtual and Augmented Reality (SVR), 2016, pp 122–126.

3) Webber, M.; Rojas, R. F. Human activity recognition with accelerometer and gyro scope: A data fusion approach. IEEE Sensors Journal 2021, 21, 16979–16989.

4) Mekruksavanich, S.; Jitpattanakul, A. A residual deep learning method for accurate and efficient recognition of gym exercise activities using electromyography and imu sensors. Applied System Innovation 2024, 7, 59.

5) Garg, S.; Saxena, A.; Gupta, R. Yoga pose classification: a CNN and MediaPipe in spired deep learning approach for real-world application. Journal of ambient intelligence and humanized computing 2023, 14, 16551–16562.

|ICAS2025|

Sri Lankan Seagrass Family Identification using Underwater Images through Image Enhancement and Deep Learning Techniques

J.Diluxshan[1], T.Keerthanaram.[2], J.Tuvensha[3], V.Athiththan[4]

[1,4]Department of Physical Science, University of Vavuniya, Sri Lanka
[2]Department of Bio Science, University of Vavuniya, Sri Lanka
[3]Department of ICT, University of Vavuniya, Sri Lanka

Abstract: Seagrass ecosystems are integral to marine biodiversity, carbon sequestration, and coastal resilience, yet their monitoring remains constrained by the complexities of underwater imaging and manual species identification. Automated identification of seagrass families is important for enabling large scale, consistent, and timely monitoring, reducing reliance on labor intensive manual classification, and improving conservation and management efforts for these vital marine ecosystems. This study proposes a novel hybrid deep learning framework for the automated classification of three predominant seagrass families in Sri Lanka's coastal waters: Hydrocharitaceae, Cymodoceaceae, and Ruppiaceae. A total of 700 underwater images were captured using iPhone 15 Pro Max and GoPro cameras from multiple coastal locations, including Mannar, Trincomalee, and Jaffna. Following a two stage enhancement pipeline combining Water-Net and DehazeFormer, 217 high quality images were retained, which were then augmented to 1,519 images across the three families to improve dataset diversity. Among five evaluated convolutional neural networks, VGG16, VGG19, and MobileNetV2 were selected as base learners in an ensemble model, achieving 99% classification accuracy on the test dataset. These findings demonstrate the potential of deep learning based, automated seagrass monitoring to enable scalable, consistent, and timely conservation efforts.

Keywords: deep learning, ensemble learning, marine biodiversity monitoring, seagrass classification, underwater image enhancement

ICAS2025

Faculty of Applied Science
University of Vavuniya

Sri Lankan Seagrass Family Identification using Underwater Images through Image Enhancement and Deep Learning Techniques

Diluxshan J.[1*], Keerthanaram T.[2],Tuvensha J.[3],Athiththan V.[4]
[1,4]Department of Physical Science, Faculty of Applied Science, University of Vavuniya.
[2]Department of Bio-Science, Faculty of Applied Science, University of Vavuniya.
[3]Department of ICT, Faculty of Technological Studies, University of Vavuniya.

Introduction

- Seagrasses are vital marine plants supporting biodiversity, carbon storage, and coastal stability
- Sri Lanka hosts three dominant families:
  - *Hydrocharitaceae*
  - *Cymodoceaceae*
  - *Ruppiaceae*


(a) *Cymodoceaceae* (b) *Hydrocharitaceae* (c) *Ruppiaceae*

- These ecosystems are threatened by climate change, pollution, and habitat loss
- Accurate identification protects marine life and supports conservation
- Manual identification is slow and resource heavy

Previous Studies

Study	Methodology	Key Findings	Limitations
Nawaz et al. (2025)	Survey of deep learning methods for seagrass monitoring	Overview of CNN, Transformer, and enhancement based techniques; compared reported accuracies from 85%–98% in different contexts	No experimental validation on Sri Lankan datasets
Stankovic et al. (2021)	Field surveys and carbon analysis in SE Asia seagrass beds	Quantified blue carbon stock; climate change mitigation role; no classification accuracy	Does not address automated classification or image based monitoring
Paul et al. (2023)	LWDS lightweight CNN for seagrass classification	Achieved ~92.49% accuracy on underwater seagrass dataset	Limited to one dataset; no advanced enhancement integration
Song et al. (2022)	Vision Transformer (*DehazeFormer*) for image dehazing	Achieved over 40 dB PSNR; introduced RS-Haze dataset for realistic dehazing	Not underwater/seagrass-specific; high computational cost
Langlois et al. (2023)	Subtidal Seagrass Detector using deep learning	Presence detection accuracy: 97.0%; cover classification accuracy: 80.7%	Focused on presence/cover estimation, not fine grained family classification
Ozaeta et al. (2024)	CNN-based multi species classification	Achieved 93.72% accuracy across five seagrass species in varied habitats	Requires large, diverse labeled datasets for generalization
Li et al. (2019)	Water-Net	Provided dataset for evaluating enhancement algorithms; improved image quality in multiple studies leading to +5–10% accuracy gains in classification tasks	Dataset not specific to seagrass; general underwater scenes

Aim & Objective

Aim:
Develop an automated system to identify Sri Lankan seagrass family in underwater images using image enhancement and deep learning

Objectives:
- Collect underwater images from Mannar, Trincomalee, and Jaffna
- Enhance image quality using **Water-Net** and **DehazeFormer**
- Train and evaluate multiple CNN architectures
- Implement an **ensemble model** to achieve high accuracy
- Develop a **Django-based system** for user friendly classification

Methodology

1. Image Acquisition
   - Underwater images collected using **iPhone 15 Pro Max** and **GoPro** over a **2-month period**
   - Locations: **Jaffna**, **Mannar**, and **Trincomalee**
   - Manually labeled into three seagrass families: *Hydrocharitaceae*, *Cymodoceaceae*, and *Ruppiaceae*
   - Images affected by low light, turbidity, and color distortion caused by underwater conditions

No	Family Name	Count
01	*Cymodoceaceae*	340
02	*Hydrocharitaceae*	100
03	*Ruppiaceae*	260

Summary of the seagrass image dataset before pre-processing

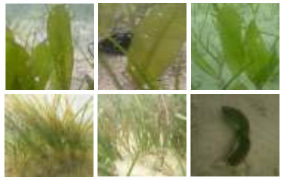

2. Image Enhancement
   - Underwater challenges: turbidity, low contrast, color distortion
   - Stage 1: **Water-Net** (pretrained) for color correction, contrast enhancement, haze reduction
   - Stage 2: **DehazeFormer** (pretrained) for residual haze removal and clarity improvement
   - Applied sequentially to all dataset images for consistent, high quality inputs
   - Data augmentation performed to expand and balance the dataset

No	Family	Count
01	*Cymodoceaceae*	576
02	*Hydrocharitaceae*	385
03	*Ruppiaceae*	576

Final seagrass image dataset after augmentation


(a) Raw *(b) WaterNet* *(c) DehazeFormer*

3. Model Training and Configuration
   - **Dataset split:** 70% training, 20% testing, 10% validation
   - Trained **five CNN models: VGG16, VGG19, MobileNetV2, Xception, and DenseNet121** for multi class seagrass family classification
   - Other models were tested but showed low accuracy; these five fit the data best
   - The **best performing** models among the five were selected for ensemble learning

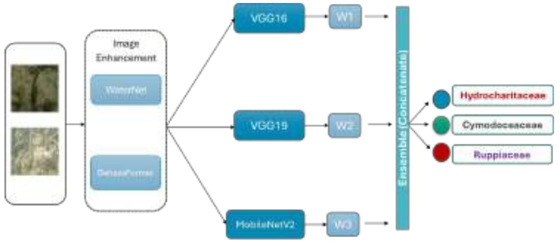

Model Development and Training Pipeline

Results and Discussion

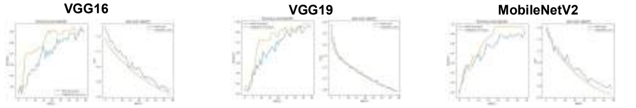

Training and Validation Performance of Best Models

Model	Accuracy (Without Enhancement)	Accuracy (With Enhancement)
VGG16	*78%*	94%
VGG19	*80%*	97%
MobileNetV2	*75%*	97%
Xception	*73%*	89%
DenseNet121	*77%*	88%

Accuracy With and Without Enhancement


User Interface *After Image Upload* *Classification Result*

System Development

- **Without enhancement**, models gave only **73–80% accuracy** due to haze, low contrast, and color issues in underwater images
- **With WaterNet and DehazeFormer**, accuracy improved greatly to **88–97%**, proving that enhancement is essential
- The best models were **VGG16, VGG19, and MobileNetV2**
- Their **ensemble achieved 99% accuracy**, showing that enhancement plus ensemble learning is a strong and reliable solution for seagrass identification

Conclusion

- The ensemble model achieved **99% accuracy**
- Implemented a two-stage image enhancement pipeline: **Water-Net** + **DehazeFormer**
- Trained and evaluated multiple CNN models (VGG16, VGG19, MobileNetV2, Xception, DenseNet121)
- Selected top 3 models (VGG16, VGG19, MobileNetV2) for ensemble learning
- Provides a practical, user-friendly tool for researchers and conservationists
- Developed an automated Django-based system for underwater seagrass family classification

References

1. Nawaz, U., Anees-ur-Rahaman, M., & Saeed, Z. (2025). A survey of deep learning approaches for the monitoring and classification of seagrass. *Ocean Science Journal*, 60, 19.
2. Stankovic, M., Ambo-Rappe, R., Carly, F., Dangan-Galon, F., Fortes, M. D., Hossain, M. S., Kiswara, W., Van Luong, C., Minh-Thu, P., Mishra, A. K., et al. (2021). Quantification of blue carbon in seagrass ecosystems of Southeast Asia and their potential for climate change mitigation. *Science of the Total Environment*, 783, 146858.
3. Paul, M. A., Kumar, K. S., Sagar, S., & Sreeji, S. (2023). LWDS: Lightweight DeepSeagrass technique for classifying seagrass from underwater images. *Environmental Monitoring and Assessment*, 195, 614.
4. Langlois, L. A., Collier, C. J., & McKenzie, L. J. (2023). Subtidal Seagrass Detector: Development of a deep learning seagrass detection and classification model for seagrass presence and density in diverse habitats from underwater photoquadrats. *Frontiers in Marine Science*, 10, 1197695.
5. Ozaeta, M. A. A., Fajardo, A. C., Brazas, F. P., & Cantal, J. A. M. (2024). Deep Learning Approach for Seagrass Species Classification. *Proceedings of the GECOST 2024 Conference*.
6. Li, C., Guo, C., Ren, W., Cong, R., Hou, J., Kwong, S., & Tao, D. (2019). An underwater image enhancement benchmark dataset and beyond. *IEEE Transactions on Image Processing*, 29, 4376–4389.
7. Song, Y., He, Z., Qian, H., & Du, X. (2022). Vision Transformers for Single Image Dehazing. *IEEE Transactions on Image Processing*, 31, 5635–5648.

|ICAS2025|

Parallelizing Reed-Solomon Codes for Enhanced DNA Data Storage

M.S.K.Alwis

Department of Physical Science, University of Vavuniya, Sri Lanka

Abstract: The rapid increase in global data is expected to reach hundreds of zettabytes soon. It has exposed the limitations of current storage technologies regarding capacity, durability, and energy efficiency. DNA, nature's own data carrier, offers a powerful alternative for data storage. It has an extremely high storage density up to hundreds of exabytes per gram and can remain stable for thousands of years. This makes DNA an ideal medium for long-term archival and biomedical data storage. However, using DNA for practical data storage faces significant challenges. These include high synthesis and sequencing error rates, as well as the need to maintain balanced GC content for reliable reading. To address these issues, this work presents a new parallelised implementation of the Reed–Solomon code over the Galois Field, specially optimised for DNA digital storage. Unlike previous methods, our design combines OpenMP-based multi-core parallelism using 8 threads with SIMD vectorised block processing, achieving up to 5.4X speedup while maintaining 100% decoding accuracy for two-symbol errors per block. The implementation extends the Schifra Reed–Solomon library with custom modifications that handle DNA-specific error patterns, improving robustness and enabling smooth integration with molecular data workflows. The proposed framework shows strong potential for large-scale archival storage, biomedical research, and energy-efficient big data systems. It highlights how computational parallelism can connect the worlds of molecular and digital information. Future work will focus on scaling to larger code parameters and exploring GPU-based acceleration for real-time applications.

Keywords: Galois Field, OpenMP, Reed Solomon, Schifra library, SIMD

ICAS2025

Faculty of Applied Science
University of Vavuniya

Parallelizing Reed-Solomon Codes for Enhanced DNA Data Storage

M.S.K.Alwis [1*]
[1]Department of Physical Science, Faculty of Applied Science, University of Vavuniya, Sri Lanka

Introduction

- **Data explosion** → traditional storage insufficient
- **DNA storage** → sustainable, ultra-high density (~215 PB/gram)
- **Challenges** → errors in synthesis & sequencing
- **Current solutions** → Reed–Solomon codes; slow for large data
- **Need** → faster, efficient error correction

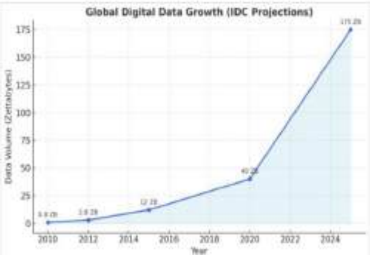

Figure 1:Data Growth

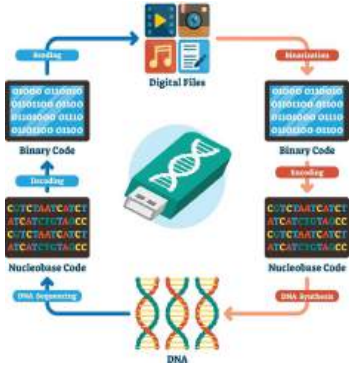

Figure 2:DNA storage process

Objective

- Parallelize Reed-Solomon encoding & decoding for DNA data storage.
- Evaluate performance improvements and error correction accuracy.
- Explore CPU thread scaling and field size trade-offs.

Methodology

- **Platform:** C++ (GF(16)) implementation with OpenMP parallelization.
- **Input:** DNA sequence split into fixed-size 11-base blocks.
- **Process:** Each block independently encoded/decoded in parallel.

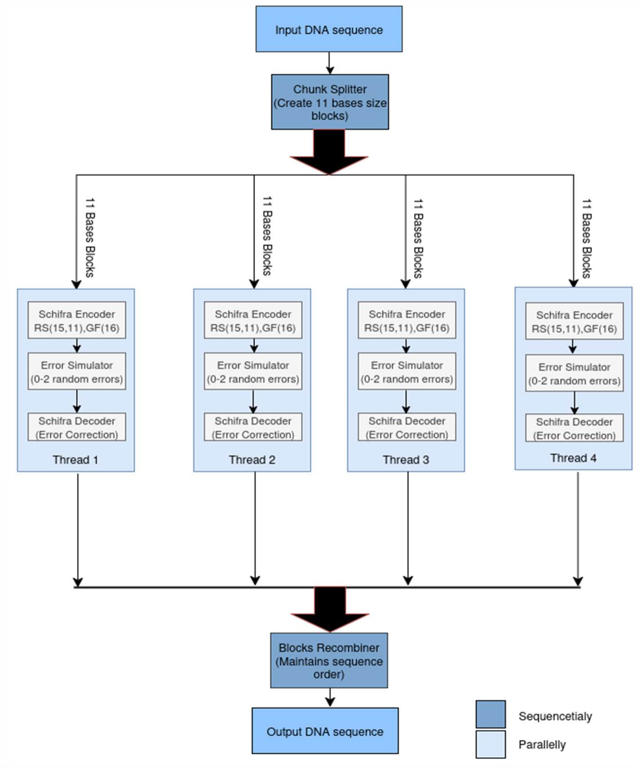

Figure 3:Parallel Architecture

Results and Discussion

- **Scalability:** Increasing threads yields a **considerable performance boost**.
- **Robust Speedup**: Speedup is **consistent for large sequence lengths.**
- Shows **minimal variation due to errors** (1 or 2 errors per block).

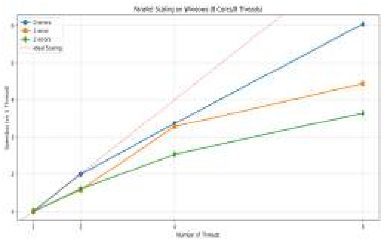

Figure 4:Parallel scaling performance on Windows (8C/8T system)

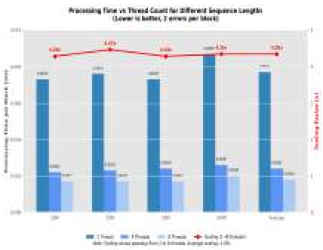

Figure 5:Parallel processing time for large sequences

Conclusion

- **Conclusion:** Parallelized Schifra RS is appropriate for **fast, large-scale DNA storage**, maintaining 100% accuracy for **minimum error rates (≤2 errors/11-base block)**.

- **Future Work:** Explore **GPU acceleration** to further enhance large-scale performance.

References

[1] N. Goldman et al., "Towards practical, high-capacity, low-maintenance information storage in synthesized DNA," *Nature*, vol. 494, no. 7435, pp. 77–80, Feb. 2013, doi: 10.1038/nature11875.

[2] J. Guan et al., "Chemical principles for novel DNA storage systems," *bioRxiv*, preprint, Jul. 2016. [Online]. Available: https://www.biorxiv.org/content/10.1101/064238v1

[3] A. Koohi and S. Hessabi, "A novel encoding algorithm for efficient DNA storage," in *Proc. ACM Great Lakes Symp. VLSI*, 2003, pp. 152–157, doi: 10.1145/764808.764848.

|ICAS2025|

Leveraging Natural Language Processing for a Centralized Digital Hub to Automate Traffic Law Enforcement and Fine Management in Sri Lanka

P.R.P.D.Bandara[1], A.V.Ann Sinthusha[1], R.Yasotha[1]

[1]Department of Physical Science, University of Vavuniya, Sri Lanka

Abstract: This paper presents a legal NLP system that maps free-text traffic violation narratives to the applicable offences and penalties under Sri Lanka's *Motor Traffic Act.* We digitize the principal Act and its amendments into a structured corpus and evaluate a progression of retrieval and reasoning methods—TF-IDF, BM25, SBERT (with a lexical–semantic hybrid), a compact local TinyLLM, and an OpenAI LLM integrated with Retrieval-Augmented Generation (RAG). A staged methodology first validates the pipeline on 42 on-the-spot fine offences and then scales to the full consolidated Act. Using 300 expert-validated scenarios (multi-offence, up to three penalties per case), we require exact section/subsection/paragraph/subparagraph matches for correctness. The implemented system outputs, for each detected offence, the exact *Motor Traffic Act* citation and the corresponding prescribed penalty/fine as defined in the Act. The OpenAI RAG approach achieves 94.00% overall accuracy and 100.00% partial accuracy, substantially outperforming TinyLLM (68.33% overall), SBERT (33.67%), BM25 (26.67%), and TF-IDF (0.67%). These results indicate that dense retrieval coupled with grounded generation handles paraphrase, multi-offence narratives, and subtle context better than sparse baselines. We enforce ethical safeguards: evidence-linked outputs, confidence scoring, and abstention under uncertainty to support transparent, auditable use. We discuss validity threats (synthetic narratives, label robustness), guardrails (citation-linked outputs, abstention), and deployment aspects (temporal indexing, bilingual support), showing that legal RAG can deliver deployment-grade accuracy for traffic enforcement in a low-resource jurisdiction.

Keywords: information retrieval, legal NLP, retrieval augmented generation, Sri Lanka, traffic law

ICAS 2025

Faculty of Applied Science
University of Vavuniya

Leveraging Natural Language Processing for a Centralized Digital Hub to Automate Traffic Law Enforcement and Fine Management in Sri Lanka

P.R.P.D. Bandara[1*], A.V. Ann Sinthusha[1], R. Yasotha[1]
[1]*Department of Physical Science, Faculty of Applied Science, University of Vavuniya, Sri Lanka*

Introduction

- Traffic enforcement in Sri Lanka is **manual and fragmented**, causing unequal penalties and officer-level inconsistency.
- No **centralized, authoritative platform** exists for offence look-up, penalty calculation, and legal citations[2].
- **Low public legal literacy** makes compliance difficult and fuels disputes[3].
- This research present the **first end-to-end legal NLP system** for Sri Lankan traffic law: scenario → offence(s) → exact citation(s) → penalty/fine.

Objectives

1. Apply natural language Processing techniques for traffic offence detection and fine calculation
2. Develop a Comprehensive Legal Data Processing Pipeline
3. Develop User-Centric Web Interface for Real-World Deployment

Methodology

- This research digitized the Motor Traffic Act[1] and its amendments into a structured corpus and built a retrieval-to-reasoning pipeline
- (TF-IDF/BM25 → SBERT/TinyLLM → OpenAI LLM + RAG) that maps free-text violations to exact citations and penalties.
- The pipeline was validated in two stages, first on 42 on-the-spot offences, then across the entire consolidated Act with evidence-linked, confidence-scored outputs (with abstention when uncertain).

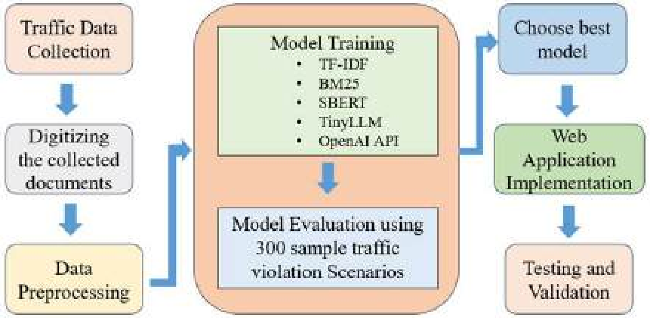

Figure 1: *Overall Methodology*

Results and Discussion

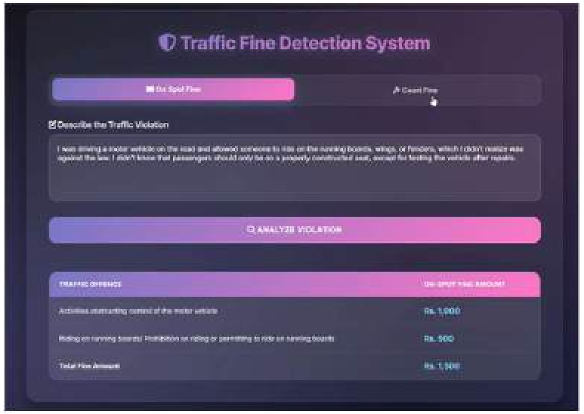

☑ Describe the Traffic Violation

I was driving a motor vehicle on the road and allowed someone to ride on the running boards, wings, or fenders, which I didn't realize was against the law. I didn't know that passengers should only be on a properly constructed seat, except for testing the vehicle after repairs.

TRAFFIC OFFENCE	ON-SPOT FINE AMOUNT
Activities obstructing control of the motor vehicle	Rs. 1,000
Riding on running boards/ Prohibition on riding or permitting to ride on running boards	Rs. 500
Total Fine Amount	Rs. 1,500

Figure 3: *User Interface*

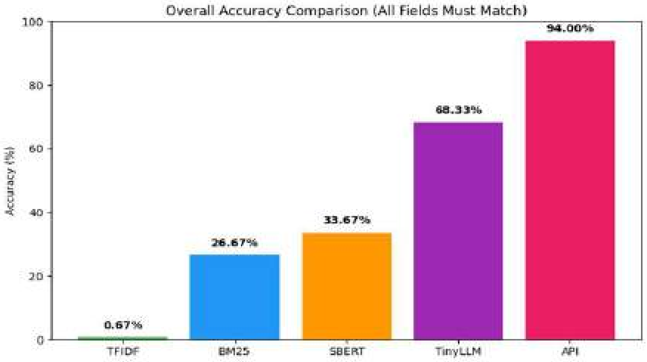

Figure 2: *Overall Accuracy Comparison*

Conclusion

- A **unified legal NLP platform** can **standardize** traffic enforcement decisions in Sri Lanka.
- **Evidence-linked** citations and **exact penalties** enhance **transparency** and **public trust**.
- **RAG-based retrieval + reasoning** achieves deployment-grade accuracy for a low-resource jurisdiction.

References

[1] Motor Traffic Act, No. 14 of 1951, Parliament of the Democratic Socialist Republic of Sri Lanka.

[2] Wijesinghe,K.; Fernando,S. Digitalization challenges in Sri Lankan law enforcement. Sri Lanka J. Technol. 2020, 12, 34–50.

[3] Katz,M.A. Natural language processing in legal informatics: A review of applications and challenges. Artif. Intell. Law 2021, 29, 201–230

|ICAS2025|

Computationally Scalable Lecture Assistance through Large Language Models and Retrieval Augmented Generation in Consumer-Grade Hardware

Ilma Jiyadh[1], S.Thirukumaran[1]

[1]Department of Physical Science, University of Vavuniya, Sri Lanka

Abstract: Taking notes during lectures is cognitively demanding and often hindered by environmental factors, with students with learning disabilities (LD) facing even greater challenges. This research addresses a critical gap by developing an automated lecture assistance tool that generates detailed notes, answers retrospective questions of students related to lectures, and produces practice questions to enhance comprehension. Existing tools either rely on proprietary, resource-intensive Large Language Models (LLMs), which require certain subscriptions, or keyword extraction mechanisms such as TF-IDF, and none of them could answer students' questions based on past lectures or generate theoretical questions based on past lectures to improve student comprehension. The primary objectives are to identify resource-efficient LLMs, fine-tune them for generating structured lecture notes, integrate an effective RAG system, and evaluate the end-to-end pipeline for accuracy and relevance. The methodology involved selecting a suitable Automated Speech Recognition (ASR) system for lecture audio transcription, creating datasets of lecture transcripts and notes, fine-tuning compact LLMs using parameter-efficient techniques, and integrating a RAG pipeline with it. The fine-tuned model's performance was evaluated with metrics including ROUGE, BERT Score and Perplexity to select the LLM that would serve as the base LLM for the tool development. RAG Assessment (RAGAS) was used to evaluate the built RAG system. Comparative analysis was conducted to evaluate the behaviour of LLM with and without RAG integration. This showed that the RAG integration significantly reduced LLM hallucinations by 37%. The proposed solution demonstrates that high-quality, accessible lecture assistance tools can be built even on modest hardware, supporting students- including those with LD- by automating notetaking, highlighting key announcements, enabling retrospective query answering, and generating practice questions. To our knowledge, this is the first study to fine-tune LLMs, integrate with RAG and deploy them on consumer-grade hardware for lecture assistance.

Keywords: fine-tuning LLMs, learning disabilities, lecture note-taking, RAG, scalable tool

Computationally Scalable Lecture Assistance through Large Language Models and Retrieval Augmented Generation in Consumer-Grade Hardware

Ilma Jiyadh[1*], S. Thirukumaran[2]
[1*,2]Department of Physical Science, University of Vavuniya, Sri Lanka

INTRODUCTION

- Lecturing is the primary method of delivering valuable information to students within the university [1], therefore effectively taking down notes during lectures is crucial.
- Students often face challenges during lectures due to factors like lighting, seating, audio-visual quality, room temperature, comfort, etc., [2] which make notetaking difficult.
- And, for students with Learning Disabilities, note-taking could be even more challenging.
- Although these difficulties have been identified and extensively studied there have been very less effort made to help these students with lectures.

AIM

Develop an automated tool using a fine-tuned LLM integrated with RAG to assist students with lectures by generating detailed lecture notes, including important announcements, generating theoretical questions based on the lectures held so far and support interactive querying of past lectures to improve students' comprehension.

OBJECTIVES

- Select compact LLMs that could be efficiently fine-tuned and evaluate their performance.
- Compare the system with and without RAG to investigate the accuracy in the responses.
- Investigate the ability of LLMs to handle long texts.

METHODOLOGY

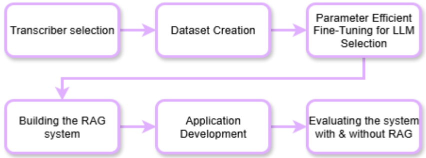

Fig 1. Methodology Pipeline

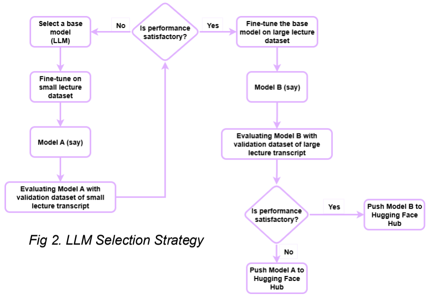

Fig 2. LLM Selection Strategy

1. Transcriber Selection
   - Whisper's small model was lightweight but inaccurate and slow, while larger versions improved accuracy at the cost of high latency and high computational overhead.
   - In contrast, Assembly AI offered notably high transcription accuracy while maintaining low latency, making it more efficient for processing long lecture audios. Therefore, it was chosen.
2. Dataset Creation
   - Two sets of data were created for LLM fine-tuning: one with 500 data of small lecture transcript and other with 124 data of large lecture transcript.
   - A set of 70 question and ground truth answer pairs were created to evaluate RAG.
3. Fine-Tuning
   - Low-rank adapters were used for PEFT.
   - TinyLlama-1.1B-ChatV1.0, Llama-3.2-1B-Instruct, Phi3-4K-mini_Instruct were chosen candidates for resource efficient fine-tuning.
4. RAG Setup
   - Chroma as Vector DB.
   - All-MiniLM-L6-V2 as embedder.
5. Application Development
   - ReactJs for frontend.
   - FastAPI for local backend.
   - Gradio Client Interface for LLM Inference.
6. With and without RAG Evaluation
   - Responses were recorded from system with and without RAG.
   - For each response it was classified as hallucinated or non-hallucinated.
   - Hallucination rate = number of hallucinated response / total response.

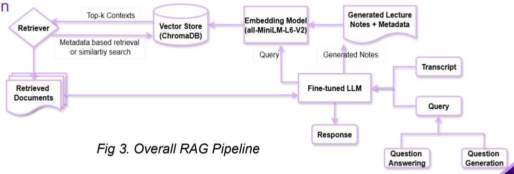

Fig 3. Overall RAG Pipeline

RESULTS & DISCUSSION

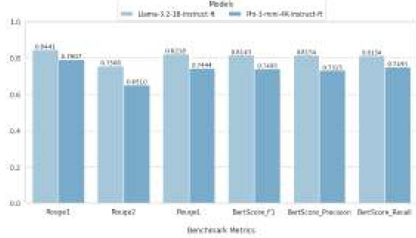

Fig 4. Evaluation of Phi3-mini-4k and Llama-3.2-1B on small lecture transcript

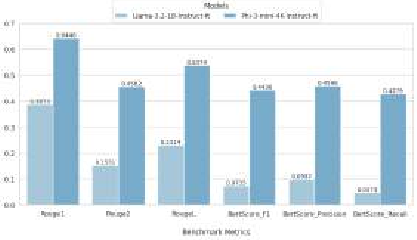

Fig 5. Evaluation of Phi3-mini-4k and Llama-3.2-1B using Split merge strategy

Metric	Phi-lecture_note-ft (ours)	Phi-3-mini-4K-Instruct
ROUGE-1	0.7907	0.6129
ROUGE-2	0.6510	0.3965
ROUGE-L	0.7444	0.5281
BertScore-F1	0.7405	0.3700
BertScore-Precision	0.7315	0.3305
BertScore-Recall	0.7493	0.4183
Perplexity	2.8920	4.9808

Table 1. Evaluation of Phi3-mini-4k after and before fine-tuning

Fig 6. Training TinyLlama-1.1B-Chat-v1.0 on large lecture transcript dataset

- TinyLlama-1.1B-ChatV1.0 performed well on small lecture transcripts, but fine-tuning with larger ones led to meaningless outputs due to exceeding its context length.
- Llama-3.2-1B-Instruct and Phi-3-4K-Mini-Instruct worked well on small transcripts but struggled with larger ones, so a split–merge approach was used. Phi-3-4K-Mini-Instruct was selected as the base model for its better performance.
- Integrating RAG reduced hallucination rates by up to 37%.

Component	Metric	Score	Interpretation
Retriever	Context Precision	0.9857	Excellent relevant context retrieval
	Context Recall	0.9571	High coverage of relevant information
Generator	Faithfulness	0.7679	Good adherence to retrieved context
	Answer Relevancy	0.9351	High alignment with user queries
End-to-End	Semantic Similarity	0.9224	Excellent meaning alignment
	Answer Correctness	0.8377	High factual accuracy

Table 2. RAGAS metric scores for RAG evaluation component-wise and end-to-end pipeline

RELATED WORKS

Ref.	Notetaking Approach	Limitations
[3]	ASR- Whisper, TF-IDF for keyword extraction and GGUF LLMs for summaries.	Only ~50% keyword relevance. Limited by transcription errors, hardware dependence, and lack of factual accuracy checks.
[4]	Mobile app using Whisper + Gemini LLM + LangChain for optimized notes.	Performance relies on internet access and requires some post-editing due to inaccurate transcription.
[5]	Web tool for humanities students using GPT-4 with customizable summarization (length, tone, format).	Risks in information loss in MapReduce and limited real-classroom testing.
[6]	LLM expands user "micronotes" into full personalized notes.	Struggles with vague micronotes, small user study, occasional hallucinations.
[7]	Collaborative whiteboard system for group note-taking.	Observed distractions and no significant quiz score improvements were noted.

CONCLUSION

- This research shows that an effective tool can be built even in resource-constrained settings, to assist students with lectures.
- Fine-tuning helps LLMs adapt to domain-specific tasks.
- Integrating RAG can help reduce LLM hallucinations.
- Simply choosing an LLM with a larger context length does not always help with its ability to handle long texts.

LIMITATIONS

- The quality of the generated notes drops when the lecture relies heavily on whiteboard explanations.
- User experience and satisfaction were not extensively evaluated in this study.

FUTURE WORKS

- Optimising the tool for mobile platforms, enabling greater accessibility.
- Incorporating ASR systems that can transcribe lectures across multiple languages would better support multilingual classrooms, particularly in regions with linguistically diverse student populations.
- Extending the tool to support video-based lectures that include whiteboard annotations.

REFERENCES

[1] Suritsky, S. K.; Hughes, C. A. Benefits of notetaking: Implications for secondary and postsecondary students with learning disabilities. Learning Disability Quarterly 1991, 14, 7–18.

[2] Imran,M.;Baig,M.;Murad,M.A.;Almurashi,S.H.Factorsdisturbingundergraduate students' interaction during lectures: A university-based survey. Pakistan Journal of Medical Sciences 2022, 38, 1945.

[3] Jaroš,M.P.Lecturesummarizer:atoolforpersonalizedlearningandassessment.2024.

[4] Karunarathna, A.; Premarathna, T.; Dilshan, R.; Wanniarachchi, W.; Bimsara, Y.; Piy atilake, I. In 2024 9th International Conference on Information Technology Research (ICITR), 2024, pp 1–6.

[5] Kolagar, Z.; Zarcone, A. In Proceedings of the 1st Workshop on Personalization of Generative AI Systems (PERSONALIZE 2024), 2024, pp 36–70.

[6]Huq, F.; Samee, A.; Lin, D. C.-E.; Tang, A. X.; Bigham, J. P. In Proceedings of the 30th International Conference on Intelligent User Interfaces, 2025, pp 1064–1081.

[7]Kam, M.; Wang, J.; Iles, A.; Tse, E.; Chiu, J.; Glaser, D.; Tarshish, O.; Canny, J. In Proceedings of the SIGCHI conference on Humanfactors in computing systems, 2005, pp 531–540.

|ICAS2025|

Identification and Analysis of Key Players and Key Connections in Brain Networks

Manoja Kumari Jeevarathnam[1], Jenusiya Jeyaseelan[1]

[1]Department of Physical Science, University of Vavuniya, Sri Lanka

Abstract: The Key Player Problem (KPP), introduced by Stephen P. Borgatti, aims to identify a set of k nodes (KP set) whose removal maximally disrupts communication within a network. These disruptions can impair the integrity, strength, or efficiency of connections. While the KPP has been applied to various complex networks, its use in brain networks remains largely unexplored. In brain networks, such disruptions are common in aging, neurological disorders, tumors, and brain injuries. However, in brain networks, edge removal representing the loss or weakening of connections between regions—is more prevalent. These edges may represent anatomical pathways or functional links. To address this research gap, we introduce the Key Connection Problem (KCP), defined as identifying a set of k edges (KC set) whose removal most severely disrupts network communication. We developed two algorithms Exhaustive k-Node Removal for Global Efficiency Minimization (EnGEM) and Exhaustive k-Edge Removal for Global Efficiency Minimization (EnGEM-E) to detect both Key Players and Key Connections in a network. For the application of these algorithms, structural brain networks were constructed from neuroimaging data of 100 cognitively normal older adults (NC) and 100 Alzheimer's disease (AD) subjects, each comprising 80 nodes and edges denoting anatomical pathways. Key Player analysis revealed that in normal aging, the most disruption-causing nodes were predominantly left-lateralized subcortical and memory related regions, whereas in Alzheimer's disease, they shifted toward the right hemisphere and frontal regions, reflecting disease-related changes in network vulnerability. Key Connection analysis revealed that normal aging networks rely on posterior and limbic connections, while Alzheimer's disease networks show disrupted frontal–subcortical connections, reflecting disease-specific structural connectivity alterations. This is the first study to formally define and investigate the KPP and KCP in brain networks, providing a new framework for analyzing structural connectivity disruptions in clinical neuroscience.

Keywords: aging, Alzheimer's disease, brain networks, EnGEM, key connection problem, key player problem, neuroimaging

Identification and Analysis of Key Players and Key Connections in Brain Networks

Manoja Kumari Jeevarathan[1*], Jenusiya Jeyaseelan[2]

[1,2]Department of Physical Science, University of Vavuniya, Sri Lanka

Introduction

Graph Theory: Unlocking Real–World Solutions

- ☐ Graphs represent entities (nodes) and their relationships (edges), making them ideal for modeling real–world systems.
- ☐ Graph theory is widely used across many fields, including Social networks, transportation networks, Biological networks, and communication systems.
- ☐ Graph-theoretical methods were chosen over deep-learning approaches to ensure interpretability of structural connectivity and direct insight into network topology.

Key Player Problem

KPP – Definition:

Given a Complex network, find a set of k nodes (a kp–set of order k) whose elimination would maximally disrupt communication among the remaining nodes.

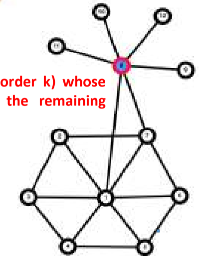

Solution of Key Player Problem

Stephen P. Borgatti

Degree of reachability, $DF = 1 - \frac{2}{N(N-1)}\sum_{i>j}\frac{1}{d_{ij}}$

- **d_{ij} is the shortest path distance between nodes i and j,**
- **N is the total number of nodes in the network.**

For kp–sets of size 1, the measure presented above can used straightforwardly to select key players by simply choosing the one with the highest score on any given measure.

For kp—sets of size k > 1, $D_R = \frac{\sum_j \frac{1}{d_{Kj}}}{N}$

where d_{Kj} is the distance from any member of the key player set to a node j not in the set. This metric evaluates the degree with which the set of key players is isolated from the rest of the nodes.

Brain Network Disruptions

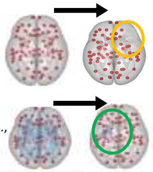

- ☐ **Network Disruption of Node Removal:**

Node removal simulates the loss of a brain region, similar to what happens in stroke, tumour , or localized degeneration.

- ☐ **Network Disruption of Edge Removal:**

Edge removal targets the connections between regions, either anatomical pathways (e.g., white matter tracts) or functional links (e.g., correlations in activity).

Global Efficiency

- ☐ The **global efficiency** is defined as the mean of the inverse of the shortest path length in a network and quantifies how efficiently information can be exchanged across the network.

$$E_{glob}(G) = \frac{1}{n}\sum_{i \in N} E_i = \frac{1}{n}\sum_{i \in N}\frac{\left(\frac{\sum_{j \in N, j \neq i} \frac{1}{d_{ij}}}{n-1}\right)}{}$$

Key Connection Problem

A Key connection Set (kc–set) of size **k** is a set of **k edges** in a network whose removal would maximally disrupt communication.

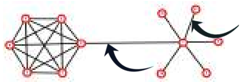

Example: Military Network

Aim & Objective

- ☐ The main aim of this study is to define the key connection problem, detect, and analyze influential edges (connections) in brain networks.
- ☐ We develop algorithms for detecting Key players and Key connections of brain networks.
- ☐ Implement algorithms for real brain Networks of Aging subjects and Alzheimer's subjects.

Implementation

Neuroimaging Data from ADNI

- ☐ 100 older adults (NC) and 100 Alzheimer's subjects (AD) cross–sectional imaging data for this study came from the Alzheimer's Disease Neuroimaging Initiative (ADNI) project's database (http://adni.loni.usc.edu).
- ☐ Unweighted 80 x 80 Brain networks.

Variable	NC (n=100)	AD (n=100)
Age (mean ± std)	72 ± 4	74±4
Gender (M:F)	14:18	19:14

- ☐ Implement EnGEM for Key players and EnGEM-E for Key connections for NC and AD, Unweighted Brain Networks.

Exhaustive k-Node Removal for Global Efficiency Minimization (EnGEM)

```
Algorithm 1 Exhaustive k-Node Removal for Global Efficiency Minimization (EnGEM)
Require: Set of graphs $\{G_1, G_2, \dots, G_N\}$, node set $V$ with $|V| = 80$, starting integer $k_{\min}$, maximum $k_{\max}$, significance level $\alpha$
Ensure: For each $k$, minimal efficiency groups MinEffGroups$_k$, stop when binomial test fails
for $k = k_{\min}$ to $k_{\max}$ do
    $Q \leftarrow$ nchoosek$(V, k)$                          ▷ All $k$-node combinations
    Initialize Eff_Results_All $\in R^{|Q| \times N}$
    for $i = 1$ to $N$ do
        Load graph $G_i$
        for $j = 1$ to $|Q|$ (parallelizable) do
            $q_j \leftarrow Q[j]$
            Remove nodes in $q_j$ from $G_i$ to get $G'_j$
            Eff_Results_All$[j, i] \leftarrow Eff(G'_j)$
        end for
        $m_i \leftarrow \arg\min_j$ Eff_Results_All$[j, i]$
        MinEffGroups$_k[i] \leftarrow Q[m_i]$
    end for
                  ▷ Count frequency of each node in all minimal groups for this $k$
    Initialize frequency vector $F \in Z^{|V|}$ with zeros
    for $i = 1$ to $N$ do
        for each node $v \in$ MinEffGroups$_k[i]$ do
            $F[v] \leftarrow F[v] + 1$
        end for
    end for
                  ▷ Perform binomial test on frequencies to check significance
    $p \leftarrow \frac{k}{|V|}$                   ▷ Probability of randomly selecting $k$ nodes
    $continue\_flag \leftarrow False$
    for $v = 1$ to $|V|$ do
        $pval \leftarrow$ binomtest$(F[v], N, p, alternative = 'greater').pvalue$
        if $pval < \alpha$ then
            $continue\_flag \leftarrow True$          ▷ At least one node is significant
            break
        end if
    end for
    if $continue\_flag = False$ then
        stop and return all results up to $k - 1$
    end if
end for
```

Exhaustive k-Edge Removal for Global Efficiency Minimization (EnGEM-E)

```
Algorithm 1 Exhaustive $k$-Edge Removal for Global Efficiency Minimization (EnGEM-E)
Require: Set of graphs $\{G_1, G_2, \dots, G_N\}$, edge list $E_i$ for each graph, starting integer $k_{\min}$, maximum integer $k_{\max}$, significance level $\alpha$, number of nodes $|V|$
Ensure: For each $k$: minimum-efficiency edge groups MinEffEdgeGroups$_k$, and stopping criterion based on binomial test
for $k = k_{\min}$ to $k_{\max}$ do
    Initialize list MinGroups$_k$ to store minimum-efficiency edge groups for all subjects
    for $i = 1$ to $N$ do
        Construct adjacency matrix $A_i$ from edge list $E_i$
        $C \leftarrow \binom{E_i}{k}$                          ▷ All $k$-edge combinations
        Initialize vector Eff$_i \in R^{|C|}$
        for $j = 1$ to $|C|$ do                     ▷ This loop is parallelizable
            $e_j \leftarrow C[j]$
            $A'_j \leftarrow A_i$
            for each edge $(u, v) \in e_j$ do
                Set $A'_j(u, v) \leftarrow 0$ and $A'_j(v, u) \leftarrow 0$
            end for
            Eff$_i[j] \leftarrow$ Eff$(A'_j)$
        end for
        minEff$_i \leftarrow$ min(Eff$_i$)
        $G_i \leftarrow$ {groups in $C$ | Eff = minEff$_i$}
        Store $G_i$ in MinGroups$_k[i]$
    end for
    Initialize frequency map FreqEdges$_k \leftarrow$ dictionary: edge $\mapsto$ count
    for $i = 1$ to $N$ do
        for each edge $e$ in all groups in MinGroups$_k[i]$ do
            FreqEdges$_k[e] \leftarrow$ FreqEdges$_k[e] + 1$
        end for
    end for
    Let $n \leftarrow N$                                  ▷ Total subjects
    for each edge $e$ in FreqEdges$_k$ do
        $k_e \leftarrow$ FreqEdges$_k[e]$
        $p \leftarrow \frac{1}{\binom{|E_i|}{k}}$             ▷ Random selection probability
        pval$_e \leftarrow$ BinomialTest$(k_e, n, p$, alternative = 'greater')
    end for
    if all significant edges satisfy pval$_e < \alpha$ then
        Continue to next $k$
    else
        MinEffEdgeGroups$_k \leftarrow$ MinGroups$_k$ for last accepted $k$
        break
    end if
end for
```

Results and Discussion

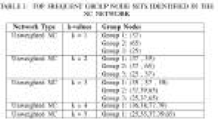

TABLE I: TOP FREQUENT GROUP NODE SETS IDENTIFIED IN THE NC NETWORK

Network Type	k-value	Group Nodes
Unweighted NC	k = 1	Group 1: [illegible] Group 2: [illegible] Group 3: [illegible]
Unweighted NC	k = 2	Group 1: [illegible] Group 2: [illegible] Group 3: [illegible]
Unweighted NC	k = 3	Group 1: [illegible] Group 2: [illegible] Group 3: [illegible]
Unweighted NC	k = 4	Group 1: [illegible]
Unweighted NC	k = 5	Group 1: [illegible]

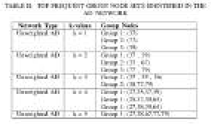

TABLE II: TOP FREQUENT GROUP NODE SETS IDENTIFIED IN THE AD NETWORK

Network Type	k-value	Group Nodes
Unweighted AD	k = 1	Group 1: [illegible] Group 2: [illegible] Group 3: [illegible]
Unweighted AD	k = 2	Group 1: [illegible] Group 2: [illegible] Group 3: [illegible]
Unweighted AD	k = 3	Group 1: [illegible] Group 2: [illegible]
Unweighted AD	k = 4	Group 1: [illegible] Group 1: [illegible] Group 1: [illegible]
Unweighted AD	k = 5	Group 1: [illegible]

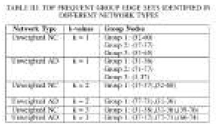

TABLE III: TOP FREQUENT GROUP EDGE SETS IDENTIFIED IN DIFFERENT NETWORK TYPES

Network Type	k-value	Group Nodes
Unweighted NC	k = 1	Group 1: [illegible] Group 2: [illegible] Group 3: [illegible]
Unweighted AD	k = 1	Group 1: [illegible] Group 2: [illegible] Group 3: [illegible]
Unweighted NC	k = 2	Group 1: [illegible]
Unweighted AD	k = 2	Group 1: [illegible]
Unweighted NC	k = 3	Group 1: [illegible]
Unweighted AD	k = 3	Group 1: [illegible]

Clinical Interpretations

- ❖ **Key Player (K=1,2,3,4,5)**

Unweighted (NC) – Top frequent Group node sets

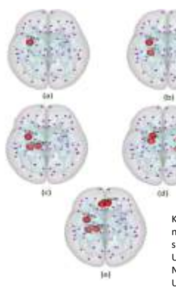

Key Players (Group1) in each network sets are shown in yellow spheres: (a) Unweighted NC k=1 (b) Unweighted NC k=2 (c) Unweighted NC k=3 (d) Unweighted NC k=4 (e) Unweighted NC k=5.

- ❖ **Key Player (K=1,2,3,4,5)**

Unweighted (AD) – Top frequent Group node sets

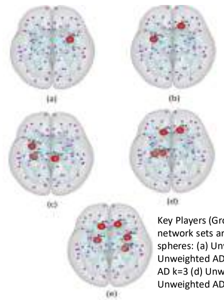

Key Players (Group1) in each network sets are shown in red spheres: (a) Unweighted AD k=1 (b) Unweighted AD k=2 (c) Unweighted AD k=3 (d) Unweighted AD k=4 (e) Unweighted AD k=5.

- ❖ **Key Connection (K=1,2,3)**

Unweighted (NC and AD) – Top frequent Group Edge sets

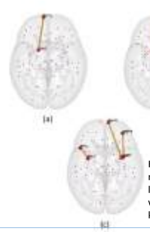

Key Connection (Group1) in each network sets are shown in yellow lines: (a) Unweighted NC k=1 (b) Un weighted NC k=2 (c) Unweighted NC k=3

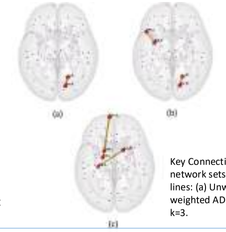

Key Connection (Group1) in each network sets are shown in yellow lines: (a) Unweighted AD k=1 (b) Un weighted AD k=2 (c) Unweighted AD k=3.

Conclusion

- ☐ Introduced the **Key Connection Problem (KCP)** alongside **Key Player analysis** for structural brain networks.
- ☐ Develop **exhaustive k – node & k – edge removal for global efficiency minimization algorithm**
- ☐ Implement algorithms for real brain Networks of Aging subjects and Alzheimer's subjects
- ☐ Identify Key – player nodes in:
  - **Normal aging (NC)** – vulnerability in **left-lateralized subcortical & memory regions**.
  - **Alzheimer's disease (AD)** – vulnerability shifted to **right hemisphere & frontal regions**.
- ☐ Key connection findings:
  - NC: Disruption mainly in **posterior & limbic pathways**.
  - AD: Disruption mainly in **frontal-subcortical circuits**.

References

1. Borgatti, Stephen P. "Identifying sets of key players in a social network." Computational & Mathematical Organization Theory 12 (2006): 21-34.
2. Ortiz-Arroyo, Daniel. Discovering sets of key players in social networks. Springer London, 2010.
3. Borgatti, Stephen P. The key player problem. na, 2003.
4. Borgatti, Stephen P. "Identifying sets of key players in a network." IEMC'03 Proceedings. Managing Technologically Driven Organizations: The Human Side of Innovation and Change (IEEE Cat. No. 03CH37502). IEEE, 2003.
5. Freeman, Linton C. "Centrality in social networks: Conceptual clarification." Social network: critical concepts in sociology. Londres: Routledge 1 (2002): 238-263.
6. Zeng, Li, Changjun Fan, and Chao Chen. "Leveraging Minimum Nodes for Optimum Key Player Identification in Complex Networks: A Deep Reinforcement Learning Strategy with Structured Reward Shaping." Mathematics 11.17 (2023): 3690.
7. Tyloo, Melvyn, Laurent Pagnier, and Philippe Jacquod. "The key player problem in complex oscillator networks and electric power grids: Resistance centralities identify local vulnerabilities." Science advances 5.11 (2019): eaaw8359.
8. Jiang, Cheng, and Zhonghua Liu. "Detecting multiple key players under the positive effect by using a distance-based connectivity approach." Physica A: Statistical Mechanics and its Applications 534 (2019): 122322.

|ICAS2025|

Automated Cashew Nut Grading using Deep Learning Techniques

R.Jalaxshi[1], Ayesh C.S.Merenchige[1], M.Sutharsan[1]

[1]Department of Physical Science, University of Vavuniya, Sri Lanka

Abstract: Grading cashew nuts is an integral process and one of the factors that greatly impacts the quality, price and value of cashew products, especially for export. Traditionally, in Sri Lanka, grading entails the manual inspection of cashew nuts using a subjective system that also takes considerable time and provides inconsistent grading. In this study, we presented deep learning systems to cater automated grading systems that are adapted to the local context. A classification system for cashew nuts was proposed, based on four varied categories: diseased, whole, half-split and broken. A new dataset of cashew nut photos from Northern province of Sri Lanka was created and labeled for the first time in the region. A unique image dataset of cashew kernels was created to enable localized model training and evaluation. Deep learning models, including VGG19 for classification and ResNet50 for detailed analysis were implemented to enhance grading accuracy across categories such as whole, half-split, broken and diseased kernels. Next, YOLOv8 nano models were applied for multi-object detection, ensuring precise identification of cashew nuts within images. The performance of the system was evaluated, yielding a mean Average Precision across IoU thresholds from 0.5 to 0.95 of 0.949. The overall mean Intersection over Union (IoU) was 0.9639 and the classification accuracy reached 0.9721, demonstrating the robustness and reliability of the system in automated cashew nut grading. The system was implemented on a Raspberry Pi 4B (4GB) device, with a connected camera for real-time detection and classification, displaying results directly on the screen. A camera mounted above the conveyor belt captures moving cashews, and live video is processed at 30 FPS into individual frames. The YOLOv8-Nano model classifies nuts in real time, with instant grading results displayed on the monitor. The proposed system significantly improves grading consistency, reduces human error and offers a scalable, practical solution for integration into local cashew processing industries.

Keywords: automated system, cashew nut grading, computer vision, deep learning, image classification, object detection, Sri Lanka

Automated Cashew Nut Grading Using Deep Learning Techniques

R.Jalaxshi[1*], Ayesh C.S.Merenchige [1], M Sutharsan[1]
[1] *Department of Physical Science, Faculty of Applied Science, University of Vavuniya, Sri Lanka*

Introduction

- **Cashew tree & nutrition:** The cashew tree (*Anacardium occidentale*) gives cashew apples and nuts.contain **heart-healthy fats**
- **Why Cashew Nut Grading**: Higher grades bring higher prices.
- **Grading & issues:** Manual grading is **slow** and **inconsistent**. Nuts are sorted by **size, shape, and color.**

Rational

 This research is conducted in response to the requirements outlined by the Sri Lanka Cashew Corporation **(Regional Office – Kilinochchi**)

Aim

 The objective of this research is to design and develop an automatic cashew nut grading system that uses deep learning techniques to lessen human effort, improve grading accuracy, and assist in increasing demand for the cashew industry in Sri Lanka

Objective

- Collected and labeled a unique dataset of terminal-stage cashew nut images from a factory in Mulliyawalai, Sri Lanka.
- Designed and trained deep learning models for single-image classification (whole, half-split, broken, diseased) and multi-object detection for grouping, typing, and grading.
- Evaluated models using accuracy, precision, sensitivity, IoU, and other relevant metrics.
- Developed an automated, lightweight grading system optimized for IoT deployment to minimize human error and support local cashew processing.

Related works

Ref	Model
[1],[2],[3]	Various computer vision-based cashew grading systems have achieved high accuracy using deep CNN with Random Forest (99.8%), K-means with Random Forest for multi-class grading, and evaluated multiple classifiers like MLP, Naive Bayes, KNN, Decision Tree, and SVM.
[4]	Classification of First Quality Fancy Cashew Kernels was performed using four deep CNN models, including ResNet50 and VGG-16 for effective kernel classification.
[5]	Precise Cashew Classification using Machine Learning employed YOLOv5, achieving the highest accuracy of 97.65% for classifying cashews into whole, broken, split-up, split-down, and defect categories.

Methodology

Data Collection

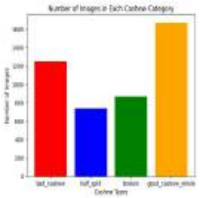

Bad Cashew	1248
Half Split	738
Broken	870
Good Cashew Whole	1673

Total: 4,529 images

Preprocessing

- From Landscape to portrait
- Add black space 640x640 image size 640×640(no dragging)


Original image


Black space added image

Preprocessing

Annotation

- Background remove
- Contour extraction (find annotation coordinate)
- Mark the border of the cashew kernel as annotation points
- Save as JSON file

Model Selection and Training

The dataset is split into 80% for training and 20% for testing. Three models, VGG19, ResNet50, and YOLOv8 Nano, were trained. The YOLOv8 Nano model was selected for its impressive ability to perform multi-class object detection with high efficiency. Moreover, its lightweight architecture makes it highly optimized for deployment on IoT devices, such as a Raspberry Pi with 4GB of RAM. This combination of features ensures it operates smoothly in resource-constrained environments.

IoT deployment

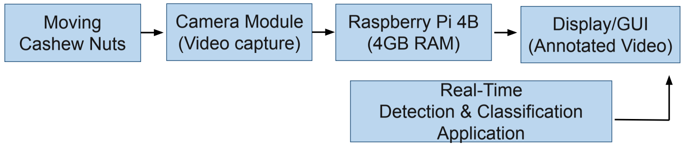
Moving Cashew Nuts → Camera Module (Video capture) → Raspberry Pi 4B (4GB RAM) → Display/GUI (Annotated Video)

Real-Time Detection & Classification Application

Industrial setup of live detection:

- Camera mounted above conveyor belt captures moving cashews
- Live video processed at 30 FPS into individual frames
- YOLOv8-Nano model classifies nuts in real-time
- Instant grading results displayed on the monitor

Industrial Impact

Scalability

Easily replicated across multiple factory lines for high-volume processing.

Broader Industrial Impact

Adaptable for grading other nuts, seeds, and agricultural products.

Results and Discussion

Model

VGG19
(ACC0.99)

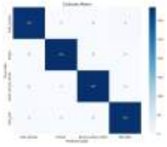

ResNet50
(ACC0.99)

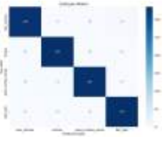

YOLO8 nano
(mAP 0.949 and IoU 0.964)

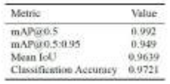

Metric	Value
mAP@0.5	0.992
mAP@0.5:0.95	0.949
Mean IoU	0.9639
Classification Accuracy	0.9721


Before Model Detection


Detected Cashew Nuts

Conclusion

- **High Accuracy Models:** VGG19 & ResNet50 reached **99% accuracy** in classifying cashew nuts (whole, half-split, broken, diseased).
- **Strong Detection Performance:** YOLOv8-Nano achieved **mAP 0.949** and **IoU 0.964**, accurately detecting multiple nuts in real-time.
- **Edge Deployment:** YOLOv8-Nano was optimized for **Raspberry Pi**, proving effective for real-world factory use in limited environments.

References

1.Sivaranjani, A.; Senthilrani, S.; Ashokumar, B.; Murugan, A. S. In 2018 IEEE International Conference on System, Computation, Automation and Networking (ICSCA), 2018, pp 1–5.
2. Arora, M.; Devi, D. A machine vision based approach to Cashew Kernel grading for efficient industry grade application. International Journal of Advance Research, Ideas and Innovations in Technology 2018, 4, 865–871.
3. Thakkar, M.; Bhatt, M.; Bhensdadia, C. Performance evaluation of classification techniques for computer vision based cashew grading system. International Journal of Computer Applications 2011, 18, 9–12
4. Vidyarthi, S. K.; Singh, S. K.; Tiwari, R.; Xiao, H.-W.; Rai, R. Classification of first quality fancy cashew kernels using four deep convolutional neural network models. Journal of Food Process Engineering 2020, 43, DOI: 10.1111/jfpe.13552.
5. Karnam, S. N.; Vaddagallaiah, V. S.; Rangnaik, P. K.; Kumar, A.; Kumar, C.; Vishwanath, B. M. Precised Cashew Classification Using Machine Learning. Engineering, Technology & Applied Science Research 2024, 14, 17414–17421.

|ICAS2025|

Comparative Study of Machine Learning Models for Non-Communicable Disease Prediction

Lenuga Mahendran[1], Banujan Kuhaneshwaran[1,2], Vasini Rasathurai[3], Luxshi Karunaharan[4], Vadivel Abishethvarman[1], Senthan Prasanth[4,5], Banage T.G.S Kumara[1]

[1]Department of Computing and Information Systems, Faculty of Computing, Sabaragamuwa University of Sri Lanka
[2]Faculty of Science and Engineering, Southern Cross University, Australia
[3]Teaching Hospital, Jaffna, Sri Lanka
[4]Department of Physical Science and Technology, Faculty of Applied Sciences, Sabaragamuwa University of Sri Lanka
[5]Faculty of Engineering and Applied Science, Memorial University of Newfoundland, Canada

Abstract: Cardiovascular and other non-communicable diseases (NCDs), especially diabetes and cancers, are some of the critical global health problems that are resulting in a high rate of morbidity and mortality. The prevalence of these conditions has been rising steadily, placing an increasing burden on healthcare systems and highlighting the need for early detection and effective preventive strategies. Early identification of individuals at risk of NCDs is critical for implementing timely interventions that can reduce disease progression and improve population health outcomes. In this context, machine learning (ML) techniques offer a promising approach for modeling disease risk by leveraging large-scale health and anthropometric data to uncover patterns not easily detected through traditional statistical methods. The paper proposes a novel machine learning (ML) scheme to model NCD risks based on anthropometric data on 300 participants in the Jaffna Teaching Hospital and Sabaragamuwa University of Sri Lanka. Important characteristics like age, gender, height, weight, body mass index (BMI), and visceral fat area were derived in order to determine risk factors for the disease. The data analysis methodology is based on strong data preprocessing, removing noise and normalisation using min-max scaling, and the correction of outliers using Python libraries such as pandas. Classification makes use of supervised ML algorithms, namely, Random Forest, Extreme Gradient Boosting, Artificial Neural Network, Decision Tree, AdaBoost, Logistic Regression, CatBoost, and Support Vector Machine. The data is divided into 80 percent training set and a 20 percent testing set, which are optimised by grid search cross-validation to provide strong model parameters. The strategy is an effective way to improve the early identification of NCDs, which allows providers to have a flexible, data-intensive resource to provide high-quality and timely interventions, leading to the overall improvement of preventive care and population health in resource-limited contexts. Overall, this study demonstrates the effectiveness of ML techniques for early identification of individuals at risk of NCDs, providing healthcare providers with a data-driven tool to deliver timely interventions. By facilitating preventive care and optimizing resource allocation, the proposed framework has the potential to improve population health outcomes of ML models for NCD risk prediction.

Keywords: anthropometric data, machine learning, non-communicable diseases, predictive modeling, risk prediction

Comparative Study of Machine Learning Models for Non-Communicable Disease Prediction

Lenuga. M[1], Banujan K.[1,2], Vasini. R[3], Luxshi. K[1], Abishethvarman V.[1], Prasanth S.[1,4], B.T.G.S Kumara[1]
[1]*Sabaragamuwa University of Sri Lanka,* [2]*Southern Cross University, Australia,* [3]*Teaching Hospital, Jaffna,* [4]*Memorial University of Newfoundland, Canada*

Abstract

Morbidity and **mortality** matters Cardiovascular and other **non-communicable diseases (NCDs).**

This analysis draws on the techniques of supervised machine learning (ML) models to predict the risks of NCDs based on **anthropometric data** drawn from 300 participants in the Jaffna Teaching Hospital and Sabaragamuwa University in Sri Lanka.

Preprocessing of data was done through eliminating noise, normalization, and correction of outliers. Such models as Random Forest, XGBoost, ANN, Decision Tree, AdaBoost, Logistic Regression, CatBoost, and SVM were trained and optimized over a grid search cross-validation. The findings present that Random Forest reported the best accuracy (98.9), whereas ensemble models were superior to other conventional classifiers. The method offers a suitable instrument in the timely detection of NCDs that facilitate preventive care where resources are scarce.

Conclusion

Among the tested models, **Random Forest** emerged as the most accurate (98.9%) and reliable, followed closely by **XGBoost** and **ANN**. Traditional models such as Logistic Regression and SVM performed less effectively. These findings confirm that ensemble learning techniques can significantly enhance NCD risk prediction using simple anthropometric data. Such models provide a low-cost, scalable, and effective tool for preventive healthcare.

Introduction

Non-communicable diseases (NCDs) cause more than **70% of deaths worldwide**. Early detection and prediction are crucial for prevention. Machine learning has shown promise in predictive healthcare, offering cost-effective, data-driven solutions. This study investigates ML models applied to anthropometric data to **predict NCD risk** in Sri Lanka.

Methodology

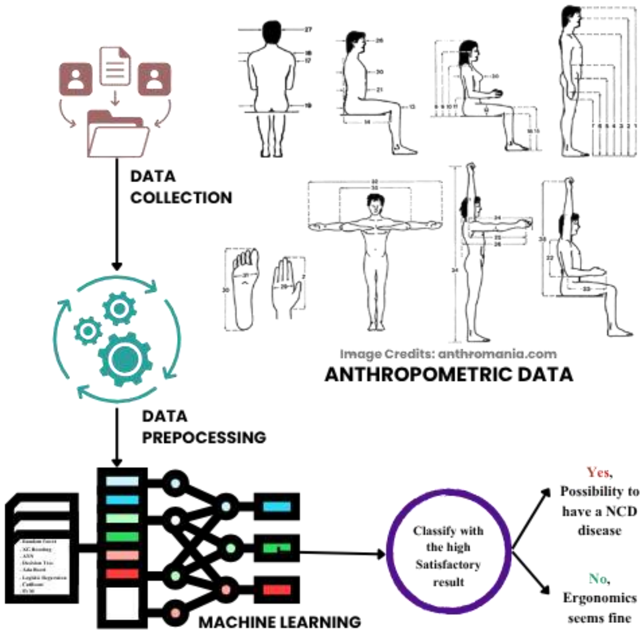

Figure 1: High-level architecture

Objective

1. To preprocess and analyze **anthropometric** data for NCD **risk prediction**.
2. To evaluate and **compare the performance** of multiple supervised ML algorithms.
3. To identify **the most effective model** for early detection of NCDs.

Results

Table 1: Algorithm's accuracy, mean squared error and absolute squared error

Algorithms	Accuracy (%)	Mean Squared Error [MSE] (%)	Absolute Squared Error [ASE] (%)
Random Forest	98.90	1.09	1.09
XG Boosting	97.80	2.19	2.19
ANN	97.80	2.19	2.19
Decision Tree	96.05	3.94	3.94
Ada Boost	93.40	6.59	6.59
Logistic Regression	88.52	11.47	11.47
Cat Boost	87.91	12.08	12.08
SVM	85.24	14.75	14.75

References

- K. Tripathi and H. Garg, "Machine Learning techniques for Cardiovascular Disease" in IOP Conference Series: Materials Science and Engineering, 2021, p. 012140. R. E. Ali, H. El
- Kadi, S. S. Labib, and Y. I. Saad, "Prediction of potential-diabetic obese-patients using machine learning techniques" 2019.

|ICAS2025|

Identification of Cotton Species and Luxury Product Recommendation using Deep Learning

Peshala S.Ariyarathna[1], N.Edwin Linosh[1]

[1]Department of Physical Science, University Of Vavuniya, Sri Lanka

Abstract: Cotton species determination has major implications for agriculture, textile manufacturing, and luxury product design. A brief yet deployable deep learning pipeline is proposed for accurately classifying four cotton species of commercial importance: *G. arboreum*, *G. barbadense*, *G. herbaceum*, and *G. hirsutum*. A curated dataset of 20,850 high-resolution images collected from public repositories and controlled photography was standardized and further augmented to promote generalization. For fiber texture, boll morphology, and vein patterns, the model utilizes ResNet50 in conjunction with a Convolutional Block Attention Module (CBAM) to emphasize spatial and channel-wise features. Transfer learning with ImageNet weights, coupled with suitable regularization, established robust performance with a Top-1 test accuracy of 94.2% and a macro F1-score of 0.938. Grad-CAM visualizations confirm that the model attended to discriminative fiber regions, enhancing interpretability. A mobile-friendly Streamlit web application delivers real-time species predictions with an average latency of 0.84 seconds and maintains 93.4% accuracy under field trials. Predicted species map to luxury product recommendations via a transparent rule-based mapper that synthesizes species identity and an image-derived quality score to suggest product categories (e.g., premium apparel, high-end home textiles, artisanal linens) with brief reasoning behind each recommendation. This integrated pipeline connects farmers, agronomists, and textile professionals to translate species-level identification into informed product decisions, quality assurance, and value-added marketing. The study demonstrates that attention-augmented residual networks constitute an effective solution for fine-grained agricultural image classification and its real-world industry implementation.

Keywords: attention mechanisms, cotton species classification, deep learning, luxury product recommendation, mobile application

IDENTIFICATION OF COTTON SPECIES AND LUXURY PRODUCT RECOMMENDATION USING DEEP LEARNING

Peshala S. Ariyarathna[1*], N. Edwin Linosh[1]

[1]Department of Physical Science, Faculty of Applied Science, University Of Vavuniya, Sri Lanka

Abstract

This study presents a deep learning model using ResNet50 with Convolutional Block Attention Module (CBAM) to classify four cotton species with 94.2% accuracy. A diverse dataset of 20,850 images was collected and augmented to improve generalization. The model was deployed through a mobile-friendly Streamlit app that provides real-time predictions and luxury product recommendations. This system offers a practical solution for farmers and textile professionals by combining precise classification with commercial insight.

Introduction

This research explores fine-grained cotton species classification using high-resolution images to support decision-making in agriculture and textile industries [1], [2]. A ResNet50 model enhanced with CBAM was trained on 20,850 images spanning four cotton species, enabling improved feature attention and classification accuracy. To boost generalization, data preprocessing included normalization and augmentation techniques.

A lightweight Streamlit app was developed for real-time predictions, offering an accessible and scalable tool for field and factory use [3], [4].

Objective

1. Develop a deep learning model to accurately classify four major cotton species.
2. Integrate CBAM attention mechanisms to refine spatial and channel-wise feature extraction.
3. Deploy the trained model in a mobile friendly app for real time species identification and luxury product recommendations.

Methodology

1. Process of Model Training

Model Compilation
Training Parameters
Handling Class Imbalance
Data Loading
Monitoring Training
Training Environment
Training Optimization Techniques

2.Cotton Species Distribution in the Dataset

Cotton Species	Number of Images	Percentage of Total
Gossypium Arboreum	4,722	20.0%
Gossypium Barbadense	5,400	22.9%
Gossypium Herbaceum	4,560	19.3%
Gossypium Hirsutum	6,168	26.1%
Total	**20,850**	**88.3%**

3. Dataset Split for Model Development

Set	Number of Images	Percentage
Training Set	16,435	70%
Validation Set	3,239	15%
Test Set	3,934	15%

4. Model Performance Metrics on Test Set

Metric	Value
Accuracy	0.942
Precision (Macro)	0.939
Recall (Macro)	0.937
F1-Score (Macro)	0.938
Balanced Accuracy	0.937
ROC-AUC (Macro)	0.989
Cohen's Kappa	0.923
Matthew's Correlation Coefficient	0.925

5. Mobile App

6. Confusion Matrix

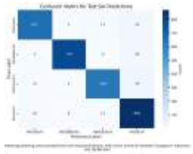

7. Training and Validation Loss and Accuracy Curves

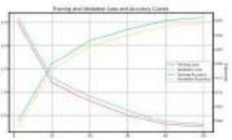

8. ROC Curve

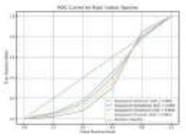

Results and Discussion

The ResNet50 + CBAM model achieved 94.2% accuracy and a macro F1-score of 0.938, showing strong performance across all cotton species. Grad-CAM visualizations confirmed the model's focus on key fiber regions. The Streamlit app maintained 93.4% accuracy in real-world use, with fast and reliable predictions. Overall, the system proved effective for both technical classification and practical deployment.

Conclusion

The ResNet50 + CBAM model achieved high accuracy and generalization in cotton species classification. The Streamlit app demonstrated practical usability with strong real-time performance. This research bridges deep learning and agriculture, offering a scalable tool for field deployment and sustainable product development.

References

1. Bilebhavi, C. M.; Arjunagi, L. The cotton industry: An overview of its global impact, trends, and challenges. International Research Journal on Advanced Engineering and Management (IRJAEM) 2024, 2, DOI: 10.47392/IRJAEM.2024.0419.
2. Radhakrishnan, S. In Sustainable fibres and textiles; Elsevier: 2017, pp 21–67.
3. Konduru, S.; Yamazaki, F.; Paggi, M. COMPETITIVE INTENSITY AND ATTRACTIVENESS OF THE US COTTON SECTOR II
4. Dristy, S. A.; Dhar, A. R.; Uddin, M. T. Sustainable practices for cotton production in Bangladesh: economic and environmental perspectives. Discover Agriculture 2024, 2, 53.

|ICAS2025|

Crop Segmentation and Prediction using Deep Learning Techniques on Satellite Images in Northern Province of Sri Lanka

Tharsika Jegatheeswaran[1], W.R.G.A.D.P. Herath[1]

[1]Department of Physical Science, University of Vavuniya, Sri Lanka

Abstract: Monitoring crop cultivation is vital for food security, land-use planning, and sustainable agriculture, especially in regions dependent on rainfall. Accurate mapping and measurement of cultivated and non-cultivated paddy lands are essential for making successful agricultural plans and climate-resilient farming in Sri Lanka, particularly in a dry zone like the Northern Province, which relies heavily on rainfall for agrarian practices. This study aims to develop an automated, deep learning-based segmentation model using high-resolution satellite images from Google Earth Pro to estimate paddy field area. A comprehensive methodology was followed, involving satellite image collection, preprocessing, manual annotation of masks using Photopea, model training, and performance evaluation. We employed four segmentation strategies: Type 1 distinguished cultivated fields from background, Type 2 separated non-cultivated fields from background, Type 3 combined cultivated and non-cultivated fields against background, and Type 4 implemented a multi-class model to segment background, cultivated, and non-cultivated areas simultaneously. This study explored four segmentation approaches using both U-Net and the Segment Anything Model (SAM). Among them, the U-Net Type 4 model that could segment multi-classes demonstrated better scalability and applicability with the validation accuracy of 94.01% and dice coefficients of 0.9145, 0.9179, and 0.8898 of background, cultivated, and non-cultivated areas, correspondingly. The pixel-based analysis was done in the Manthai East division, Northern Province, Sri Lanka, to determine the actual area estimation and verify the real-world relevance of this model. The suggested model shows that deep learning has the potential to segment crops accurately and provides a cost-effective approach for monitoring agricultural land use practices. This research enables agrarian officers to estimate paddy lands using freely available high-resolution satellite images to monitor paddy fields, plan resources, and assess seasonal yields. Future work will expand this framework to include other crop types and longitudinal analysis for prediction. The limitation is performance variation due to seasonal changes and cloud interference in satellite images.

Keywords: crop segmentation, multi-class segmentation, satellite imagery, segment anything model, U-Net

Faculty of Applied Science
University of Vavuniya

Crop Segmentation and Prediction using Deep Learning techniques on Satellite Images in Northern Province of Sri Lanka

Tharsika Jegatheeswaran[1*], W.R.G.A.D.P Herath[2]

[1,2]Department of Physical Science, Faculty of Applied Science, University of Vavuniya

INTRODUCTION

- Sri Lanka, with strong agricultural roots, relies heavily on paddy cultivation in the Northern Province. Agriculture covers 42% of land, contributes 7–8% to GDP, and employs over a quarter of the population.
- However, urbanization, deforestation, and changing rainfall patterns threaten sustainability.
- Accurate monitoring of cultivated and non-cultivated paddy fields using high-resolution Google Earth Pro imagery aids reliable area estimation and resource planning.
- Satellite images provide a bird's-eye view of the Earth's surface for crop monitoring, environmental analysis, and planning by capturing visible, infrared, and radar data.

AIM AND OBJECTIVES

Aim

To apply deep learning techniques (U-Net and SAM) on high-resolution Google Earth Pro satellite imagery for accurate segmentation and estimation of cultivated and non-cultivated paddy field areas in the Northern Province of Sri Lanka.

Objectives

- To acquiring cultivated and non-cultivated paddy areas in Northern Province
- To pre-process images and annotation
- To apply U-Net and Segment Anything Model (SAM) for segmentation
- To estimate the cultivated and non-cultivated paddy areas

PREVIOUS WORKS

Title	Model	Data Type	Study Area	Crops	Accuracy
[1]	Malaysia	FCN	Pleiades satellite	Paddy	89.7%
[2]	Thailand	U-Net model with CRF	Sentinel-1	Paddy	91%
[3]	Kenya	FCN	Sentinel-2	Seven type of crops	95.3%
[4]	USA	Swin Transformer	Sentinel-2	paddy	95.5%
[5]	India	U-Net	Sentinel satellite	Wheat Ricinus	94.6%

METHODOLOGY

Dataset

- ❖ Freely available high-resolution (8192 × 4320, 8K UHD) satellite images of the Northern Province of Sri Lanka were obtained from **Google Earth Pro**.
- ❖ A total of 57 high-resolution satellite images were collected, with patches from 100 selected images used for training, validation, and testing to segment cultivated and non-cultivated paddy areas.

Data Annotation

Masks were manually created in **Photopea** Tool. Four types of segmentation were used, so separate masks were created for each category.

- ▪ Type 1– Cultivated Paddy vs Background
- ▪ Type 2– Non-Cultivated Paddy vs Background
- ▪ Type 3– Cultivated and non-cultivated vs Background
- ▪ Type 4– Multi-Class Segmentation (0– Background, 1– Cultivated Paddy, 2– Non-Cultivated Paddy)

Type 1

Type 2

Type 3

Type 4

Model Training

Each of the four annotated datasets was used to train four U-Net model variants and three SAM (Segment Anything Model) variants to evaluate segmentation performance.

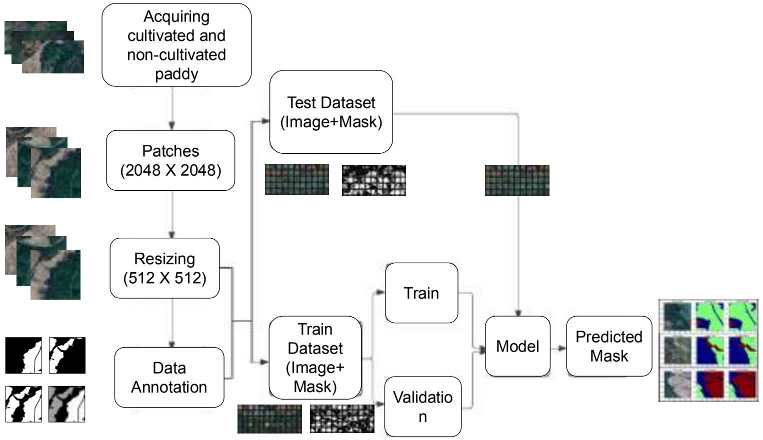

Workflow of cultivated and non-cultivated Paddy Field Segmentation

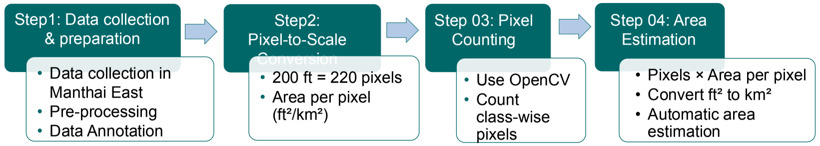

Step1: Data collection & preparation

- Data collection in Manthai East
- Pre-processing
- Data Annotation

Step2: Pixel-to-Scale Conversion

- 200 ft = 220 pixels
- Area per pixel (ft²/km²)

Step 03: Pixel Counting

- Use OpenCV
- Count class-wise pixels

Step 04: Area Estimation

- Pixels × Area per pixel
- Convert ft² to km²
- Automatic area estimation

Workflow of Paddy Field Area Estimation in Manthai East

RESULTS AND DISCUSSION

Results Comparison between segmentation models

Metric	Type1		Type2		Type3		Type4
	UNET	SAM	UNET	SAM	UNET	SAM	UNET
Dice	0.8873	0.9093	0.8751	0.9412	0.8253	0.9265	**0.9074**
IoU	0.8073	0.8395	0.8022	0.8935	0.7200	0.8692	**0.8308**
Sensitivity	0.8914	0.9289	0.9556	0.9491	0.8124	0.9088	**0.9101**
Specificity	0.9291	0.9298	0.8709	0.9019	0.8450	0.9225	**0.9550**

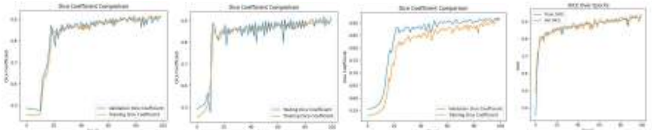

Type 1 Type 2 Type 3 Type 4

Dice Coefficient Comparison Across Four U-Net Models

Segmentation output & Area Estimation from U-Net Type 4 Segmentation in Manthai East

- The U-Net Type 4 model accurately segmented cultivated and non-cultivated paddy fields and enabled pixel-based area estimation. In previous studies, that focused on different crop types or land use classes, this work uniquely distinguishes cultivation status within paddy fields using freely available GEP satellite data.
- The complete end-to-end pipeline provides a practical and scalable tool for field-level agricultural monitoring in Sri Lanka.

CONCLUSION

- There is **no existing** automated paddy mapping in Sri Lanka for agricultural monitoring.
- Developed U-Net Type 4 for paddy field segmentation in Northern Province, Sri Lanka, achieving **94%** accuracy and estimating 56.03 km² of paddy fields in Manthai East.
- Future research should focus on multi-year imagery to estimate and predict paddy field area growth and extend the model to other crops in Sri Lanka.
- The limitation is performance variation due to seasonal changes and cloud interference in satellite images.
- **Agrarian officers** can use the tool to monitor paddy areas, plan resources, and assess seasonal yields.

REFERENCES

1. Abiddin, N. Z.; Hasan, Z. A.; Zulkifley, M. A.; Abdani, S. R.; Hassan, B.; Azmi, A.; Aziz, N. A. A. Deep Learning Segmentation Technique for Mapping and Updating PaddyCultivations at Plot Level Using High Resolution Satellite Data, Available from Malaysian Space Agency (MYSA), 2021.
2. Xu,L.;Zhang,H.;Wang,C.;Wei,S.;Zhang,B.;Wu,F.;Tang,Y.PaddyRiceMapping in Thailand Using Time-Series Sentinel-1 Data and Deep Learning Model. 2021, 13, 3994.
3. Ayushi; Buttar, P. K. Satellite Imagery Analysis for Crop Type Segmentation Using U-Net Architecture. Procedia Computer Science 2024, 235, 3418–3427.
4. Xu, H.; Song, J.; Zhu, Y. Evaluation and Comparison of Semantic Segmentation Net works for Rice Identification Based on Sentinel-2 Imagery. Remote Sensing 2023, 15, 1499.
5. Thakkar,M.;Vanzara,R.; Patel, A. Semantic segmentation approaches for crop classi fication with multi-altitude Google Earth imagery. Journal of Integrated Science and Technology 2024, 12, 832.

|ICAS2025|

Parallel Algorithms for Maximal-Clique Problems on Multi-Core Shared Memory Systems

A.Thuvaajini[1], M.Sangeetha[1]

[1]Department of Physical Science, University of Vavuniya, Sri Lanka

Abstract: Maximal clique enumeration is combinatorial graph problem, which identifies the largest fully connected subgroups within a graph, uncovering tightly-knit communities and critical relationships essential for analyzing complex networks in social science, biology, and computer science. However, due to its exponential complexity, this combinatorial problem is computationally intensive. The Bron–Kerbosch algorithm is a popular method for finding maximal cliques, but its sequential execution limits performance on large-scale graphs. Previous methods mostly focused on GPU-based parallelization (using SIMD and data parallelism) and distributed memory systems. With the advent of multi-core processors in mainstream devices such as laptops, tablets, and mobiles, these machines now have the capability to leverage shared-memory parallelization. Utilizing the parallelism of multi-core hardware offers a promising way to improve execution efficiency on common platforms. However, prior shared-memory parallelization approaches often involving SIMD instruction sets and cloud resources, have not sufficiently simplified the parallelization process for mainstream machines. This study presents parallel implementations of the Bron–Kerbosch algorithm and its pivot variant using OpenMP, optimized for multi-core shared-memory systems. The parallel algorithms employ recursive decomposition and load balancing techniques while avoiding race conditions and duplicate results. Performance was evaluated by varying thread counts and input graph sizes, spanning sparse to dense graphs. Comparisons between parallel and serial versions on identical hardware demonstrate significant speedups, with the pivot-based parallel variant showing superior load balancing and reduced redundant computations. These results confirm that shared-memory parallelism substantially improves scalability and execution time for maximal clique enumeration, making it a practical approach for large-scale combinatorial graph problems in mainstream machines.

Keywords: mainstream machines, maximal clique enumeration, parallel algorithms, recursive decomposition, shared memory multi-core

Parallel Algorithms for Maximal-Clique Problems on Multi-Core Shared Memory Systems

A.Thuvaajini[1]*, M.Sangeetha[2]

Department of Physical Science, University of Vavuniya, SL

Introduction

Maximal Clique

- A **Clique** in an undirected graph $G = (V, E)$ is a subset of the vertex set C, such that for every two vertices in C, there exists an edge connecting the two.

All cliques (every complete subgraph)
(single vertices are cliques of size 1)
•Size 1: {1}, {2}, {3}, {4}, {5}, {6}
•Size 2 (edges): {1,2}, {1,5}, {2,3}, {2,5}, {3,4}, {4,5}, {4,6}
•Size 3: {1,2,5}

Maximal Clique: A Clique that cannot be extended by including one more adjacent vertex.

Maximal cliques (not contained in any larger clique)
•{1,2,5} (a triangle)
•{2,3}
•{3,4}
•{4,5}
•{4,6}

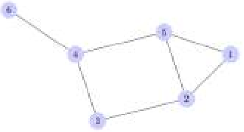

Maximal Clique Enumeration (MCE)

- **Maximal clique enumeration** is the process of **listing all the maximal cliques** in a given graph
- Listing all the maximal cliques is a combinatorial NP-Hard problem, since we are not able to predict how many vertices are going to be added. It will be solved in exponential time.
- MCE has been widely used in diverse research areas

Bron-Kerbosch Algorithm

- The Algorithm was Designed by the Dutch scientists Joep Kerbosch and Coenradd Bron for Finding the Maximal Cliques in undirected graph. It is Known to be one of the most efficient algorithm.

```
BK (R,P,X)
    if P and X are empty:
        Output R
    for each v ∈ P:
        BK (R ∪ {v}, P ∩ N(v), X ∩ N(v) )
        P = P \ {v}
        X= X ∪ {v}
```

Backtracking
Recursive

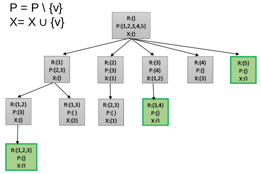

Bron-Kerbosch Algorithm with Pivoting Algorithm

- **Pivoting** chooses a vertex (pivot) and avoids exploring branches that cannot yield new maximal cliques, drastically reducing recursive calls in practice.

```
BK (R,P,X)
  if P and X are empty:
      Output R
  choose pivot vertex u ∈ P u X
  for each v ∈ P \ N(u) :
     BK (R ∪ {v}, P ∩ N(v), X ∩ N(v) )
      P = P \ {v}
      X= X ∪ {v}
```

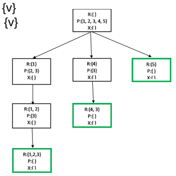

Parallelization of MCE

- Sequential MCE on large graphs is slow.
- Even optimized **sequential** methods struggle on very large graphs.
- **Larger or more complex graphs** become impractical.
- **MCE's high computational complexity → need for parallel methods**.

Objective

- Design and develop efficient **parallel algorithms** for the **Bron-Kerbosch** and **Pivot Bron-Kerbosch algorithms** on mainstream **shared-memory multi-core architectures** using OpenMP.
- Evaluates the serial and parallel algorithms by changing the **number of threads** and **size of the graphs** on sparse to dense graphs using static and dynamic scheduling
- Compare the parallel implementations' performance with the Serial implementation through the performance metrics such as **speedup**, and **memory usage**.

Methodology

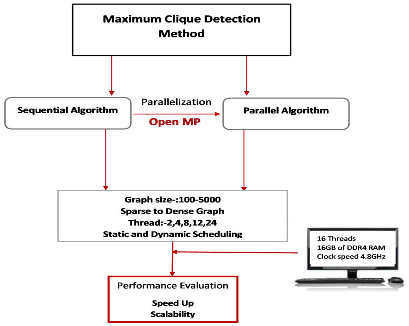

Maximum Clique Detection Method

Sequential Algorithm

Parallelization
Open MP

Parallel Algorithm

Graph size-:100-5000
Sparse to Dense Graph
Thread:-2,4,8,12,24
Static and Dynamic Scheduling

16 Threads
16GB of DDR4 RAM
Clock speed 4.8GHz

Performance Evaluation
Speed Up
Scalability

Experimental Setup: Hardware and Software Specification:
Hardware: 16-core Intel(R) Core(TM) i7-10700 (4.8 GHz), 16 GB DDR4 RAM, shared-memory architecture. Ubuntu 25.04, Visual Studio Code 1.102.1 (IDE), C programming, GCC 14.2.0 compiler with OpenMP library.

Recursive Decomposition and Thread Parallelism

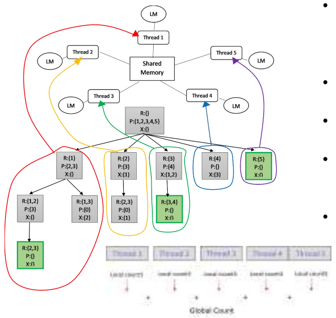

- **Parallelize the top-level loop:** Each thread is responsible for exploring maximal cliques starting from a **different initial vertex** v.
- Each starting vertex leads to a **disjoint search tree**
- Each thread maintains a local_count for the cliques it finds.
- This avoids race conditions on global_clique_count during recursive calls.
- Only at the end of each thread's work, you update the global counter inside a lock

Novel Parallel Bron-Kerboch Algorithm

```
Procedure ParallelBK0(G = (V, E))
Initialize global_count ← 0
for v ∈ V do  // Parallel (in parallel)
    R ← {v}
    P ← neighbors of v with ID > v
    X ← neighbors of v with ID < v
    local_count ← 0
    BK0(R, P, X, local_count)  // Serial recursive
   Atomically update global_count += local_count
end for
return global_count
```

Novel Parallel Bron-Kerboch with Pivot Algorithm

```
Procedure ParallelBK_Pivot(G = (V, E))
Initialize global_count ← 0
for v ∈ V do                    // Parallel (in parallel)
    R ← {v}
    P ← neighbors of v with ID > v
    X ← neighbors of v with ID < v
    local_count ← 0
    BK_Pivot(R, P, X, local_count)  // Serial recursive with pivot
      Atomically update global_count += local_count
end for
return global_count
```

Results and Discussion

Bron-Kerbosch Algorithm

Dynamic Scheduling

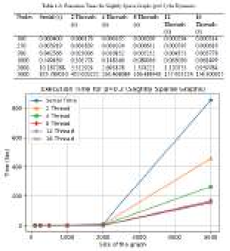

Statics Scheduling

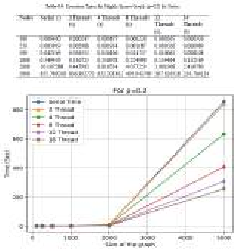

Bron-Kerbosch with pivoting Algorithm

Dynamic Scheduling

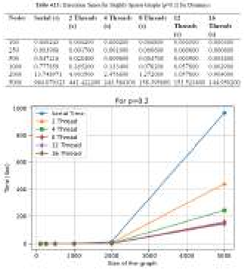

Statics Scheduling

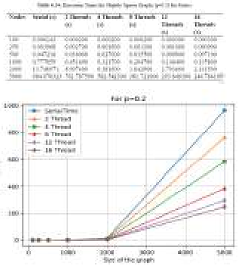

- **Graph Density:** Both Bron–Kerbosch and Bron–Kerbosch Pivot algorithms show increasing execution time with graph density(0.1 to 0.5) in both serial and parallel implementations, but parallel versions significantly reduce it.
- **Static vs Dynamic scheduling**: Dynamic scheduling outperformed static for moderated to large-sized graphs, especially in dense cases, by balancing workloads and reducing idle time.
- **Multi-threading:** With the change of the number of threads, parallel algorithms show significant improvement in both scheduling techniques. However, the dynamic scheduling achieved a much higher speedup of up to 10x.

Conclusion

- Successfully developed and implemented serial and parallel versions of the Bron-Kerbosch algorithm for maximum clique using OpenMP for multi-core systems
- Parallel implementations showed significant performance improvements:
  - ✓ Up to 3.7Œ speedup for sparse graphs (p=0.1, 5000 nodes, 12 threads).
  - ✓ Up to 12.1Œ speedup for dense graphs (p=0.5, 500 nodes, 16 threads).
- Dynamic scheduling outperformed static scheduling, enhancing thread utilization.
- Pivoting strategy reduced recursive calls, improving performance, especially for dense graphs.

References

1. Gergely Palla, Imre Derenyi, Illes Farkas, and Tamas Vicsek. 2005. Uncovering the overlapping community structure of complex networks in nature and society. Nature 435, 7043 (2005), 814–818.
2. Shungo Koichi, Masaki Arisaka, Hiroyuki Koshino, Atsushi Aoki, Satoru Iwata, Takeaki Uno, and Hiroko Satoh. 2014 Chemical structure elucidation from 13C NMR chemical shifts: Efficient data processing using bipartite matching and maximal clique algorithms. JCIM 54, 4 (2014), 1027–1035
3. Helen M Grindley, Peter J Artymiuk, David W Rice, and Peter Willett. 1993. Identification of tertiary structure resemblance in proteins using a maximal common subgraph isomorphism algorithm. JMB 229, 3 (1993), 707–721.

|**ICAS2025**|

Disease Classsification in Sugarcane using Deep Learning Technologies

P.Nivithasini[1], A.V.Ann Sinthusha[1]

[1]Department of Physical Science, University of Vavuniya, Sri Lanka

Abstract : This document presents a study on improving sugarcane disease detection in Sri Lanka, where productivity is significantly hindered by diseases such as White Leaf Disease, Red Rot, Rust, and Yellow Leaf Disease. Although these diseases severely impact yield, there is currently limited research in Sri Lanka addressing their automated detection. Traditional manual diagnosis methods are often time-consuming, error-prone, and require substantial agricultural expertise. To address these challenges and the lack of ensemble-based approaches in existing work, this study leverages deep learning techniques, employing four state-of-the-art Convolutional Neural Network (CNN) architectures VGG16, ResNet50, InceptionV3, and EfficientNetB0. A hard-voting weighted ensemble approach is applied to combine these models, enhancing both accuracy and reliability in automated disease classification. A custom dataset of 1,543 annotated sugarcane leaf images, collected from the Palwatta Sugar Company, was used with data augmentation techniques employed to improve model generalization. Individually, VGG16, ResNet50, and EfficientNetB0 achieved 95% accuracy, while InceptionV3 reached 94%. The ensemble method further boosted performance, achieving an overall F1 score of 99.57%, demonstrating the effectiveness of this approach for robust and reliable sugarcane disease detection in the Sri Lankan context.

Keywords: agriculture, convolutional neural networks, data augmentation, deep learning, hard voting ensemble, Sri Lanka, sugarcane disease detection.

ICAS2025

Faculty of Applied Science
University of Vavuniya

DISEASE CLASSIFICATION IN SUGARCANE USING DEEP LEARNING TECHNOLOGIES

Nivithasini P[1]*, A.V. AnnSinthusha[1]
[1]Department of Physical Science, Faculty of Applied Science, University of Vavuniya, Sri Lanka

Introduction

Sugarcane yield in Sri Lanka is threatened by diseases such as White Leaf, Yellow Leaf, Red Rot, and Rust, while manual detection remains slow and impractical for large-scale farming. CNNs have shown strong potential for plant disease classification, but most local studies focus only on White Leaf Disease. Research on multiple sugarcane diseases in Sri Lanka is limited. Single CNN models lack robustness, whereas ensemble methods can enhance accuracy and reliability in disease detection.

Aim

To identify sugarcane leaf diseases from locally collected images in Sri Lanka, enabling early classification and supporting improved crop management for better yield and quality.

Objective

- To construct a locally collected dataset of multiple sugarcane leaf diseases in Sri Lanka.
- To implement and evaluate multiple CNN models for effective disease classification.
- To explore different ensemble learning techniques such as hard voting, soft voting, stacking, and weighted ensembling.
- To identify the best-performing ensemble mechanism that achieves the highest accuracy and robustness for sugarcane disease detection.

Literature Review

Title	Dataset	Methods	Accuracy
Optimized CNN with Environmental Adaptation	Kaggle (175 healthy, 174 red rot, 73 red rust, 100 bacterial blight)	CNN with Environmental Adaptation	89%
Image Processing for Sugarcane Disease	Not mentioned	AHE, K-means, GLCM, PCA, SVM	95%
CNN-Based Sugarcane Disease Detection – India	Collected in India Total=580	Deep learning based CNN	98.69%
White Leaf Disease Detection in Sugarcane Using UAV RGB Imagery in Sri Lanka	UAV RGB Imagery of Sugarcane – Gal- Oya Plantation(White Leaf Disease (WLD)) in Sri Lanka	YOLOv5, YOLOR, DETR, Faster R-CNN	95%
Deep Learning for Leaf Disease	Farms, Kolhapur, India	CNN	95.4%
Ensemble Deep Learning for Sugarcane Disease Classification	Existing Datasets + 2569 images	MobileNet-V2 Ensemble model	84 to 86.53%

- Most existing studies in Sri Lanka focus only on White Leaf Disease, with limited attention to multiple sugarcane leaf diseases.
- Single CNN models lack robustness and generalization.
- Although CNNs have shown strong performance in plant disease detection, single CNN models lack robustness and struggle with generalization.
- Very few studies have explored ensemble deep learning methods for sugarcane disease detection using locally collected datasets in Sri Lanka.

Methodology

DATA COLLECTION

Dataset collected from the **Pelwetta Sugar Company**.
1543 Images across 5 classes

DATA PREPROESSING

Resize images to 493 × 1040
Rotation, Flipping, Scaling, Zooming, Brightness & Contrast
Training set 70% | Validation set 15% | Testing set 15%

MODEL TRAINING

VGG16 | ResNet50 | InceptionV3 | EfficientNetB0 | MobileNetV2

MODEL EVALUATION

Review performance metrics & Compare outcomes.

ENSEMBLING MODEL BUILDING

Techniques: **Stacking, Average Weighted, Soft Voting, Hard Voting**

FINAL ENSEMBLE SELECTION

Choose the best ensemble method based on performance.

Results and Discussion

Individual Models

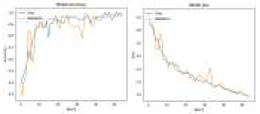

Fig1 : Accuracy & Loss Graph for VGG16

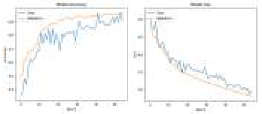

Fig2 : Accuracy & Loss Graph for EfficientNetB0

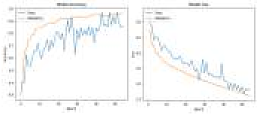

Fig3: Accuracy & Loss Graph for ResNet50

Model	Healthy	Red Rot	Rust	White-leaf	Yellow	Accuracy
MobileNetV2	**0.75**	**0.88**	**0.87**	**0.88**	**0.67**	**0.83**
VGG16	0.98	0.98	0.98	0.98	0.96	0.95
EfficientNetB0	0.95	0.94	0.85	0.94	0.95	0.95
ResNet50	0.95	0.95	0.92	1.00	0.96	0.95
InceptionV3	0.94	0.94	0.88	1.00	0.94	0.94

Table 1: F1-Scores of Individual Models

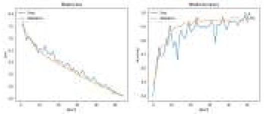

Fig4: Accuracy & Loss Graph for InceptionV3

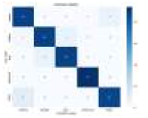

Fig5: Confusion Matrix for InceptionV3

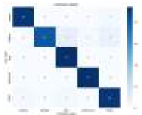

Fig6: Confusion Matrix for VGG16

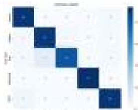

Fig7: Confusion Matrix for EffiecientNetB0

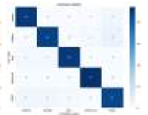

Fig8: Confusion Matrix for RestNet50

Ensemble Performance

- The hard voting ensemble outperformed all single models with 99.57% accuracy.
- Other ensemble methods (soft voting, weighted averaging, stacking) also performed well, but hard voting was the best.

Model	Healthy	Red Rot	Rust	White-leaf	Yellow	Accuracy
Stacking	1.00	0.97	0.96	1.00	0.98	0.98
Soft Voting	1.00	0.99	0.98	0.99	1.00	0.99
Average Weighted	1.00	0.99	0.98	1.00	1.00	0.99
Hard Voting	**1.00**	**1.00**	**0.98**	**1.00**	**1.00**	**1.00**

Table 2 : Comparison table for Ensemble methods

Ablation Study

- Removing EfficientNetB0 dropped accuracy to 71.98%, proving it was the most critical model in the ensemble.
- Removing VGG16 , ResNet50 or InceptionV3 did not reduce performance

Model	Weak Classes	Well Classified Classes
VGG16	RedRot (3), Yellow (2)	Healthy, Rust,WLD
ResNet50	Yellow (6), Rust (2)	Healthy, RedRot, WLD
EfficientNetB0	**Rust (5), Yellow (2), RedRot (1)**	**Healthy, WLD**
InceptionV3	Yellow (4), Rust (3), RedRot (2)	Healthy, WLD

Table 3: Model-wise Misclassifications and Class-wise Performance

Models	Accuracy (%)
Without InceptionV3	99.57
Without VGG16	99.57
Without ResNet50	99.57
Without EfficientNetB0	**71.98**

Table 4 : Table for Model Exclusion Analysis for Hard Voting Ensemble

Conclusion

Why EfficientNetB0 is significant

- EfficientNetB0 balances depth, width, and resolution, making it efficient yet powerful.
- Captures fine details in sugarcane leaves, improving disease recognition.
- Consistently strong predictions made it the key contributor to ensemble success.

Why Hard Voting Ensemble performed best (99.57% accuracy)

- Combines the strengths of multiple CNN models, reducing the weaknesses of individual models.
- Aggregated decisions improved overall stability and robustness.
- EfficientNetB0's influence boosted the ensemble's reliability.

References

[1] Daphal, S. D.; Koli, S. M. *Enhancing sugarcane disease classification with ensemble deep learning: A comparative study with transfer learning techniques.* **Heliyon**, 2023, 9.
[2] Wickramasinghe, K.; Wijesuriya, A.; Ariyawansha, B.; Perera, A.; Chanchala, K.; Manel, D.; Chandana, R. *Performance of sugarcane varieties in a White Leaf Disease (WLD)—prone environment at Pelwatte.* 2019.
[3] Shovon, M. S. H.; Mozumder, S. J.; Pal, O. K.; Mridha, M. F.; Asai, N.; Shin, J. *PlantDet: A robust multi-model ensemble method based on deep learning for plant disease detection.* **IEEE Access**, 2023, 11, 34846–34859.
[4] Srivastava, S.; Kumar, P.; Mohd, N.; Singh, A.; Gill, F. S. *A novel deep learning framework approach for sugarcane disease detection.* **SN Computer Science**, 2020, 1, 87

|**ICAS2025**|

Machine Learning Approaches for Early Diagnosis of Liver Diseases using Sri Lankan Patient Data

Kobika Balasubramaniyam[1], Tuvensha Jegatheeswaran[2], V.Thusyanthan[3], M.Thayalini[4]

[1]Department of Physical Science, University of Vavuniya, Sri Lanka
[2]Department of ICT, University of Vavuniya, Sri Lanka
[3]Teaching Hospital, Jaffna, Sri Lanka
[4]District General Hospital, Kilinochchi, Sri Lanka

Abstract: The liver is one of the most vital organs in the human body, responsible for essential functions such as detoxification, metabolism, protein synthesis, and regulation of biochemical processes necessary for survival. Damage or impaired liver function can therefore lead to serious health complications and significantly reduce life expectancy. In recent decades, the global burden of liver diseases has steadily increased, affecting both developed and developing countries. Liver disease represents a growing health burden in Sri Lanka, where Alcohol-Associated Liver Disease (ALD) and Metabolic Dysfunction-Associated Steatotic Liver Disease (MASLD, formerly NAFLD) are major causes of illness and death. Importance of early liver disease detection in Sri Lanka is emphasized, addressing a critical real-world healthcare challenge through data-driven approaches that enable timely treatment, reduce complications, and improve patient survival.Clinical data were collected from Jaffna Teaching Hospital and Kilinochchi General Hospital, comprising 538 records, including ALD, MASLD, and healthy subjects. Data preprocessing involved advanced techniques such as Multiple Imputation by Chained Equations (MICE) for missing data, outlier removal using Z-score, Interquartile Range (IQR), and K-Nearest Neighbour (KNN) methods, and feature selection with LASSO and Variance Inflation Factor (VIF). To handle class imbalance, Synthetic Minority Oversampling Technique (SMOTE) was applied. The dataset was divided into 80% training and 20% testing for model validation.Eight machine learning algorithms were evaluated for both binary (healthy vs. liver disease) and multi-class (healthy, ALD, MASLD) classification. Random Forest achieved the highest binary accuracy of 99.03%, with precision 100%, recall of 97.96%, F1-score of 98.97%, and AUC-ROC of 99.92% confirming robust performance. In multi-class classification, Decision Tree performed best, achieving 86.4% accuracy with precision of 88.46%, recall of 86.4%, F1-score of 87.23%, and AUC-ROC of 84.94%. These findings demonstrate that robust preprocessing and appropriate model selection substantially improve early liver disease prediction. Future work will integrate deep learning techniques, particularly Convolutional Neural Networks (CNNs) with ultrasound imaging, to enhance diagnostic precision and support non-invasive, region-specific liver disease detection in Sri Lanka.

Keywords: ALD, clinical data, early detection, liver disease, machine learning, MASLD, Sri Lanka

ICAS2025

Faculty of Applied Science
University of Vavuniya

MACHINE LEARNING APPROACHES FOR EARLY DIAGNOSIS OF LIVER DISEASES USING SRI LANKAN PATIENT DATA

Kobika Balasubramaniyam[1*], Tuvensha Jegatheeswaran[2], Dr.V.Thusyanthan[3], Dr. M.Thayalini[4]

[1]Department of Physical Science, University of Vavuniya, Sri Lanka, [2]Department of ICT, University of Vavuniya, Sri Lanka, [3]Teaching Hospital Jaffna, Sri Lanka, [4]District General Hospital Kilinochchi, Sri Lanka

Introduction

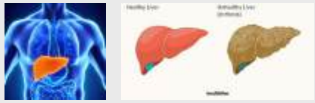

Figure 1: Liver and its healthline

- The liver is a vital organ located in the upper right abdomen.
- Functions:
  - Filters blood and removes toxins (alcohol, drugs, waste).
  - Produces bile to aid fat digestion.
  - Regulates blood sugar by storing glucose as glycogen.
  - Stores essential vitamins (A, D, E, K, B12), iron, and copper.
- Common Liver Diseases:
  - Hepatitis (A–E): Viral inflammation.
  - Fatty Liver Disease:
    - NAFLD (linked to obesity, diabetes).
    - AFLD (due to excessive alcohol).
    - Cirrhosis: Scarring from long-term liver damage.
    - Liver Cancer: Often linked to chronic liver disease.

Figure 2: stages of Liver Damage

Importance of early diagnosis of Liver disease: Statistical Results

- Liver disease causes 2 million deaths annually (4% of global deaths – 1 in 25).
- Two-thirds of liver-related deaths occur in men.
- Main global causes: Alcohol use & Metabolic Dysfunction Associated Steatotic Liver Disease (MASLD, formerly NAFLD).
- ALD & MASLD show high worldwide mortality rates.
- In Sri Lanka, major causes are ALD & MASLD.
- Unsafe alcohol use (54.7%) is the leading cause among Sri Lankan men.
- NAFLD is the most common liver disease burden in Sri Lanka.

Diagnosis of Liver disease

- Imaging Tests: Abdominal and Pelvic CT, Abdominal Ultrasound
- Other Tests: Numerical data testing for liver disease includes blood tests for bilirubin, blood glucose, albumin etc.
- Traditional diagnostic methods: Biopsies and imaging.

Aim & Objective

Aim

Developing a machine learning-based diagnostic model for the early detection of liver diseases (ALD, MASLD) Sri Lankan data

Objective

1. Obtain ethical clearance and collect relevant patient data from Sri Lankan hospitals, followed by comprehensive preprocessing.
2. Perform systematic feature selection and conduct statistical analysis on the clinical dataset for the correctness.
3. Apply various machine learning algorithms to accurately classify and predict liver disease types based on the selected clinical features.
4. Develop a region-specific, noninvasive diagnostic model tailored to the healthcare needs of the Sri Lankan population.

Methodology

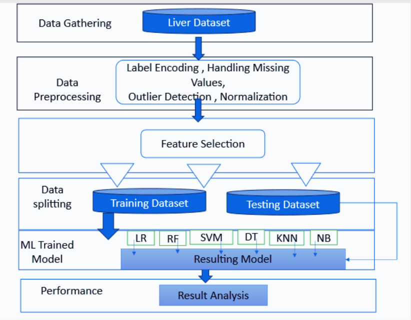

Figure 3: Overall Methodology of Liver Disease Diagnosis

Data Collection

- Necessary approvals for collecting the dataset are given by our university's ethical committee (Ethical Clearance).
- **Data was collected from Jaffna Teaching Hospital and Kilinochchi General Hospital.** (2025)
- We visited the hospital directly and retrieved the clinical data and biochemical measurements.
- We gathered both ALD, MASLD/NAFL, and Healthy data. (**Totally 538 data**)
- Binary classification 271 liver disease cases and 267 Healthy cases .
- Multi-class Classification 267 Healthy cases, 213 MASLD/NAFLD, and 58 ALD

Table 1: Dataset Variable Descriptions

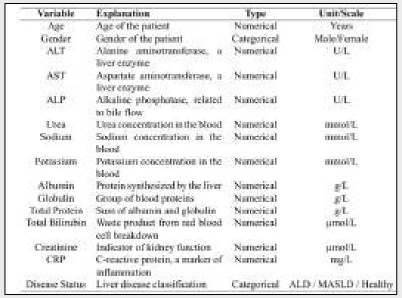

Variable	Explanation	Type	Unit/Scale
Age	Age of the patient	Numerical	Years
Gender	Gender of the patient	Categorical	Male/Female
ALT	Alanine aminotransferase, a liver enzyme	Numerical	U/L
AST	Aspartate aminotransferase, a liver enzyme	Numerical	U/L
ALP	Alkaline phosphatase, related to bile flow	Numerical	U/L
Urea	Urea concentration in the blood	Numerical	mmol/L
Sodium	Sodium concentration in the blood	Numerical	mmol/L
Potassium	Potassium concentration in the blood	Numerical	mmol/L
Albumin	Protein synthesized by the liver	Numerical	g/L
Globulin	Group of blood proteins	Numerical	g/L
Total Protein	Sum of albumin and globulin	Numerical	g/L
Total Bilirubin	Waste product from red blood cell breakdown	Numerical	µmol/L
Creatinine	Indicator of kidney function	Numerical	µmol/L
CRP	C-reactive protein, a marker of inflammation	Numerical	mg/L
Disease Status	Liver disease classification	Categorical	ALD / MASLD / Healthy

- **MICE imputation** was used to **handle missing values.**
- The **SMOTE technique** was used to **handle imbalanced data**
- **KNN, Z-score, and IQR methods** were used to **remove outliers.**
- **Feature Selection** was done using LASSO and VIF-8 features were selected.
- The **dataset was split into 80% training and 20% testing.** Eight machine learning models were evaluated for binary and multi-class classification.
- **Random Forest showed the best binary performance, while Decision Tree achieved the highest multi-class performance.**

Results

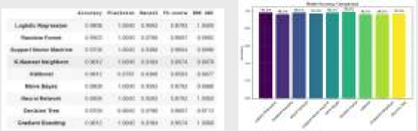

Figure 4: Test accuracy of the Machine Learning Models: Binary-class

- **binary classification:Random Forest achieved the highest accuracy of 99.03%** among all models, with precision 100%, recall 97.96%, F1-score 98.97%, and AUC-ROC 99.92%, confirming robust performance.
- Logistic Regression, Naive Bayes, and Neural Network models performed well, each achieving an accuracy of 98.06%.
- Compared to previous research, our model achieved the best overall accuracy, demonstrating superior performance.

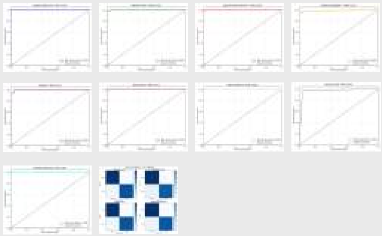

Figure 5: ROC curves of the Machine Learning Models: Binary-class

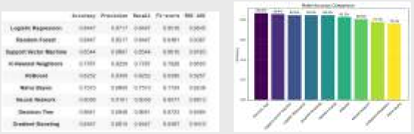

Figure 6: Test accuracy of the Machine Learning Models: Multi-class

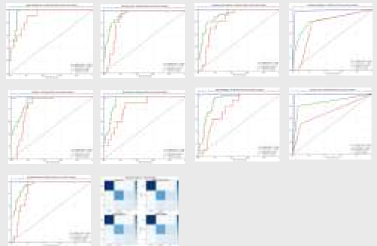

Figure 7: ROC curves of the Machine Learning Models: Multi-class

- multi-class classification:Decision Tree performed best, achieving 86.41% accuracy, precision 88.46%, recall 86.41%, F1-score 87.23%, and AUC-ROC 84.94%, outperforming other models.
- Logistic Regression, Random Forest, and Gradient Boosting models performed well, each achieving an accuracy of 84.47%.

Conclusion

•The Random Forest model achieved the highest accuracy among all tested machine learning models, reaching **99.03% for binary classification**.

•Decision tree achieved the highest accuracy among all tested machine learning models, reaching **86.41% for Multi-class classification.**

•The **limitation** is the dataset size, and demographic focus on Sri Lankan patients may limit generalizability to other populations. Additionally, class imbalance and the absence of certain clinical features could influence model performance.

•**Our Future work will apply CNN-based deep learning with ultrasound imaging for region-specific liver disease detection in Sri Lanka.**

Previous Work

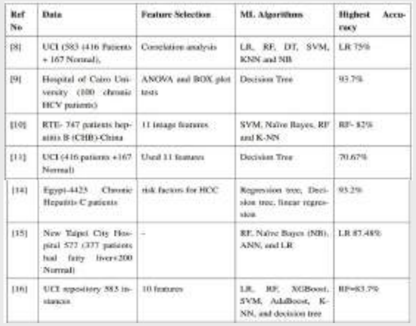

Ref No	Data	Feature Selection	ML Algorithms	Highest Accuracy
[8]	UCI (583 (416 Patients + 167 Normal),	Correlation analysis	LR, RF, DT, SVM, KNN and NB	LR 75%
[9]	Hospital of Cairo University (100 chronic HCV patients)	ANOVA and BOX plot tests	Decision Tree	93.7%
[10]	RTE- 747 patients hepatitis B (CHB)-China	11 image features	SVM, Naïve Bayes, RF and K-NN	RF- 82%
[11]	UCI (416 patients +167 Normal)	Used 11 features	Decision Tree	70.67%
[14]	Egypt-4423 Chronic Hepatitis C patients	risk factors for HCC	Regression tree, Decision tree, linear regression	93.2%
[15]	New Taipei City Hospital 577 (377 patients had fatty liver+200 Normal)	–	RF, Naïve Bayes (NB), ANN, and LR	LR 87.48%
[16]	UCI repository 583 instances	10 features	LR, RF, XGBoost, SVM, AdaBoost, K-NN, and decision tree	RF=83.7%

References

1. Asrani, S. K.; Devarbhavi, H.; Eaton, J.; Kamath, P. S. Burden of liver diseases in the world. Journal of hepatology 2019, 70, 151–171.
2. Park, I.-g.; Yoon, S. J.; Won, S.-m.; Oh, K.-K.; Hyun, J. Y.; Suk, K. T.; Lee, U. Gut microbiota-based machine-learning signature for the diagnosis of alcohol-associated and metabolic dysfunction-associated steatotic liver disease. Scientific Reports 2024, 14, 16122.
3. Wijewantha, H. S. Liver Disease in Sri Lanka. Euroasian journal of hepato-gastroenterology 2017, 7, 78.
4. Dassanayake, A. S. Nonalcoholic fatty liver disease: identifying the disease burden in Sri Lanka. Euroasian journal of hepato-gastroenterology 2018, 8, 69.
5. Singh, S. P.; Panigrahi, S.; Mishra, D.; Khatua, C. R. Alcohol-associated liver disease, not hepatitis B, is the major cause of cirrhosis in Asia. Journal of hepatology 2019, 70, 1031–1032.
6. Li, J.; Nguyen, M. H.; Valenti, L. Non-alcoholic fatty liver disease (NAFLD) in Asia— More efforts are needed. Liver International 2020, 40.
7. Wu, T.; Cooper, S. A.; Shah, V. H. Omics and AI advance biomarker discovery for liver disease. Nature Medicine 2022, 28, 1131–1132.
8. Rahman, A. S.; Shamrat, F.; Tasnim, Z.; Roy, J.; Hossain, S. A. A comparative study on liver disease prediction using supervised machine learning algorithms. International Journal of Scientific & Technology Research 2019, 8, 419–422.
9. Ayeldeen, H.; Shaker, O.; Ayeldeen, G.; Anwar, K. M. In 2015 Third World Conference on Complex Systems (WCCS), 2015, pp 1–6.
10. Chen, Y.; Luo, Y.; Huang, W.; Hu, D.; Zheng, R.-q.; Cong, S.-z.; Meng, F.-k.; Yang, H.; Lin, H.-j.; Sun, Y., et al. Machine-learning-based classification of real-time tissue elastography for hepatic fibrosis in patients with chronic hepatitis B. Computers in biology and medicine 2017, 89, 18–23.
11. Nahar, N.; Ara, F. Liver disease prediction by using different decision tree techniques. International Journal of Data Mining & Knowledge Management Process 2018, 8, 01–09.
12. Perveen, S.; Shahbaz, M.; Keshavjee, K.; Guergachi, A. A systematic machine learning based approach for the diagnosis of non-alcoholic fatty liver disease risk and progression. Scientific reports 2018, 8, 2112.
13. Wei, R.; Wang, J.; Wang, X.; Xie, G.; Wang, Y.; Zhang, H.; Peng, C.-Y.; Rajani, C.; Kwee, S.; Liu, P., et al. Clinical prediction of HBV and HCV related hepatic fibrosis using machine learning. EBioMedicine 2018, 35, 124–132.
14. Zhang, Z.-M.; Tan, J.-X.; Wang, F.; Dao, F.-Y.; Zhang, Z.-Y.; Lin, H. Early diagnosis of hepatocellular carcinoma using machine learning method. Frontiers in bioengineering and biotechnology 2020, 8, 254.
15. Ghosh, M.; Raihan, M. M. S.; Raihan, M.; Akter, L.; Bairagi, A. K.; Alshamrani, S. S.; Masud, M. A Comparative Analysis of Machine Learning Algorithms to Predict Liver Disease. Intelligent Automation & Soft Computing 2021, 30. 39

|ICAS2025|

Colour-Based Feature Analysis for Aloe Vera Leaf Disease Classification using Deep Learning

P.Tharsika [1], S.Thirukumaran[1]

[1]Department of Physical Science, University of Vavuniya, Sri Lanka

Abstract: Accurate classification of Aloe vera leaf diseases is challenging due to overlapping colour patterns between healthy and infected regions under varying lighting conditions. Traditional methods often fail to capture these subtle colour features, emphasizing the need for robust colour based analysis to improve deep learning model accuracy. This research introduces an advanced automated system for classifying Aloe vera leaf diseases, categorising them as healthy, aloe rust, or leaf spot, to facilitate early detection and support sustainable agriculture in Sri Lanka's expanding Aloe vera leaf sector. Utilizing a dataset of 847 images collected from farms in Jaffna and Peradeniya, the approach integrates sophisticated colour based feature analysis across multiple colour spaces (HSV, LAB, YCbCr, Normalized RGB, Opponent, and YUV) with Discrete Wavelet Transform (DWT) for enhanced representation. State of the art deep learning models, including DenseNet, EfficientNetV2B3, VGG16, and ResNet50, were employed for classification. DenseNet achieved superior performance with 98% accuracy (precision: 0.99, recall: 0.99 for aloe rust), underscoring the efficacy of colour based feature analysis in discerning visually prominent disease patterns. However, dataset imbalance (698 aloe rust, 139 healthy, 276 leaf spot images) led to biases. These results validate the integration of colour based feature analysis and deep learning for plant disease detection, advancing prior computer vision applications in agriculture while revealing challenges with imbalanced data. The framework enhances theoretical insights into colour based feature analysis and DWT for capturing disease specific cues, surpassing manual inspections and offering practical benefits for farmers in arid regions like Hambantota and Puttalam by minimizing crop losses. Limitations include the dataset's modest size and regional focus, potentially limiting generalization to varied conditions or emerging diseases. Future efforts will prioritize larger, balanced datasets, incorporate texture or spectral features, and investigate ensemble models for greater robustness, with potential extensions to other crops.

Keywords: Aloe vera, colour based features, deep learning, discrete Wavelet Transform, disease classification, plant pathology

Colour-based Feature Analysis for Aloe Vera Leaf Disease Classification using Deep Learning

P.Tharsika[1*], S.Thirukumaran[2]

[1,2]*Department of Physical Science, Faculty of Applied Science, University of Vavuniya*

Introduction

- Aloe vera (*Aloe barbadensis Miller*) is a valuable plant with medicinal, cosmetic, and nutritional benefits, widely cultivated in Sri Lanka's dry zones.
- Its leaves contain polysaccharides, antioxidants, enzymes, and vitamins, making them essential for pharmaceutical, cosmetic, and food industries.
- Leaf diseases such as aloe rust and leaf spot cause discoloration and tissue damage, reducing yield and commercial value.
- Manual inspection methods are time-consuming, labor-intensive, and often fail to detect early infections.
- This research develops an AI-based Aloe vera leaf disease classification system using multiple colour models and Discrete Wavelet Transform (DWT) for accurate and early disease detection.

Symptoms of Aloe Vera Diseases

Aloe Rust disease:

- Black or brown circular spots appear on leaves, hardening over time as the fungus oxidizes plant compounds, giving a distinct crusty texture.
- Thrives in moderate temperatures (60–82°F) with prolonged leaf wetness, primarily affecting older leaves while sparing new growth.

Leaf Spot disease:

- Small, circular to oval dark brown or black sunken spots form, often starting at leaf tips, potentially spreading across the leaf surface if untreated.
- Caused by fungal (*Alternaria alternata*) or bacterial infections, worsened by excessive moisture on leaves and poor air circulation.

Aim and Objectives

Aim

- This study aims to develop an automated system for classifying aloe vera leaf diseases (healthy, aloe rust, leaf spot) using colour-based feature analysis and deep learning to achieve high accuracy and assist farmers in early disease detection.

Objectives

- Preprocess aloe vera leaf images by resizing, normalizing, and organizing by disease class.
- Convert images to HSV, LAB, YCbCr, Normalized RGB, Opponent, and YUV colour spaces for better feature extraction.
- Use Discrete Wavelet Transform (DWT) to extract texture-based features from images.
- Train nine deep learning models (CNN+DWT, VGG16, ResNet50, EfficientNetB0, EfficientNetV2B0, ConvNeXtBase, DenseNet121, ConvNeXt, EfficientNetV2B3) for disease classification.
- Evaluate models using accuracy, precision, recall, F1-score, and confusion matrices, assessing colour space impact on accuracy.

Related work

Ref No.	Dataset	Methodology	Accuracy
1	3000 Aloe vera leaf images	This architecture is typical of a Convolutional Neural Network (CNN). CNNs are widely applied in tasks such as image recognition, object detection, and computer vision applications.	85.4%
2	Data from 7 trials, sourced from PubMed, Wiley, and Cochrane.	Faster-RCNN Based Deep Learning Model	91%
3	Data obtained from Optical Coherence Tomography (OCT) and optical microscopy images of Aloe Vera leaves images	• Optical Coherence Tomography (OCT). • Microscopy.	77.6%
4	Data from 7 trials, sourced from PubMed, Wiley, and Cochrane	KAloe vera farms, like gels and patches, were evaluated in clinical trials.	93%
5	The dataset from Arkansas Plant Disease Database and Reddit, has 237 images of diseases like Alterrnaria, Alternata and Canker, with 200 for training and 37 for testing	The KNN Arkansas image acquisition, LAB* conversion, KNN segmentation, morphological operations, and GLCM-based feature extraction for classification	96.76%

Methodology

Dataset

A total of 847 Aloe Vera images (Healthy, Aloe Rust Disease, Leaf Spot Disease) were

collected. Dataset Composition

- Aloe Rust Diseases: 698 images
- Leaf Spot Diseases: 276 images
- Healthy Leaves: 139 images

Data Pre-processing

- Organized images into three class-wise folders: healthy, aloe rust, and leaf spot for efficient data handling.
- Ensured correct labeling and accessibility of images for preprocessing and model training.
- Resized all images to a uniform 224x224 resolution using OpenCV for CNN compatibility.
- Removed low-quality or duplicate images and standardized formats to JPEG.
- Applied normalization to enhance consistency and support effective feature extraction.

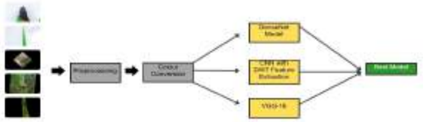

DenseNet121

- DenseNet121 uses dense connectivity to enhance feature reuse, effectively classifying aloe rust and leaf spot diseases in Aloe vera leaf images.
- It processes images in multiple colour spaces (HSV, LAB, YCbCr, etc.) to capture disease-specific visual patterns.
- Combined with Discrete Wavelet Transform (DWT), it extracts texture features for better detection of subtle disease symptoms.
- Compared with VGG16 and ResNet50, DenseNet121 achieves a strong balance between accuracy and efficiency in disease classification.

VGG16

- VGG16's 16-layer architecture with 3×3 convolutional filters effectively classifies aloe rust and leaf spot in Aloe vera images.
- It processes images in multiple colour spaces (HSV, LAB, YCbCr) to capture disease-specific features like rust's orange hues.
- Combined with DWT, it extracts detailed texture features, improving detection of subtle and complex disease patterns.
- Achieves competitive accuracy, precision, recall, and F1-score compared with models like DenseNet121 and ResNet50.

CNN with DWT Feature Extraction

- Custom CNN with DWT combines deep learning and texture analysis for accurate classification of aloe rust and leaf spot.
- DWT decomposes 224×224 images into sub-bands, capturing disease-specific texture patterns.
- Processes images in multiple colour spaces (HSV, LAB, YCbCr) to enhance both colour and texture feature detection.
- Evaluated against VGG16 and DenseNet121, showing strong performance in accuracy, precision, recall, and F1-score.

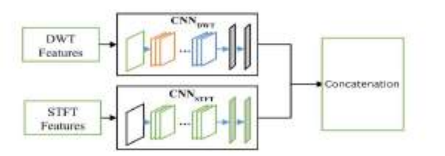

Results and Discussion

Confusion Matrices across Models

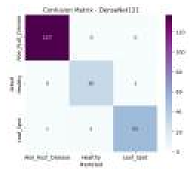

DenseNet121

VGG16

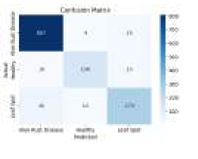

CNN with DWT Feature Extraction

Accuracy and Loss Accuracy Performance

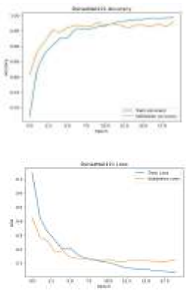

DenseNet121

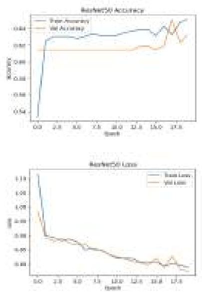

VGG16

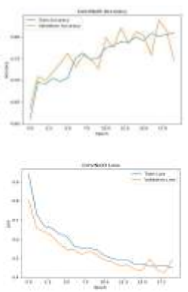

CNN with DWT Feature Extraction

Performance Metrics

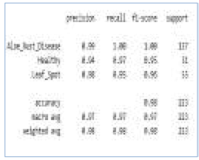

DenseNet121

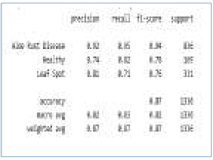

VGG16

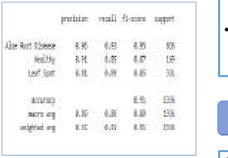

CNN with DWT Feature Extraction

Sample Data Set

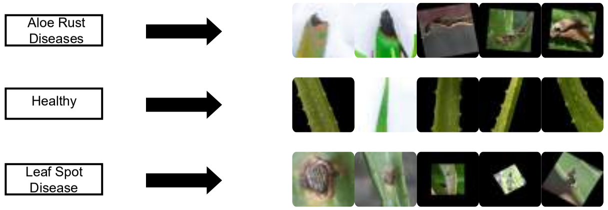

Accuracy Comparison

Models		Precision	Recall	F1- Score	Accuracy
DenseNet121	Aloe Rust Disease	0.99	1.00	1.00	0.98%
	Healthy	0.94	0.97	0.95	
	Leaf Spot	0.98	0.95	0.96	
	Macro Avg	0.97	0.97	0.97	
	Weighted Avg	0.98	0.98	0.98	
CNN with DWT	Aloe Rust Disease	0.96	0.93	0.95	0.91%
	Healthy	0.91	0.85	0.87	
	Leaf Spot	0.81	0.89	0.85	
	Macro Avg	0.89	0.89	0.89	
	Weighted Avg	0.92	0.91	0.91	
VGG-16	Aloe Rust Disease	0.92	0.95	0.94	0.87%
	Healthy	0.74	0.82	0.78	
	Leaf Spot	0.81	0.71	0.76	
	Macro Avg	0.82	0.83	0.82	
	Weighted Avg	0.87	0.87	0.87	

Conclusion

- Developed an automated system to classify Aloe vera leaf diseases (Healthy, Aloe Rust, Leaf Spot) using colour-based feature analysis, DWT, and deep learning models.
- Explored multiple colour spaces and architectures like DenseNet, ResNet50, VGG16, and EfficientNet, with DenseNet achieving the highest accuracy of 98%.
- Faced challenges with dataset imbalance and overlapping symptoms, impacting accurate classification of healthy and leaf spot leaves.
- Established a robust framework for early disease detection, reducing manual inspection and supporting sustainable Aloe vera cultivation.

References

1. Smith, J.; Brown, K. Bioactive Compounds in Aloe barbadensis miller: Therapeutic and Cosmetic Applications. Journal of Medicinal Plants Research 2020, 14, 123–135.
2. Perera, A.; Silva, R. Cultivation of Aloe vera Varieties in Sri Lanka's Dry Zones: Economic and Agricultural Perspectives. Tropical Agricultural Research 2018, 29, 210– 225.
3. Fernando, M.; Wijesekara, S. Pathogens Affecting Aloe vera: Challenges and Management Strategies in Sustainable Cultivation. Plant Pathology Journal 2021, 17, 89– 102.
4. Jones, A.; Kumar, R. Challenges in Traditional Plant Disease Detection: Limitations and Opportunities for Automation. Journal of Agricultural Science and Technology 2019, 21, 456–467.
5. Johnson, E., Historical Uses of Aloe vera in Ancient Civilizations; Academic Press: London, 2015.

|ICAS2025|

Machine Learning and Deep Learning Techniques for Betel Leaf Disease Detection in Imbalanced Datasets

R.A.N.M.Rajapaksha[1], N.Edwin Linosh[1]

[1]Department of Physical Science, University of Vavuniya, Sri Lanka

Abstract: The cultivation of betel leaf (*Piper betle*) is an important supplementary livelihood for many farmers in Sri Lanka's wet zone, particularly in the districts of Gampaha, Kalutara, and Colombo. However, the productivity and quality of betel leaves are frequently threatened by diseases such as bacterial leaf blight, fungal infections, pest attacks, and mite infestations. Timely and accurate identification of these issues is critical, yet traditional diagnostic methods used by farmers are often outdated, inefficient, or inaccessible. This research project addresses these challenges by developing an automated image classification system using both machine learning and deep learning approaches. A dataset of betel leaf images was collected and categorized into four classes: bacterial leaf blight, pest attack, mites attack, and healthy leaves. Using this dataset, five traditional machine learning models (Decision Tree, LightGBM, Random Forest, Support Vector Machine, and XGBoost) and four deep learning models (VGG16, VGG19, ResNet50, and ResNet101) were trained using consistent preprocessing, augmentation, and training strategies. Model performance was evaluated using balanced accuracy, macro F1-score, and AUC-ROC to ensure fair and robust comparison. Among all models tested, ResNet50 emerged as the top performer, achieving the highest scores across all evaluation metrics. This best-performing model was then integrated into a user-friendly web application, allowing real-time disease prediction from uploaded leaf images. The study demonstrates how deep convolutional neural networks, when paired with proper preprocessing techniques, can significantly enhance plant disease classification accuracy. The proposed solution offers a scalable and practical tool to support early detection and disease management, thereby promoting precision agriculture in Sri Lanka's betel leaf farming communities.

Keywords: betel leaf, CNN, data augmentation, deep learning, disease detection, image classification, machine learning

Machine Learning and Deep Learning Techniques for Betel Leaf Disease Detection In Imbalanced Datasets

R.A.N.M. Rajapaksha, N. Edwin Linosh
Department of Physical Science, Faculty of Applied Science, University of Vavuniya

Abstract

Betel leaf farming is vital to many Sri Lankan farmers, especially in the wet zone, but diseases such as bacterial blight, pest attacks, and mite infestations threaten yield and quality. This study introduces an automated system for detecting these diseases using both machine learning and deep learning techniques. A custom image dataset was collected from local betel farms and categorized into four classes: healthy, bacterial blight, pest, and mite-infested leaves. Five ML models (Decision Tree, Random Forest, SVM, XGBoost, LightGBM) and four DL models (VGG16, VGG19, ResNet50, ResNet101) were trained and evaluated using balanced accuracy, macro F1-score, and AUC-ROC to ensure fair comparison across imbalanced data. ResNet50 achieved the best performance across all metrics and was deployed in a web application enabling users to upload leaf images for instant predictions. This work bridges the gap in localized datasets and ML–DL comparative studies, offering a scalable, practical solution for timely and accurate betel leaf disease detection.

Introduction

Economic Importance in Sri Lanka
Betel (*Piper betle*) is a valuable cash crop, especially in districts like Gampaha, Kalutara, and Colombo. Sri Lanka exports betel leaves to countries like Pakistan and the Middle East, earning millions in foreign income annually.

Support for Farmers' Livelihoods
Over 25,000 rural families depend on betel farming as their main source of income. It's a long-term crop that provides steady earnings when managed well.

Challenges in Cultivation
Farmers face serious problems due to leaf diseases like:

- Bacterial leaf blight (oil blight)
- Fungal infections
- Mite attacks
- Pest damage

These reduce leaf quality and yield, affecting both local sales and exports.


Bacterial Leaf Blight


Fungal Infection


Mites Attack


Pest Attack


Healthy

Limitations of Traditional Detection
Most farmers rely on visual inspection or traditional knowledge, which can be slow and inaccurate. This often leads to late diagnosis and crop loss.

Objective

- To identify and classify common betel leaf diseases in Sri Lanka's wet zone.
- To collect a real-world image dataset of healthy and diseased betel leaves.
- To evaluate ML and DL models to determine the most accurate approach for disease classification.

Methodology

01
- **Data Collection**
  - Collect images of healthy and diseased betel leaves from betel farmers in the Gampaha District.

02
- **Data Preprocessing**
  - Standardizes images (resize) - Removes noise (median blur)
  - Focuses on relevant area (background removal)
  - Enhances visibility of features (CLAHE)
  - Extracts useful descriptors (color histograms + texture features)

03
- **Data Splitting & Augmentations**
  - Rotates, zooms, flips and Brightness changes(random transformations from *ImageDataGenerator*)

04
- **Model Training (Machine Learning)**
  - Decision Tree
  - Random Forest
  - SVM
  - XGBoost
  - LightGBM

05
- **Model Training (Deep Learning)**
  - VGG16
  - VGG19
  - ResNet50
  - ResNet101

06
- **Model Evaluation & Comparison.**

Table 3.1: Collected Raw image counts

Disease	Count
Bacterial Leaf Blight	113
Fungal Infection	12
Healthy	252
Mites Attack	114
Pests Attacks	161
Total	652

Table 3.2: Data After Splitting

Disease	Total	Training	Validation	Testing
Bacterial Leaf Blight	113	79	16	18
Fungal Infection	12	8	1	3
Healthy	252	176	37	39
Mites Attack	114	79	17	18
Pests Attacks	161	112	24	25
Total	652	454	95	103

Table 3.3: Augmentations on Training Set

Disease	Training	Augmented
Bacterial Leaf Blight	79	474
Healthy	176	1056
Mites Attack	79	474
Pests Attacks	112	672
Total	446	2676

Results and Discussion

Table 4.1: Evaluation Metrics for Each Model

Model Type	Accuracy	Balanced Accuracy	Macro F1	Weighted F1	ROC-AUC
ResNet50	0.93	0.9219	0.9233	0.9297	0.9954
VGG19	0.92	0.9155	0.9116	0.9198	0.9940
ResNet101	0.89	0.8816	0.8839	0.8890	0.9856
VGG16	0.89	0.8706	0.8727	0.8872	0.9899
LightGBM	0.85	0.8267	0.8293	0.8431	0.9610
Random Forest	0.84	0.8203	0.8275	0.8357	0.9520
XGBoost	0.80	0.7608	0.7704	0.7956	0.9439
SVM	0.78	0.7405	0.7487	0.7762	0.9206
Decision Tree	0.73	0.6974	0.6974	0.7224	0.8086

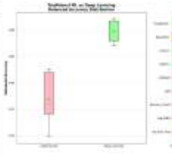

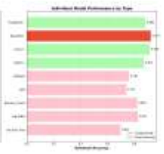

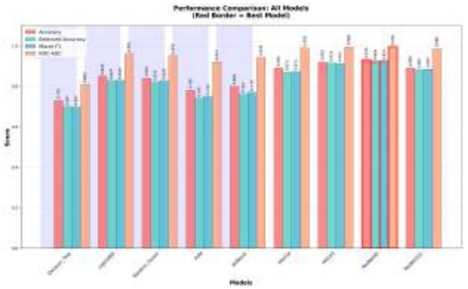

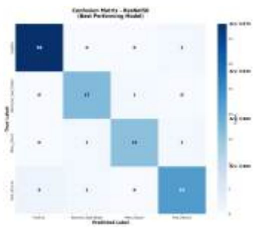

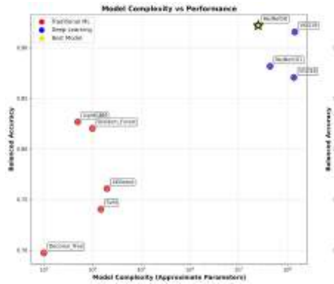

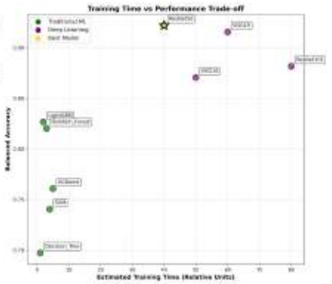

By analyzing the performance outcomes of the machine learning and deep learning models applied to betel leaf disease classification , Among the models, deep learning architectures such as ResNet50 and VGG19 showed superior performance compared to traditional ML models.

Conclusion

According to the research, the ResNet-50 model proved to be the most effective for automated betel leaf disease detection, demonstrating superior accuracy, robustness, and suitability for real-time deployment in agricultural monitoring systems.

References

1. Hussein, M. A., & Abbas, A. H. (2019). Plant leaf disease detection using support vector machine. *Al-Mustansiriyah Journal of Science*, *30*(1), 105–110.
2. Kale, M. R., & Shitole, M. S. (2021). Analysis of crop disease detection with SVM, KNN and random forest classification. *Information Technology in Industry*, *9*(2), 364–372.
3. Jadhav, S. B., Udup, V. R., & Patil, S. B. (2019). Soybean leaf disease detection and severity measurement using multiclass SVM and KNN classifier. *International Journal of Electrical and Computer Engineering*, *9*(5), 4092–4099.
4. Nikith, B., Keerthan, N., Praneeth, M., & Amrita, T. (2023). Leaf disease detection and classification. *Procedia Computer Science*, *218*, 291–300.
5. Aravind, K., PraylaShyry, S., & Felix, Y. (2019). Classification of healthy and rot leaves of apple using gradient boosting and support vector classifier. *International Journal of Innovative Technology and Exploring Engineering*, *8*(9), 2278–3075.
6. Chauhan, D., Walia, R., Singh, C., Deivakani, M., & Kumbhkar, M. (2021). Detection of maize disease using random forest classification algorithm. *Turkish Journal of Computer and Mathematics Education*, *12*(10), 715–720.

|ICAS2025|

Towards Generalisable Brain Age Prediction Across Heterogeneous Biomechanical Imaging Data

Jakob Träuble[1], Alex Christey[1], Gabriele Kaminski Schierle[1]

[1]Department of Chemical Engineering and Biotechnology, University of Cambridge, Cambridge, United Kingdom

Abstract: Brain age prediction from biomechanical brain imaging is a promising approach for identifying early signs of neurodegeneration. By estimating the deviation between predicted and chronological age, it is possible to quantify accelerated brain aging, which can serve as a sensitive biomarker for disease risk. Biomechanical properties derived from Magnetic Resonance Elastography (MRE) offer greater age sensitivity than anatomical measures and can reveal early neurodegenerative changes in multicentre datasets. Consistent performance across heterogeneous datasets poses a challenge, as demographic variability and acquisition-site differences can introduce confounding effects that limit generalisation. To address this, we investigate contrastive learning approaches tailored for regression, enabling models to capture fine-grained biomechanical patterns associated with ageing. Furthermore, these are combined with and compared to different domain adaptation strategies, including an adversarial classifier and distribution measure penalties such as Maximum Mean Discrepancy (MMD) and Hilbert Schmidt independence criterion (HSIC), designed to reduce site- and demographic-specific biases while preserving biologically meaningful variation. Our results show that the model combining contrastive regression with MMD achieved the most accurate brain age estimation. However, improvements in predictive accuracy did not consistently correspond to reductions in domain-specific confounding. This underscores the importance of evaluating both accuracy and robustness when developing generalisable biomarkers for brain ageing. Through this integration and systematic comparison, the work aims to identify representation learning strategies that improve generalisation in brain age prediction, supporting the development of biomechanical imaging as a reliable biomarker in multi-centre studies.

Keywords: brain age, magnetic resonance elastography, maximum mean discrepancy, neuro-degeneration

Towards Generalisable Brain Age Prediction Across Heterogeneous Biomechanical Imaging Data

Jakob Träuble[1*], Alex Christey[1], Gabriele Kaminski Schierle[1]

[1]Department of Chemical Engineering and Biotechnology, University of Cambridge, Cambridge, United Kingdom

ABSTRACT

Brain age prediction from Magnetic Resonance Elastography offers greater age sensitivity than anatomical imaging[1]. We investigate contrastive regression[2] and domain adaptation strategies[3,4] for brain age prediction. Our goal is to improve generalisation across heterogeneous datasets, advancing biomechanical imaging as a multi-centre biomarker.

BACKGROUND

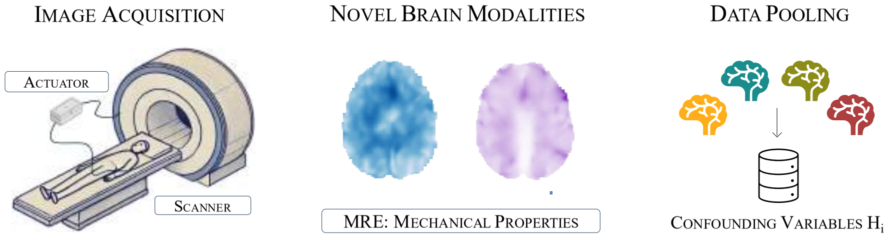

- **Magnetic Resonance Elastography (MRE):** novel imaging technique that measures the brain's mechanical properties
- **Domains:** Data is pooled from various clinical studies

OBJECTIVE

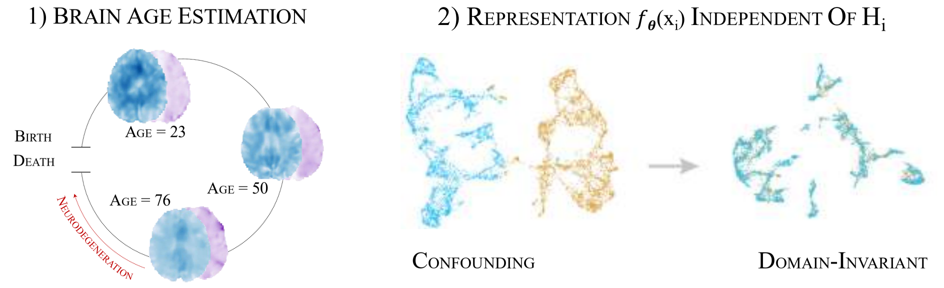

METHODOLOGY

1) CONTRASTIVE REGRESSION LEARNING

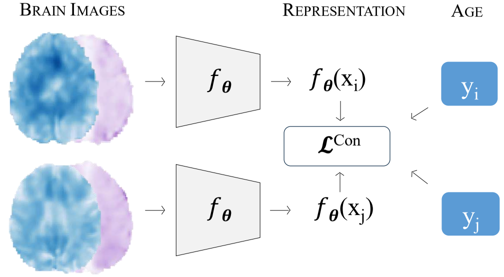

2) DOMAIN ADAPTATION

$$L_{adv} = -\sum_{x \in sites} s_X \log D(z)_X$$

ADVERSARIAL DOMAIN CLASSIFIER

$$HSIC(X,Y) = \frac{1}{(n-1)^2} Tr(HKH \cdot HLH) \qquad MMD^2(X,Y)$$

$$L_{CORAL}(X,Y) = \frac{1}{4d^2} \|C_X - C_Y\|_F^2$$

PROBABILITY MEASURES

$$\rightarrow \mathcal{L}^{\text{Total}} = \mathcal{L}^{\text{Con}} + \mathcal{L}^{\text{Dom}}$$

RESULTS

Method	MAE (Years)
Contrastive (no DA term)	3.42 ± 0.189
+ Classification	3.32 ± 0.178
+ MMD	$\mathbf{3.21 \pm 0.160}$
+ Classification + MMD	3.58 ± 0.109
+ Coral	3.54 ± 0.216
+ HSIC	3.46 ± 0.215

Table 1: Benchmark of brain age estimation objective

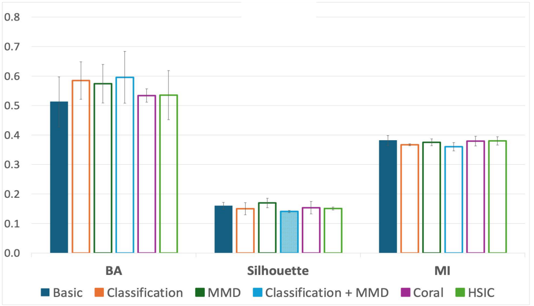

Figure 1: Benchmark of confounding metrics

CONCLUSION

- The model combining contrastive learning with a Maximum Mean Discrepancy (MMD) term yielded the most accurate brain age estimation result
- However, benchmarked methods show only minor changes in the quantitative confounding metrics

→ Suggests that gains in predictive accuracy do not automatically translate to gains in removal of domain-specific information

GATES Cambridge

C2 D3 Cambridge Centre for Data-Driven Discovery

AP SCI ACCELERATE PROGRAMME FOR SCIENTIFIC DISCOVERY

[1]Träuble et al., 2025 - Contrastive Learning on Regional Biomechanical Properties (bioRxiv); [2]Zha et al., 2023 - Rank-n-contrast (NeurIPS); [3]Smola et al., 2006 - Maximum mean discrepancy (ICONIP); [4]Gretton et al., 2005 – HSIC (ALT)

|ICAS2025|

The Landscape of Single Cells in Atherosclerotic Plaques

Korbinian Träeuble[1,2], Matthias Heinig[1,2,3]

[1]Institute of Computational Biology, German Research Center for Environmental Health, Helmholtz Zentrum München, Neuherberg, Germany
[2]Department of Computer Science, TUM School of Computation, Information and Technology, Technical University of Munich, Garching, Germany
[3]German Center for Cardiovascular Research, partner site Munich Heart Alliance, Berlin, Germany

Abstract: Atherosclerosis, the underlying driver of major cardiovascular events such as myocardial infarction and stroke, is marked by chronic inflammation and lipid accumulation within arterial walls, leading to the formation of plaque lesions. Despite its global burden, many cellular mechanisms underpinning plaque initiation, progression, and destabilization remain incompletely understood. Notably, immune-mediated transformations of vascular smooth muscle cells (SMCs), endothelial cells (ECs), and fibroblasts during plaque development are areas of intense investigation. Single-cell RNA sequencing (scRNA-seq) has revolutionized our understanding of tissue complexity by revealing cell-type heterogeneity at unparalleled resolution. In our study, we utilize a comprehensive scRNA-seq reference atlas that spans over 250,000 cells derived from carotid, coronary, and femoral artery samples. The atlas provides hierarchical annotations at two levels of granularity: Level 1 defines 13 broad cell classes, while Level 2 refines these into more specific subtypes. Using this atlas as a reference, we apply cell2location-based spot deconvolution on 10x Genomics Visium spatial transcriptomics data from coronary artery plaques. This integration allows us to map the spatial organization of these diverse cell types in early versus advanced lesions. Our results reveal that while both immune and structural cells are present across all stages, immune populations are enriched in advanced lesions, highlighting the pivotal role of inflammation in disease progression.

Keywords: atherosclerosis plagues, immune cells, RNA reference atlas, single-cell RNA sequencing

The Landscape of Single Cells in Atherosclerotic Plaques

Korbinian Traeuble[1,2], Matthias Heinig[1,2,3]

[1]*Institute of Computational Biology, German Research Center for Environmental Health,Helmholtz Zentrum München, Neuherberg, Germany.* [2]*Department of Computer Science, TUM School of Computation, Information and Technology, Technical University of Munich, Garching, Germany.* [3]*German Center for Cardiovascular Research, partner site Munich Heart Alliance, Berlin, Germany,*

Abstract

Atherosclerosis is characterized by chronic inflammation and the buildup of lipids in the arteries, leading to plaque formation and potential rupture. We utilize a single-cell transcriptomic reference atlas to characterize the landscape of cells in these plaques as well as their spatial location in early and advanced lesions. This marks a step forward in understanding atherosclerosis.

Introduction

- Atherosclerosis is the major cause for myocardial infarction and stroke.
- The immune-driven transformation and differentiation of arterial smooth muscle cells (SMCs), endothelial cells (ECs), and fibroblasts in plaque progression are still poorly understood and under active study.
- Single-cell RNA sequencing (scRNA-seq) sheds light into the cell type composition of tissues.
- scRNA-seq atlases harmonize different datasets into one annotated object which can be used for downstream tasks.

Objective

We characterized the cellular composition of atherosclerotic plaques in scRNA-seq and spatial transcriptomics.

Methodology

- We utilize a scRNA-seq reference atlas [1] to investigate cell type composition of plaques:
  - ➢ This atlas consists of more than 250,000 cells from 79 carotid, coronary and femoral artery samples
  - ➢ Annotations on broad level 1 and fine-grained level 2
- Apply spot deconvolution using cell2location [2] on 10x Visium samples from coronary arteries [3] and atlas as reference.

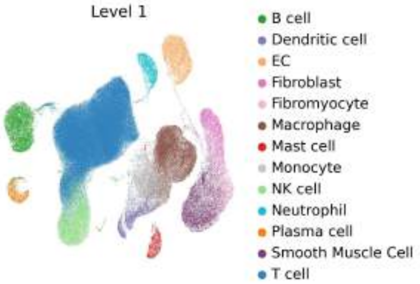

Figure 1: UMAP representation of scRNA-seq atlas of atherosclerotic plaques including level 1 cell type annotation.

Atlas cell type composition

Cell type composition of unsorted datasets

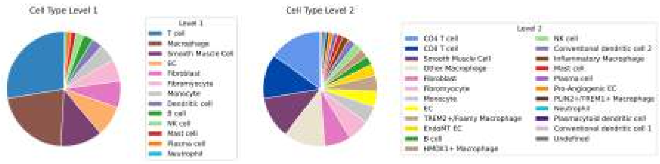

Figure 2: Cell types present in plaques

Spot deconvolution

Spatial distribution of cell types in control and advanced plaques

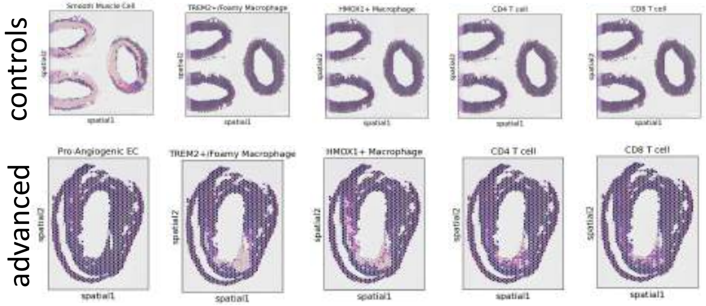

Figure 3: Spatial abundance of control and advanced plaques

Conclusion

Many structural and immune cells are present in plaques, while the later are more abundant in more advanced lesions.

Limitations

- Only cell types characterized in atlas investigated
- Cell2location algorithm has no validation
- Deconvolution with only two samples currently → Future studies could include more spatial samples and investigate differences quantitively.

References

[1] Traeuble, K. et al. Integrated single-cell atlas of human atherosclerotic plaques. (2024) doi:10.1101/2024.09.11.612431.

[2] Kleshchevnikov, V. et al. Cell2location maps fine-grained cell types in spatial transcriptomics. Nat Biotechnol 40, 661–671 (2022).

[3] Bleckwehl, T. et al. Encompassing view of spatial and single-cell RNA sequencing renews the role of the microvasculature in human atherosclerosis. Nat Cardiovasc Res 4, 26–44 (2024).

|ICAS2025|

Deep Learning-Based Biomarkers of Brain Aging: Structural and Functional Changes Across the Lifespan

Thuraisamy Vaitheeswaran[1], Logiraj Kumaralingam[2]

[1]Department of Physical Science, University of Vavuniya, Sri Lanka
[2]Department of Radiology and Diagnostic Imaging, University of Alberta, Canada

Abstract: Normal brain aging refers to the gradual, natural changes in brain structure and function that occur with advancing age, in the absence of neurodegenerative disease. Identifying biomarkers of normal aging is essential for distinguishing healthy brain development from pathological conditions and for understanding the mechanisms underlying cognitive resilience, especially given the global increase in the aging population. Most existing studies employ deep learning for brain age prediction rather than classification into discrete age groups, even though aging is a gradual process in which group-based analysis can better capture meaningful structural brain changes than individual age-based analysis. In this study, we propose a deep learning framework with integrated explainable AI to identify and interpret biomarkers of brain aging. We analyzed diffusion-weighted and T1-weighted MRI data from healthy individuals in the publicly available IXI dataset, categorized into three age groups: Group 1 (early adulthood, 20–39 years, n = 119), Group 2 (middle age, 40–59 years, n = 124), and Group 3 (later life, 60–79 years, n = 133). Structural brain networks were constructed, and graph attention networks (GATs) were trained to perform pairwise classification between Group 1 vs. Group 2 and Group 2 vs. Group 3, achieving accuracies of 86% and 87%, respectively. Using a GNN explainer, we identified discriminant brain regions and connections contributing to aging. From early adulthood to middle age, we found six highly robust discriminant connections indicating broad network reorganization involving multimodal integration, social cognition, and visual–memory pathways. In contrast, the transition from middle age to later life revealed only four discriminant connections, suggesting that many midlife changes stabilize, but specific left-hemisphere memory and semantic/cognitive networks continue to decline. These structural biomarkers have clear functional relevance for monitoring healthy cognitive aging.

Keywords: diffusion-weighted MR imaging, explainable artificial intelligence, graph attention network, normal brain aging, structural brain network

DEEP LEARNING-BASED BIOMARKERS OF BRAIN AGING: STRUCTURAL AND FUNCTIONAL CHANGES ACROSS THE LIFESPAN

Thuraisamy Vaitheeswaran[1*], Logiraj Kumaralingam[2*]

[1] *Department of Physical Science, Faculty of Applied Science, University of Vavuniya, Vavuniya, Sri Lanka,*
[2] *Department of Radiology and Diagnostic Imaging, University of Alberta*

Introduction

- Normal brain aging refers to the **natural and gradual changes** that occur in the brain's structure and function over time, Typically starts in the 20s - 30s, Aging is a natural, **inevitable, and irreversible biological process** characterized by the gradual decline of physiological functions [1].
- Normal brain aging is a natural process, while neurodegenerative diseases like Alzheimer's and Parkinson's involve abnormal, progressive brain damage [2].
- The American Federation for Aging Research (AFAR) defines aging biomarkers as measurable biological indicators that reflect **macroscopic brain changes with age**, such as **decreased neuron density** and **synaptic connections** that **reduce grey** matter and **affect learning, sensory, motor, and memory functions** [3–9].
- In Southeast Asia, the **older population (60+) is projected** to grow from 9.8% in 2017 to 20.3% by 2050. Identifying brain aging **biomarkers** helps **distinguish normal aging from neurodegenerative diseases**, supporting early detection, better healthcare planning, and neuroscience research.[10]

Research Gap

•**Focus on Prediction Rather than Classification:** Most existing studies concentrate on **brain age prediction** (a regression task) rather than **classification** into discrete age groups.

• **Limitations of Individual Age-Based Analysis:** Aging is a gradual process, unlike diseases that cause sudden changes. Analyzing individual ages may not capture meaningful differences, whereas **group-based analysis** can better reveal structural changes during aging.

•**Traditional deep learning models** often rely on raw image-based MRI inputs. In contrast, our **graph-based approach** models MRI-derived connectivity networks, allowing for a more explicit representation of **structural and functional brain interactions**.

•**Lack of Explainability in Aging Studies :** No previous studies have applied **explainable AI** to interpret the gradual structural changes that occur in the brain during normal aging.

Aim and Objective

Aim

- To identify structural and functional biomarkers of normal brain aging using neuroimaging data from different age groups (20–39, 40–59, and 60–79) through explainable deep learning techniques.

Construct Brain Networks from Neuroimaging Data

- Acquire structural neuroimaging data from the three age groups.
- Preprocess the data and construct brain networks suitable for deep learning analysis.

Develop Deep Learning Models for Classification

- Design and train **Graph Attention Network (GATs)** on the brain network data.
- Classify aging-related brain patterns across the age groups.

Integrate Explainable AI

- Apply **GNNExplainer** methods to interpret the deep learning models.
- Identify specific brain connections that act as biomarkers of normal aging.

Methodology

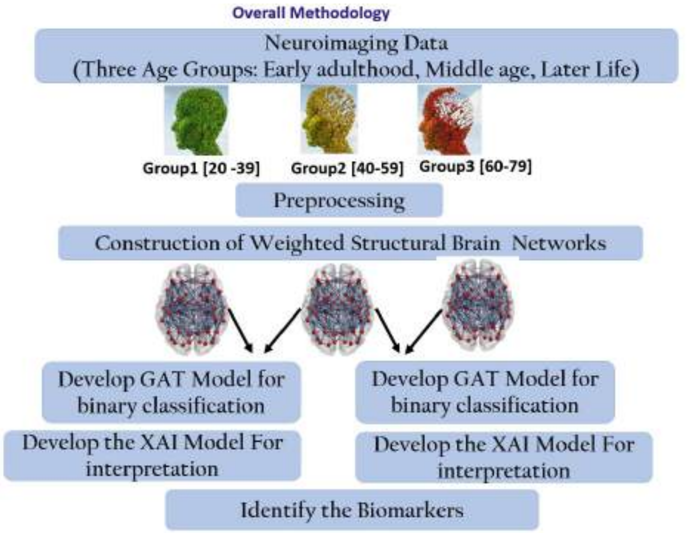

Overall Methodology

Neuroimaging Data
(Three Age Groups: Early adulthood, Middle age, Later Life)

Group1 [20 -39] Group2 [40-59] Group3 [60-79]

Preprocessing

Construction of Weighted Structural Brain Networks

Develop GAT Model for binary classification

Develop GAT Model for binary classification

Develop the XAI Model For interpretation

Develop the XAI Model For interpretation

Identify the Biomarkers

The dataset used in this study was obtained from the **Information eXtraction from Images project (IXI)** database.

Variables	Group 1 [20 -39] Early adulthood	Group 2 [40-59] Middle age	Group 3 [60-79] Later Life
Number of subjects	119	124	133
Male : Female	63:56	52:72	52:81
Age(Mean +/- std)	30.09 +/- 5.49	51.26 +/- 6.46	67.82 +/- 5.7

Pre-processing & Weighted Structural Brain Network

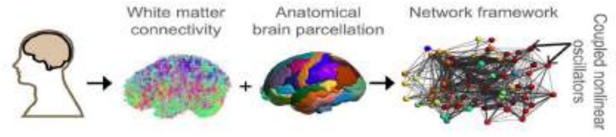

Proposed GAT Model

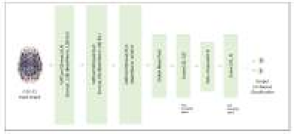

Implementation

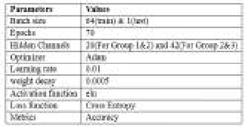

Parameters	Values
Batch size	64(train) & 1(test)
Epochs	70
Hidden Channels	28(For Group 1&2) and 42(For Group 2&3)
Optimizer	Adam
Learning rate	0.01
weight decay	0.0005
Activation function	elu
Loss function	Cross Entropy
Metrics	Accuracy

Evaluation Metrics

$$accuracy = \frac{TP + TN}{TP + FN + FP + TN}$$

$$recall = \frac{TP}{TP + FN}$$

$$specificity = \frac{TN}{FP + TN}$$

$$precision = \frac{TP}{TP + FP}$$

$$F1score = 2 \times \frac{precision \times recall}{precision + recall}$$

Results and Discussion

Binary Classification Result

Group1(20- 39 years) vs Group2(40- 59 years)
Accuracy: **86%**

classes	Precision	Recall	F1-score
Group1(20 - 39)	0.88	0.85	0.86
Group2(40 - 59)	0.83	0.87	0.85

Group2(40- 59 years) vs Group3(60- 79 years)
Accuracy: **87%**

classes	Precision	Recall	F1-score
Group2(40 - 59)	0.88	0.84	0.86
Group 3(60 - 79)	0.86	0.89	0.87

Visualize Classifier's Decision Using GNN Explainer

Average of Explanation Heatmap of all Group2 subjects, and resulting maps

Discriminant structural connections and corresponding discriminant edge weights in axial view, and resulting maps of thresholding at 60%, 65%, 70%, and 75% For **Early Adulthood-> Middle Age**

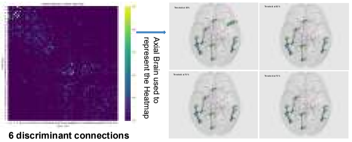

6 discriminant connections

- **Multimodal integration & cognition** (bankssts–inferior parietal, bilateral).
- **Visual memory integration** (entorhinal–fusiform, left).
- **Visuospatial-object recognition** (inferior parietal–inferior temporal, bilateral).
- **Episodic memory integration** (isthmus cingulate–cuneus, left).

Functional Changes

This stage shows **widespread network reorganization**, with declines in **processing speed**, **social cue interpretation**, and **integration of sensory and memory systems**.

Early Adulthood –> Middle Age

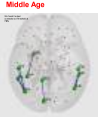

Average of Explanation Heatmap of all Group3 subjects, and resulting maps

Discriminant structural connections and corresponding discriminant edge weights in axial view, and resulting maps of thresholding at 60%, 65%, 70%, and 75% For **Middle Age –> Later life**

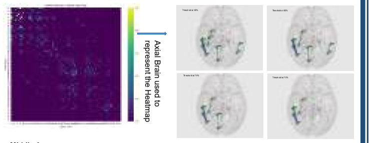

Middle Age –> Later life

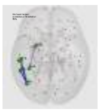

4 discriminant connections

- **bankssts–inferior parietal (Left)**
- **entorhinal–fusiform (Left)**
- **inferior parietal–inferior temporal (Left)**
- **inferior parietal–Middle temporal (Left)**

Functional Changes

- This suggests that **many middle age structural differences stabilize** into later life.
- **Specific left-hemisphere networks** continue to decline.
- These are heavily **memory** and **semantic/cognitive processing pathways.**

Conclusion

- **First study** to classify brain aging stages (20–39, 40–59, 60–79) using deep learning integrated with explainable AI to interpret structural brain changes.
- The **Graph Attention Network (GAT)** achieved high-accuracy classification (86%, 87%) for both Early Adulthood → Middle Age and Middle Age → Later Life transitions.
- Key structural connections distinguishing age groups were identified using a **GNN Explainer.**

  •Early → Middle Age: 6 discriminant connections indicating broad network reorganization involving multimodal integration, social cognition, and visual–memory systems.

  •Middle Age → Later Life: 4 discriminant connections showing that many midlife changes stabilize, but left-hemisphere memory and semantic/cognitive networks continue to decline. Identified structural biomarkers demonstrate clear functional relevance for monitoring healthy cognitive aging.

- Future work: Extend the analysis to multimodal (structural + functional) neuroimaging for deeper insights into brain aging dynamics.

References

1. Riddle, D. R. (Ed.). (2007). Brain aging: models, methods, and mechanisms.
2. Rossini, P. etc (2007). Clinical neurophysiology of aging brain: from normal aging to neurodegeneration. Progress in neurobiology, 83(6), 375-400.
3. Butler RN,et al. Aging: the reality: biomarkers of aging: from primitive organisms to humans. J Gerontol A Biol Sci Med Sci. 2004; 59(6).
4. Scheibel, A. B. (1992). Structural changes in the aging brain. Handbook of mental health and aging, 147-173.
5. Lockhart, S. N., & DeCarli, C. (2014). Structural imaging measures of brain aging. Neuropsychology review, 24, 271-289.
6. Dickstein, D. L., Kabaso, D., Rocher, A. B., Luebke, J. I., Wearne, S. L., & Hof, P. R. (2007). Changes in the structural complexity of the aged brain. Aging cell, 6(3), 275-284.
7. Tomasi, D., & Volkow, N. D. (2012). Aging and functional brain networks. Molecular psychiatry, 17(5), 549-558.
8. Ferreira, L. K., & Busatto, G. F. (2013). Resting-state functional connectivity in normal brain aging. Neuroscience & Biobehavioral Reviews, 37(3), 384-400.
9. Joaquin, A. M., & Gollapudi, S. (2001). Functional decline in aging and disease: a role for apoptosis. Journal of the American Geriatrics Society, 49(9), 1234-1240.
10. United Nations, Department of Economic and Social Affairs,Population Division World Population Prospects 2024, https://population.un.org/wpp/.

|ICAS2025|

Optimized Enhancement of Pelvic CT Scan Images using Image Processing Techniques

Anchana Rajakumaran

Department of Physical Science, University of Vavuniya, Sri Lanka

Abstract: Computed Tomography (CT) imaging plays a crucial role in diagnosing pelvic disorders such as cancers, vascular abnormalities, and traumatic injuries. However, reducing radiation dose in pelvic CT scans—a key priority under the ALARA (As Low As Reasonably Achievable) principle—often leads to increased noise and reduced contrast, impairing diagnostic accuracy. Addressing this trade-off, the present research aims to minimize radiation exposure while maintaining diagnostic-quality imaging through a hybrid image enhancement framework combining Non-Local Means (NLM) filtering for noise suppression and wavelet-based transform techniques for contrast enhancement. A dataset of 140 anonymized low-dose pelvic CT images from Thellipalai Base Hospital, Jaffna, was used. The proposed two-stage approach first applies NLM denoising to reduce random noise while preserving fine structures, followed by wavelet decomposition and thresholding to selectively enhance high-frequency details. A grid search across NLM smoothness parameters (5–30) and wavelet thresholds (0.01–0.09) identified the optimal configuration ($h = 5$, threshold $= 0.01$). Quantitative analysis using Peak Signal-to-Noise Ratio (PSNR) and Signal-to-Noise Ratio (SNR) showed marked improvement over standalone enhancement methods, achieving mean PSNR above 44 dB and substantially enhanced SNR values. These improvements indicate clearer structural delineation and reduced visual fatigue, as confirmed by radiologist feedback. Compared with conventional single-stage methods, the hybrid approach demonstrated superior balance between noise reduction and anatomical detail preservation, directly supporting accurate diagnoses without additional radiation burden. This research highlights how optimized hybrid enhancement can bridge the gap between dose reduction and image interpretability, offering a scalable, low-cost solution for clinical settings—especially in low-resource environments. Future work will integrate machine learning– based adaptive parameter tuning to further automate and personalize the enhancement process for diverse diagnostic needs.

Keywords: hybrid enhancement, low-dose imaging, medical image processing, non-local means, pelvic CT, wavelet transform

Optimized Enhancement of Pelvic CT Scan Images Using Image Processing Techniques

Anchana Rajakumaran[1]*
[1]Department of Physical Science, University of Vavuniya, Sri Lanka

Abstract

This study develops a hybrid framework using Wavelet Transform and Non-Local Means filtering to enhance low-contrast, noisy pelvic CT images. Tested on 140 scans with optimized parameters, it improved PSNR (45.85 dB) and SNR (34.88 dB). Radiologist feedback confirmed better visualization, aiding accurate diagnoses. Future work includes ML automation.

Introduction

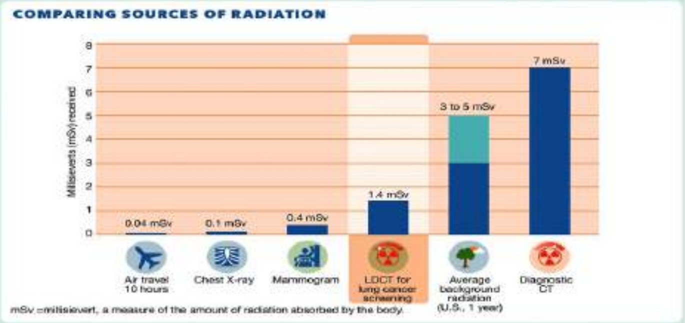

CT is essential for pelvic diagnostics, but low-dose scans cause noise and low contrast, reducing accuracy. This study proposes a hybrid method using NLM denoising and wavelet enhancement to improve image quality, highlight critical structures, and support accurate diagnosis while minimizing radiation (ALARA principle).

Objective

Minimize CT radiation exposure while preserving diagnostic-quality imaging of the pelvic region of the human body.

→ Develop a hybrid enhancement framework

→ Optimize parameters for effective noise reduction and fine-detail preservation

→ Validate performance through quantitative metrics and expert radiologist evaluation

Methodology

Data Collection

Thellipalai Base Hospital, Sri Lanka

140 anonymized LDCT Pelvic images

Image Parameters

▪ **Resolution**	**512 x 512 pixels**
▪ **Pixel Spacing**	**0.5 – 1.00 mm/pixels**
▪ **Aspect ratio**	**1:1**
▪ **Field of View**	**250 – 400 mm**
▪ **Bit depth**	**original**

Enhancement

NLM with *h* = 5–30
DWT thresholds 0.01–0.09

Grid search (4200 combinations)

Validation

Evaluation: PSNR & SNR metrics

Radiologist qualitative review

Results and Discussion

Optimal Settings
NLM h = 5
WT = 0.01

Outperformed Results
PSNR : 45.85 dB
SNR : 34.88 dB

Quantitatively, PSNR increased to **45.85 dB** and SNR to **34.88 dB**, indicating a marked reduction in noise & clear structural visibility.

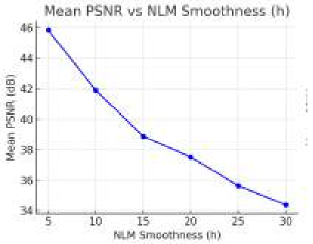

Conclusion

The hybrid method improves low-dose pelvic CT by enhancing PSNR, SNR, and organ clarity, with radiologist validation confirming reduced noise and better delineation. It enables accurate diagnosis with minimal radiation, supporting the ALARA principle..

References

- Improving Signal to Noise Ratio of Low-Dose CT Image Using Wavelet Transform – A study
- Applications of nonlocal means algorithm in low-dose X-ray CT image processing and reconstruction: A review

|ICAS2025|

A Graph Neural Network Approach to Parkinson's Disease Detection with Multi-Modal Brain Imaging

Varaniya Varatharasa[1], Pavithira Sivasothy[1]

[1]Department of Physical Science, University of Vavuniya, Sri Lanka

Abstract: Parkinson's Disease (PD) is a progressive neurodegenerative disorder characterized by the gradual loss of dopamine-producing neurons in the substantia nigra, resulting in both motor symptoms such as tremors, rigidity, and bradykinesia, and non-motor symptoms including cognitive decline and sleep disturbances. Early detection of PD remains a significant challenge due to the absence of reliable biomarkers prior to the onset of motor symptoms. Consequently, diagnosis often occurs only after substantial neuronal loss, reducing the efficacy of treatment. According to the World Health Organization (WHO), over 8.5 million people worldwide were affected by PD in 2023, emphasizing its growing global burden and the urgent need for improved diagnostic methods. Existing neuroimaging-based PD detection studies commonly employ Convolutional Neural Networks (CNNs) that analyze voxel-level information, which limits their ability to capture the brain's complex networked organization. Since PD disrupts both structural and functional connectivity across brain regions, representing the brain as a graph provides a biologically meaningful way to model inter-regional relationships. In this study, we propose a Graph Neural Network (GNN) based multi-modal framework for PD detection using diffusion-weighted MRI (dwMRI) and resting-state fMRI (rsfMRI) data from 115 PD and 118 normal control (NC) participants. Structural and functional brain networks were constructed for each modality, and five node-level features including degree, degree mean, external edges, external edges mean, and internal edges were extracted from all nodes in each subject. In functional networks, positive and negative edge weights were separately modeled through two GNN pipelines, and their outputs were ensembled. The structural and functional GNNs achieved accuracies of 88% and 75%, respectively, while the multi-modal ensemble improved classification performance to 90%. These findings demonstrate the potential of GNN based brain network analysis for effectively capturing PD related connectivity alterations and advancing neuroimaging based diagnostics.

Keywords: ensembling, functional brain network, graph neural network, Parkinson's disease, structural brain network

A Graph Neural Network Approach to Parkinson's Disease Detection with Multi-Modal Brain Imaging

Varaniya Varatharasa[1*], Pavithira Sivasothy[2]
[1] Department of Physical Science, Faculty of Applied Science, University of Vavuniya, [2]Department of Physical Science, Faculty of Applied Science, University of Vavuniya

Introduction

- **Parkinson's Disease (PD)** is a progressive neurological disorder caused by the loss of dopaminergic neurons in the substantia nigra.
- PD is the **second most common neurodegenerative disease** after Alzheimer's, affecting over 8.5 million people globally [1].
- PD mainly impacts **older adults** and is a growing public health concern, including in countries like Sri Lanka.

Figure 1: Symptoms of PD

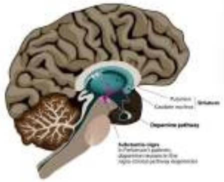

Figure 2: substantia nigra and dopamine pathway in PD

Diagnostic Methods

- **Neurological Examination:** Assessment of movement, coordination, and balance by a neurologist.
- **Genetic Testing:** Recommended for younger patients or those with family history.
- **Neuroimaging:** MRI, fMRI, PET, and CAT detect brain changes at the macro level.

Figure 3: Neurological Examination

Figure 4: Genetic Testing

Figure 5: Neuroimaging

Previous Works

Table 1: fMRI-based studies

Ref No	Modality	Subjects	Model	Accuracy
[2]	fMRI	603	CNN	88.5%
[3]	fMRI	30	CNN	97.92%
[4]	fMRI	40	CNN	86.07%
[5]	fMRI	183	CNN	77.80%

Table 2: Multimodal-based studies

Ref No	Modality	Subjects	Model	Accuracy
[6]	MRI + SPECT	30	CNN Ensemble	99.94%

Table 3: GNN-based multimodal studies

Ref No	Modality	Subjects	Model	Accuracy
[7]	T1-MRI, fMRI, DWI	109	GAT	73%

Research Gaps

- Most studies focus on whole-brain imaging, with limited analysis of **brain network** connectivity and interactions.
- Limited research uses **dwMRI** to assess disease-related micro structural changes.
- Sparse **multi-modal** fusion approaches.

Aim and Objectives

Aim : Develop a deep learning framework using Graph Neural Network (GNN) for accurate detection of PD from multi-modal brain imaging (dwMRI and rsfMRI).

Objectives:

- Build structural and functional brain networks from dwMRI and rsfMRI.
- Extract microstructural connectivity features for PD classification from dwMRI.
- Develop a GNN-based multimodal fusion model for accurate PD detection.

Methodology

Neuroimaging data collection and preprocessing

- We have collected and preprocessed PPMI data (dwMRI, rsfMRI, T1-MRI).

Table 4: Demographic characteristics of Subjects

Variable	Parkinson's Disease : PD (115)	Normal Control: NC (118)
Male : Female	79 : 36	44 : 74

Construction of structural and functional networks

- Converted raw data of all modalities from DICOM to NIfTI using MRIcron.

Table 5: Details of Network construction

Modality	Atlas Used	Network Dimension	Tools Used
Structural (dwMRI)	Desikan – Killiany	80 x 80	MRIcron, FSL, Camino (UCL), MATLAB
Functional (rsfMRI)	Harvard - Oxford	164 x 164	MRIcron, CONN Toolbox, SPM12, MATLAB

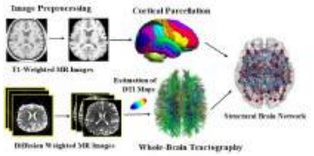

Figure 6: Pipeline for Structural network construction

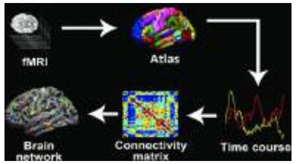

Figure 7: Pipeline for Functional network construction

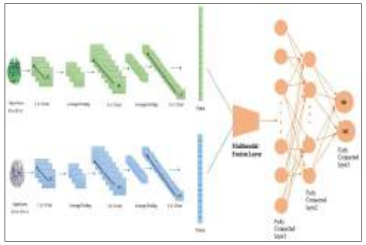

Figure 8: Developed CNN Ensembling Architecture

- As shown in **Table 5**, brain networks were constructed using the specified preprocessing and connectivity tools.
- Voxel-level features from **115 PD** and **118 NC** subjects were used to develop **three CNN models**: one for structural data, one for functional data, and one combined model.
- The outputs of these models were integrated through a **CNN ensembling architecture**, as shown in **Figure 8**, to standardize predictions and improve classification robustness.

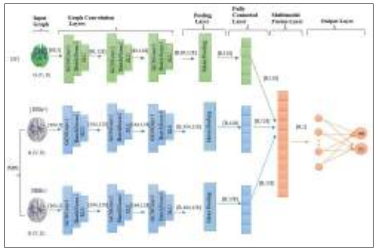

Figure 9: Proposed GNN Ensembling Architecture

- **Figure 9** shows the **proposed GNN ensembling architecture**.
- Structural and functional brain networks with **five node-level features**: **degree, degree (mean), external edges, external edges (mean), internal edges** for all **nodes per subject** were used as input.
- Separate GNN models were tested on structural and functional networks, and their outputs were combined in the **proposed GNN ensembling model** to improve classification performance.

Results and Discussion

- Implemented in Python using PyTorch on Visual Studio Code.

Table 6: CNN Ensembling results

Modality	Model	Accuracy
dwMRI	CNN	86%
fMRI	CNN	82%
dwMRI, rsfMRI, T1-MRI	CNN Ensemble	88%

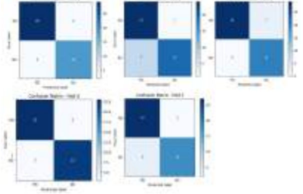

Figure 10: CNN Ensembling Confusion Matrices

Table 7: GNN Ensembling results

Modality	Model	Accuracy
dwMRI	GNN	88%
fMRI	GNN	75%
dwMRI, rsfMRI, T1-MRI	GNN Ensemble	90%

- A previous graph-based study [7] reported 73% accuracy with 109 subjects. In comparison, our proposed GNN ensemble achieved 90% accuracy on 233 subjects from the PPMI dataset, highlighting its superior performance.

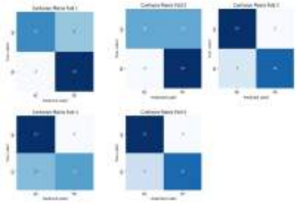

Figure 11: GNN Ensembling Confusion Matrices

Conclusion

- We proposed a multi-modal GNN ensembling framework leveraging structural (dwMRI) and functional (rsfMRI) brain networks, achieving 90% accuracy and surpassing previous CNN and GNN approaches for PD detection.
- **Future work:** extend to multiclass disease stages and integrate explainable AI methods.

References

1) Vathanakumar, M.; Ratnarajah, N. In 2024 Moratuwa Engineering Research Conference (MERCon), Moratuwa, Sri Lanka, 2024, pp 642–647.
2) A. Sajeeb and et al. "Parkinson's disease detection using FMRI images leveraging transfer learning on convolutional neural network". In: Proceedings - International Conference on Machine Learning and Cybernetics. IEEE Computer Society, 2020, pp. 131–136. doi: 10.1109/ICMLC51923.2020.9469530.
3) S. Yadav Babasaheb Ambedkar and S. Yadav. "Bayesian deep learning based convolutional neural network for classification of Parkinson's disease using functional magnetic resonance images".
4) N.U. Islam, R. Khanam, and A. Kumar. "Using 3D CNN for classification of Parkinson's disease from resting-state fMRI data". In: Journal of Engineering and Applied Science 70.1 (2023). doi: 10.1186/s44147-023-00236-2.
5) P. Patil and W.R. Ford. "Parkinson's Disease Recognition Using Decorrelated Convolutional Neural Networks: Addressing Imbalance and Scanner Bias in rs-fMRI Data". In: Biosensors 14.5 (2024). doi: 10.3390/bios14050259.
6) B. Majhi and et al. "An improved method for diagnosis of Parkinson's disease using deep learning models enhanced with metaheuristic algorithm". In: BMC Medical Imaging 24.1 (2024). doi: 10.1186/s12880-024-01335-z
7) A. Safai et al. "Multimodal Brain Connectomics-Based Prediction of Parkinson's Disease Using Graph Attention Networks". In: Frontiers in Neuroscience 15 (2022), p. 741489. doi: 10.3389/fnins.2021.741489.

|**ICAS2025**|

Electrocardiogram Signal Classification for Heart Disease Diagnosis with Deep Learning – A Sri Lankan Study

B.Ushanthika[1], S.Thirukumaran[1]

[1]Department of Physical Science, University of Vavuniya, Sri Lanka

Abstract: Heart disease remains a significant health concern worldwide, including in Sri Lanka, where timely and accurate diagnosis is crucial for improving patient outcomes. The 12-lead electrocardiogram (ECG) is a widely used, cost-effective tool for detecting cardiac abnormalities. This study presents a deep learning-based approach for classifying 12-lead ECG images into normal and not normal categories using a region-specific dataset collected from Jaffna Teaching Hospital in Sri Lanka. ECG records were digitized from printed paper using a mobile application that converts physical documents into high-quality digital images. The dataset was organized into three formats: scanned images, digitized signals in Comma-Separated Values format, and clean ECG traces without grid lines. The preprocessing pipeline focused on creating standard-sized 3×4 combined lead images through segmentation, binarization, and noise removal. These images served as inputs for convolutional neural network architectures such as ResNet-18, SqueezeNet1.1, MobileNetV2, EfficientNet-B1, and a custom BasicDenseNet. The Convolutional Neural Network models were trained end-to-end using 12-lead ECG image inputs. Each lead was treated as a separate channel, enabling the model to learn spatial and morphological dependencies across multiple leads. The network automatically extracted discriminative features such as waveform shapes, lead-specific variations, and inter-lead correlations that influenced the classification outcome. Models were trained and evaluated to optimize classification accuracy and generalization. Model performance was assessed using accuracy, precision, recall, F1-score, and confusion matrices to ensure balanced evaluation. ResNet-18 achieved the highest validation accuracy of 93%, followed by SqueezeNet1.1 at 90%. To enhance interpretability and clinical trust, Gradient-weighted Class Activation Mapping visualizations were used to identify discriminant ECG regions influencing predictions. These visualizations, reviewed by cardiographers, confirmed that the model focused on clinically relevant leads and waveform patterns. This study demonstrates the potential of combining deep learning with explainable AI to build reliable ECG classification systems. It highlights the effectiveness of deep learning for ECG-based abnormality detection, providing a scalable pipeline to aid early diagnosis of heart abnormalities in the Sri Lankan population.

Keywords: deep learning, digitization, ECG, explainable AI, Grad-CAM, Sri Lanka

Electrocardiogram Signal Classification for Heart Disease Diagnosis with Deep Learning – A Sri Lankan Study

B. Ushanthika [1*], S. Thirukumaran [2]

[1, 2] Department of Physical Science, Faculty of Applied Science, University of Vavuniya.

Introduction

- Heart disease remains a critical health issue in Sri Lanka, requiring early and accurate diagnosis.
- The 12-lead Electrocardiogram (ECG) is a cost-effective and widely used tool for detecting cardiac abnormalities.
- Explainable AI techniques were applied to highlight influential ECG regions, ensuring model transparency and clinical trust.
- ECG data from Jaffna Teaching Hospital was digitized, pre-processed, and standardized into image formats.
- Multiple Convolutional Neural Network(CNN) models were trained and evaluated to classify ECGs as normal or abnormal with improved accuracy.

Fig.1 Scanned ECG Image

Literature Review

Ref. No.	Dataset	Model	Accuracy
01	Mendeley Dataset	1D-CNN model	98.42%
02	Collected Dataset	A 3-layer dense model	97%
03	MIT-BIH Arrhythmia Database	2D-CNN Model	97.42%
04	PTB_XL	CNN SincNet CNN+Entrpy	88.2% 85.8% 89.82%
05	PhysioNet	AlexNet SqueezeNet Vgg16 InceptionV3 ResNet-18	84.38% 93.75% 87.50% 71.88% 81.25%

Objectives

- To develop a scalable pre-processing pipeline and train multiple CNN architectures for classifying paper-based ECG images.
- To evaluate model performance with comprehensive metrics while ensuring clinical relevance through real-world ECG format alignment.
- To integrate model explainability to localize clinically meaningful ECG segments and validate these highlights with cardiographers, improving interpretability and clinical trust.

Methodology

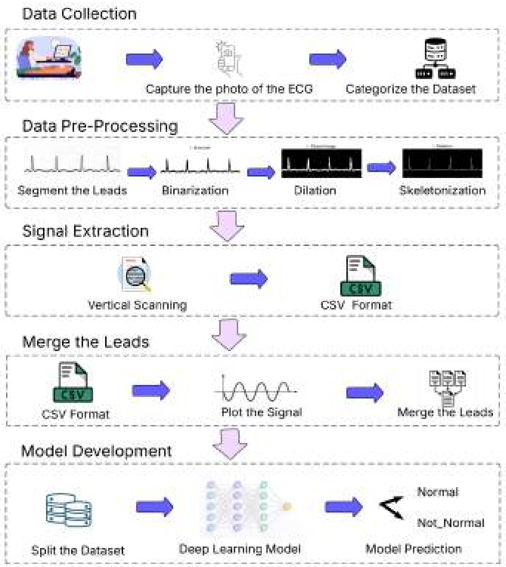

Fig.2 Overall workflow

- ECG scan images were collected from Jaffna Teaching Hospital and categorized into normal and not normal sets with guidance from cardiographers.
- Each ECG scan was manually segmented into 12 leads, converted to binary, processed with dilation, and skeletonized for cleaner signals.
- Vertical scanning was applied on skeletonized ECG traces to extract waveform points, which were then digitized and stored in Comma-Separated Values (CSV) format.
- Individual leads were reconstructed from CSV signals and combined into a standardized 3×4 grid image mimicking real-world ECG format.
- Five CNN architectures were trained and evaluated on the processed ECG images for accurate classification.

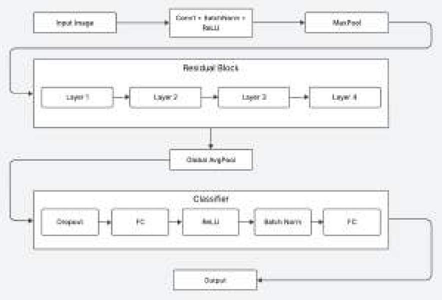

Fig.3 Architecture Diagram of ResNet-18

Results and Discussion

- CNN models achieved high accuracy in classifying ECG images as normal or abnormal.
- ResNet-18 demonstrated the best validation performance, with accuracy 93%.
- Evaluation metrics (precision, recall, F1-score) confirmed balanced and reliable model performance.
- the study highlights that deep learning-based ECG classification can significantly enhance early diagnosis and improve patient outcomes.

Model	Accuracy
ResNet-18	0.93
SqueezeNet1.1	0.90
EfficientNet-B1	0.90
MobileNetV2	0.86
BasicDenseNet	0.86

Table.1 Model Comparison Table

	Precision	Recall	F1-Score	Support
Normal	0.87	0.87	0.87	15
Not_Normal	0.87	0.87	0.87	15
Accuracy			0.87	30
Macro avg	0.87	0.87	0.87	30
Weighted avg	0.87	0.87	0.87	30

Table.2 Classification Report for ResNet-18

Fig.4 Confusion Matrix for ResNet-18

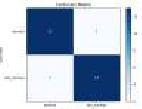

The dataset is balanced, and the model performs equally well on both classes.

Model Interpretability

- Grad-CAM visualizations, evaluated by cardiographers, highlighted abnormal ECG regions and confirmed reliable model focus.
- Explainable AI improves transparency and trust, supporting clinical adoption of deep learning models.

Fig.5 Grad-CAM visualization of important ECG areas

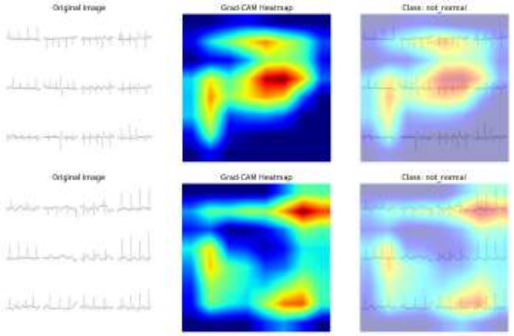

Conclusion

- Deep learning models effectively classify 12-lead ECGs as normal or abnormal.
- ResNet-18 showed the best validation performance.
- Explainable AI validated model focus and enhanced interpretability.
- The system demonstrates potential as a clinical decision-support tool.

References

[1] Nguyen, T.; Pham, H. H.; Le, K. H.; Nguyen, A.-T.; Thanh, T.; Do, C. Detecting COVID-19 from digitized ECG printouts using 1D convolutional neural networks. PLoS ONE 2022, 17, e0277081.

[2] Mishra, S.; Khatwani, G.; Patil, R.; Sapariya, D.; Shah, V.; Parmar, D.; Dinesh, S.; Daphal, P.; Mehendale, N. ECG Paper Record Digitization and Diagnosis Using Deep Learning. Journal of Medical and Biological Engineering 2021, 41, 422–432.

[3] Izci, E.; Ozdemir, M. A.; Degirmenci, M.; Akan, A. In 2019 IEEE (Conference Name Not Provided), 2019, pp 1–4.

[4] Śmigiel, S.; Pałczyński, K.; Ledziński, D. ECG Signal Classification Using Deep Learning Techniques Based on the PTB-XL Dataset. Entropy 2021, 23, 1121.

[5] Al-Fahoum, A. Enhanced Cardiac Arrhythmia Detection Utilizing Deep Learning Architectures and Multi-Scale ECG Analysis. Unknown Journal 2023, 44, 5539–5548.

|ICAS2025|

Assessing Heart Disease Risk in Patients with Anemia through Predictive Modeling

R.Thulashika[1], R.Elango[2]

[1]Department of Physical Science, University of Vavuniya, Sri Lanka
[2]Jaffna Teaching Hospital, Sri Lanka

Abstract: Cardiovascular diseases are one of the leading causes of death worldwide and anemia is a common condition marked by low hemoglobin levels. Despite its prevalence anemia is often overlooked even though it plays a significant role in increasing the risk of heart disease. This study aims to develop a predictive model to assess the heart disease risk in patients with anemia. For this research, hematological and cardiovascular data were collected from 800 Bed Head Tickets at Jaffna Teaching Hospital, Sri Lanka. The data included patients with heart failure, myocardial infarction and those without heart disease. Manual data collection is difficult and takes time so MIMIC database was chosen as a backup. It is a publicly available dataset containing deidentified patient details and supported the initial stages of model implementation. After completing the manual data collection we applied multiple machine learning algorithms along with two ensemble approaches to train the data. The ensemble combining Logistic Regression and Support Vector Machine (SVM) achieved the highest accuracy of 79.38% and ROC-AUC of 82.02% with strong performance in other metrics. The proposed model demonstrates strong potential for clinical application by enabling early detection of high risk anemia patients. This will help facilitate timely medical check ups and reduce the risk of heart complications.

Keywords: anemia, cardiovascular diseases, clinical application, ensemble model, hematological data, machine learning

Assessing Heart Disease Risk In Patients With Anemia Through Predictive Modeling

Thulashika Raveendran[1*], Elango Rasu[2]
[1] *Department of Physical Science, University of Vavuniya, Sri Lanka* , [2] *Jaffna Teaching Hospital, Sri Lanka*

Introduction

- **Cardiovascular disease** is a major health issue that includes heart attack and heart failure.
- **Anemia** is a blood disorder that lowers hemoglobin and reduces oxygen delivery increasing the **risk of heart disease**
- These two conditions are closely related but they have **complex link**.
- **Machine learning models** can identify complex patterns in data and enable **early detection.**

Objectives

- Develop a model to identify anemia patients at high risk of heart disease.
- Identify key hematological and cardiovascular indicators for heart disease risk prediction.

Methodology

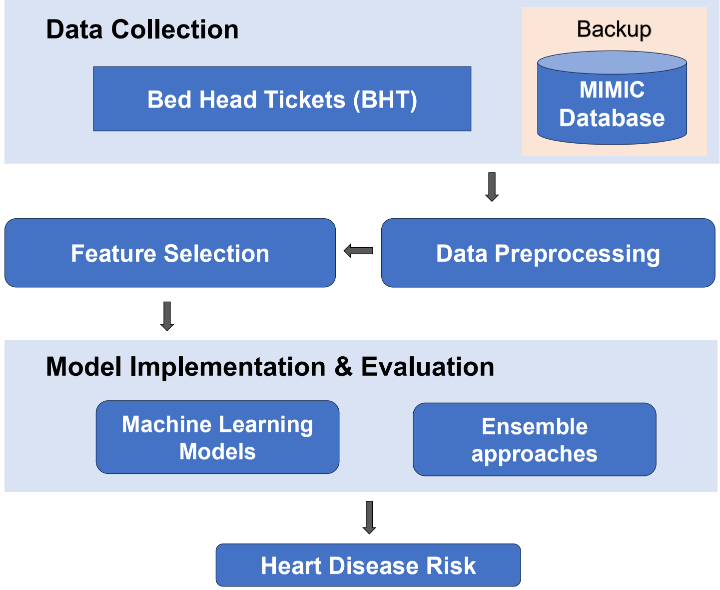

Data Collection

Bed Head Tickets (BHT)

Backup

MIMIC Database

Data Preprocessing

Feature Selection

Model Implementation & Evaluation

Machine Learning Models

Ensemble approaches

Heart Disease Risk

Dataset

- **Heart Failure & Myocardial Infarction Patients**
- **Non Heart Disease Patients**

12 Features

Table1:Data table

Hematological Parameters	Cardiovascular parameters
Hemoglobin(Hb) Red Blood Cells(RBC) Mean Corpuscular Volume(MCV) Mean Corpuscular Hemoglobin(MCH) Mean Corpuscular Hemoglobin concentration(MCHC) Hematocrit(HCT) Red Cell distribution width(RDW)	Diabetes : yes/ no Cholesterol :yes/no Blood Pressure :yes/no Age Gender

Results and Discussion

800BHTs

Selected Features:

RBC	Cholesterol
Hb	Blood Pressure
MCV	Diabetes
HCT	Age
RDW-CV	Gender

Top Performer **Logistic Regression-SVM Ensemble**

Accuracy	Precision	Recall	F1-Score	ROC-AUC
79.38%	80%	79%	79%	82.02%

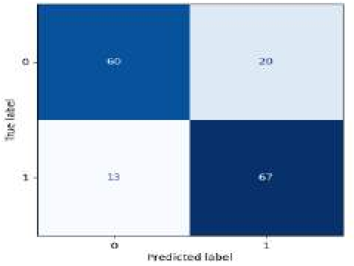

Figure1:Confusion Matrix

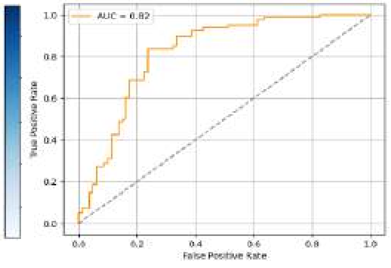

Figure2:ROC Curve

Conclusion

Simple Blood Tests and **Risk factors** with **Machine learning model** may help to assess heart disease risk in anemia patients.

References

[1] A. Minj and S. Mishra, “A study to correlate iron deficiency anemia with heart failure using hematological parameters and ECG,” 2021.

[2] L. Cheng et al, “An ensemble machine learning model for predicting one-year mortality in elderly coronary heart disease patients with anemia,”2024.

|ICAS2025|

Diagnosis of Acute Lymphoblastic Leukemia through White Blood Cell Segmentation from Multi-Microscope Imaging using Deep Learning

Thanushiga Chandrasegaram[1], W.R.G.A.D.P.Herath[1], S.Thirukumaran[1]

[1]Department of Physical Science, University of Vavuniya, Sri Lanka

Abstract: Acute Lymphoblastic Leukemia, as a severe type of blood cancer, can be characterized by the uncontrolled increase of white blood cells, and it is crucial to make an early and accurate diagnosis to provide effective treatment. The traditional method of using manual examination of peripheral blood smear slides is slow and very reliant on the expertise of the examiner, which introduces variability. To address this, this research introduces an interpretable deep learning method that integrates both the segmentation and classification of WBCs based on the images created by multi-microscopic scanner imaging to better reflect a real-world lab setting. A combined dataset was created using publicly available blood smear images and a custom LeukemiAttri dataset. Training of the segmentation model was done through manual annotation of preprocessed images. A refined Segment Anything Model was used as a robust method of WBC segmentation, achieving an average segmentation accuracy of 87%. The segmented cells have been subsequently grouped as healthy or leukemic on the basis of five deep learning models, namely DenseNet-169, DenseNet-121, VGG16, VGG19, and MobileNet, with DenseNet-169 reporting the best classification accuracy of 92%. Compared to previous single-scanner approaches, this multi-scanner framework achieved better generalization and higher accuracy, offering a practical solution for reliable automated leukemia detection in clinical practice.

Keywords: CNN classification, deep learning models, Leukemia diagnosis, multi-scanner datasets, segment anything model, WBC segmentation

ICAS2025

Faculty of Applied Science
University of Vavuniya

Diagnosis of Acute Lymphoblastic Leukemia through White Blood Cell Segmentation from Multi-Microscope Imaging using Deep Learning

Thanushiga Chandrasegaram[1*], W.R.G.A.D.P Herath[2], S.Thirukumaran[3]
[1,2,3]*Department of Physical Science, Faculty of Applied Science, University of Vavuniya*

Introduction

- Leukemia is a serious blood cancer caused by uncontrolled WBC growth; early detection is critical, but current manual PBS analysis is slow, subjective, and error-prone.
- Deep learning can automatically learn subtle features from PBS images to distinguish healthy and leukemic cells, though challenges remain with irregular shapes, inconsistent staining, and overlapping cells.
- Robust segmentation is essential to isolate nucleus shape and cytoplasm irregularity, which significantly improves classification accuracy and reliability.
- This research uses a segmentation-based deep learning system to handle scanner differences and improve accuracy and reliability in clinics

Aim and Objectives

Aim

Develop a deep learning method for accurate leukemia diagnosis using WBC segmentation from multi-scanner images.

Objectives

- Build a diverse multi-scanner dataset.
- Standardize and preprocess images with resizing and manual masks for quality segmentation input.
- Fine-tune the Segment Anything Model for WBC Segmentation.
- Classify segmented WBCs as healthy or leukemic using multiple deep learning models (DenseNet-169, DenseNet-121, VGG16, VGG19, MobileNet).

Previous Works

Ref.No.	Methodology	Source Of Data	Accuracy
1	ResNet	Self Annotated Dataset	92%
2	CNN	Utilized a dataset of blood cell images	96%
3	U-Net SVM	Public Repository	90%
4	CNN	Public Dataset	90%
5	CNN	Microscopic images annotated by medical experts	95%

Methodology

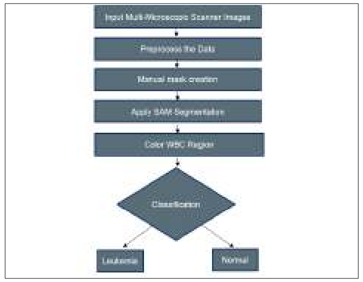

Workflow for WBC Segmentation and Classification

Dataset	Scanner Type	Camera Model	Resolution (Pixel)
ALL-IDB 	300x to 500x	Optical laboratory microscope with Canon PowerShot G5	2592 × 1944
Mehradaria Leukemia 	100x to 400x	Zeiss microscope	Not specified
LeukemiAttri 	100x to 600x	Three local lab scan ners (Scanner A, B, C) with varying optical systems	224× 224

Multi-Microscope Scanner Dataset

Pre-processing

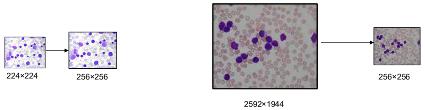

Manual Mask Creation

Used ImageJ to draw WBC masks for ground truth.

Segmentation

Dataset divided into training (80%) and validation (20%) - total 665 images. Segmentation was done using Segment Anything Anything(SAM) Model.

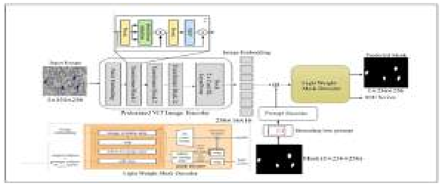

SAM Architecture

Classification

Data Splitting	Training	Testing
Leukemia	221	65
Normal	300	69

Data Augmentation

- Ensured at least 100 images per class to address class

Selected Architectures

1) VGG Net 2) DenseNet 3) MobileNet

Results and Discussion

Segmentation Results

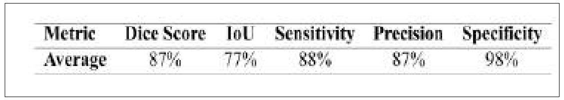

Metric	Dice Score	IoU	Sensitivity	Precision	Specificity
Average	87%	77%	88%	87%	98%

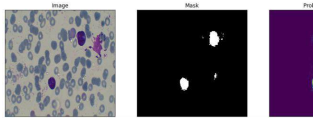

Image, mask, and probability map

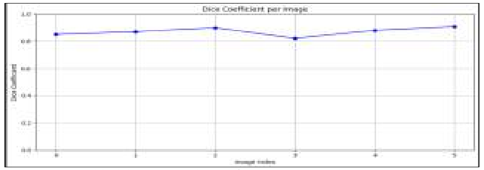

Model segmentation performance across images

Classification Results

CNN Models	Accuracy
DenseNet 169	92%
VGG 16	90%
VGG 19	72%
DenseNet 121	85%
MobileNet	84%

DenseNet 169

Accuracy Graph

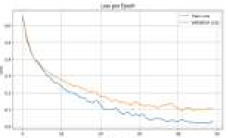

Loss Graph

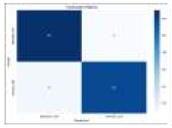

Confusion Matrix

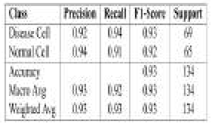

Class	Precision	Recall	F1-Score	Support
Disease Cell	0.92	0.94	0.93	69
Normal Cell	0.94	0.91	0.92	65
Accuracy			0.93	134
Macro Avg	0.93	0.92	0.93	134
Weighted Avg	0.93	0.93	0.93	134

Classification Report

Model	Accuracy With Segmentation (%)	Accuracy Without Segmentation (%)
DenseNet169	92	84
VGG16	90	82
DenseNet121	87	79
MobileNet	84	76
VGG19	72	65

- Five CNN models (DenseNet-169, DenseNet-121, VGG16, VGG19, MobileNet) showed higher accuracy with segmented WBC images compared to original images. Segmentation improved performance by 5–13%, with DenseNet-169 achieving the best accuracy (92%).
- The improvement came from segmentation removing background noise, staining variations, and overlapping cells, allowing models to focus on key WBC morphological features for better classification.

Conclusion

- Developed a deep learning framework for WBC segmentation and leukemia classification using multi-scanner image
- Fine-tuned SAM successfully segmented WBCs across varied imaging conditions.
- Classified cells with five models; DenseNet-169 gave the best accuracy.
- Multi-scanner data improved model generalization over single-scanner methods.

References

[1] Yan, G.; Mingyang, G.; Wei, S.; Hongping, L.; Liyuan, Q.; Ailan, L.; Xiaomei, K.; Huilan, Z.; Juanjuan, Z.; Yan, Q. Diagnosis and typing of leukemia using a single peripheral blood cell through deep learning. *Cancer Science* 2025, 116, 533–543.
[2] El-Seoud, M. S. A.; Siala, M. H.; McKee, G. Detection and Classification of White Blood Cells Through Deep Learning Techniques. *International Journal of Online En gineering (iJOE) 2020, 16, 93–105.*
[3] Rejula, M. A.; Jebin, B. M.; Selvakumar, R.; Amutha, S.; George, E. Detection of Acute Lymphoblastic Leukemia Using a Novel Bone Marrow Image Segmentation. *Tsinghua Science and Technology* 2025, 30, 610–623.
[4] Saleem,S.;Amin,J.;Sharif,M.;Anjum,M.A.;Iqbal,M.;Wang,S.-H.Adeepnetwork designed for segmentation and classification of leukemia using fusion of the transfer learning models. *Complex & Intelligent Systems* 2021, 7, 1–16.
[5] Raphael, R. T. Segmentation and Classification Techniques of Leukemia Using Image Processing: An Overview. *International Conference on Intelligent Sustainable Systems (ICISS)* 2019, 378–384

|ICAS2025|

Machine Learning Approaches to Discover Novel Biomarkers in Lung Cancer

M.Mithushika

Department of Physical Science, University of Vavuniya, Sri Lanka

Abstract: Lung cancer is one of the leading causes of cancer related deaths worldwide. For early diagnosis and better treatment, finding reliable biomarkers is essential. In lung cancer patients, certain genes identified as biomarkers, can be expressed at much higher or lower levels compared to normal. In previous studies, many methods have been used to find biomarkers. Most researchers rely on machine learning models, but there is still a gap in applying these approaches effectively for biomarker discovery. In this study, we developed a combined feature selection approach for transcriptomic data containing 20,000 genes' protein coding from different cell lines, from the publicly available Human Protein Atlas (HPA) dataset. Based on recent research, we applied eight suitable feature selection methods, such as Variance, ANOVA, Fisher's Score, Chi-squared, LASSO, Kruskal-Wallis, Mutual Information, and Standard Deviation, individually to the preprocessed data and selected the top 1000 important genes from each. From each method, the top 1000 genes were selected, and overlapping results were compared using visual analytics. Among these, Mutual Information, Chi-squared, and Fisher's Score showed more overlapping results. It led to the identification of six key genes, which are ANO10, CD63, FAS, PARVA, PHF11, and TMEM115. Interestingly, all six are associated with lung related diseases and immune functions, which strengthens their potential relevance in lung cancer. Among them, ANO10, CD63, FAS, PARVA, and TMEM115 have already been recognized in previous studies as lung cancer biomarkers, either being highly or under expressed, and our analysis further confirmed their roles through Gene Ontology (GO), Kyoto Encyclopedia of Genes (KEGG), and Reactome enrichment results.The exception is PHF11, which has not yet been reported as a lung cancer biomarker. Interestingly, previous studies have linked PHF11 mainly to immune regulation and asthma, both of which influence lung-associated inflammatory pathways. This observation aligns with recent insights that epigenetic alterations, such as DNA methylation, play crucial roles not only in tumorigenesis but also in immune modulation. In this way, our study not only reconfirmed several established biomarkers described in prior research but also highlighted PHF11 as a promising candidate that could bridge immune and epigenetic mechanisms in lung cancer. Our results demonstrate that by integrating multiple feature selection methods with biological validation, we can identify biomarkers that may have been overlooked, offering new possibilities for early detection and treatment in lung cancer.

Keywords: biomarkers, feature selection, gene expression, lung cancer, machine learning

MACHINE LEARNING APPROACHES TO DISCOVER NOVEL BIOMARKERS IN LUNG CANCER

Ms.M.Mithushika
Department of Physical Science, University of Vavuniya

Introduction

- Lung cancer is the leading cause of cancer related deaths worldwide.

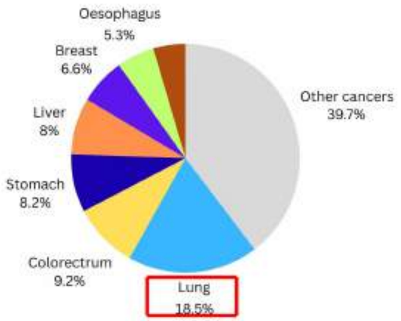

Source: GLOBOCAN 2018

- **Biomarkers** play a crucial role in improving early detection and enabling personalized treatments.
- Machine learning techniques provide efficient tools to analyze genomic data.

Objective

- Develop a **new pipeline** to find biomarkers
- Identify **novel biomarkers** for lung cancer

Data set

We used Human Protein Atlas (HPA) transcriptomic data

- 20,000 genes
- 1055 cell lines
- Transcriptomic values in Transcripts Per Million(TPM)

Methodology

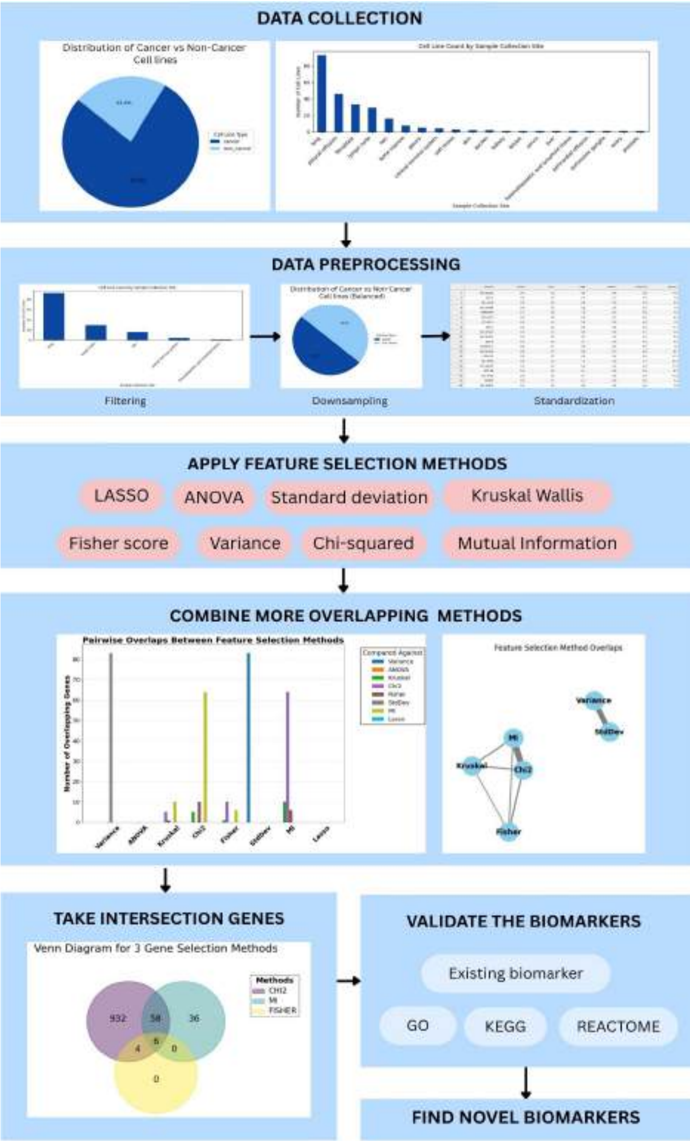

DATA COLLECTION

DATA PREPROCESSING

Filtering → Downsampling → Standardization

APPLY FEATURE SELECTION METHODS

LASSO, ANOVA, Standard deviation, Kruskal Wallis, Fisher score, Variance, Chi-squared, Mutual Information

COMBINE MORE OVERLAPPING METHODS

TAKE INTERSECTION GENES

VALIDATE THE BIOMARKERS

Existing biomarker, GO, KEGG, REACTOME

FIND NOVEL BIOMARKERS

Results and Discussion

- **Top overlapping genes :** ANO10, CD63, FAS, PARVA, TMEM115, PHF11
- Novel biomarker: **PHF11** (Linked with asthma and immune system)

Conclusion

- Combined feature selection method identified biomarkers
- PHF11 may be a novel biomarker
- Future work requires validation using independent dataset

References

[1] Xie Y. et al., “Early lung cancer diagnostic biomarker discovery by machine learning,” 2020.
[2] Jalili M. et al., “CentiServer: a comprehensive resource for centrality analysis,” *PLOS ONE*, 2016.
[3] Fangwei et al., “Functional enrichment validation of lung cancer biomarkers,” 2025.
[4] Sheng et al., “Validation of lung cancer biomarkers via enrichment analysis,” 2025.
[5] Abdelwahab O. A. et al., “Biomarker discovery in lung adenocarcinoma using feature selection,” 2022.

|ICAS2025|

Identifying Novel Diagnostic Biomarkers in Bladder Cancer

M.N.Fathima Nufla

Department of Physical Science, University of Vavuniya, Sri Lanka

Abstract: Bladder cancer remains a significant clinical challenge due to limitations in current diagnostic methods, which are invasive, costly, or lack sensitivity particularly for early-stage detection. This study aimed to identify novel transcriptomic biomarkers that enable non-invasive and accurate detection of bladder cancer using machine learning and bioinformatics approaches. Publicly available gene expression datasets from bladder tumor and normal tissues were analyzed using differential expression analysis and weighted gene co-expression network analysis (WGCNA) to identify genes within tumor-associated modules. From an intersection of 408 candidate genes, LASSO regression selected 21 potential biomarkers. These were further evaluated using cross-validation and model performance metrics, and an 11-gene diagnostic signature was prioritized based on consistent discriminatory power (AUC > 0.80) and biological relevance.The diagnostic performance of this signature was rigorously assessed using multiple machine learning classifiers, including Support Vector Machines, Artificial Neural Networks, and Random Forests, across three independent validation cohorts. The signature consistently achieved high area under the ROC curve (AUC) values ranging from 0.926 to 0.963, demonstrating strong cross-platform generalizability. To enhance biological and clinical interpretation, Shapley Additive Explanations (SHAP) were employed to highlight key genes contributing to tumor classification and to reveal their potential roles in tumor biology and immune microenvironment signaling.Overall, this study presents a biologically coherent, interpretable, and robust 11-gene transcriptomic signature for bladder cancer diagnosis. While the findings are derived from publicly available datasets, they provide a reproducible analytical framework and a promising foundation for future prospective validation and clinical translation toward non-invasive diagnostic testing.

Keywords: biomarkers, bladder cancer, LASSO, machine learning, SHAP

Identifying Novel Diagnostic Biomarkers in Bladder Cancer

MN. Fathima Nufla[1*]

[1]*Department of Physical Science, Faculty of Applied Science, University of Vavuniya, Sri Lanka*

Introduction

- Bladder cancer is the **10th most common cancer worldwide** (~573,000 cases/year).
- **High recurrence risk**: 50–80% in non-muscle invasive bladder cancer (NMIBC), progression to MIBC possible.
- **Current diagnosis**: cystoscopy (invasive, costly) + urine tests (low sensitivity for early-stage detection).
- **Unmet need**: reliable, **non-invasive biomarkers** for early and accurate diagnosis.
- **Transcriptomics (gene expression profiling)** reflects tumor biology → promising for biomarker discovery.

Objective

Primary Objective :

- Identify novel transcriptomic biomarkers for accurate bladder cancer diagnosis using machine learning techniques.

Secondary Objectives :

- Validate biomarkers across independent patient cohorts
- Perform comprehensive model interpretability analysis using SHAP
- Establish pathway for clinical translation

Methodology

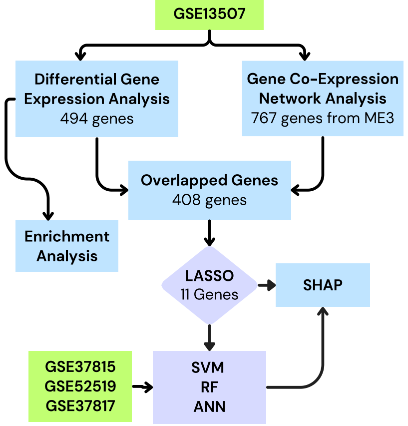

GSE13507

Differential Gene Expression Analysis
494 genes

Gene Co-Expression Network Analysis
767 genes from ME3

Overlapped Genes
408 genes

Enrichment Analysis

LASSO
11 Genes

SHAP

GSE37815
GSE52519
GSE37817

SVM
RF
ANN

Figure 1: Flow diagram of methodology

Datasets:
Training and validation: GSE13507 (255 samples)
Testing: GSE52519, GSE37815, GSE37817

Analysis:
DEG → WGCNA → 21 genes → Final 11 genes panel (AUC > 0.80)

Machine Learning Models:
SVM, RF, ANN

Interpretability:
SHAP analysis

Results and Discussion

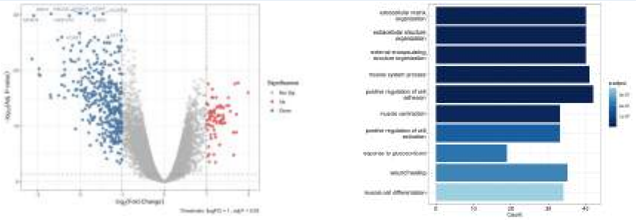

Figure 2 :Volcano plot tumor vs normal and GO BP enrichment (Bar plot)

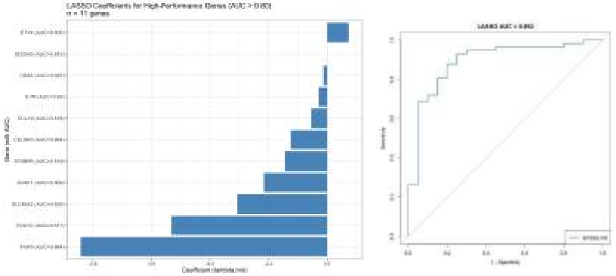

Figure 3 :LASSO coefficients and ROC curve for the LASSO model.

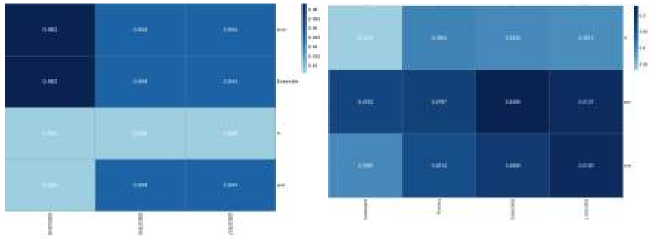

Figure 4 : Heat map of Model Performance and Model-Dataset SHAP Importance

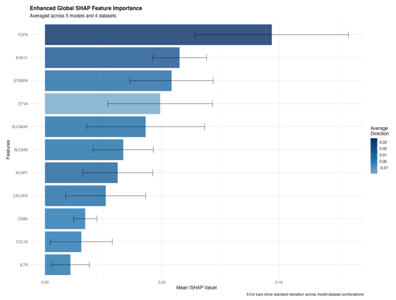

Figure 5 : Global SHAP importance (all models, all datasets).

494
DEGs

11
Final
Biomarker

11-Gene Signature:

CD8A 0.92	FGF9 0.88	ACAP1 0.87	CELSR3 0.86
IL7R 0.85	SLC9A9 0.84	SLC46A2 0.83	EVA1C 0.81
STXBP6 0.81	CCL19 0.81	ETV4 0.80	

Model Performance (AUC):

0.963	0.944	0.926
SVM (Best)	ANN Average	RF Average

SHAP Analysis Revealed :

- Top Contributors**:** FGF9, EVA1C, STXBP6, ETV4
- Stable Directionality **:** Most genes consistently tumor-associated
- Biological Coherence **:** Immune, transport, and signaling pathways

Cross-Platform Validation :

- Consistent high performance across three independent datasets demonstrates robust generalizability.

Functional Enrichment :

- Extracellular matrix organization, Cell adhesion processes, Immune system activation, Muscle system processes

Novel Findings :

- **6 genes** with prior bladder cancer links, **5 genes** emerging as novel diagnostic biomarkers,Strong immune microenvironment signatures

Conclusion

Successfully identified an 11-gene transcriptomic signature with high diagnostic accuracy (AUC 0.926-0.963) and robust cross-platform generalization.

Key Achievements :

- Network-aware discovery pipeline reducing false positives
- Parsimonious, interpretable biomarker panel
- Rigorous external validation across multiple cohorts
- Model explainability through SHAP analysis

Future Directions:

- Clinical assay development (qPCR/NanoString)
- Prospective multi-center validation
- Urine-based version for non-invasive testing
- Mechanistic validation of novel genes

References

1) **Abudurexiti, M., Xie, H., Jia, Z., et al. (2019).** Development and External Validation of a Novel 12-Gene Signature for Prediction of Overall Survival in Muscle-Invasive Bladder Cancer. *Frontiers in Oncology*, 9, 856.
2) **Statnikov, A., Wang, L., & Aliferis, C. F. (2008).** A comprehensive comparison of random forests and support vector machines for microarray-based cancer classification. *BMC Bioinformatics*, 9, 319.
3) **Lundberg, S. M., & Lee, S. I. (2017).** A unified approach to interpreting model predictions. *Advances in Neural Information Processing Systems*, 30, 4765-4774.

|ICAS2025|

Assessing GAN and VAE Augmentation Methods in Malignant Pleural Mesothelioma Prediction

M.A.Fathima Azka

Department of Physical Science, University of Vavuniya, Sri Lanka

Abstract: Malignant Pleural Mesothelioma (MPM) is a rare and aggressive cancer that is strongly associated with asbestos exposure. Its severity has led to growing research interest in finding effective solutions. In recent years, computational methods and machine learning approaches have been increasingly applied in oncology to classify tumor and normal samples using transcriptomic data. However, such models typically require large and balanced datasets to achieve robust performances, which are not available for rare cancers like MPM due to the very limited number of patients and under-representation of normal samples. This data scarcity poses a significant challenge in building predictive models that are reliable and generalizable. To address this limitation, we employ computational analysis with data augmentation as a strategy to increase the effective sample size. Specifically, we evaluate two deep generative models, Generative Adversarial Networks (GANs) and Variational Autoencoders (VAEs) to generate synthetic tumor and normal samples. Importantly, synthetic samples were used strictly in the training process, while test sets contained only real data, ensuring no data leakage during evaluation. To validate the augmentation strategy, a comparative evaluation framework was introduced using both the naturally imbalanced MPM dataset and an originally balanced breast cancer dataset, which is further manipulated to simulate imbalance, resulting in four experimental conditions: original balanced data, artificially imbalanced data, GAN-augmented data, and VAE-augmented data. Classification is performed using Support Vector Machines (SVM) and Random Forests (RF), and model performance is assessed through accuracy, F1 score, precision, recall, and ROC AUC. In addition, Principal Component Analysis (PCA) and t-Distributed Stochastic Neighbor Embedding (t-SNE) are applied to visually examine the quality and separability of synthetic data. The results show that GAN-based augmentation consistently improves classification performance more than VAE-based augmentation, particularly under imbalanced conditions. For instance, in the imbalanced breast cancer setting, GAN improved SVM accuracy by 5.6% and recall by 7.1% compared to the baseline without augmentation. In MPM, performance gains were smaller due to high baseline separability, indicating a ceiling effect. Overall, GAN achieved a mean performance score of 0.9247, compared to 0.9081 for VAE. This study presents a reproducible computational pipeline for benchmarking generative models in transcriptomics, and demonstrates that augmentation can effectively mitigate class imbalance in cancer prediction, while highlights the importance of dataset specific characteristics. The findings also motivate further research into hybrid generative architectures and biologically grounded validation strategies in precision oncology.

Keywords: breast Cancer, generative adversarial networks, Malignant Pleural Mesothelioma, random forests, support vector machines, variational autoencoders

Assessing GAN and VAE Augmentation Methods in Malignant Pleural Mesothelioma Prediction

MA. Fathima Azka[1]*
[1]Department of Physical Science, Faculty of Applied Science, University of Vavuniya, Sri Lanka

Introduction

- **Malignant Pleural Mesothelioma**:
  - Rare, aggressive, asbestos-linked cancer.
  - Long latency (>30 years), late diagnosis (median survival ~12 months).
  - Public datasets are **imbalanced**, limiting reliable prediction and making ML models biased toward the majority class.
- **Significance**: Demonstrates generative models as powerful tools for **rare cancer prediction**, with clinical implications for early detection and personalized treatment.

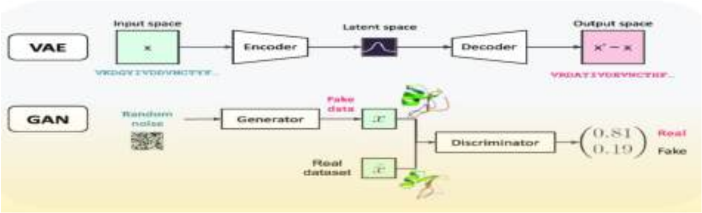

Figure 1 : Architecture of VAE and GAN

Objective

- Evaluate GAN and VAE for augmentation in bioinformatics
- Improve MPM predictive accuracy using augmentation
- Validate the model for imbalanced dataset

Methodology

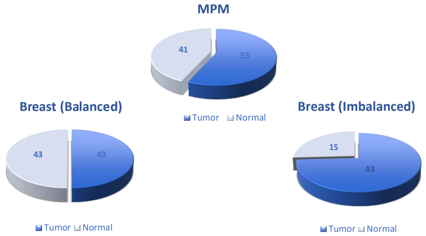

Figure 2 : Summary of Datasets

Experimental Settings:
- Original balanced data.
- Original imbalanced data.
- Artificially imbalanced data.
- GAN-augmented data.
- VAE-augmented data.

Classifiers: SVM, Random Forest.
Evaluation Metrics: Accuracy, F1-score, Precision, Recall, ROC-AUC.
Validation: PCA & t-SNE for synthetic data realism.

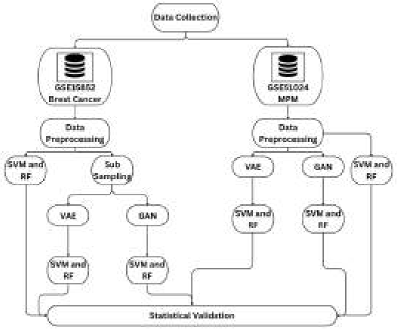

Figure 3 : Flow Diagram of Methodology

Results and Discussion

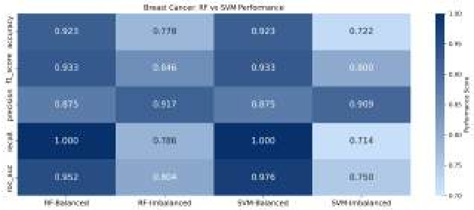

Figure 4 : Heat map Comparison of classifier performance between the original balanced and artificially imbalanced Breast Cancer datasets

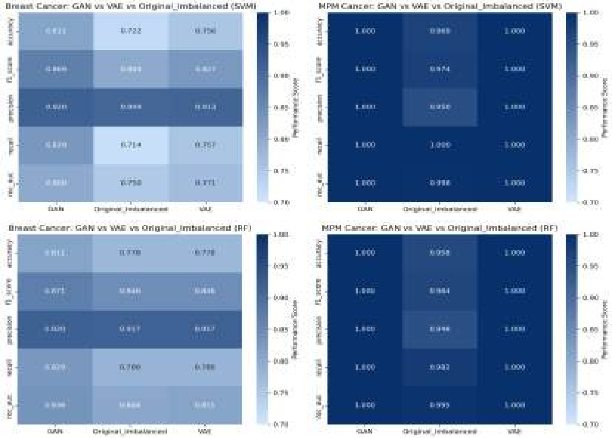

Figure 5 : Heatmap of mean metric scores for Original, GAN augmented, and VAE augmented datasets

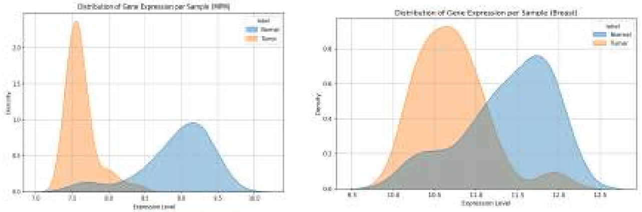

Figure 6 : Baseline distribution analysis of MPM and Breast cancer

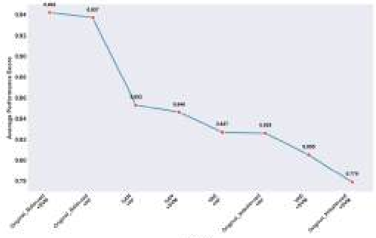

Figure 7 : Method ranking plot for Breast Cancer dataset

GAN vs VAE:
- GAN consistently improved classifier performance, especially under imbalance.
- In breast cancer (imbalanced), SVM showed +5.6% accuracy, +7.1% recall gain with GAN.
- In MPM, improvements smaller due to near perfect baseline separability.

Overall Performance:
- GAN mean score: **0.9247**
- VAE mean score: **0.9081**

Statistical Validations:
- Effect sizes were medium to large across all metrics for breast cancer in both classifiers.
- Consistency analysis showed high stability across all evaluation metrics, confirming that the results are robust and not dependent on random initialization.

Conclusion

- **GAN outperformed VAE** in augmenting transcriptomic datasets.
- Greatest benefit under class imbalance, enhancing minority class detection.
- Establishes reproducible pipeline for synthetic data benchmarking.
- **Implication**: Supports early detection strategies for rare cancers and robust machine learning pipelines in precision oncology.
- **Future Work**: Explore hybrid GAN-VAE models, integrate biological priors, and extend validation to multi omics datasets.

References

[1] C. Kwon, S. Park, S. Ko, and J. Ahn, “Increasing prediction accuracy of pathogenic staging by sample augmentation with a GAN,” *PLOS ONE*, vol. 16, ed. by P. Pławiak, e0250458, 2021.

[2] B. Karlberg, R. Kirchgaessner, J. Lee, M. Peterkort, L. Beckman, J. Goecks, and K. Ellrott, “SyntheVAEiser: augmenting traditional machine learning methods with VAE-based gene expression sample generation for improved cancer subtype predictions,” *Genome Biology*, vol. 25, 2024, doi: 10.1186/s13059-024-03431-3.

|**ICAS2025**|

Removal of Total Hardness from Surface water using Chemical Softening Techniques

S.Pirapakaran[1], S.Saravanan[2], S.Devaisy[1]

[1]Department of Bio Science, University of Vavuniya, Sri Lanka
[2]National Water Supply and Drainage Board, Vavuniya, Sri Lanka

Abstract: Water hardness, primarily caused by dissolved calcium and magnesium ions, is a common significant challenge in surface water sources, leading to scale formation and operational issues in both domestic and industrial systems. Conventional softening methods typically employ calcium hydroxide ($Ca(OH)_2$), sodium hydroxide (NaOH), and sodium carbonate (Na_2CO_3) to precipitate hardness-causing ions. In this study, the combined use of lime ($Ca(OH)_2$) and Polyaluminium Chloride (PACL) was investigated to enhance hardness removal through a series of controlled jar tests. Surface water samples collected from the Per Aru reservoir exhibited total hardness levels ranging from 120 to 400 mg/L, determined by EDTA titration. Six parallel experiments were performed using a constant lime dose sufficient to achieve pH 10.5, followed by varying PACL dosages. The experimental procedure involved rapid mixing at 250 rpm for 1 minute, followed by slow mixing at 40 rpm for 10 minutes, further mixing at 10 rpm for 10 minutes, and finally 10 minutes of settling. Lime addition effectively raised the pH to promote precipitation of calcium and magnesium, while subsequent PACL dosing improved flocculation and particle settling. Results revealed that hardness removal efficiency was strongly influenced by pH, lime dose, PACL concentration, and the timing of PACL addition. The maximum hardness reduction (66.7%) was achieved with lime at pH 10.5 combined with 28.5 ppm PACL addition. However, higher PACL doses reduced the final pH from 10.5 to 8.46, thereby suppressing precipitation. Overall, the study demonstrates that optimizing the balance between lime and PACL dosages is essential for achieving hardness and turbidity removal in a cost-effective manner, offering practical guidance for surface water treatment applications.

Keywords: flocculation, hardness, softening, surface water, turbidity

Removal of Total Hardness from Surface Water Using Chemical Softening Techniques

S. Pirapakaran[1*], S. Saravanan[1], S. Devaisy[2]
[2]*Faculty of Applied science, University of Vavuniya, Sri Lanka.*
[1]*National Water Supply and Drainage Board, Vavuniya, Sri Lanka.*
(** Corresponding author*)

Abstract

Water hardness caused by calcium and magnesium leads to scaling and treatment challenges. This study tested lime [$Ca(OH)_2$] with PACL on Per Aru reservoir water (120–400 mg/L hardness) using jar tests. Lime was added until pH 10.5 was reached, followed by varying PACL doses. The optimum was 28.5 ppm PACL, achieving 66.7% removal. Lime–PACL proved effective and low-cost.

Introduction

Rising hardness in the Per Aru reservoir poses health and scaling challenges in drinking water. This study presents a low-cost treatment using lime and PACL, where lime removes temporary hardness through precipitation and PACL improves overall removal efficiency.

$$Ca(HCO_3)_{2()} + Ca(OH)_{2(aq)} \longrightarrow 2CaCO_{3(s)} + 2H_2O_{(l)}$$

$$Mg(HCO_3)_{2(s)} + Ca(OH)_{2(aq)} \longrightarrow Mg(OH)_{2(s)} + 2CaCO_{3(s)} + 2H_2O_{(l)}$$

Objective

- To evaluate cost-effective chemical treatments for hardness removal.
- To assess lime performance at varying pH.
- To study the influence of PACL dosage and addition time.
- To identify the most suitable method for Per Aru water treatment.

Methodology

Surface water were collected

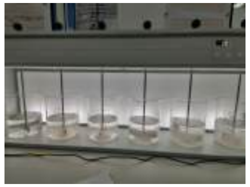

Jar test

Hardness test

Surface water from the Per Aru reservoir, Vavuniya, was tested using jar experiments with Na_2CO_3, NaOH, lime, and lime–PACL. Parameters such as pH, EC, turbidity, hardness, Ca^{2+}, and Mg^{2+} were measured. The study varied pH, PACL dosage (14–85 ppm), and addition time to evaluate hardness, calcium, magnesium, and turbidity removal efficiency.

Results and Discussion

Before and after treatment

Lime achieved 57% hardness removal at pH 10, while the lime–PACL combination (pH 10.5, 28.5 ppm PACL) reached 66.7% removal with turbidity below 2 NTU. Excess PACL reduced efficiency due to pH drop, and the best results occurred when PACL was added after 20 minutes, showing this method as a low-cost option for surface water softening.

Conclusion

Lime combined with PACL offers an effective, low-cost solution for hardness removal from surface water. Optimum performance was achieved with lime at pH 10.5 and 28.5 ppm PACL at pH 10.5. This method balances hardness and turbidity removal, making it suitable for application in regional water treatment plants.

References

WHO (2017). Sri Lanka.
Edzwald (2011). Coagulation in Water Treatment.
Guidelines for Drinking Water Quality.
Kausley et al. (2022). Chemical Softening Methods for Hardness Removal.
Piyasiri & Senanayake (2016). Water Quality in Dry Zone .

|ICAS2025|

Rainfall and Extreme Rainfall Trend Analysis in the Malwathu Oya River Basin, Sri Lanka: A 40-Year Assessment (1985–2024)

T.Vinith Steeban[1], R.Lakshan[2], T.Keerthanaram[2]

[1]State Key Laboratory of Tropical Oceanography, South China Sea Institute of Oceanology, University of Chinese Academy of Science, Guangzhou, China
[2]Department of Bio Science, University of Vavuniya, Sri Lanka

Abstract: The Malwathu Oya river basin, Sri Lanka's second-largest watershed, covering 10,500 km^2, lacks a comprehensive rainfall and extreme rainfall trend analysis, despite its critical importance for water resource management and climate adaptation planning. We address this knowledge gap by systematically assessing long-term precipitation patterns and extreme rainfall trends in this climatically sensitive dry zone basin. This research analyzed 40 years (1985–2024) of daily precipitation data from the CHIRPS v2.0 satellite dataset at 0.1° resolution across 25 strategically distributed locations throughout the basin. Statistical analyses included Mann–Kendall trend tests for non-parametric trend detection, Sen's slope estimator for quantifying trend magnitude, extreme value analysis using the Generalized Extreme Value (GEV) distribution, monsoon onset/withdrawal analysis using the pentad method, and assessment of the Precipitation Concentration Index (PCI). The basin was divided into upper, middle, and lower zones for spatial pattern analysis.Significantly increasing trends in annual rainfall were observed at all 25 locations ($p < 0.05$), with Sen's slope estimates ranging from 8.47 to 13.69 mm yr^{-1}. Spatially, the lower basin exhibited the strongest trends (11.0–12.3 mm yr^{-1}), followed by the upper basin (9.6–11.7 mm yr^{-1}) and middle basin (8.5–10.8 mm yr^{-1}). The Southwest monsoon contributed most significantly to annual increases (2.1–3.8 mm yr^{-1}), while the Northeast monsoon showed moderate increases (1.8–3.2 mm yr^{-1}). Extreme rainfall analysis revealed an intensification of daily maximum events, with 23 out of 25 locations showing increasing trends in annual maximum rainfall. Return period analysis indicated that 10-year extreme events now occur with 6–8 year frequencies. Monsoon timing remained relatively stable, with the Southwest monsoon onset occurring around early May and the Northeast monsoon onset in mid-October. PCI values (13.95–16.37) indicated moderate to irregular precipitation concentration patterns, with higher irregularity in upper and lower basin areas.Using satellite-based observational data, this study provides the first comprehensive evidence of significant rainfall intensification across the Malwathu Oya basin over the past four decades. The basin-wide increasing trends, coupled with the intensification of extreme events and spatial variability, indicate clear impacts of climate change on regional precipitation regimes. Annual rainfall has increased by approximately 14% across the basin, with particularly pronounced changes in the characteristics of extreme events. These findings have critical implications for water resource management, flood risk assessment, and agricultural planning, necessitating adaptive strategies for reservoir operations, early warning systems, and climate-resilient development planning. The results fill a critical knowledge gap in Sri Lankan hydro-climatology and provide essential baseline information for evidence-based climate adaptation and sustainable water resource management in one of the country's most important river basins. The documented trends support regional climate change projections and highlight the urgent need for adaptive management strategies in water-stressed dry zone environments.

Keywords: climate change, extreme precipitation, Malwathu Oya basin, Mann-Kendall analysis, monsoon variability, rainfall trends

Rainfall and Extreme Rainfall Trend Analysis in the Malwathu Oya River Basin, Sri Lanka: A 40-Year Assessment (1985-2024)

Vinith Steeban. T.[1*], Lakshan.R.[2], Keerthanaram. T.[2]

[1]State Key Laboratory of Tropical Oceanography, South China Sea Institute of Oceanology, University of Chinese Academy of Science, Guanzhou, People's Republic of China
[2]Department of Bio-science, Faculty of Applied Science, University of Vavuniya, Sri Lanka

Abstract

A 40-year analysis of Sri Lanka's Malwathu Oya basin reveals significant rainfall intensification, with annual precipitation increasing by approximately 14% basin-wide. The study identifies stronger increasing trends in the lower basin and a pronounced intensification of extreme rainfall events, indicating clear climate change impacts. These findings are critical for updating water resource management, flood risk assessment, and climate-resilient agricultural planning in this vital dry zone watershed.

Introduction

- The Malwathu Oya basin is Sri Lanka's second-largest watershed, a vital lifeline for the country's dry zone [1]
- Despite its importance, a critical knowledge gap exists: a comprehensive, basin-wide analysis of long-term rainfall trends has been absent.
- Current water infrastructure and agricultural practices are based on historical climate assumptions.
- accelerating climate change, understanding how precipitation patterns are shifting is essential for building resilience.[2]
- This study addresses this urgent need by conducting the first systematic investigation into four decades of rainfall patterns, trends, and extremes

Objective

- Quantify long-term (1985-2024) rainfall trends in Malwathu Oya River basin
- Analyze spatial patterns (upper, middle, lower basin) of Malwathu Oya
- Assess extreme rainfall and monsoon timing changes during last 40 years

Methodology

- Data: 40 years of CHIRPS v2.0 satellite data (0.1° resolution) at 25 locations [3]
- Trend Analysis: Mann-Kendall test; Sen's Slope
- Extremes: Generalized Extreme Value (GEV) distribution for return periods [4]
- Indices: Pentad method (monsoons), Precipitation Concentration Index (PCI)

Results and Discussion

- Universal positive trends: All 25 locations show significant annual increases
- Spatial heterogeneity: Lower basin (11.64 mm/yr) > Upper basin (10.51 mm/yr) > Middle basin (9.73 mm/yr)
- Extreme events: Enhanced intensity and frequency across most locations
- Seasonal patterns: Inter-monsoon periods driving annual increases
- Monsoon timing: Remarkable stability despite intensity changes
- PCI analysis: Moderate to irregular precipitation concentration patterns

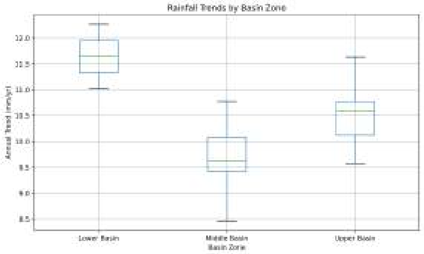

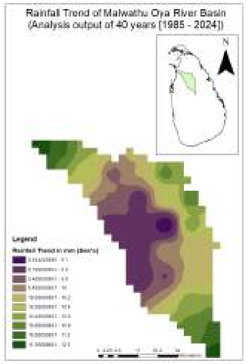

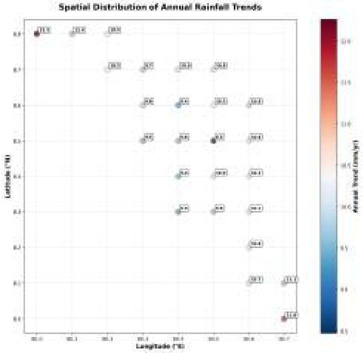

Conclusion

- Clear climate change signal with all the locations showing an increase in annual rainfall of ~14%
- Increased flood risk due to more intense extremes
- Urgent adaptive strategies for agriculture and disaster planning

References

[1] Fors, A. (2022). Improved understanding of water balance in the Malwathu Oya River basin using SWAT and remote sensing.

[2] Bastiaansen, R., Doelman, A., Eppinga, M. B., & Rietkerk, M. (2020). The effect of climate change on the resilience of ecosystems with adaptive spatial pattern formation. Ecology letters, 23(3), 414-429.

[3] Arachchillage, J. G. S. T. (2020). Process based modelling of future variations in river flows and fluvial sediment supply to coasts due to climate change and human activities: Data poor regions.

[4] Huang, W. K., Stein, M. L., McInerney, D. J., Sun, S., & Moyer, E. J. (2016). Estimating changes in temperature extremes from millennial-scale climate simulations using generalized extreme value (GEV) distributions. Advances in Statistical Climatology, Meteorology and Oceanography, 2(1), 79-103.

|ICAS2025|

Developing a Carbon Neutrality Roadmap for the University of Vavuniya: A Step Towards a Climate-Smart University

A.Aneeqa[1], S.Vijitharan[1]

[1]Department of Bio Science, Faculty of Applied Science, University of Vavuniya

Abstract: This study aims to present a carbon neutrality roadmap for the University of Vavuniya, to make it a climate-smart institution. The research focused only on carbon dioxide (CO_2) emissions, excluding other greenhouse gases, from university-owned vehicle fuel consumption (Scope 1) and purchased electricity (Scope 2). Emissions were estimated using the IPCC (2006) Tier 2 guidelines, applying nationally relevant emission factors derived from IPCC and national energy reports. Significant findings of this study are as follows: In 2024, emissions from purchased electricity were measured at 351.69 tonnes CO_2 (88.74%) and fuel use by university vehicles at 42.93 tonnes CO_2 (10.88%), totaling 394.62 tonnes CO_2. These findings confirm that Scope 2 emissions are the dominant contributor to the university's carbon footprint. The per-person emission, based on registered students and academic and non-academic staff, was 0.12 tonnes CO_2. A seven-year analysis (2018–2024) of electricity emissions showed temporal variations and helped identify pathways to reduce emissions. Remote sensing and biomass methods were used to estimate forest carbon stored on campus (2024), which amounted to 4,086.27 tonnes CO_2. With its substantial carbon stock, the campus forest demonstrates a significant capacity to offset emissions, highlighting the university's potential to serve as an effective carbon sink. The study faced challenges, including limited electronic data (with most records in hard copy) and time constraints. It is recommended to expand renewable energy capacity, building upon the existing 251 kW solar photovoltaic system, to enhance energy efficiency, promote sustainable transportation, and strengthen carbon management frameworks. The proposed roadmap emphasizes progressive reductions in carbon emissions while leveraging the potential for carbon removal, aiming to achieve carbon neutrality and establish the University of Vavuniya as a model for climate-smart higher education in Sri Lanka.

Keywords: carbon emission accounting, carbon neutrality, climate-smart university, renewable energy

Developing a Carbon Neutrality Roadmap for the University of Vavuniya
A Step Towards a Climate-Smart University

Aneeqa. A1[1*], Vijitharan. S 2[2]

[1,2] Department of Bio-science, Faculty of Applied Science, University of Vavuniya, Sri Lanka

Abstract

This study develops a carbon neutrality roadmap for the University of Vavuniya by quantifying emissions from purchased electricity (Scope 2) and university-owned vehicles (Scope 1). In 2024, total emissions were 394.62 tCO_2, dominated by electricity use (88.74%). The campus forest's carbon stock was 4,086.27 tCO_2, demonstrating high offset potential. The study recommends expanding renewables and sustainable practices to achieve carbon neutrality

Introduction

- ❖ Climate change presents urgent challenges, and universities play a crucial role.
- ❖ offers the first systematic assessment of the University of Vavuniya's carbon footprint.
- ❖ By focusing on direct (Scope 1) and indirect (Scope 2) emissions, and proposes strategies for achieving carbon neutrality.

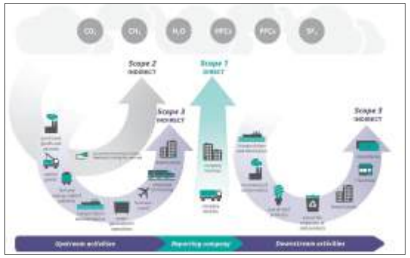

Overview of GHG Protocol scopes and emissions across the value chain (Environmental Protection Agency, 2025)

Objective

- To quantify the carbon emissions from electricity and fuel consumption by university-owned vehicles.
- To analyse and evaluate the effectiveness of existing energy and fuel management practices at the university.
- To propose a carbon neutrality roadmap integrating mitigation strategies and policies

Methodology

(1) Data collection

University-owned vehicle fuel data (2024)

Institutional electricity record (2018-2024)

▼

(2) Emission Calculation

$Emission\ (kgCO_2) = Activity\ Data \times Emission\ factor$ (IPCC 2006 Tier 2)

▼

(3) Forest carbon estimation(2024)

NDVI → Forest area → Biomass → Carbon stock (Vijitharan *et al.*, 2022)

$$Total\ forest\ carbon\ stocks\ (Mg\ C) = Area\ of\ forest\ cover\ (ha) \times Carbon\ stocks\ (MgC\ ha^{-1})$$

▼

(4) Net Carbon Balance

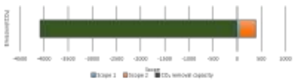

Results and Discussion

- **Total Emissions (2024):** 394.62 tCO_2
  Purchased Electricity (Scope 2): 351.69 tCO_2
  University-owned Vehicle Fuel (Scope 1): 42.93 tCO_2
- **Campus Forest Carbon Stock:** 4,086.27 tCO_2
- **Scenario Analysis:** Progressive 10% annual reduction with 3% annual stock increment could achieve neutrality in 2036

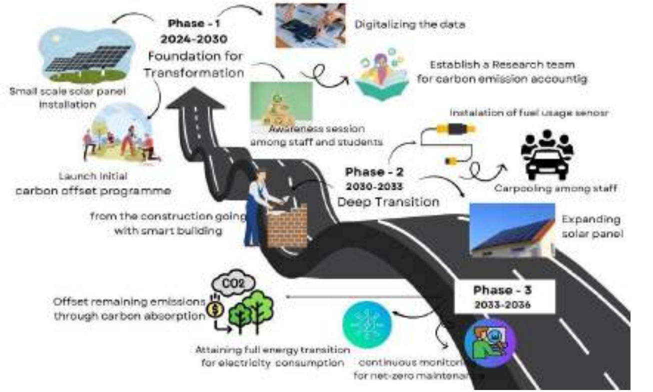

Conclusion

Electricity consumption is the primary source of emissions, while the university forest offers significant offset potential. Through the proposed Phases 1–3 transition plan, including activities such as expanding renewable energy systems, installing fuel consumption sensors, and introducing engaging initiatives like Green Certificates for the lowest-emission faculty and drivers, the University of Vavuniya can achieve carbon neutrality, transforming from foundation to full transition into a climate-smart, zero-carbon institution.

References

- IPCC (2006). *Guidelines for National Greenhouse Gas Inventories*.
- Oxford University Saïd Business School, & Oxford University Estates Services. (2022, April)
- Herth, A., & Blok, K. (2021). Quantifying universities' direct and indirect carbon emissions: The case of Delft University of Technology. *University Carbon Footprint*

|ICAS2025|

Allometric Estimation of Above-Ground Biomass for Selected Tree Species of the University of Vavuniya

L.A.N.N.Liyanaarachchi[1], S.Vijitharan[1]

[1]Department of Bio Science, University of Vavuniya, Sri Lanka

Abstract: Forest ecosystems play a vital role in carbon sequestration, helping mitigate the effects of climate change. However, urban and institutional green spaces, which also serve as potential carbon sinks, are often overlooked in carbon stock assessments. This study aims to estimate the above-ground biomass (AGB) and carbon stock of dominant tree species within the University of Vavuniya to assess their contribution to local climate mitigation. This study assessed the biomass of selected dominant tree species within the academic area (24 ha) of the University of Vavuniya, Pampaimadu premises. Biomass was determined by non-destructive methods. Four species were selected for the study, comprising two native and two exotic species, based on their dominance in the area. *Azadirachta indica*, *Bauhinia racemosa*, *Tectona grandis*, and *Mangifera indica* were the selected tree species. Measurements included Diameter at Breast Height (DBH), height, and GPS locations. Biomass was estimated using allometric equations. A total of 644 trees from the selected species were recorded, with 539 native and 105 exotic trees. Among the selected species, *Azadirachta indica* was the most dominant across the area. The total biomass of the study area was estimated at 433.17 Mg, comprising 329.97 Mg of above-ground biomass and 103.20 Mg of below-ground biomass. The average biomass per tree was highest for *Bauhinia racemosa* (1.18 Mg/tree), followed by *Tectona grandis* (0.67 Mg/tree), *Azadirachta indica* (0.48 Mg/tree), and *Mangifera indica* (0.33 Mg/tree). The corresponding average carbon stock values were *Bauhinia racemosa* (0.55 Mg C/tree), *Tectona grandis* (0.31 Mg C/tree), *Azadirachta indica* (0.22 Mg C/tree), and *Mangifera indica* (0.15 Mg C/tree). Comparison among species showed that native trees, particularly *Bauhinia racemosa* and *Azadirachta indica*, contributed substantially more to total biomass and carbon stock than the exotic species. In terms of total biomass, *Bauhinia racemosa* (208.31 Mg) contributed the most, followed by *Azadirachta indica* (172.93 Mg), *Tectona grandis* (33.59 Mg), and *Mangifera indica* (18.32 Mg). The results provide baseline information for future carbon monitoring and contribute to the University of Vavuniya's efforts to promote a carbon-neutral campus. These findings can also inform urban greening and climate adaptation strategies in institutional landscapes.

Keywords: allometric equations, biomass estimation, climate change mitigation

ICAS 2025

Faculty of Applied Science
University of Vavuniya

Allometric Estimation of Above-Ground Biomass for Selected Tree Species of the University of Vavuniya

L A N N Liyanaarachchi[1*], S Vijitharan[2]
Department of Bio-science, Faculty of Applied Science, University of Vavuniya

Abstract

Climate change driven by rising CO_2 emissions highlights the importance of trees as carbon sinks. Urban and institutional forests remain underexplored in carbon research. This study estimates aboveground biomass (AGB) in the University of Vavuniya, Using allometric equations, particularly *Bauhinia racemosa* and *Azadirachta indica*, stored higher carbon, highlighting their importance in campus sustainability and climate mitigation.

Introduction

CO_2 Emissions ↑
→ Climate Change Intensifies 🌍
→ Need for Effective Mitigation Strategies ⚙
→ Trees Act as Carbon Sinks 🌳
→ Store Carbon in Biomass & Support Ecosystems 🌿
→ University Green Spaces = Potential Carbon Reservoirs 🏫
→ Dry Zone Campuses in Sri Lanka Understudied
→ University of Vavuniya Has Diverse Tree Species 🌾
→ But Biomass Data Lacking ❌
→ This Study Estimates Tree Biomass Using Allometric Methods 📏
→ Provides Baseline Data for Climate Action & Sustainable Campus Planning 🌍

Objective

To estimate the above-ground biomass of selected tree species within the University of Vavuniya premises

Methodology


Figure 1- Study zones

🗺 Study Area Selection
⬇
📍 Division into 5 Zones
⬇
🌳 Species Selection
(*Azadirachta indica, Mangifera indica, Bauhinia racemosa, Tectona grandis*)
⬇
📏 Field Measurements
{DBH (≥10 cm), Height (trees <3 m excluded}
⬇
Biomass Estimation
(Using species-specific allometric equations)
⬇
☁ Carbon Stock Calculation
(Using carbon fraction: 0.47 × biomass)
⬇
📊 Data Analysis & Comparison
(Biomass and carbon stock per species)

Results and Discussion

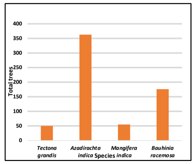

Figure 2 Abundance of tree species within the study area

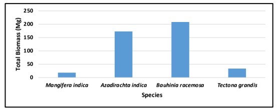

Figure 3- Species-wise distribution of total biomass

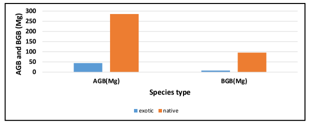

Figure 4- Contribution of AGB and BGB by spices type

- **Average biomass/tree *Bauhinia racemosa* was highest (1.18 Mg/tree)**
- **Highest average carbon stock value was *Bauhinia racemosa* (0.55 Mg C/tree).**

Conclusion

- Biomass and carbon storage varied among species, with ***Bauhinia racemosa*** and ***Azadirachta indica*** contributing the most.
- Native species dominated overall carbon stock, while exotics contributed less due to lower abundance.
- Campus greenery plays a key role in carbon sequestration, emphasizing the importance of conserving and expanding native trees.

References

Chave, J., Réjou-Méchain, M., et al. (2014). Improved allometric models to estimate the aboveground biomass of tropical trees. *Global Change Biology, 20*(10), 3177–3190.
Jayasinghe, R. N. K., Dilini, R. M. A., et al. (2025). Assessment of carbon sequestration and biodiversity for sustainable urban campus management. *Sri Lanka Technological Campus Conference Proceedings, August 2025*

|ICAS2025|

Assessment of Water Quality Parameters in the Cascade Systems that Feed Peraru Reservoir

P.P.M.Sathsarani[1], S.Suntharalingam[2], S.Devaisy[1]

[1]Department of Bio Science, University of Vavuniya, Sri Lanka

[2]National Water Supply and Drainage Board, Vavuniya, Sri Lanka

Abstract: The water resources of the Peraru reservoir are treated by the National Water Supply and Drainage Board, Vavuniya and distributed to the public for potable and non-potable purposes. However the water hardness fluctuate with season and exceeds the standards in dry season. Therefore, this study aims to analyze the water quality, primarily focusing on hardness of the water in the tanks and channels along the cascade systems that feed the Peraru reservoir in the Vavuniya District. The Peraru Reservoir is fed by a cascade system made up of many tanks and channels connected one after another. Water samples were taken from these tanks and channels, and pH, electrical conductivity (EC), chloride, alkalinity, hardness, and fluoride were tested. The data was processed using ArcMap spatial platform to develop Inverse Distance Weighting interpolation maps.The temporal and spatial analysis of water quality parameters from 2022 to mid-2025 reveals that pH and chloride levels generally remain stable within permissible limits, while hardness, alkalinity, electrical conductivity (EC), and fluoride show significant variations influenced by seasonal changes and geological factors. Hardness and alkalinity frequently exceed Sri Lanka Standards (SLS) limits in key tanks and the Peraru reservoir, especially during dry seasons. Fluoride levels exceed safe limits at several sites, notably in Peraru surface and channels connected to Charnockite and amphibolite formations. Statistical tests confirm a strong correlations between EC, hardness, alkalinity and fluoride highlight their common mineral sources related to the different type of geology of the cascade system. From that it is found that there is a significant variation of key water quality parameters in different locations. EC, alkalinity, hardness, and fluoride show a strong positive relationship across the cascade system. Elevated levels of these parameters occur at several locations, particularly near the Nochchimoddai Bridge and along the Madukanda–Peraru cascade line. In June and July, there was more variation in water quality in channels than in tanks. Hornblende-biotite gneiss and Biotite–rich amphibolite zones are mostly contribute for the hardness.

Keywords: alkalinity, cascade system, electrical conductivity, fluoride, geology, hardness, Peraru reservoir, water quality

ICAS2025

Faculty of Applied Science
University of Vavuniya

ASSESSMENT OF WATER QUALITY PARAMETERS IN THE CASCADE SYSTEMS THAT FEED PERARU RESERVOIR

Sathsarani. P.P.M. [1], Suntharalingam.S and Devaisay.S [2]
Department of Bio-Science, University of Vavuniya, Sri Lanka

Introduction

- The Peraru Reservoir supplies water to the Vavuniya scheme.
- The water hardness, especially during the dry season, remains a concern.
- This study identifies cascade locations contributing to increased hardness during the dry.

Objective

To analyze the water quality, with a primary focus on hardness, of the tanks and channels in the cascade system feeding the Peraru reservoir in Vavuniya District.

Methodology

- Identified tanks and built the cascade system map
- Measured water quality parameters.
- Created spatial maps and time series(2022–2025) using Minitab.
- Performed ANOVA, Post Hoc, and Pearson correlation analyses
- Developed the geology map to assess geological influence on hardness.

Results and Discussion

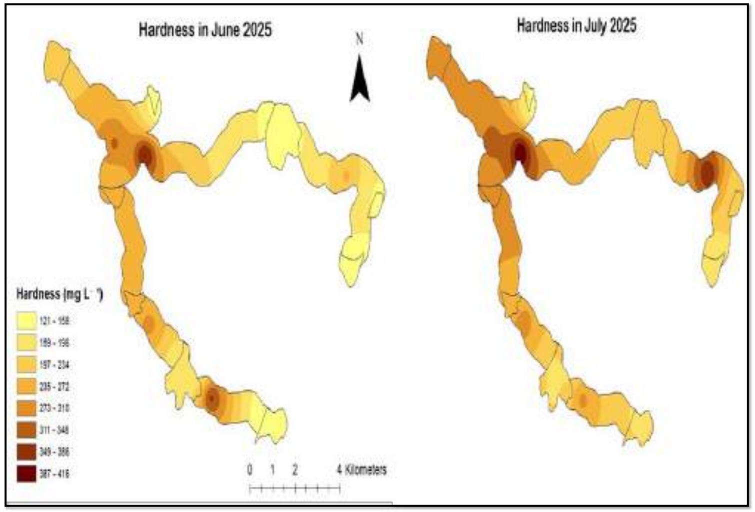

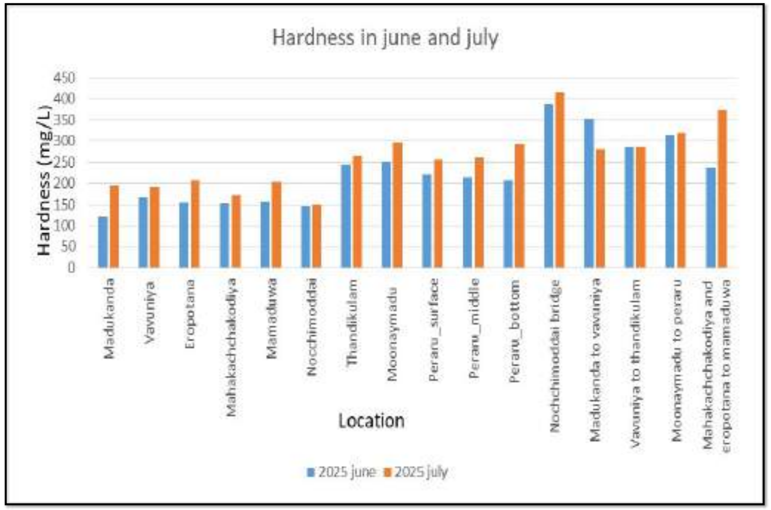

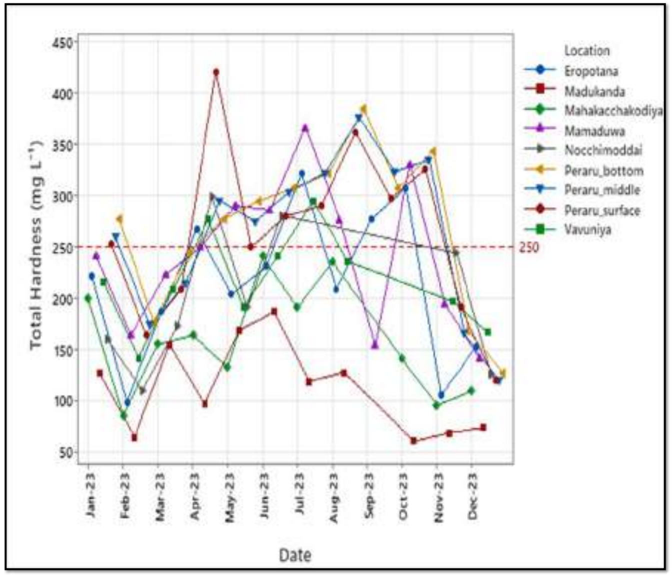

Conclusion

There is a significant variation of key water quality parameters in different locations. EC, alkalinity, hardness, and fluoride show a strong positive relationship across the cascade system. Elevated levels of these parameters occur at several locations, particularly near the Nochchimoddai bridge and along the Madukanda–Peraru cascade line, indicating naturally higher concentrations.

|ICAS2025|

Canteen Effluent Treatment using Phytoremediation Techniques: A Case Study at the University of Vavuniya

H.Adikari[1], S.Devaisy[1]

[1]Department of Bio Science, University of Vavuniya, Sri Lanka

Abstract: Canteen wastewater, also known as greywater, primarily contains organic matter such as oils, grease, food particles, and cleaning agents. When discharged untreated into the environment, it can significantly affect soil quality, structure, landscape, and vegetation. At the University of Vavuniya (UoV), the discharge of large volumes of effluent from a campus canteen has caused water stagnation and unsanitary conditions. This study evaluates the feasibility of using a laboratory-scale phytoremediation unit to treat canteen wastewater from the UoV. Two constructed wetland setups were developed—one as a control and the other for testing—using *Lemna minor* as the phytoremediation plant. Effluent collected from the university canteen was fed into the system at a flow rate of 5 mL/min, maintaining a hydraulic retention time (HRT) of 24 hours. The raw effluent was found to contain high levels of contaminants: Turbidity (225±20 NTU), Total Kjeldahl Nitrogen (TKN) (25.21±4 mg/L), Electrical Conductivity (EC) (1249±6 μS/cm), Phosphate (14.23±3 mg/L), Total Dissolved Solids (TDS) (2633±9 mg/L), and Chemical Oxygen Demand (COD) (2400±8 mg/L), with several parameters exceeding Central Environmental Authority (CEA) standards. The *Lemna minor*-based phytoremediation unit showed removal efficiencies of 97% (Turbidity), 59% (TKN), 13% (EC), 59% (Phosphate), 48% (TDS), and 53% (COD) over a continuous four-week experimental period. A small sample t-test confirmed that the reductions in Phosphate, TKN, TDS, Turbidity, and COD were statistically significant ($p < 0.05$). As the treated water met CEA standards for discharge onto land for irrigation, this phytoremediation system is recommended as a cost-effective and environmentally friendly solution for canteen wastewater treatment. Furthermore, the treated water can be safely reused for gardening and irrigation purposes.

Keywords: canteen wastewater, constructed wetlands, Greywater, Lemna minor, Phytoremediation

WATER AUDIT AND EFFLUENT TREATMENT ASSESSMENT AT THE UNIVERSITY OF VAVUNIYA

Adikari,H[1], Devaisy,S[1].
Department of Bio-Science, Faculty of Applied Science, University of Vavuniya

Abstract

This study conducted a water audit to identify canteen wastewater as a major source of pollution and treated it using a laboratory-scale phytoremediation unit with *Lemna minor* and *Spirodela polyrhiza*. Both species showed significant removal of turbidity, phosphate, TKN, TDS, and COD, meeting CEA standards. The findings recommend phytoremediation as a cost-effective, eco-friendly wastewater treatment method..

Introduction

- Kitchen wastewater, a major contributor to greywater, which contains high levels of organic matter, oils, grease, and detergents that harm the environment, groundwater, and human health if untreated.

- Conventional treatment methods are costly, energy-intensive, and often unsuitable for resource-limited regions.

- Phytoremediation, using Duck weed (*Lemna minor)* offers an eco-friendly, cost-effective solution for treating kitchen wastewater

Objective

- **To assess the performance of a duckweed-based constructed wetland system for the treatment of canteen wastewater and to evaluate its environmental compliance with CEA standards**.

Methodology

- Setting up a constructed wetland (**Control and Experimental setup**)
- Characteristics of raw feed water
- Determination of treated water quality

  COD- Titrimetric analysis,

  Phosphate-Spectrometric analysis

  TDS – Gravimetric analysis

  TKN- Kjeldahl method (Digestion, Distillation, Titration)
- Assess the performance of wetland system

Figure1:*Lemna minor*

Figure 2: Prepared constructed wetlands

Results and Discussion

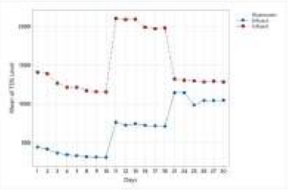

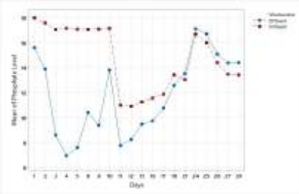

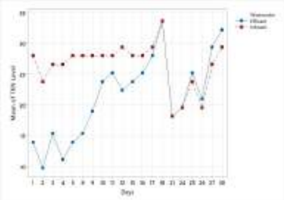

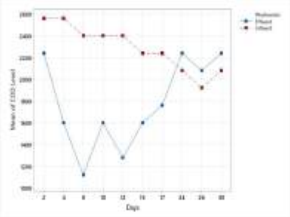

Conclusion

- This study treated canteen wastewater at the University of Vavuniya using duckweed (*Lemna minor)*
- The wastewater exceeded CEA standards, posing health and environmental risks.
- *Lemna minor* significantly reduced COD, TKN, phosphates, TDS, and turbidity, with results statistically significant. Phytoremediation proved eco-friendly, low-cost, and produced useful byproducts like compost and animal feed.

References

Adhikari, U., Harrigan, T. and Reinhold, D.M. (2014) 'Use of duckweed-based constructed wetlands for nutrient recovery and pollutant reduction from dairy wastewater,' *Ecological Engineering*, 78, pp. 6–14. https://doi.org/10.1016/j.ecoleng.2014.05.024.

Hadidi, L.A. (2021) 'CONSTRUCTED WETLANDS A COMPREHENSIVE REVIEW,' *International Journal of Research -GRANTHAALAYAH*, 9(8), pp. 395–417. https://doi.org/10.29121/granthaalayah.v9.i8.2021.4176.

Adnan, A.A. and Ismayana, A. (2022) 'Removal of cyanide from an artificial wastewater in constructed wetland system with Pistia stratiotes and C. Zizaniodes,' *IOP Conference Series Earth and Environmental Science*, 1063(1), p. 012018. https://doi.org/10.1088/1755-1315/1063/1/012018.

|ICAS2025|

Solid Waste Management of Wafer Production Process in Sri Lanka

H.N.Kuruppuarachchi[1], S.Kayanan[1]

[1]Department of Bio Science, University of Vavuniya, Sri Lanka

Abstract: Globally, the wafer industry is rapidly expanding within the food manufacturing sector, contributing significantly to consumer demand while generating considerable volumes of solid waste at various production stages. In developing countries such as Sri Lanka, where food industries are growing quickly, waste management practices often lag behind industrial expansion, leading to resource inefficiencies, environmental impacts, and increased operational costs. This study aims to assess the magnitude and causes of solid waste generation in wafer production facilities and to propose recommendations for sustainable waste management. A combined methodology of process flow mapping, material balance analysis, and on-site audits was employed to quantify solid waste in each process and to evaluate current management practices. Results showed that total solid waste generation amounts to 882.46 kg per day, with cutter waste contributing the highest share at 20.35%, followed by plain sheet waste at 20.22% and oven lumps at 17.58%. The remaining portion consists mainly of cream sheet waste and sweeping waste, underscoring the concentration of waste in a few critical process stages. The findings highlight that weak process control, outdated equipment, and limited preventive measures exacerbate waste generation. Approximately 50.78% of the total waste, originating from plain sheet damages, cream sheet damages, and cutter waste, is reused for cream preparation and chocolate-coated products, while oven lumps are sold to private parties for chicken feed production. In contrast, sweeping waste, amounting to 115 kg per day, is directly disposed of. Current practices emphasize reuse and recycling, while neglecting waste prevention and reduction at the source. In conclusion, strengthening solid waste management in wafer production requires the development of standard operating procedures, equipment modifications, process optimization, and workforce training to enhance prevention and reduction. Aligning these interventions with extended producer responsibility, as emphasized in Sri Lanka's waste management policy, will foster more sustainable production practices.

Keywords: extended producer responsibility, material balance analysis, process flow mapping, wafer production process, waste generation

Solid Waste Management of Wafer Production Process in Sri Lanka

H.N. Kuruppuarachchi[1]*, S. Kayanan[1]
[1]*Department of Bio Science, University of Vavuniya, Sri Lanka*

Abstract

The wafer industry is rapidly expanding within the global food manufacturing sector, contributing significantly to consumer demand but also generating considerable amounts of solid waste at multiple stages of production. In developing countries such as Sri Lanka, where food industries are growing quickly, waste management practices often fail to keep pace with industrial expansion, leading to operational inefficiencies, environmental degradation, and higher production costs. This study aimed to assess the magnitude and causes of solid waste generation in wafer production facilities and to recommend sustainable management strategies. A combined methodology of process flow mapping, material balance analysis, and on-site audits was employed to quantify waste generated in each stage and evaluate current practices. Results revealed that total solid waste generation amounts to 882.46 kg per day, with cutter waste (20.35%), plain sheet waste (20.22%), and oven lumps (17.58%) as the largest contributors. Approximately 50.78% of waste, including plain sheet, cream sheet, and cutter waste, is reused for cream preparation and chocolate-coated products, while oven lumps are diverted for poultry feed production. However, sweeping waste, amounting to 115 kg per day, is disposed of directly. Strengthening standard operating procedures, upgrading equipment, optimizing processes, and training the workforce are essential for sustainable wafer production in Sri Lanka.

Introduction

The wafer industry has emerged as a rapidly expanding segment of the global confectionery market, driven by increasing consumer demand for convenient, affordable, and versatile snack products. Characterized by its crisp texture, layered structure, and diverse range of flavors, wafer production has gained significant popularity worldwide. In Sri Lanka, the food manufacturing sector, including wafer production, has shown steady growth over recent decades, contributing to both economic development and changing consumption patterns.

However, the expansion of wafer manufacturing has been accompanied by challenges in managing the solid waste generated across different stages of the production process. Unlike developed countries, where advanced waste reduction and recycling systems are often integrated into industrial operations, many developing countries, including Sri Lanka, face gaps in technological capacity, regulatory enforcement, and resource efficiency. These shortcomings result in large volumes of production waste, inefficient use of raw materials, and escalating environmental impacts.

Understanding the magnitude, sources, and management practices of solid waste in wafer production is essential for improving operational efficiency, reducing costs, and mitigating environmental harm. By focusing on the Sri Lankan context, this study highlights the pressing need to develop sustainable waste management strategies, integrating prevention, reduction, reuse, and recycling within the wafer production process.[1,2].

Figure 1: Wafer Biscuit

Objectives

- To quantify the amount and types of solid waste generated in wafer production.
- To identify key process stages contributing to high waste generation.
- To propose sustainable waste management strategies aligned with national policy.

Methodology

The methodology combined process flow mapping, material balance analysis, and on-site audits to quantify solid waste generation at each stage of wafer production and review existing management practices. These approaches enabled the identification of waste hotspots, assessment of efficiency, and evaluation of recycling and disposal strategies within the rapidly expanding wafer manufacturing process.

Figure 3: Material Balance Analysis

Process Flow Mapping
- Traced each stage of wafer production (raw material → mixing → baking → sndwiching → cooling → cutting → packaging)
- Identified where losses (e.g., cutter waste, sheet damage, oven lumps) occur
- Helped visualize waste hotspots cdearly

Material Balance Analysis
- Compared inputs vs, outputs at every stage
- Quantified raw material use, product yield, and waste fractions
- Highlighted inefficiencies and estimated potential recovery gains

On-site Audits
- Direct observation of operations, equipment use, and worker practices
- Collected photographic evidence, staff feedback, and daily records
- Captured real-world issues such as poor process control, outdated machinery, and handling

Integration & Outcomes
- Identified waste hotspots and inefficiencies
- Quantified waste flows & derived recovery percentages
- Evaluated recycling and disposal strategies within the rapidly expanding wafer industry

Figure 2: General Methodology

Raw Material Receiving & Storage
Weighing and Mixing
Baking
Cream Preparation
Sandwiching
Cutting and Trimming
Packaging

Figure 4: Process Flow Analysis

Results and Discussion

Results showed that total solid waste generation amounts to 882.46 kg per day, with cutter waste contributing the highest share at 20.35%, followed by plain sheet waste at 20.22% and oven lumps at 17.58%. The remaining portion consists mainly of cream sheet waste and sweeping waste, underscoring the concentration of waste in a few critical process stages. The findings highlight that weak process control, outdated equipment, and limited preventive measures exacerbate waste generation. Approximately 50.78% of the total waste, originating from plain sheet damages, cream sheet damages, and cutter waste, is reused for cream preparation and chocolate-coated products, while oven lumps are sold to private parties for chicken feed production. In contrast, sweeping waste, amounting to 115 kg per day, is directly disposed of. Current practices emphasize reuse and recycling, while neglecting waste prevention and reduction at the source.

Contributing Factors
- Weak process control
- Outdated equipment
- Limited preventive measures

Figure 5: Types of waste and contributing factors

Reuse and Disposal
- 50.78% reused for cream preparation, chocolate products
- Oven lumps sold for chicken feed; sweeping waste disposed

Figure 6: Reuse and disposal

Conclusion

In conclusion, strengthening solid waste management in wafer production requires the development of standard operating procedures, equipment modifications, process optimization, and workforce training to enhance prevention and reduction. Aligning these interventions with extended producer responsibility, as emphasized in Sri Lanka's waste management policy, will foster more sustainable production practices..

Develop standard operating procedures
Make equipment modifications
Optimize processes
Train workforce

Figure 6: Recommendations

References

1. Sahoo, A., Sahu, J. N., Bandopadhyay, T. K., & Rajendran, S. (2023). Insights into the management of food waste in developing countries: Current challenges and future perspectives. Journal of Environmental Management, 337, 117868.
2. Thi, N. B. D., Kumar, G., & Lin, C. Y. (2015). An overview of food waste management in developing countries: Challenges and opportunities. Science of the Total Environment, 505, 307-314.

|**ICAS2025**|

Effect of Different Feeds on the Growth and Survival of *Holothuria scabra* (Sea cucumber) in Nursery Culture

S.Keerthana[1], A.E.S.Patrick[2], W.S.Thulasitha[3], H.A.Thamiliny[4], B.Nirooparaj[5]

[1,2]Department of Bio Science, University of Vavuniya, Sri Lanka
[3]Department of Zoology, University of Jaffna, Sri Lanka
[4]Suganth Sea Food (Pvt) Ltd, Jaffna, Sri Lanka
[5]National Aquaculture Development Authority of Sri Lanka

Abstract: Increased harvest pressure and local harvesters' intensifying collection have led to a critical decline in *Holothuria scabra* populations in Sri Lanka. Aquaculture provides a practical solution to reduce the overexploitation of sea cucumbers. In Sri Lanka, juvenile post-release survival and growth performance have been scarce. Therefore, this study aims to evaluate the growth performance and percentage of survival of juveniles under different feed treatments along with control setups. The present study was conducted at Suganth Seafood (Pvt) Ltd, Kakkaitheevu, Jaffna. Juveniles (2–3 g) were selected randomly from the hatchery and stocked in indoor nursery tanks (120 L). Three replicate tanks were maintained for each treatment (T1, T2, T3) and the control, with a stocking density of 20 juveniles per tank. Varying ratios of three types of seaweeds and sea mud were utilized in feed preparation as follows: *Sargassum crassifolium* : *Gracilaria salicornia* : *Kappaphycus alvarizii* : sea mud in T1 = 4:3:2:1, T2 = 2:4:3:1, T3 = 3:2:4:1, and in the control, sea mud alone (100%) was utilized. Growth performances were evaluated by measuring total body weight, total body length, growth rate, along with survival rate and food conversion ratio. Although all seaweed-based feeds supported 100% survival with moderate growth, the feed containing a higher proportion (40%) of *Kappaphycus alvarizii* (T3) produced significantly higher growth performance compared to the other treatments (T1 and T2). This was observed in mean weight (14.72 ± 0.39 g, $p < 0.05$), mean length (5.48 ± 0.18 cm, $p < 0.05$), and growth rate (0.39 ± 0.01 g/day, $p < 0.05$). Interestingly, the control setup showed the lowest growth performance. Statistically, there was a significant difference among treatments ($p < 0.05$), and the *K. alvarizii* (40%) showed improved growth performance among indoor nursery systems. Therefore, this study suggests that indoor culture using seaweed-based feeds such as *Kappaphycus alvarizii* seems to be a stable and effective approach for post-release hatchery juveniles in sea cucumber culture.

Keywords: food conversion ratio, growth performance, *Holothuria scabra*, seaweed-based feeds, survival rate

Effect of different feeds on the growth and survival of *Holothuria scabra* (Sea cucumber) in nursery culture

Keerthana S[1*], Patrick A E S[1], Thulasitha W S[2], Thamiliny H A[3], Nirooparaj B[4],

[1]Department of Bio-Science, Faculty of Applied Science, University of Vavuniya, [2]Department of Zoology, Faculty of Science, University of Jaffna,[3]Suganth Sea Food (pvt) Ltd, [4]National Aquaculture Development Authority of Sri Lanka

Abstract

This study evaluated the growth and survival of Sea cucumber juveniles fed with seaweed-based feeds in indoor tanks. Varying ratios of three seaweeds and sea mud were utilized in feed preparation. All seaweed treatments ensured 100% survival and significant differences among treatments ($p < 0.05$). Interestingly, the treatment fed with *Kappaphycus alvarizii* (40%) showed the highest growth performance (14.72 ± 0.39 g), suggesting optimal indoor juvenile production.

Introduction

- *Holothuria scabra* is a valuable sea cucumber threatened by overharvesting
- Aquaculture is essential to meet market demand and protect wild stocks
- There is a need to improve hatchery production, survival rates of post-release juveniles in Sri Lanka
- Nursery stage feeding is critical for improving growth and survival before grow-out
- Seaweeds are potential cost-effective and locally available feeds: *Sargassum* sp. (Sa), *Gracilaria* sp. (Gr), *Kappaphycus* sp. (Ka)

Fig 1: Sea cucumber Juveniles

Sargassum sp.

Gracilaria sp.

Kappaphycus sp.

Fig 2: Varieties of seaweeds

Aim & Objective

-To evaluate the growth and survival performance of *H. scabra* juveniles under different seaweed-based feeds in a nursery culture

- Evaluate growth performance under varying seaweed feed ratios
- Determine survival rates in response to different seaweed feed ratios
- Identify the most effective feed composition for nursery culture

Methodology

- Experimental Design: 8-week trial; 3 treatments ($T_{1\text{-}3}$) & control (Ctrl), 3 replicates, 20 juveniles/tank (2-3g)
- ratios of feed preparation as follows: *Sa*: *Gr*: *Ka*: sea mud
  - T_1 = 4:3:2:1 -T_2 = 2:4:3:1-T_3 = 3:2:4:1
- Control = sea mud (100%)
- Feeding: Daily at 8% body weight (W) (Al-Harbi, 2022)
- Measurements: W, Growth Rate (GR), Food Conversion Ratio (FCR), Survival Rate (SR) (Indriana et al., 2024)
- Water Quality: Monitored weekly (Temp 27–31°C, Salinity 30–35 ppt, pH 8.0–8.2)
- Data analysis: One-way ANOVA with Tukey's test (95% CI, Minitab 22.2.2)

$$GR(g/d) = \frac{W_F - W_I}{t}$$

$$FCR\ (\%) = \frac{C}{W_F - W_I}$$

$$SR\ (\%) = \left(\frac{N_t}{N_0}\right)100$$

Where,
W_F = Final weight
W_I = Initial weight
t = Days
C = Dry weight of feed consumed
N_t = Surviving juveniles at the end
N_0 = Initial stocked juveniles

Fig 3: Indoor tank setup

Fig 4: Weighing juveniles *H. scabra*

Results and Discussion

- Survival: $T_{1\text{-}3}$ = 100±0.00^a %, Ctrl= 95±5.00^a %
- Highest weight gain: T_3 (23.88±0.39^a g), Lowest weight gain: Ctrl (6.57±0.30^c g)
- Length gain was highest in T_3 (5.27 ± 0.15^a cm) and lowest in Ctrl (1.70 ± 0.10^c cm)
- GR: Highest in T_3 (0.39±0.01^a g/d), Lowest in Ctrl (0.11±0.01^c g/d)
- Statistical Analysis: Significant differences ($p < 0.05$) among treatments for growth

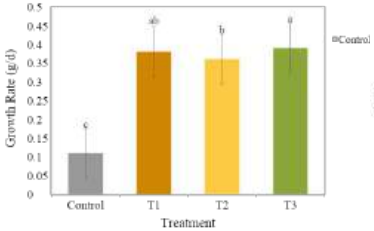

Fig 5: GR for all $T_{1\text{-}3}$ and Ctrl

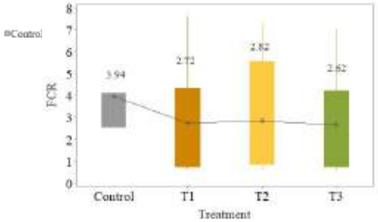

Fig 6: FCR for all $T_{1\text{-}3}$ and Ctrl

- Seaweed-based feeds enhanced growth compared to sea mud alone
- *Kappaphycus alvarizii* (40%) in T_3 supported the best indoor performance, likely due to high polysaccharides and digestibility & also the lowest FCR value
- Indoor systems provide stable conditions and high survival, suitable for juvenile-stage rearing

Conclusion

- Seaweed-based feeds, especially *Kappaphycus*-rich feed, is effective for nursery-stage *H. scabra*
- Indoor nursery culture ensures consistent production for aquaculture and restocking programs

References

- Al-Harbi, M. (2022). *Effects of diet quantity on growth performance of juvenile sea cucumbers Holothuria scabra Oceanological and Hydrobiological Studies 51*(2) https://doi.org/10.26881/oahs-2022.2.04
- Indriana, L. F., Kunzmann, A., & Slater, M. J. (2024). Dietary effect of different fermented feed sources on growth performance of early juvenile sea cucumber *Holothuria scabra*. *Aquaculture Reports*, *34* https://doi.org/10.1016/j.aqrep.2023.10189
- Yuval, B., Sudai, L., & Ziv, Y. (2014). Abundance and diversity of holothuroids in shallow habitats of the northern Red Sea. *Journal of Marine Biology*, *2014*. https://doi.org/10.1155/2014/631309

|ICAS2025|

Evaluation of Cytogeno toxic Effects of Automobile Service Station Effluents on *Allium cepa*: A Comparative Study of Treated and Untreated Samples

S.Alojini[1], J.Nimalan [1]

[1]Department of Bio Science, University of Vavuniya, Sri Lanka

Abstract: Effluents from automobile service stations are a major source of water pollution, releasing toxic substances into aquatic systems that pose risks to both ecosystems and human health. This study evaluated the cytotoxic and genotoxic effects of treated and untreated effluents from selected service stations near the Vavuniya Tank using the *Allium cepa* assay, a well-established bioindicator system. The genotoxicity assay was conducted after 48 hours of exposure to effluents at concentrations of 0.01%, 0.1%, 1%, and 10%, with tap water serving as the control. The *Allium cepa* assay followed standard protocols, where cytogenetic parameters such as mitotic index (MI), limit value of cytotoxicity (LCV), phase index (PI), and chromosomal aberrations were evaluated under oil immersion at high magnification (2500 cells per sample). Results revealed that cytogenetic responses varied with effluent treatment and concentration. A concentration-dependent reduction in MI was observed, with the control, treated, and untreated effluents showing 38.96%, 21.40%, and 17.44% MI, respectively, at 10% concentration. Similarly, LCV decreased with increasing concentrations: from 100% (control) to 54.93% in treated and 44.76% in untreated effluents at 10%. Chromosomal aberration analysis showed that both treated and untreated effluents induced abnormalities, with the frequency of aberrations increasing with concentration. Untreated effluents exhibited genotoxic effects, producing higher numbers of abnormal interphases (54) and sticky prophases (26), compared to treated effluents (abnormal interphases (31) and sticky prophases (21)). Dominant aberrations included abnormal interphase, sticky prophase, and sticky metaphase. Overall, both treated and untreated effluents demonstrated cytotoxic and genotoxic effects on *Allium cepa* root meristem cells, with untreated effluents exerting a greater impact. The severity of these effects increased with effluent concentration, peaking at 10%.

Keywords: *Allium cepa*, Chromosomal aberration, Cytogeno toxicity, Mitotic index, service station effluents

Evaluation of Cytogenotoxic Effects of Automobile Service Station Effluents on *Allium cepa*: A Comparative Study of Treated and Untreated Samples.

[1]S. Alojini and [1]J. Nimalan

1Department of Bio Science, Faculty of Applied Science,
University of Vavuniya

Abstract

This study evaluated cytogeno toxic impacts of treated and untreated automobile service station effluents near Vavuniya Tank using the *Allium cepa* assay. Parameters including mitotic index, cytotoxicity, phase index, and chromosomal aberrations were analyzed. Results revealed concentration-dependent toxicity, with untreated effluents showing stronger effects. Both effluents induced chromosomal abnormalities including abnormal interphase and sticky prophase, highlighting environmental risks, particularly at 10% concentration.

Introduction

- Water pollution arises from sewage, agriculture, and industrial effluents.
- Automobile service stations release oils, grease, detergents, PAHs, and heavy metals.
- Genotoxic effects include DNA damage, mutations, and chromosomal aberrations.
- Vavuniya reservoir, situated in the urban region, is particularly vulnerable to oil and grease contamination resulting from petroleum-based automobile service activities
- Assessing the genotoxic effects of water pollution by the service stations is important to predict this effect on living organism

Objective

To assess the cytogeno toxic effects of automobile effluents using the *Allium cepa* assay .

Methodology

- Experiments was designed with four effluent concentrations: 10%, 1%, 0.1%, and 0.01% (v/v, effluent/tap water) and control for treated and untreated water.
- Onion bulbs were exposed to each concentration for 48 hours with five replicates.
- Tips were fixed in ethanol and glacial acetic acid (3:1, v/v).
- Samples were hydrolyzed in 1N HCl at 60 °C for 5 minutes.
- Root tips were stained with aceto-carmine for 30 minutes
- Cells were Observed and count under a microscope oil immersion.

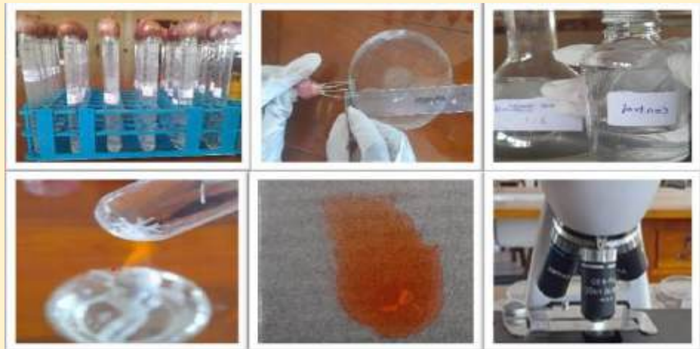

Results and Discussion

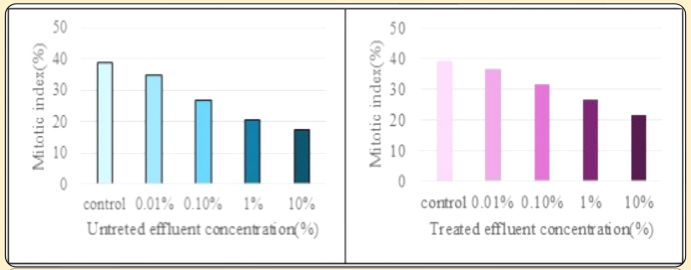

- Both treated and untreated effluents reduced mitotic index (MI) compared to control (38.96%).. At 10% concentration, MI dropped to 21.40% and 17.44% for treated and untreated effluents, respectively.
- Chromosomal aberrations increased with effluent concentration in both treated and untreated samples.
- Most frequent aberrations were abnormal interphase, sticky prophase, sticky metaphase.
- Untreated effluent showed stronger genotoxicity than treated (e.g., more abnormal interphase and sticky prophase).

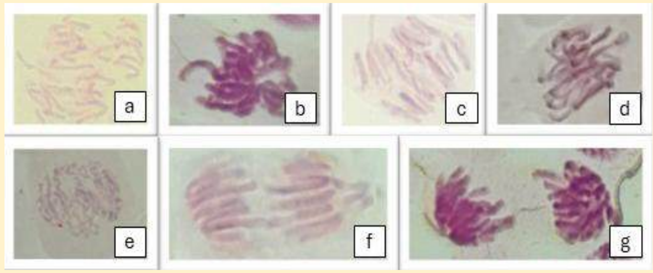

(a) C metaphase, (b) Chromosome stickiness, (c) Disturbed spindle, (d) Chromosomal adherence in metaphase, (e) Disturbed prophase, (f) Chromosomal bridge and (g) Chromosomal bridge.

Conclusion

- Chromosomal aberrations increased, and the mitotic index decreased with increasing effluent concentration.
- The untreated effluent exhibited a higher number of aberrations compared to the treated effluent.
- The major types of abnormalities observed in the untreated effluent included abnormal interphase, sticky prophase, and sticky metaphase. In the treated effluent, disturbed metaphase and multipolar anaphase were observed.
- Both effluents may pose cytogeno toxic risks to living organisms.

References

- Fiskesjö, G. (1985). The Allium test as a standard in environmental monitoring. Hereditas, 102(1), 99–112.
- Grosu, L., Ferenț, E., Nicuță, D., & Alexa, I.-C. (2024). Approach regarding the biosafety evaluation of black and red currant pomace extracts using *Allium cepa* test. Ovidius University Annals of Chemistry, 35(2), 126–136.

|**ICAS2025**|

Fabrication and Characterization of Nanocomposites (Cu-Sn) and Treating the Organic Dyes Blended Domestic Wastewater and Drainage Water

P.Rajesh[1], K.Sivakumar[1]

[1]Centre for Materials Engineering and Regenerative Medicine, Bharath Institute of Higher Education and Research, Selaiyur, Chennai, India

Abstract: Amalgamation of colours are generally utilized consistently. The symptom of their boundless use in 12% of these colours are squandered during passing on process 20% of this wastage enters into the environment. There is a requirement for expulsion colours from nearby waste water with cost and compelling innovation. The study has gotten significant interest on account of its increased efficiency as a photocatalysts to corrupt a broad scope of natural material. The $CuSO_4$ is utilized to kills the microorganisms present in wastewater, since it has an anti-bacterial property. The synthesized nanoparticles were kept in magnetic stirrer for 2 hrs after that the solution was kept in autoclave for multiple times for breaking particles at high pressure. Tests were pipetted into the petri plate and 1ml of dye were added into plate. The plates were held for recognition under apparent light notification the progressions recorded. Major dyes are used in this study namely methylene blue, methyl red, malachite green commercially available in our laboratory and dye degrading results for $CuSO_4$. We have future aspects for waste water treatment, sewage treatment, agro-water treatment for recycling purposes.

Keywords: antioxidant assay, Cu-Sn nanocomposite, dye degradation, wastewater, UV-visible spectroscopy

International Conference on Applied Sciences - 2025
Faculty of Applied Science, University of Vavuniya, Sri Lanka
ICAS 2025

Fabrication and Characterization of Nanocomposites (Cu-Sn) and Treating the Organic Dyes Blended Domestic Wastewater and Drainage Water

Rajesh Pandiyan [a]*, Sivakumar Kumaraguru [a]
Centre for Materials Engineering and Regenerative Medicine, Bharath Institute of Higher Education and Research, Selaiyur, Chennai, India – 600073.

ABSTRACT

Synthetic dyes cause severe water pollution, with ~12% wasted during dyeing and 20% entering the environment. $CuSO_4$ nanoparticles were synthesized, stirred, and autoclaved to enhance photocatalytic efficiency. These nanoparticles effectively degraded methylene blue, methyl red, and malachite green under visible light. The study highlights their dual role in dye degradation and microbial control, offering scope for wastewater, sewage, and agro-water treatment.

Antioxidant Potential of Cu–Sn Bimetallic Nanoparticles: A DPPH Assay Approach

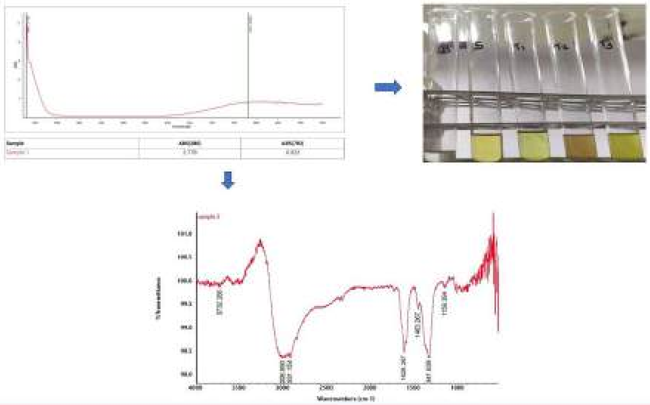

INTRODUCTION

Water, the universal solvent, is essential for all living organisms, yet contamination from sewage, industries, and domestic sources poses a global challenge. Wastewater treatment aims to remove pollutants through physical, chemical, and biological methods for safe reuse. Nanotechnology, especially metal-based nanocomposites, offers promising solutions for dye degradation and microbial control. In this study, chemically synthesized nanoparticles were tested for photocatalytic dye degradation under sunlight using methylene blue, methyl red, and malachite green.

MATERIALS AND METHODS

Nanoparticles were synthesized using copper sulphate and tin chloride precursors, dissolved separately in distilled water. Both solutions were combined with 0.1 g urea (catalyst) to form Solution C and stirred magnetically for 2 hours. The mixture was then subjected to six autoclave cycles at high pressure to obtain fine nanoparticles. Nanoparticles were synthesized by a facile method using copper sulphate and tin chloride as precursors. Solution A: 1 g $CuSO_4$ in 50 mL distilled water. Solution B: 1.0 g $SnCl_2$ in 50 mL distilled water. Solution C: A mixture of A and B with 0.1 g urea as a catalyst. The prepared solution was stirred magnetically for 2 hours, followed by six autoclave cycles at high pressure to obtain fine nanoparticles.

RESULTS AND DISCUSSION

SUMMARY & CONCLUSION

Nanoparticles were effectively synthesized using the free-facile method, ensuring a simple and eco-friendly preparation route. UV-Visible spectroscopy confirmed nanoparticle formation through distinct absorption peaks, while FTIR analysis revealed the presence of functional groups responsible for stability and reactivity. The synthesized nanoparticles showed effective dye degradation capability, indicating their potential in wastewater treatment applications. The observed color change during the antioxidant assay confirmed significant free radical scavenging ability, proving the nanoparticles' bioactive potential.

REFERENCES

1. Rajesh Pandiyan, Revathi Rajagopal, Suresh Kumar Subbiah. 2023. Methyl Red (2-(N, N-dimethyl-4-aminophenyl) azobenzene carboxylic acid) Incorporated Domestic Wastewater Treated Upon (Ag-Pb) Nanosynthesis. *Biomass Conversion and Biorefinery*.
2. Rajesh Pandiyan, Revathi Rajagopal. (2023). Fabrication and Characterization of Silver and Lead Nanoparticles and Application upon Synthetic Azo Dye Degradation. *Biomass Conversion and Biorefinery.*, Web of Science. https://doi.org/10.1007/s13399-023-04073-4.

ACKNOWLEDGEMENTS

I am pleased to acknowledge my sincere thanks to :

- The Board of Management Bharath Institute of Higher Education and Research, Bharath University (Deemed to be University), Selaiyur, Chennai -600073, Tamil Nadu, India.
- Management and to my esteemed guide, **Dr. Rajesh Pandiyan,** for their insightful supervision and unwavering support.

|ICAS2025|

Anti-Bacterial and Seed Germination Potential of Bimetallic Na–Ni Diamond Crystal Nanoparticles for Wastewater Treatment

K.Sivakumar[1], P.Rajesh[1]

[1]Centre for Materials Engineering and Regenerative Medicine, Bharath Institute of Higher Education and Research, Selaiyur, Chennai, India

Abstract: Hydrothermal synthesis stands out as a highly effective method for creating nanostructures due to its eco-friendly and straightforward process. In this study, we successfully produced sodium nitrate and nickel (II) chloride nanoparticles using hydrothermal methods. Sodium nitrate ($NaNO_3$) and nickel (II) chloride hexahydrate ($NiCl_2{\cdot}6H_2O$) were synthesized through precise chemical methods. The resulting samples underwent thorough characterization and analysis using a range of advanced techniques, including UV–visible spectroscopy, microscopic analysis, FTIR, anti-bacterial activity testing, zeta potential measurement and SEM. The UV–visible spectroscopy results confirmed that the synthesized bimetallic Na–Ni nanoparticles possessed a size range of 300–600 nm. FTIR analysis identified the functional groups of the bimetallic Na–Ni nanoparticles, with peaks at 2853.016, 2080.025, 1607.706, 1363.261 and 834.847 cm^{-1}, corresponding to C–H stretching, C=O stretching, N–H bending, O–H bending and C–H bending. Anti-bacterial activity tests demonstrated the effectiveness of the synthesized bimetallic Na–Ni nanoparticles against Gram-positive (Staphylococcus aureus) and Gram-negative (Pseudomonas aeruginosa) bacterial strains. Additionally, the study decisively showcased the capabilities of these bimetallic nanoparticles in dye degradation. Our findings revealed that these bimetallic nanoparticles can efficiently remove pollutants from highly contaminated water, rendering the treated water suitable for various applications, including agricultural use. Furthermore, we rigorously evaluated their performance as fertilizers. In seed germination experiments, they affirmed their potential in sustainable agriculture.

Keywords: antibacterial activity, bimetallic nanoparticles, dye degradation, seed germination, SEM

International Conference on Applied Sciences - 2025
Faculty of Applied Science, University of Vavuniya, Sri Lanka
ICAS 2025

Anti-bacterial and Seed Germination Potential of Bimetallic Na–Ni Nanoparticles for Wastewater Treatment

Sivakumar Kumaraguru [a], Rajesh Pandiyan [a]*
Centre for Materials Engineering and Regenerative Medicine, Bharath Institute of Higher Education and Research, Selaiyur, Chennai, India – 600073.

ABSTRACT

- Na–Ni nanoparticles were synthesized by the hydrothermal method and characterized by UV–Vis, FTIR, SEM, and zeta potential.
- The particles (300–600 nm) showed strong antibacterial activity, FTIR showed peaks at 2853, 2080, 1607, 1363, and 834 cm^{-1}, corresponding to C–H stretching, C=O stretching, N–H bending, O–H bending, and C–H bending, respectively.
- Effective dye degradation and improved seed germination highlight their potential in wastewater treatment and sustainable agriculture.

INTRODUCTION

- Nanoparticles have superior properties over bulk materials, with applications in agriculture, medicine, and the environment.
- Agricultural and Environmental Applications
- They enhance seed germination, neutralize soil toxins, and are effective in degrading hazardous dyes such as azo dyes from industrial effluents.
- This study synthesized Sodium–Nickel nanoparticles by the hydrothermal method for antibacterial, seed germination, and dye degradation applications.

Antibacterial, Seed Germination, and Dye Degradation Potential of Na–Ni Nanoparticles

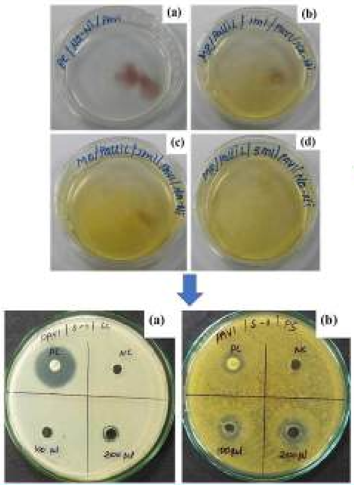

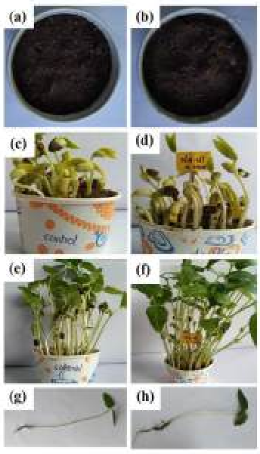

MATERIALS AND METHOD

- Precursor Solution – 0.25 M Sodium nitrate + 0.25 M Nickel (II) chloride in 100 mL distilled water with 100 mg urea.
- Stirring – Mixture stirred for 30 minutes.
- Hydrothermal Treatment – Transferred to autoclave at 100 °C for 1 hour.
- Post-treatment – Solution cooled, filtered, washed with deionized water, and dried under a lamp.

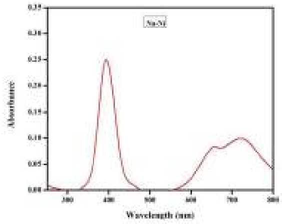

RESULTS AND DISCUSSION

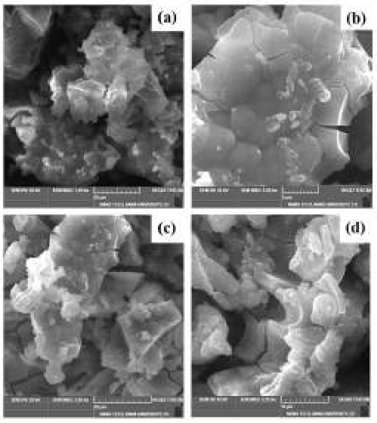

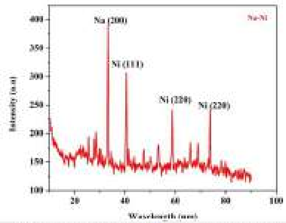

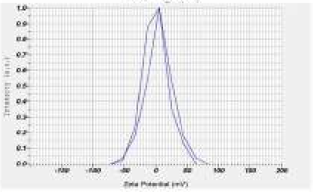

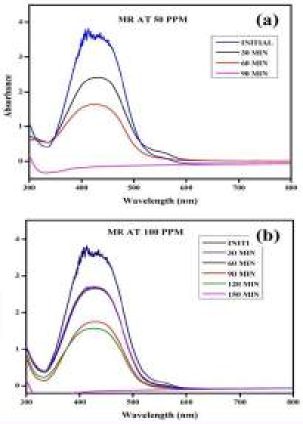

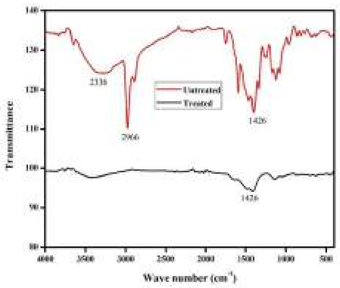

SUMMARY & CONCLUSION

- Na–Ni nanoparticles were successfully synthesized using the hydrothermal method and well-characterized by XRD, FTIR, UV–Vis, SEM, and zeta potential.
- UV–Vis confirmed nanoparticle formation with a peak at 354 nm; SEM showed particle sizes of 50–100 nm.
- The NPs achieved high dye degradation efficiency (93% at 50 ppm and 75% at 100 ppm).
- They exhibited strong antibacterial activity against pathogenic bacteria.
- Na–Ni nanoparticles enhanced seed germination, highlighting their potential in agriculture and wastewater treatment.

REFERENCES

1. Rajesh Pandiyan, Revathi Rajagopal, Suresh Kumar Subbiah. 2023. Methyl Red (2-(N, N-dimethyl-4-aminophenyl) azobenzene carboxylic acid) Incorporated Domestic Wastewater Treated Upon (Ag-Pb) Nanosynthesis. *Biomass Conversion and Biorefinery*.
2. Rajesh Pandiyan, Revathi Rajagopal. (2023). Fabrication and Characterization of Silver and Lead Nanoparticles and Application upon Synthetic Azo Dye Degradation. *Biomass Conversion and Biorefinery.*, Web of Science. https://doi.org/10.1007/s13399-023-04073-4.

ACKNOWLEDGEMENTS

I am pleased to acknowledge my sincere thanks to :
- The Board of Management Bharath Institute of Higher Education and Research, Bharath University (Deemed to be University), Selaiyur, Chennai -600073, Tamil Nadu, India.
- Management and to my esteemed guide, **Dr. Rajesh Pandiyan,** for their insightful supervision and unwavering support.

|**ICAS2025**|

Effect of Animal Fat on Anaerobic Co-Digestion and Process Optimization

N.G.B.S.M.Nawagamuwa[1], P.G.Rathnasiri[2], S.Devaisy[1]

[1]Department of Bio Science, University of Vavuniya, Sri Lanka
[2]Department of Chemical and Process Engineering, University of Moratuwa, Sri Lanka

Abstract: One of the emergent challenges in meat processing industries is producing biogas with animal waste associated with high-fat content. This research attempts to find out the effect of animal fat (poultry) on anaerobic co-digestion and process optimization by means of food waste as the co-substrate and cow dung (CD) as the inoculum by considering the trend in biomethane production at different quantities of animal fat. A series of batch fermentations were carried out in a lab-scale batch reactor (>500 mL) based on the VDI 4630 protocol. One control batch experiment was conducted with inoculum alone and five other different co-digestion experiments were implemented in triplicates with the proportions of rendered chicken fat emulsion:food waste at 0:100, 25:75, 50:50, 75:25, and 100:0 (w/w) in the presence of inoculum. The proportion of substrates to inoculum was 100:300 (w/w) in all the co-digestion experiments. Each experiment was implemented for four (4) days continuously under mesophilic (35 °C) conditions and at 200 rpm mixing speed by ensuring continuous mixing. Experimental data proved that the highest total biogas potential is achievable with co-digestion experiments incorporated with high quantities of food waste (0:100, 25:75), though a sudden process failure of acidification occurred eventually, along with minimal organic material conversion rate ($mL/gCOD_{removal}$). Experiments utilizing relatively high quantities of fat emulsion showed relatively low total biogas production without any sudden process failure and with a high organic material conversion rate. The highest pH reduction with high COD and volatile solid removal efficiencies were represented by high-quantity food waste incorporated batch experiments. The most viable co-digestion proportion was 50:50 (w/w) among the batch experiments incorporated by food waste with regard to the limited pH drop of the feedstock mixture. Another satisfactory fermentation was the co-digestion of animal fat associated with inoculum (cow dung) without using food waste (100:0), which produced continuous biomethane production with a high rate of organic material conversion. Continuous mixing and stable temperature at 35 °C may optimize gas production efficiency, and pH adjustment will be a further optimization technique for achieving the highest possible biomethane production.

Keywords: anaerobic digestion, animal fat inhibition, biochemical methane potential, co-digestion, process optimization

ICAS2025

Faculty of Applied Science
University of Vavuniya

EFFECT OF ANIMAL FAT ON ANAEROBIC CO-DIGESTION AND PROCESS OPTIMIZATION

Nawagamuwa N.G.B.S.M.[1*], Rathnasiri P.G.[2], Devaisy S.[1]

[1]*Department of Bio Science, University of Vavuniya, Sri Lanka* , [2]*Department of Chemical and Process Engineering, University of Moratuwa, Sri Lanka*

Abstract

This research attempts to find out the effect of animal fat (poultry) on anaerobic co-digestion and process optimization by means of food waste as the co-substrate and cow dung (CD) as the inoculum. Fat : food waste proportions of 0:100, 25:75, 50:50, 75:25, 100:0 (w/w) were tested with batch experiments at 35°C and 200 rpm. Most prolific proportions were 50:50 and 100:0. pH adjustment is a further recommendation for optimal biomethane yield.

Introduction

Livestock and processing industries such as dairy, swine and poultry (meat processing) are some of the prominent ventures in Sri Lanka. Poultry based meat production in Sri Lanka has found to be the pioneering meat producing sector based on the data published by DAPH in Sri Lanka which has been about 140,000MT by 2013. Improper disposal of decomposable animal waste fat may cause significant environmental pollution problems, including surface and groundwater contamination and unpleasant odors (Karim et al., 2004). Anaerobic digestion can be a sustainable solution for this waste generation.

Objectives

- To develop a lab-scale experimental set-up for anaerobic co-digestion.
- To evaluate biogas generation potential by varying ratios of input feedstock.
- To determine threshold limit for inhibition due to anaerobic degradation of animal fat.

Methodology

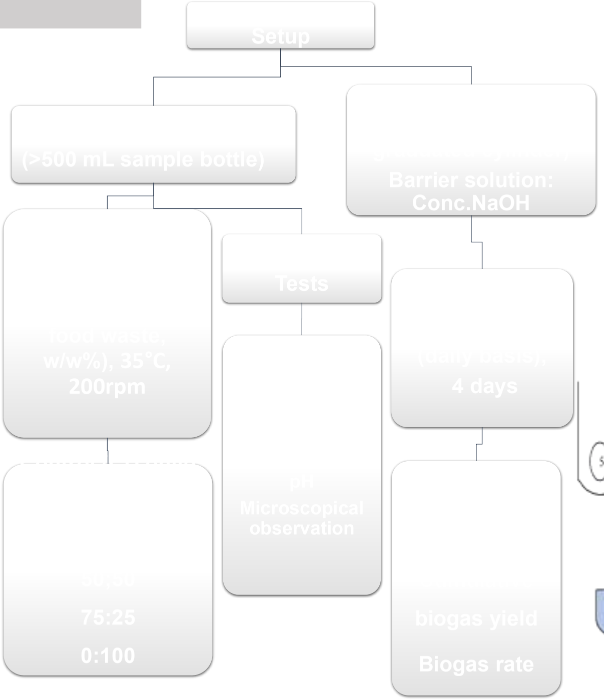

Figure 1.1: Graphical methodology

Figure 1.3 : Digested feedstock

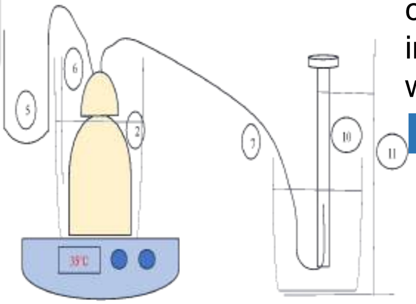

Figure 1.2: Schematic diagram of complete experimental setup

Results and Discussion

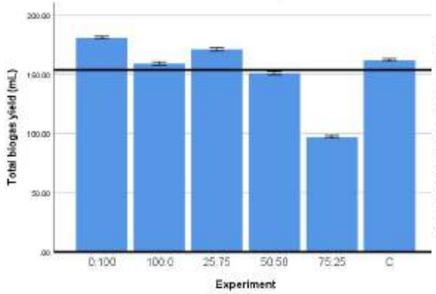

Figure 2.1: Total biogas yield plot

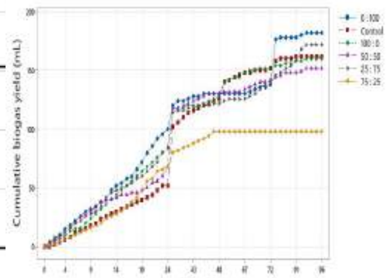

Figure 2.2 Cumulative biogas yield plot

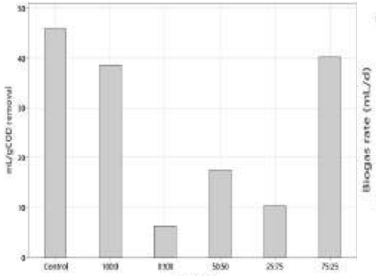

Figure 2.3: Conversion rate of organic materials

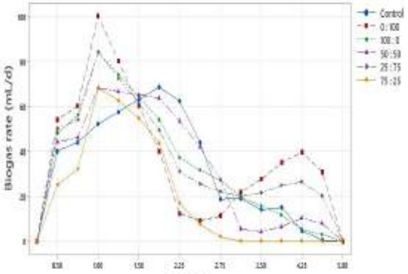

Figure 2.4: Biogas rate plot

Conclusion

Most prolific proportions for the co-digestions were 50:50 (w/w) among FW incorporated experiments and 100:0(w/w) was the other effective option.

References

- Mhlanga, P., Marenya, M. O., Tavengwa, N. T., & Tinarwo, D. (2023). Anaerobic co-digestion of canteen food waste and cow dung.
- Dhar, H., Kumar, P., Kumar, S., Mukherjee, S., & Vaidya, A. N. (2016). Effect of organic loading rate during anaerobic digestion of municipal solid waste. Bioresource Technology,

|ICAS2025|

Optimization of Anaerobic Codigestion Process for Biogas Production by Treating Food Waste with Water Hyacinth

K.Thadshayini[1], A.Nanthakumaran[1], P.G.Rathnasiri[2]

[1]Department of Bio Science, University of Vavuniya, Sri Lanka
[2]Department of Chemical and Process Engineering, University of Moratuwa, Sri Lanka

Abstract: Sri Lanka faces increasing challenges in waste management and renewable energy due to rising food waste generation and the proliferation of invasive *Water Hyacinth* (*Eichhornia crassipes*). This study investigated the optimization of biomethane production through co-digestion of food waste and pretreated water hyacinth, using cow dung as inoculum. Laboratory-scale experiments were conducted in 500 mL batch digesters under mesophilic conditions (37 °C) with agitation at 200 rpm. Biomethane volume was measured using the water displacement method, with carbon dioxide (CO_2) absorbed using 9 N sodium hydroxide (NaOH). Four trials were performed: cow dung alone, cow dung with food waste, cow dung with water hyacinth, and cow dung with food waste and water hyacinth. Cumulative biomethane production in the trials was 115, 158, 216, and 240 mL, respectively. The highest methane yield of 11.04 mL/g VS and maximum production rate of 1.288 mL/g VS/h were observed in the co-digestion of all three substrates, with 21.74 g VS added. Pretreatment of water hyacinth contributed to increased biomethane production. The Modified Gompertz model closely fitted the experimental data ($R^2 = 0.8847$–0.9952), with minor deviations attributed to substrate heterogeneity and microbial adaptation. These results demonstrate that co-digestion enhances biomethane yield, production rate, process stability, and organic waste conversion efficiency. This study recommends adopting this approach in existing biogas systems to support sustainable energy recovery, effective control of invasive water hyacinth, and improved organic waste management in Sri Lanka.

Keywords: anaerobic digestion, biogas production, co-digestion, food waste, renewable energy, water hyacinth

Optimization of Anaerobic Co-Digestion Process for Biogas Production by Treating Food Waste with Water Hyacinth

Thadshayini Karunakaran, Prof. (MS). A. Nanthakumaran,Prof. P.G. Rathnasiri

Introduction

- Sri Lanka faces dual challenges.
- Rising food waste (65–66% of municipal solid waste).
- Proliferation of invasive water hyacinth *(Eichhornia crassipes)*.
- Both resources remain underutilized, causing environmental problems (GHG emissions, eutrophication, clogged waterways).
- Anaerobic digestion (AD) offers a sustainable waste-to-energy solution.

- Gap: In Sri Lanka there is a lack of localized studies on co-digestion of food waste and water hyacinth with cow dung.

Objectives

- Design and test a lab-scale anaerobic digester.

- Evaluate biogas yield from different substrate combinations.

- Assess physicochemical characteristics of feedstocks.

Abstract

Sri Lanka faces challenges in managing food waste and invasive water hyacinth. This study optimized biogas production via co-digestion with cow dung in 500 mL batch digesters. The highest methane yield (11.04 mL/g VS) and rate (1.288 mL/g VS/h) occurred with all three substrates, demonstrating improved biomethane yield, stability, and waste-to-energy potential.

Methodology

Experimental Setup:

- 500 mL batch digesters, mesophilic (37 °C), agitation at 200 rpm.
- Gas collection: water displacement; CO_2 absorbed with NaOH.

Feedstocks:

- Cow dung -CD(inoculum), Food waste -FW(canteen), pretreated Water hyacinth - WH (sun-dried & ground).

Results and Findings

Key Results

- Cumulative methane volume:
  - Trial 1 (CD): 115 mL
  - Trial 2 (CD+FW): 158 mL
  - Trial 3 (CD+WH): 216 mL
  - Trial 4 (CD+FW+WH): 240 mL (highest yield).
- Maximum methane yield: 11.04 mL/g VS.
- Highest production rate: 1.288 mL/g VS/h.
- Gompertz model fitted well ($R^2 = 0.8847–0.9952$).
- Pretreatment (sun-drying & grinding) improved hydrolysis and gas yield.

Analysis

Analysis: COD, TS, VS, TN, TOC, pH, biogas yield.
Modeling: Modified Gompertz equation for cumulative biogas prediction.

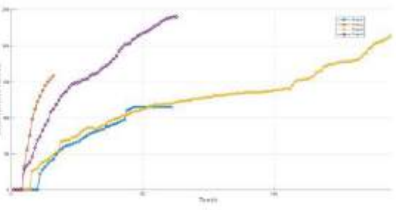

Figure 1 : Cumulative biomethane volume for all trails

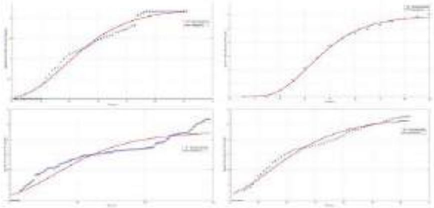

Figure 2 :Gompertz model fit curves for all trails

Conclusions

- Co-digesting food waste and water hyacinth with cow dung improves methane yield and process efficiency, supporting sustainable biogas production.
- Co-digestion provides a sustainable approach to manage waste and invasive species while producing renewable energy.

Recommendations

- Scale-up to community biogas plants.
- Further studies on retention time & pretreatment of raw materials.

Reference

Mata-Alvarez J, Dosta J, Macé S, Astals S. 2014. Codigestion of solid wastes: A review of its uses and perspectives including modeling. Critical Reviews in Biotechnology. 34(1):46–63.

|ICAS2025|

Sustainable Biogas Production using Food Waste and Animal Excreta

B.Kathusika[1], A.Nanthakumaran[1], P.G.Rathnasiri[2]

[1]Department of Bio Science, University of Vavuniya, Sri Lanka
[2]Department of Chemical and Process Engineering, University of Moratuwa, Sri Lanka

Abstract: The rising fossil fuel dependence and organic waste generation increase the need for sustainable energy such as biogas. In Sri Lanka, food waste and animal manure remain underutilized despite their potential for renewable energy and nutrient recovery. This study aimed to assess the feasibility of biogas production through *co-digestion* using food waste and animal excreta. Experiments were conducted in four separate trials for both substrates using a 500 mL batch anaerobic digester operated at mesophilic temperature (35–37 °C) with constant agitation at 200 rpm. Biogas volume was quantified by the water displacement method, with 9 N Sodium Hydroxide (NaOH) used as a Carbon Dioxide (CO_2) scrubber to allow direct measurement of methane. Substrate quality was analyzed before and after digestion, including Total solids, Volatile solids, pH, COD removal efficiency, and C/N ratio. Methane yields were further modeled using the Modified Gompertz equation to assess kinetic performance. The results revealed that *co-digestion* significantly enhanced methane generation compared to mono-digestion. Buffalo dung with food waste in 2:1 ratio achieved the highest cumulative methane yield, with experimental values of 8.99 mL/g VS and a Gompertz fit of 9.03 mL/g VS ($R^2 = 0.9893$). The higher yield may result from buffalo dung's stable buffering and rich microbial content. Followed by cow dung with food waste, yielding 7.25 mL/g VS experimentally and 6.85 mL/g VS by Gompertz fit ($R^2 = 0.9790$), dung-only trials produced lower methane volumes. These findings confirm the superior biogas potential and stability of buffalo dung-based *co-digestion.* Future research is recommended to scale up biogas production systems using the ratio of buffalo dung with food waste in 2:1 and to improve slurry utilization, and expand large-scale applications to reduce food waste and animal manure while addressing local energy demands.

Keywords: anerobic digestion, buffalo dung, biogas, cow dung, co-digestion, food waste

Sustainable Biogas Production Using Food Waste and Animal Excreta

Kathusika Balakirishnan, Prof.(MS).A.Nanthakumaran, Prof. P.G.Rathnasiri

01 Abstract

Co-digestion of food waste with animal excreta enhanced methane output compared to mono-digestion. The buffalo dung–food waste mix (2:1) achieved the highest yield (8.99 mL/g VS), followed by cow dung–food waste (7.25 mL/g VS). Dung-only systems produced lower volumes. Buffalo dung-based co-digestion showed improved stability. The Gompertz kinetic model confirmed strong predictive accuracy.

02 Introduction

Global Challenge:
- Rising energy demand & waste.
- Fossil fuel dependence.

Local Context:
- Sri Lanka generates 7,000-8,000 tons of waste/day.
- >50% is organic (food waste, manure)

03 Objective

- To quantify the input and the biogas output with the co- digestion of food waste and cow dung.
- To quantify the input and the biogas output with the co- digestion of food waste and buffalo dung.
- To compare the efficiency of different substrate combinations and determine the optimal mixing ratios.
- To analyze the physicochemical characteristics of the feedstock before and after anaerobic digestion.

04 Methodology

1.Lab-Scale Experiment
- Setup: 500 mL batch digesters.
- Conditions: 35-37°C, 200 rpm.
- Substrates: Cow Dung (CD), Buffalo Dung (BD), Cooked Rice (CR), Food Waste (FW).
- Trials: 8 trials (Mono & Co-digestion).
- Gas Analysis: Water displacement, CO_2 scrubbed with NaOH.

Figure 1. Lab scale experimental set-up for the anaerobic digestor system

05 Analysis

- Data modeling : MATLAB R2024a,MS Excel
- Parameters: pH, TS, VS, COD, C/N.
- Experimental data analysis: Cumulative methane yield, Biomethane production rate
- Kinetic Modeling data analysis: Modified Gompertz equation.

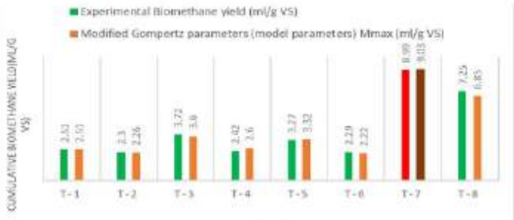

Figure 2. Comparison of Experimental and Gompertz-Fitted Cumulative Biomethane Yield

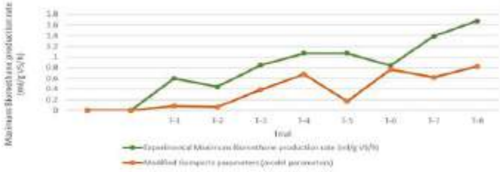

Figure 3. Experimental vs Gompertz Model Biomethane Production Rate

06 Results and discussion

- Co-Digestion Enhances Methane Yield
- Buffalo dung co-digested with food waste (2:1) yielded ~3.5x more methane than dung alone.
- 2. Kinetic Modeling
- The Modified Gompertz model fitted the data excellently (R^2 > 0.97), predicting a maximum potential yield of 9.03 mL CH_4/g VS for the BD+FW 2:1 mixture

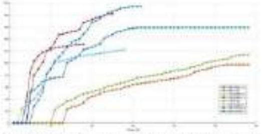

Figure 4. Cumulative biomethane production in each trial

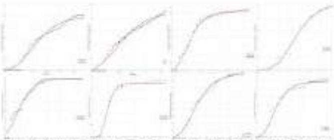

Figure 5. Gompertz Equation to Predict Biomethane Yield in Each Trials

07 Conclusion

- Buffalo dung + Food Waste (2:1) is the optimal substrate mix.
- It achieved the highest methane yield (8.99 mL CH_4/g VS).
- Co-digestion significantly outperforms mono-digestion.

References

Adiotomre, K. O., & Ukrakpor, E. F. (2015). Production of biogas from kitchen waste and cow dung. International Journal of Innovative Scientific & Engineering Technologies Research, 3(2), 52–64. SEAHI Publications.
Iqbal, A., Jarwar, A. I., Laghari, A. Q., Maitlo, G., Qureshi, K., Bhutto, A. W., Shah, A. K., Jatoi, A. S., & Ahmed, S. (2021). Biological assisted treatment of buffalo dung and poultry manure for biogas generation using laboratory-scale bioreactor. Biomass Conversion and Biorefinery, 12, 2961–2972

|**ICAS2025**|

Utilization of Alligator Weed as Organic Liquid Fertilizer: A Comparative Study on Okra (*Abelmoschus esculentus*) Growth and Yield

P.Kabisha[1], A.Nanthakumaran[1]

[1]Department of Bio Science, University of Vavuniya, Sri Lanka

Abstract: Alligator weed (*Alternanthera philoxeroides*) is a highly invasive species causing severe ecological and economic consequences by affecting water quality, hydrological flow, and the growth of native flora and fauna due to its rapid growth and dense mat formation. It thrives in both aquatic and terrestrial habitats and has become a significant ecological concern in Sri Lanka. In Trincomalee, a two-hectare farm pond in Anpuvalipuram has been infested annually, typically from November to May (up to 1.5-hectare level), disrupting fishing and irrigation activities. Although local communities have attempted control measures such as mulching and feeding it to poultry because of its high nutrient availability, these practices have further encouraged its spread into surrounding terrestrial areas. This study was conducted to evaluate the potential of alligator weed as an organic liquid fertilizer and to compare its effectiveness on the growth and yield of the okra crop with that of a conventional organic fertilizer mix and an inorganic fertilizer. Liquid fertilizers were prepared using four concentrations of alligator weed (25%, 50%, 75% and 100%). A traditional organic mixture of Gliricidia and neem leaves, an inorganic fertilizer treatment, and an untreated control were also included. The experiment was arranged in a Completely Randomized Design with four replicates. Fertilizer samples were analyzed for nitrogen, phosphorus, potassium (NPK), pH, and electrical conductivity (EC). Growth and yield performance were evaluated by measuring crop height, stem circumference, total pod number and total pod weight. Despite relatively low NPK concentrations, the 50% alligator weed liquid fertilizer treatment achieved the highest yield performance (1,145.26 g and 64 pods), which was comparable to inorganic fertilizer and superior to both the organic mixture and the control. Utilizing alligator weed not only provides a sustainable alternative to inorganic fertilizers but also offers an eco-friendly strategy for managing a problematic invasive species while recycling nutrients within agricultural areas.

Keywords: alligator weed, effectiveness, replicates, treatment

Utilization of alligator weed as organic liquid fertilizer: A comparative study on okra (*Abelmoschus esculentus*) growth and yield

Kabisha.P[1*], A. Nanthakumaran[1]

[1]Department of Bio-science, Faculty of Applied Science, University of Vavuniya, Sri Lanka

Abstract

This study evaluated the use of alligator weed liquid fertilizer on okra crop compared with inorganic fertilizer, a traditional organic mixture, and a control. Four concentrations (25–100%) were tested under a Completely Randomized Design. The 50% concentration produced nearly similar growth and yield inorganic fertilizer, proving a sustainable, eco-friendly alternative.

Introduction

Alligator weed (*Alternanthera philoxeroides*), an invasive aquatic plant, poses severe ecological and agricultural threats in Sri Lanka. Despite its challenges, recent studies highlight its potential (high nutrient content, rapid biomass availability) as a sustainable resource for organic fertilizer production, improving soil health, enhancing nutrient availability, and supporting environmentally friendly agricultural practices

Objective

- To prepare liquid fertilizers
- To analyze physicochemical parameters (N, P, K, pH, EC) of prepared liquid fertilizers
- To evaluate effects on okra growth and yield.

Methodology

Liquid fertilizer preparation

↓

Okra cultivation and maintenance

↓

Physicochemical parameter analysis of liquid fertilizer

↓

Data collection of crop observational variables

↓

Data analysis using Minitab statistical software

Figure 01: Flow diagram showing the process of research

Results and Discussion

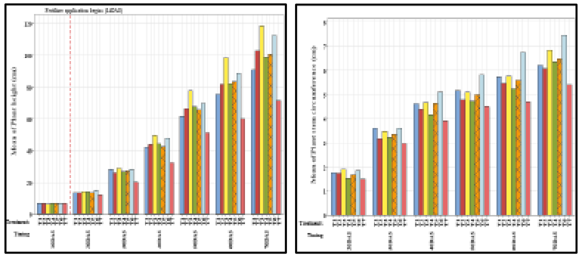

Figure 02: Bar chart showing the effect of different fertilizer applications on okra growth performance at different timings

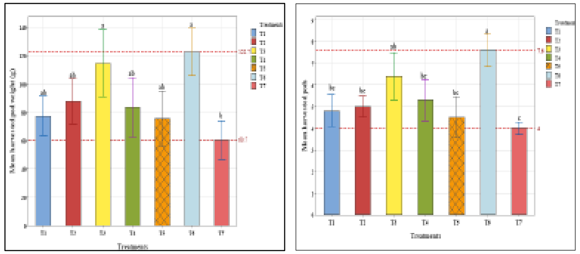

Figure 03: Bar chart showing the effect of different fertilizer applications on okra yield performance at different timings

The results indicate that fertilizer treatments significantly enhanced plant height, stem circumference, and yield attributes. Among treatments, T6 and T3 performed best, producing the highest pod weight and number, suggesting their superior effectiveness in promoting okra growth and productivity

Conclusion

This study concludes that 50% alligator weed liquid fertilizer is the most effective treatment for enhancing okra growth and yield, comparable to inorganic fertilizer. Utilizing this invasive weed as fertilizer not only improves crop productivity but also supports sustainable agriculture and weed management. Wider testing across crops, soils, and climates is recommended to validate long-term benefit

References

Dissanayake, N.P. (2020). Review article on Alternanthera philoxeroides (Mart.) Griseb (alligator weed); an invasive plant species in Sri Lanka and its control measures. *Journal of the University of Ruhuna*, 8(2), pp.93–103. doi: https://doi.org/10.4038/jur.v8i2.7937

Ekanayake, E. and Fernando, K. (2022). *Influence of organic liquid fertilizers on growth and yield of Abelmoschus esculentus, Raphanus sativus and Amaranthus spp in container gardening*. [online] Available at: https://seu.ac.lk/sljot/publication/v3n2/Influence_of_organic_liquid_fertilizers_on_growth_and_yield_of_Abelmoschus_esculentus__Raphanus_sativus_and_Amaranthus_spp_in_container_gardening.pdf

.Viveka, S. and Grace, L. (2020). *Conversion of Water Hyacinth (Eichhornia crassipes) into Nutrient-Rich Fertilizer by Pit Methods*. [online] Available at: https://www.researchgate.net/publication/343207308_Conversion_of_Water_Hyacinth_Eichhornia_crassipes_into_Nutrient-Rich_Fertilizer_by_Pit_Methods

Author index

Published by:

FACULTY OF APPLIED SCIENCE,
UNIVERSITY OF VAVUNIYA,
SRI LANKA

CARE FOR EDUCATION
Empowerment & Prosperity Through Education

HEMSONS

ALTRA SCIENTIFIC

DA

9786246269210